

# Relationship Between Construction Costs and Reliability of Quay Walls

R. Wesstein





# A research into the relationship between the construction costs and the reliability index $\beta$ of quay walls

By

**R. Wesstein**

in partial fulfilment of the requirements for the degree of

**Master of Science**

in Civil Engineering – Hydraulic Structures & Flood Risk

at the Delft University of Technology,

to be defended publicly on March 28, 2019 at 10:30 AM.

*Graduation committee:*

Prof. dr. ir. S.N. Jonkman	TU Delft – Hydraulic Structures & Flood Risk
Dr. ir. J.G. de Gijt	TU Delft – Hydraulic Structures & Flood Risk
Dr. ir. J.G. Verlaan	TU Delft – Integral Design & Management
Ir. A.A. Roubos	TU Delft – Hydraulic Structures & Flood Risk
Dr. ir. O.M. Heeres	Arcadis

An electronic version of this thesis is available at <http://repository.tudelft.nl/>



# Acknowledgements

This thesis has been established as the final work for my master program Hydraulic Engineering at the Delft University of Technology. In this thesis, research has been done into the relation between the construction costs and reliability index of quay walls. The research was conducted at the department of ports and hydraulic engineering of Arcadis, in cooperation with the Port of Rotterdam.

First of all, I would like to express my gratitude to Arcadis for providing me the opportunity and all the resources to conduct this research. Special thanks to my daily supervisor dr. ir. O.M. Heeres for your advice and time advocated during the different stages of my research. Your geotechnical knowledge and experience were very valuable. Besides that, I would like to thank all the colleagues at Arcadis for your help and making my stay comfortable.

Furthermore, my gratitude goes to all the members of my graduation committee for their guidance and support during my graduation. Especially the committee meetings gave relevant new insights. Your contributions made this research possible and were highly appreciated.

Finally, I want to express my appreciation to Deltares for providing me with an upgraded bug-fix version of the software package D-SheetPiling, before their public release. Therefore, I was able to perform reliability calculations and meet the research objective.

*R. Wesstein  
Delft, March 2019*



# Summary

Structures, such as quay walls, have to meet a particular level of safety. Therefore, in the European design codes (Eurocodes), three reliability classes (RC) are introduced based on the potential consequence of failure of the structure. For each of these RC's, a maximum allowable probability of failure is introduced, corresponding to a reliability index ( $\beta$ ). In recent research by Roubos et al. (2018), it was suggested that the marginal costs of safety investments for quay walls are quite low. Therefore, it is questionable whether the current reliability classes and the corresponding set of partial factors, as defined in the Eurocodes and CUR 211, are functional for quay walls. This gave rise to the present study. This study investigates the relationship between the construction costs and the reliability index  $\beta$  for two case study quay walls located in the Port of Rotterdam; 1) a double anchored combi-wall and 2) a combi-wall with a relieving platform. The double anchored combi-wall has a retaining height of about 17 m and is located in the Waalhaven. Besides that, the combi-wall with a relieving platform has a retaining height of about 24 m and is located in the Maasvlakte 1.

Accordingly, the objective of this study is to acquire more insight into the relationship between the construction costs and the reliability index  $\beta$  of quay walls. It is emphasised that this relationship is considered as the marginal costs of safety investments, given specific functionality and boundary conditions of a quay wall. Firstly, the two quay walls were designed semi-probabilistic in RC1, RC2 and RC3, using D-Sheet Piling for the double anchored combi-wall and using Plaxis 2D for the combi-wall with a relieving platform. Thereafter, the construction costs of these designs were calculated and compared. Besides that, the influence of the partial factors, which are defined in the Eurocodes and distinguish the reliability classes, on the construction costs was quantified. The same was done for the influence of three of the critical failure mechanisms; 'passive resistance inadequate', 'sheet pile profile fails' and 'tension member anchorage fails'. For these failure mechanisms the  $\beta$ 's were estimated using the reliability analyses module of D-Sheet Piling, which is based on a probabilistic level II analysis, the First Order Reliability Method (FORM). In figure 1 the results of the relative construction costs increase of the quay walls designed in RC1, RC2 and RC3 are depicted.

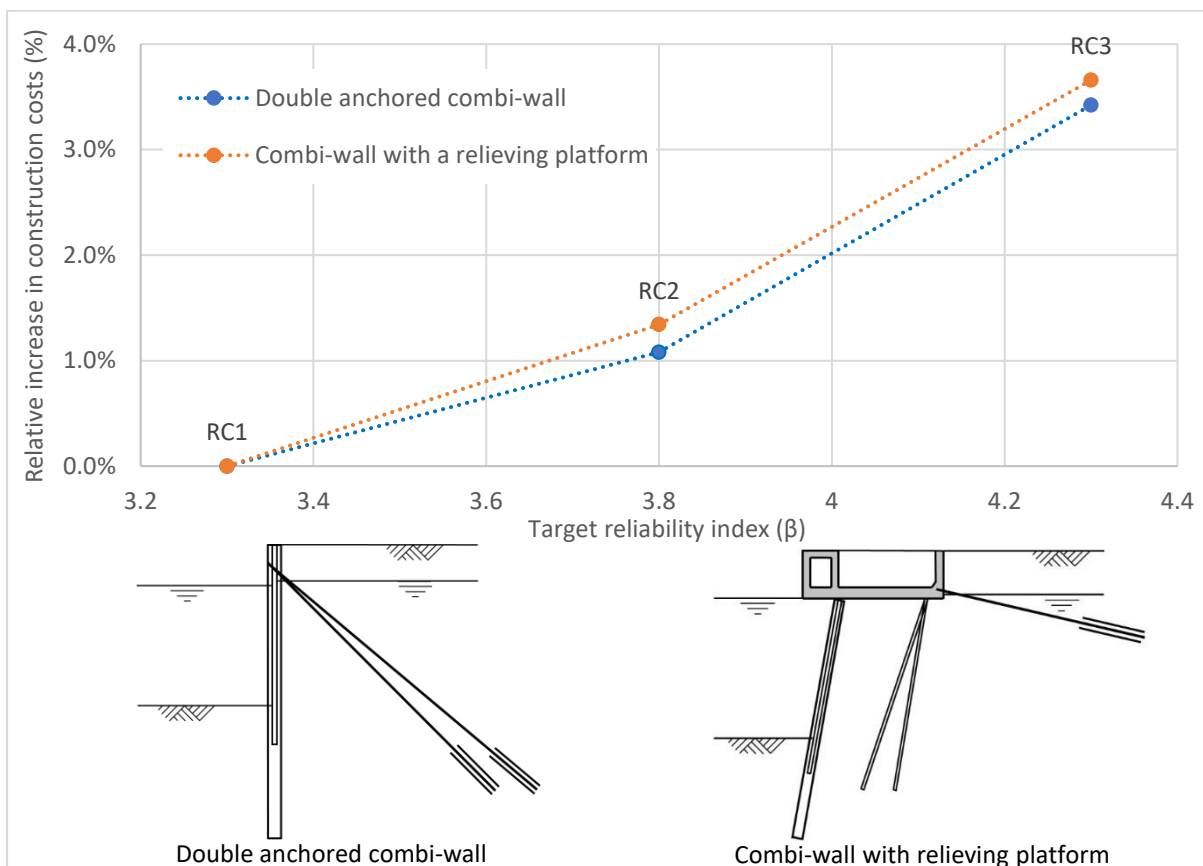


Figure 1 – Construction cost increase of quay walls designed semi-probabilistic in RC1, RC2 and RC3

It appeared that the estimated relationship between the construction costs and the target  $\beta$  of the quay walls are generally comparable and the marginal costs of safety investments are relatively low. Even significantly lower than suggested by Roubos et al. (2018). For both quay walls, the construction costs difference increases between the designs in RC2 and RC3, suggesting that the relationship between the construction costs and  $\beta$  increases for higher  $\beta$ -values. It followed that the differentiation in construction costs between the reliability classes is considerably less than the differentiation in construction costs between quay walls in practice. Therefore, it seems that the current reliability classes and the corresponding set of partial factors, as defined in the Eurocodes and CUR 211, are non-functional for quay walls and have to be revalidated.

Furthermore, the influence of the partial factors on the construction costs was evaluated by performing a sensitivity analysis by increasing the partial factors from the optimised design in RC1 alternately. From this sensitivity analysis can be concluded that in the initial phase of a quay wall design, the determination of  $\phi$  strongly influences the construction costs and the  $\beta$  of the quay wall, in contrast to  $c$ . Besides that, the influence of the surface load on the construction costs is reasonable.

The influence of the failure mechanisms on the construction costs of the double anchored combi wall was evaluated by combining the results of two sensitivity analyses, in which the dimensions of the corresponding structural components were varied. In these analyses the sensitivities of both the construction costs and the  $\beta$  to the dimensions of structural components were determined. The obtained  $\beta$ 's for these failure mechanisms of the double anchored combi-wall are very high because these failure mechanisms are not normative in the design verifications. In the development of probabilistic design of quay walls, it is essential that reliability calculations can be performed for the normative failure mechanisms; 'bearing capacity of tubular piles inadequate', 'local buckling of combi-wall' and 'soil mechanical failure of tension member'. The influence of the failure mechanisms on the construction costs of the double anchored combi-wall is depicted in figure 2, and it appeared that the influences of the failure mechanisms 'passive resistance inadequate' and 'tension member anchorage fails' are relatively low. Therefore, the reliability index  $\beta$  of the quay wall can be increased in an economically attractive manner by increasing the length of the tubular piles of the combi-wall or the steel sectional area of the anchor rod. Due to these influences, economic optimisation in the probabilistic design of quay walls is possible by increasing the target  $\beta$  of the failure mechanism 'passive resistance inadequate' and decrease the  $\beta$  of 'sheet pile profile fails'. Further research would be required in order to determine the optimised target  $\beta$ 's, considering other (normative) failure mechanisms as well.

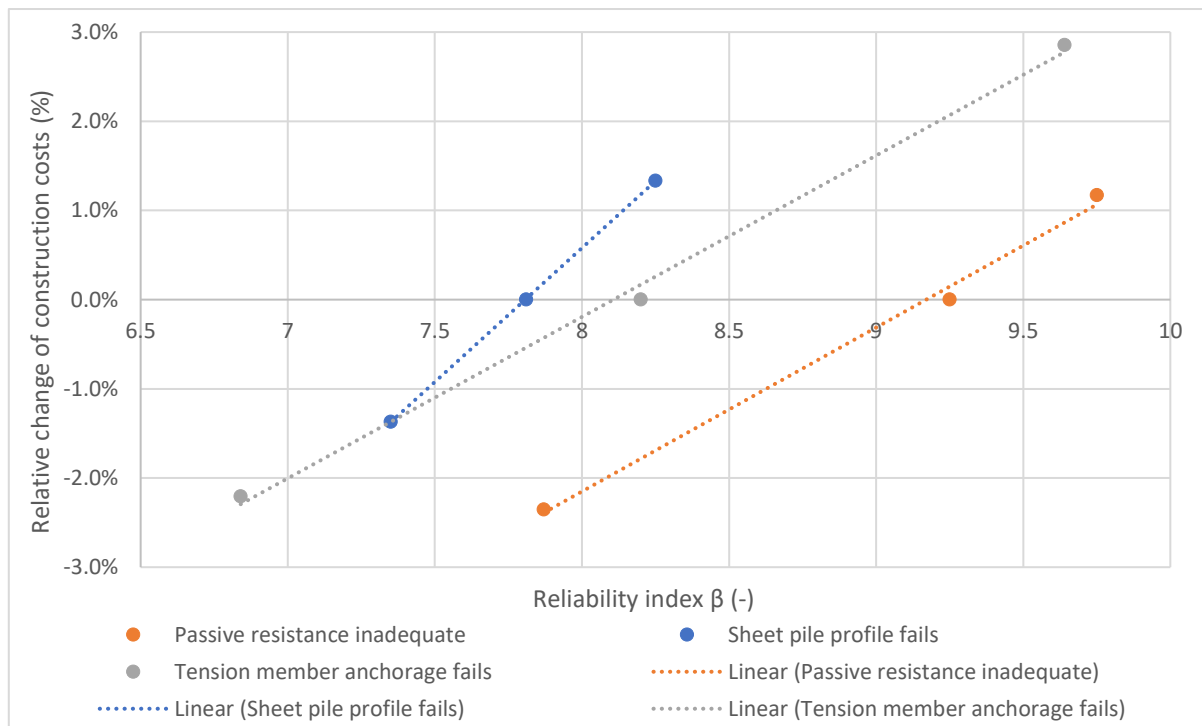


Figure 2 – Influence of failure mechanisms on construction costs of the combi-wall with a relieving platform

# List of symbols

## Reliability symbols

$\alpha$	Sensitivity factor	[-]
$\beta$	Reliability index	[-]
$\beta_{\text{target}}$	Target reliability index	[-]
$\gamma$	Partial factor	[-]
$\mu$	Mean	[-]
$\sigma$	Standard deviation	[-]
$\psi$	Load combination factor	[-]
$\Phi$	Cumulative normal distribution	[-]
$E(X)$	Expected parameter value	[-]
$P_f$	Probability of failure	[-]
$t_{\text{ref}}$	Reference period	[years]
$V$	Coefficient of variation	[-]
$X_k$	Characteristic value	[-]
$X_d$	Design value	[-]
$Z$	Limit state function	[-]

## Geotechnical symbols

$\alpha_p$	Pile class factor	[-]
$c$	Cohesion	[kPa]
$\gamma_{\text{dry}}$	Unsaturated volumetric weight	[kN/m <sup>3</sup> ]
$\gamma_{\text{wet}}$	Saturated volumetric weight	[kN/m <sup>3</sup> ]
$\gamma_w$	Specific weight of water	[kN/m <sup>3</sup> ]
$\varphi'$	Angle of internal friction	[°]
$\delta$	Wall friction angle	[°]
$E_{\text{oed}}$	Oedometer stiffness	[kN/m <sup>2</sup> ]
$E_{50}$	Secant stiffness	[kN/m <sup>2</sup> ]
$E_{\text{ur}}$	Unloading / Reloading stiffness	[kN/m <sup>2</sup> ]
$G_0$	Shear modulus for small strains	[kN/m <sup>2</sup> ]
MSF	Safety factor from $\varphi$ -c reduction	[-]
$K_0$	Neutral lateral earth pressure coefficient	[-]
$K_a$	Active lateral earth pressure coefficient	[-]
$K_p$	Passive lateral earth pressure coefficient	[-]
$k_h$	Modulus of subgrade reaction	[kN/m <sup>3</sup> ]
$t$	Embedded depth	[m]
$q_c$	Cone resistance	[MPa]

## Structural symbols

$A$	Cross-sectional area	[m <sup>2</sup> ]
$\Delta C$	Relative change in construction costs	[%]
$D$	Diameter	[m]
$\Delta D$	Relative change in structural dimensions	[%]
$E$	Elasticity modulus	[kPa]
$f_y$	Yield strength	[N/mm <sup>2</sup> ]
$I$	Moment of inertia	[m <sup>4</sup> ]
$L$	Length	[m]
$t$	Wall thickness	[m]
$M$	Moment force	[kNm]
$N$	Normal force	[kN]
$R_{\text{inter}}$	Interface strength ratio	[-]

UC	Unity check	[-]
V	Shear force	[kN]
w	Displacement	[m]
W	Elastic section modulus	[m <sup>3</sup> ]

# Index

<b>ACKNOWLEDGEMENTS</b> .....	<b>V</b>
<b>SUMMARY</b> .....	<b>VII</b>
<b>LIST OF SYMBOLS</b> .....	<b>IX</b>
<b>INDEX</b> .....	<b>XI</b>
<b>1 INTRODUCTION</b> .....	<b>1</b>
1.1 BACKGROUND OF QUAY WALLS.....	1
1.2 PROBLEM DEFINITION.....	3
1.3 RESEARCH OBJECTIVE .....	3
1.4 RESEARCH QUESTIONS .....	4
1.5 RESEARCH METHOD.....	5
1.6 SCOPE AND LIMITATIONS .....	7
1.7 RESEARCH OUTLINE.....	7
<b>2 THEORETICAL FRAMEWORK</b> .....	<b>9</b>
2.1 QUAY WALLS.....	9
2.1.1 <i>Types of quay walls</i> .....	9
2.1.2 <i>Quay walls in the Netherlands</i> .....	16
2.1.3 <i>Technical failure of quay walls</i> .....	17
2.2 RELIABILITY OF STRUCTURES .....	21
2.2.1 <i>Probability of failure &amp; reliability index</i> .....	21
2.2.2 <i>Reliability methods</i> .....	23
2.2.3 <i>Economic optimum</i> .....	28
2.2.4 <i>Limit states</i> .....	28
2.3 DESIGN GUIDELINES.....	29
2.3.1 <i>Eurocodes</i> .....	29
2.3.2 <i>NEN 9997-1</i> .....	33
2.3.3 <i>CUR 166</i> .....	33
2.3.4 <i>CUR 211</i> .....	35
2.4 CALCULATION METHODS .....	35
2.4.1 <i>Blum Method</i> .....	36
2.4.2 <i>Subgrade reaction method</i> .....	36
2.4.3 <i>Finite element method</i> .....	37
2.5 COST OF QUAY WALLS.....	38
2.5.1 <i>Indexing</i> .....	40
2.5.2 <i>Cost estimation</i> .....	40
2.6 CONCLUSION .....	41
<b>3 STARTING POINTS</b> .....	<b>42</b>
3.1 BENCHMARK 1: DOUBLE ANCHORED COMBI-WALL.....	42
3.1.1 <i>Introduction of benchmark 1</i> .....	42
3.1.2 <i>Project location</i> .....	42
3.1.3 <i>Boundary conditions</i> .....	43
3.1.4 <i>Existing design of benchmark 1</i> .....	43
3.1.5 <i>Partial factors of semi-probabilistic design</i> .....	44
3.1.6 <i>Reliability calculations</i> .....	46
3.2 BENCHMARK 2: COMBI-WALL WITH A RELIEVING PLATFORM.....	48
3.2.1 <i>Introduction of benchmark 2</i> .....	48
3.2.2 <i>Project location</i> .....	49
3.2.3 <i>Boundary conditions</i> .....	49
3.2.4 <i>Existing design of benchmark 2</i> .....	49
3.2.5 <i>Partial factors of semi-probabilistic design</i> .....	50
3.2.6 <i>The plaxis model of benchmark 2</i> .....	52
<b>4 RESULTS BENCHMARK 1: DOUBLE ANCHORED COMBI-WALL</b> .....	<b>54</b>
4.1 DESIGN PRINCIPLES .....	54
4.1.1 <i>Optimised design</i> .....	55

4.2	SEMI-PROBABILISTIC DESIGN RESULTS .....	56
4.3	CONSTRUCTION COSTS ESTIMATION .....	57
4.3.1	<i>Construction costs estimation of optimised designs</i> .....	58
4.3.2	<i>Execution classes steel structures</i> .....	60
4.4	RELIABILITY RESULTS .....	61
4.5	INFLUENCE OF PARTIAL FACTORS ON THE CONSTRUCTION COSTS.....	63
4.6	INFLUENCE OF STRUCTURAL COMPONENTS ON THE CONSTRUCTION COSTS .....	66
4.7	INFLUENCE OF FAILURE MECHANISMS ON THE CONSTRUCTION COSTS .....	67
4.8	CONCLUSION .....	69
<b>5</b>	<b>RESULTS BENCHMARK 2: COMBI-WALL WITH A RELIEVING PLATFORM.....</b>	<b>71</b>
5.1	DESIGN PRINCIPLES .....	71
5.1.1	<i>Optimised design</i> .....	72
5.2	SEMI-PROBABILISTIC DESIGN RESULTS .....	72
5.3	CONSTRUCTION COSTS ESTIMATION .....	74
5.3.1	<i>Construction costs estimation of optimised designs</i> .....	74
5.3.2	<i>Execution class steel structures</i> .....	77
5.4	INFLUENCE OF PARTIAL FACTORS ON THE CONSTRUCTION COSTS.....	77
5.5	INFLUENCE OF STRUCTURAL COMPONENTS ON THE CONSTRUCTION COSTS .....	81
5.6	CONCLUSION .....	82
<b>6</b>	<b>CONCLUSION AND DISCUSSION .....</b>	<b>84</b>
6.1	CONCLUSIONS.....	84
6.2	DISCUSSION.....	90
6.2.1	<i>Execution class</i> .....	90
6.2.2	<i>Fraction <math>\Delta C/\Delta\beta_{target}</math> estimations</i> .....	90
6.2.3	<i>Fraction <math>\Delta C/\Delta\beta</math> estimations</i> .....	90
6.3	RECOMMENDATIONS .....	91
6.3.1	<i>Recommendations for science</i> .....	91
6.3.2	<i>Recommendations for practice</i> .....	92
	<b>REFERENCES.....</b>	<b>93</b>
	<b>APPENDICES.....</b>	<b>96</b>
APPENDIX A	ADDITIONAL THEORETICAL FRAMEWORK	
APPENDIX B	FICTIONAL CASES	
APPENDIX C	BOUNDARY CONDITIONS OF BENCHMARK 1	
APPENDIX D	CHARACTERISTIC VALUES OF SOIL PROPERTIES	
APPENDIX E	BOUNDARY CONDITIONS OF BENCHMARK 2	
APPENDIX F	SPIRALLY WELDED STEEL PIPES OF ARCELORMITTAL	
APPENDIX G	DESIGNS BASED ON STANDARD DIMENSIONS OF BENCHMARK 1	
APPENDIX H	DESIGN CALCULATIONS OF OPTIMISED DESIGN OF BENCHMARK 1 IN RC1	
APPENDIX I	OPTIMISED DESIGN OF BENCHMARK 1 IN SLS WITH INCREASED $\phi'$	
APPENDIX J	INFLUENCE OF THE MODULUS OF SUBGRADE REACTION ON THE RELIABILITY INDEX OF BENCHMARK 1	
APPENDIX K	RELIABILITY RESULTS OF BENCHMARK 1	
APPENDIX L	ANCHORS OF JETMIX	
APPENDIX M	DESIGNS BASED ON STANDARD DIMENSIONS OF BENCHMARK 2	
APPENDIX N	DESIGN CALCULATIONS OF OPTIMISED DESIGN OF BENCHMARK 2 IN RC1	
APPENDIX O	Z-TYPE SHEET PILE PROFILES OF ARCELORMITTAL	
APPENDIX P	VERIFICATION REPORTS OF OPTIMISED DESIGN OF BENCHMARK 1 IN RC1	
APPENDIX Q	VERIFICATION REPORTS OF OPTIMISED DESIGN OF BENCHMARK 2 IN RC1	

# 1 Introduction

## 1.1 Background of quay walls

Ports are essential for international maritime transport, handling over 80 per cent of the global trade by volume (UNCTAD/RMT, 2015). Accommodating vessels in ports several types of structures can be used, such as quay walls, wharfs, jetties or dolphins for instance. In this respect, quay walls are used very commonly. In the Netherlands already a considerable number of kilometres of quay walls have been built already. Quay walls are retaining structures that are primarily intended to moor vessels. In order to do so, they have to resist horizontal soil pressures. Soil retaining structures are needed when the required slope of the surface exceeds the angle of repose of the soil. Basically, the retaining structure prevents the soil from sliding. Quay walls are mostly used when cranes or other heavy equipment must be able to move along the quay. In general, quay walls are provided with bollards to moor the vessels and fenders to absorb the berthing forces. The superstructure is usually provided with crane rails, and the foundation must take care of the stability of the quay wall.

Especially for decision makers and clients, the construction costs of quay walls are essential for evaluating the feasibility of a project or for determining the most economical, technical solution. The Port of Rotterdam indicated from experience and expert judgement that the construction costs of a quay wall are determined for approximately 75% by the retaining height and 25% by other factors, as shown in figure 1.1 (De Gijt, 2010).

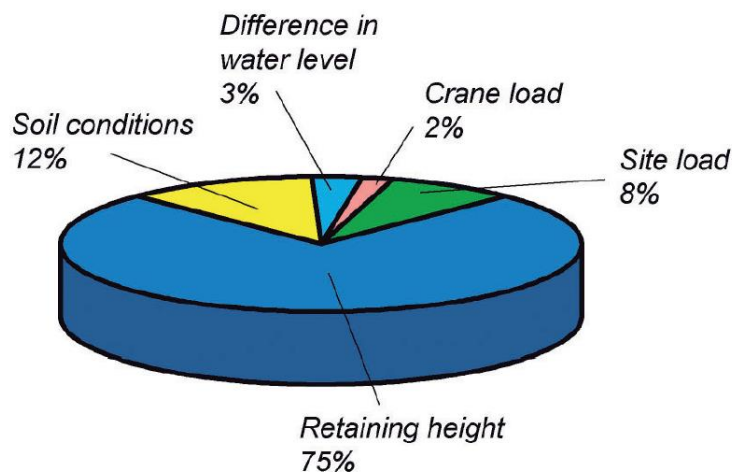


Figure 1.1 – Analysis of factors driving the construction costs of quay walls in Rotterdam (De Gijt, 2010)

To fulfil the varied requirements of quay walls, depending on their purpose and location, a large number of different types of quay walls have arisen during the years in various countries. The choice for a particular type of quay wall predominantly depends on the local soil conditions, the water levels and the requirements imposed by the client. The most frequently applied types of quay walls in the Port of Rotterdam, the Netherlands are:

- anchored combi-wall. In figure 1.2 an anchored combi-wall is depicted.

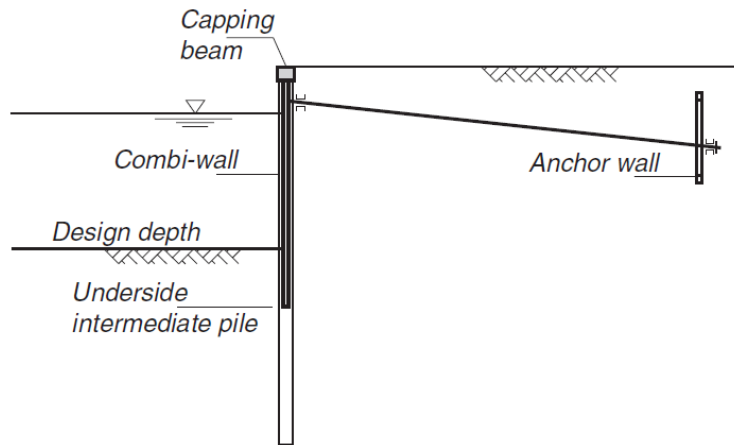


Figure 1.2 – Principle of an anchored combi-wall (Stichting CURNET, 2014)

- sheet pile structure with a relieving platform. In figure 1.3 a combi-wall with a relieving platform is illustrated.

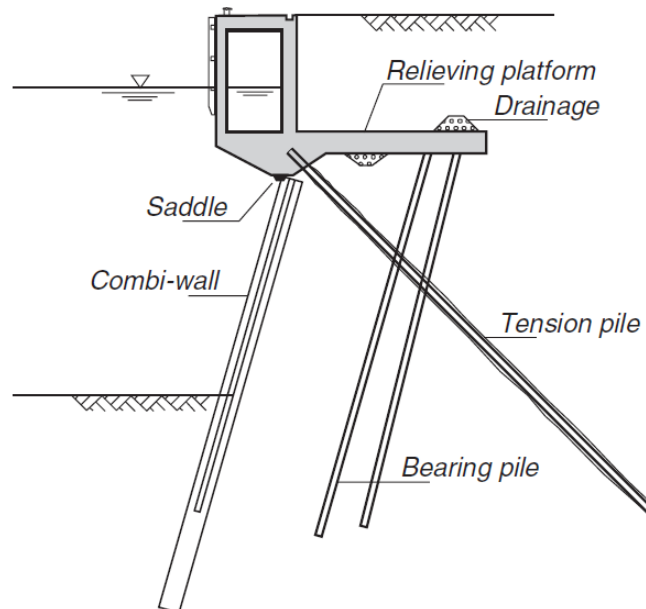


Figure 1.3 – Principle of a combi-wall structure with a relieving platform (Stichting CURNET, 2014)

Anchored combi-walls are mostly used for lower retaining heights, in contrary to sheet pile structures with a relieving platform. Furthermore, the sheet pile structures with a relieving platform are mostly used when the loads on the site are heavy or when there are high demands considering the allowable deformations (Stichting CURNET, 2014).

Structures, like quay walls, have to meet a particular level of reliability, defined in design requirements. Therefore, in the Eurocodes, three reliability classes are introduced based on the potential consequence of failure. These reliability classes influence the design requirements. This reliability classification is initially developed for the design of bridges and buildings and can be considered as subjective (Smit, 2016). In the very beginning of the design process, every structure designed following the Eurocodes is classified into one of the reliability classes. For each of the reliability classes, a maximum allowable probability of failure is introduced, corresponding to a reliability index  $\beta$ . The maximum allowable probability of failure and the reliability index are directly related to each other. The reliability index of a structure is divided into target reliability indices per failure mechanism, corresponding to a maximum allowable probability of failure per failure mechanism (Jonkman et al., 2017).

This reliability index determines for each of the reliability classes a set of partial factors, which are defined in the National Annexes of the Eurocodes. The partial factors defined in the Dutch National

Annex act on the loads, the material characteristics and the geometrical variables of the design and they are, among others, based on the target reliability indices per failure mechanism (The Netherlands Standardisation Institute, 2017).

## 1.2 Problem definition

Even before the start of the design process of a quay wall, a decision has to be made about the required reliability class. In theory, a higher reliability class, and a higher reliability index, for the quay wall, means a more reliable structure with a lower maximum allowable probability of failure. The differences between the maximum allowable failure probabilities of the reliability classes are known, but the construction costs differences between quay walls with different reliability classes (and reliability indices) are not known.

In recent research by Roubos et al. (2018) the target reliability indices for quay walls were derived from various risk acceptance criteria, such as economic optimisation, individual risk, societal risk, the life quality index and the social and environmental repercussion index. For the economic optimisation, a first estimation of the marginal safety investments for quay walls was determined. The findings included that the marginal costs of safety investments for quay wall are quite low, which gave rise to this study. The research by Roubos et al. (2018) also concluded that it is possible that the optimal annual and lifetime reliability indices of commercial quay walls are lower than the current standards prescribe.

In the Eurocodes, every reliability index corresponds to a reliability class. In the past, the target reliability indices per failure mechanism were allocated by expert judgement, and these indices were evaluated and adapted using validation studies in the following years. These validation studies mainly consisted of probabilistic calculations of several failure mechanisms. From these studies also the influence of every stochastic parameter on the failure probability is obtained, but their influence on the cost of the quay walls is currently unknown.

The Port of Rotterdam already estimated the factors driving the construction costs of quay walls in Rotterdam, illustrated in figure 1.1. This study considered a large number of different quay walls with different requirements and functionalities, such as retaining heights for instance. Therefore, figure 1.1 cannot be used for an estimation of the marginal costs of safety investments of quay walls.

## 1.3 Research objective

From the problem the following objective of this research is defined:

*Acquire more insight into the relationship between the construction costs and the reliability index  $\beta$  of quay walls.*

On the one hand, the relationship between the construction costs and the reliability index of quay walls can be considered as the marginal costs of safety investments, given a particular functionality of a quay wall. On the other hand, the reliability index of a quay wall is also influenced by the functionality of a quay wall, such as the retaining height or type of crane. The marginal costs of safety investments are directly influenced by the partial factors, defined in the reliability classes of the Eurocodes. In contrast, the functionality of a quay wall is independent of the partial factors. This is an important differentiation. It is emphasised that this study is focused on the marginal costs of safety investments of quay walls.

This research is performed in order to obtain insight into the distribution of reliability and construction cost of quay walls, which can be useful for the future design of quay walls. With the help of this study, quay wall designs can be adapted more economically when a different reliability level has to be reached as well. So, this research is useful for Arcadis, the Port of Rotterdam and also for other quay wall design engineers. Besides that, this research contributes to the development of probabilistic design of quay walls. For instance, it is possible that the target reliability indices per failure mechanism can be optimised based on the sensitivity of the cost of quay walls to the failure mechanisms. When the cost of a quay wall is sensitive for a particular failure mechanism, it may be economically beneficial to lower the target reliability index for this failure mechanism and increase another target reliability index for which the sensitivity of the cost is lower. Then it is possible that the cost of the quay wall decreases, but the overall reliability index of the quay wall remains constant. This is comparable to the failure probability distribution principle for flood defences.

## 1.4 Research questions

The main research question, corresponding to the research objective is defined as follows:

**Main question:** What is the relationship between the construction costs and the reliability index  $\beta$  of quay walls?

In order to answer the main question, the following research questions are formulated:

- **Research question 1:** What are the construction cost differences between quay walls designed with a different reliability index  $\beta$ ?

Recent research estimated this marginal costs of safety investments, but thorough research is required in order to answer this question (Roubos et al., 2018).

Only the direct construction costs of the defined quay wall structure and the cost influenced by the reliability class are considered in this study. The quay wall is defined as the retaining wall, including its possible anchoring, pile foundation, relieving platform, bollards and fenders. This means that the cost of the pavement of the terminal and the bed protection in front of the quay wall are not taken into account. Besides that, costs of planning, design, engineering, maintenance, demolition, insurance and one-off costs, such as profit, risks and general costs, are not considered, because they are not depending on the RC of the quay wall. The construction costs mainly consist of material, labour and equipment costs.

This study is mainly focused on quay walls in the Port of Rotterdam, the Netherlands. Therefore, two cases of the most frequently applied types of quay walls in the Port of Rotterdam are considered in this study (Stichting CURNET, 2014):

1. Benchmark 1: a double anchored combi-wall;
2. Benchmark 2: a combi-wall with a relieving platform.

These results were used, together with the target reliability indices defined in the Eurocodes, in order to find a first estimate of the relationship between the construction costs and the target reliability index of quay walls (The Netherlands Standardisation Institute, 2017). These codes were used, because all European standards correspond to these. Next, the reliability indices of the designs were evaluated for three of the critical failure mechanisms using the reliability analyses module of D-Sheet Piling.

- **Research question 2:** What are the influences of the partial factors on the construction costs of quay walls?

The Port of Rotterdam estimated the factors driving the construction costs of quay walls in Rotterdam (De Gijt, 2010), but this analysis considered a large number of different quay walls with different requirements and functionalities. In contrast, this study is focusing on the marginal costs of safety investments of quay walls, based on a particular constant functionality.

The most important factors influencing the marginal costs of safety investments are determined by the reliability class, namely the partial factors. The influences of the partial factors on the construction costs were determined using a sensitivity analysis in this study. Utilising the sensitivity analysis the sensitivity of the construction costs of the quay wall to every partial factor was determined, representing the influence of each of the partial factors on the construction costs.

- **Research question 3:** What are the influences of failure mechanisms on the construction costs of quay walls?

The influences of failure mechanisms on the construction costs of quay walls were estimated by comparing the influence of the corresponding structural components on the construction costs with their influence on the reliability index of quay walls. Through a sensitivity analysis the sensitivity of the construction costs of the quay wall to the structural components was determined, representing the influence of each of the structural component. Besides that, for every situation from this sensitivity analysis, the reliability index was estimated using reliability calculations.

The reliability calculations were performed using the reliability analyses module of D-Sheet Piling, in which it is possible to perform probabilistic calculations for the following failure mechanisms:

- passive resistance inadequate;
- sheet pile profile fails;
- tension member (anchorage) fails.

These failure mechanisms are indicated as some of the most critical ones (Calle & Spierenburg, 1991). Other failure mechanisms need to be analysed with different models.

## 1.5 Research method

This research started with a literature study, which is presented in the following chapter 2. It contains descriptions and evaluations of relevant literature about this subject. The objective of the literature study is to treat previous studies about this subject and provide a starting point for this research. From this literature study, more insight was acquired into the currently still missing knowledge about the relationship between the construction costs and the reliability index of quay walls.

The research questions were answered based on the design of the two benchmark quay walls. Previously, this research started by examining fictional sheet pile structures in order to become familiar with the research steps and possible results. The different (fictional) quay walls were designed consecutively using stepwise refinement. At first, a fictional cantilever sheet pile structure was considered because this type of quay wall is a straightforward retaining structure and the failure mechanisms of this type of quay wall are well known. The fictional cantilever sheet pile wall was designed semi-probabilistic using three calculation methods: the Blum method, the hand calculation and the subgrade reaction method. The hand calculation was used as a first estimate of the results. The Blum Method was used as validation of the subgrade reaction method. The other fictional cases were designed using the subgrade reaction method. For all three fictional cases also reliability calculations were performed.

Thereafter, the two benchmark quay walls were considered, from which both the final design in RC2 was already performed by the designer on behalf of the Port of Rotterdam. The first benchmark quay wall, a double anchored combi-wall, has a retaining height of about 17 m and is located in the Waalhaven, Port of Rotterdam. The second benchmark quay wall, a combi-wall with a relieving platform, has a retaining height of about 24 m and is located in the Maasvlakte 1. Benchmark 1 is used because the soil properties are relatively well known as this quay wall is constructed in a land reclamation. Both benchmarks have been designed following the CUR 211, with the help of the CUR 166 and the NEN 9997-1, as these were used by the designer as well.

The following research steps were performed two times, for both benchmark quay walls. An overview of these research steps is depicted in an flow diagram in figure 1.4. First, the particular quay wall was designed semi-probabilistic for the three different reliability classes (RC1, RC2 and RC3), based on their actual design. Three different reliability classes mean three different reliability indices, defined in the Eurocodes. Thereafter, the construction costs for these semi-probabilistic designs were determined deterministic, and the results were reviewed. Only the direct construction costs of the defined quay wall structure and the cost influenced by the reliability class were considered. The cost are estimated using the standard cost estimate system (standaardsystematiek voor kostenramingen – SSK), which is widely accepted in the Netherlands. Moreover, the system is accessible (CROW, 2010). In the existing designs of both benchmarks, SSK calculation sheets were prepared by cost specialists. In these calculation sheets, the activities accompanying to the construction of the quay walls were collected and expressed per unit of length, area, volume, number or weight. The cost of these activities were estimated using unit prices, which are based on standard prices and prices of previous quay wall projects. In this study, this calculation sheet was validated using construction costs unit prices of quay walls of the Port of Rotterdam (Koene, 2018). The activities in the calculation sheet consist of the supply of materials and construction of structures, including labour- and equipment costs.

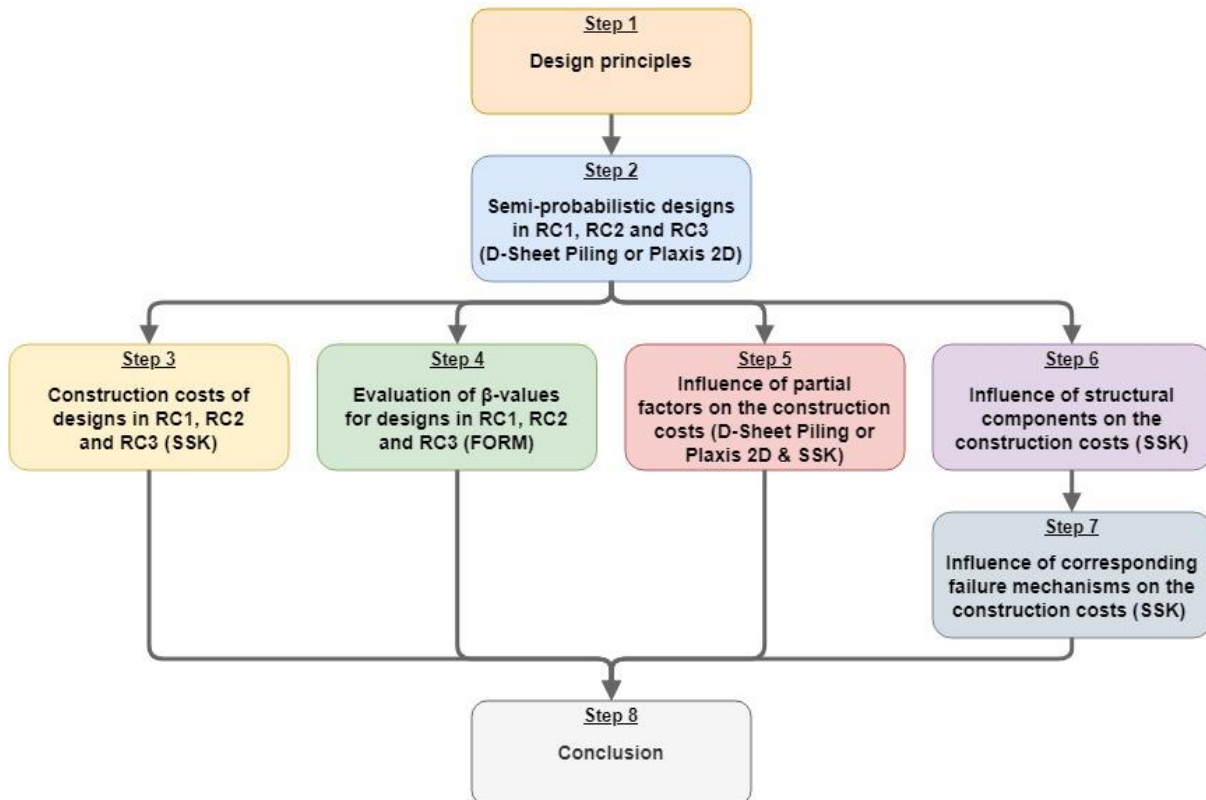


Figure 1.4 – Flow diagram of research steps per benchmark quay wall

With these results, the construction cost differences between quay walls designed with a different reliability index  $\beta$  has been obtained, together with a first estimate of the relationship between the construction costs and target  $\beta$ -values. Next, for benchmark 1 the reliability indices were evaluated for three of the critical failure mechanisms using the reliability analyses module of D-Sheet Piling.

The design of a quay wall can be related to a corresponding reliability index using several methods, from which a few are discussed here. It was possible to perform probabilistic calculations using level III reliability methods, for instance with the ProbAna software of Plaxis. The results of these methods are reliable, but this software is complex and requires very long computational time. Plaxis can also be used to calculate the safety factor of 'soil mechanical failure' of a design, using a phi-c-reduction. The computational time of this method is relatively long, and it is hard to relate this safety factor to the reliability index of a structure. Besides that, level II reliability methods are possible as well. Level II methods are approximating the probability of failure, but the computational time is in general considerably lower. For instance, the point estimate method can be used with the help of Plaxis. In this method, the probability density function is estimated using simplified equivalent distributions of the parameters. This method requires a few numbers of input parameters, but the accuracy of this method is uncertain due to its simplification. Another possible level II reliability method is the reliability analyses module of D-Sheet Piling. The reliability analyses module of D-Sheet Piling is based on the First Order Reliability Method (FORM). FORM is approximating the probability of failure of designs based on the design point of the limit state function. The design point is the failure point with the highest probability density, so most probably failure occurs in this point. With the help of probabilistic level III methods more reliable results will be produced because the probability of failure can be calculated more exactly. However, these methods are very time-consuming. Because of the limited time that is reserved for this study, the probabilistic level II analysis, the FORM was used in this study. FORM is considered as a good alternative of level III methods because it requires less mathematical computations and generally gains accurate results (Jonkman et al., 2017). It is very likely that this method is more accurate than the point estimate method. This is because the inaccuracy in the results increases for increasing non-linearity in the input data for the point estimate method (Valley & Kaiser, 2010). Non-linearity certainly applies to the benchmarks of this study.

Thereafter, several sensitivity analyses were performed. In these sensitivity analyses, the influence of the partial factors and three failure mechanisms on the construction costs was determined first. Utilising the sensitivity analysis the sensitivity of the construction costs of the quay wall to every partial factor was determined, representing the influence of each of the partial factors. From this analysis, the essential partial factors concerning the construction costs of quay walls were determined. Sensitivity analyses are used as computational models because this method is straightforward and capable of obtaining the influence of the different factors.

Next, the influence of the three failure mechanisms on the construction costs of quay walls was estimated. First, the influences of the structural components, corresponding to these failure mechanisms, on the construction costs were determined using a sensitivity analysis varying the dimensions of these components. For every relevant situation of the sensitivity analysis, the reliability index has been estimated for three of the critical failure mechanisms using the reliability analyses module of D-Sheet Piling. In this way, the reliability index and the design of a quay wall has been related.

So, for both quay walls, the influence of the partial factors on the construction costs were obtained as well as the influence of three of the critical failure mechanisms. The influence of the failure mechanisms on the construction costs was estimated by combining the influences of the structural components on the construction costs and on the reliability index. Using the results of this study all research questions and the main question of this study has been answered.

## 1.6 Scope and limitations

This study is mainly focused on quay walls in the Port of Rotterdam, the Netherlands. Therefore, the two benchmark quay walls considered in this study are based on the two most frequently applied types of quay walls in the Port of Rotterdam (Stichting CURNET, 2014). Both benchmark quay walls and their soil characteristics are specific for the Port of Rotterdam and therefore not immediately applicable for other ports in the Netherlands.

Both benchmark quay walls have been designed following the CUR 211, with the help of the CUR 166 and the NEN 9997-1. In these codes design approach 3 is used, in which the partial factors are applied to the load or the load effects and to the soil parameters. This design approach is typically used in Dutch design standards. Because of the limited time that is reserved for this study, only a limited number of quay walls can be analysed. More analysed quay walls would increase the reliability of the conclusions.

In the determination of the construction costs, the influence of the execution classes (EXC) is neglected in this study. The construction costs are determined using present (2016) unit prices, which can deviate in the future. Besides that, model uncertainties of the design and project risks are not considered in the construction costs.

The reliability results are performed using the reliability analyses model of D-Sheet Piling, based on the FORM. A restriction of the reliability analyses module of D-Sheet Piling is that correlations between variables cannot be implemented. Besides that, not all parameters can be chosen as stochastic and model uncertainties are not taken into account. Using this software, reliability calculations can only be performed for three of the critical failure mechanisms, regardless of whether these failure mechanisms are normative.

## 1.7 Research outline

This study starts with the theoretical framework, obtained by a literature study in the preparation of this research. The theoretical framework describes important background theory and treats previous studies about this subject. In the starting points, the two benchmark quay walls are introduced, and the starting points and boundary conditions of these cases are treated. From these starting points, the calculations and results are gathered in the subsequent chapters. Thereafter, the results are collected and evaluated in the successive chapter, leading to the conclusions, discussion and recommendations. A flow diagram of the research outline is depicted in figure 1.5.

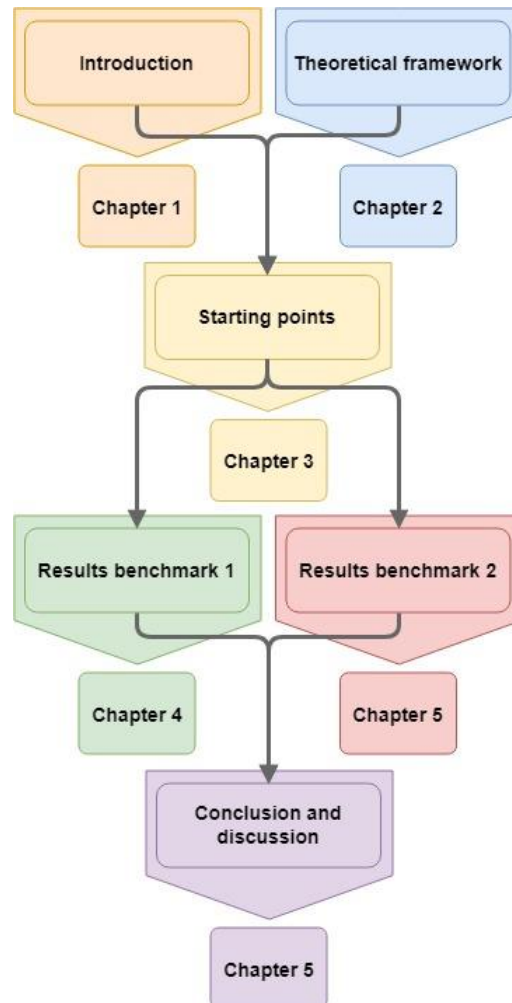


Figure 1.5 – Research outline

## 2 Theoretical framework

This chapter contains the theoretical framework of this research, which is obtained in the literature study. In the first subchapter, a general description is given. Furthermore, the different types of quay walls applied in the world and the Netherlands are being discussed. Besides that, the failure of quay walls and the development of defining failure is considered. In the second subchapter the reliability methods of structures are briefly explained and the most important one, the semi-probabilistic method, is further treated. After that, the most crucial design guidelines in the Netherlands are considered in the third subchapter, and the different calculation methods are discussed in the fourth subchapter. The fifth subchapter describes the cost of quay walls, in which previous studies about the cost of quay walls are evaluated. This theoretical framework does not include all the literature considered in the literature study of this research. Additional literature, which has an indirect connection with this study, is attached in Appendix A.

### 2.1 Quay walls

In this subchapter, the importance of quay walls and the different types of quay walls applied in the world are being discussed. The most frequently applied types of quay walls in the Netherlands are compared, and the development of defining quay wall failure is given.

Quay walls are soil retaining structures primarily intended to moor vessels, and therefore they have to resist lateral soil pressures. Vessels are moored at quay walls when cranes or heavy equipment must be able to move along the quay. In general quay walls are provided with bollards to moor the vessels and fenders to absorb the berthing forces. The superstructure is usually provided with crane rails, and the foundation must take care of the stability of the quay wall.

#### 2.1.1 Types of quay walls

The quay structure has to meet multiple requirements, depending on the users. For instance, for vessels, there must be sufficient draught for the largest vessels to berth. The terminal behind the quay wall must be sufficiently elevated to protect it from overflow, even at high tide. For the handling of freight, it is also essential to have a storage area that is large enough to provide for current and future transshipment, storage and transport. Furthermore, the quay wall must retain soil for the terminal behind it, provide bearing capacity to carry loads imposed by the transshipment of freight and possibly also serve as a water retaining wall during a period with high water for low areas lying behind the quay structure (Stichting CURNET, 2014).

In order to fulfil the varied requirements of quay walls, a large number of different types of quay walls have arisen over the years in various countries. Quay wall types are useful for this research when they are representative of quay walls with considerable retaining heights in the Netherlands. Quay walls can differ in complexity very much, and several important structural types are discussed below. For this end, provided information in CUR 211 is used as this source is widely used in the Netherlands (Stichting CURNET, 2014).

The different types of quay walls can be divided into four categories (using stepwise refinement):

- sheet pile structures;
- gravity structures;
- open berth structures;
- sheet pile structures with a relieving platform.

The characteristics of these categories with their quay wall types, except for the open berth structure, are discussed below. The open berth structures are not treated in this literature study, because they are not relevant in this study. Open berth structures can be favourable because of the wave reduction due to the slope underneath the deck but are hardly used in the Netherlands.

##### 2.1.1.1 Sheet pile structures

The most straightforward quay walls are sheet pile structures, which obtain their stability from the fixation capacity of the soil. Sheet pile structures are used at locations where the soil is easily penetrable

and has poor conditions, like in the Netherlands. So, these types of quay walls can be used for this research.

Sheet pile structures can be performed using single sheet piling, combined sheet piling, diaphragm walls or fixed cofferdams. The single sheet pile can be made of wood, concrete or steel, which are driven into the soil. Steel sheet piling is suitable for quay walls with high retaining heights and heavy loads. If even heavier structures are needed these can be constructed from various types of combi-walls. Combi-walls consists of heavy primary elements that are embedded in the soil and intermediate sheet piles which may be shorter than the primary elements. Diaphragm walls are reinforced concrete walls, which are made in situ. A cofferdam wall consists of two sheet pile structures, using the soil filling between the two walls to obtain their stability. Failure of this type of quay wall can occur when the sheet pile profile fails, the sheet pile structure is unstable or, if possible, the anchorage fails (Stichting CURNET, 2012b).

The sheet pile structures can be cantilevered or combined with an anchor system. These two types are considered here.

- Cantilever sheet pile structure:** The cantilever sheet pile wall is embedded into the soil and transfers the soil pressure to the subsoil. So, the sheet pile wall is elastically fixed into the ground and is usually used for smaller retaining heights. Cantilever sheet pile structures are applied for retaining heights up to about 5 metres (Stichting CURNET, 2012b). With larger retaining heights some kind of anchoring or strut system is necessary. The principle of a cantilever sheet pile structure is depicted in figure 2.1.

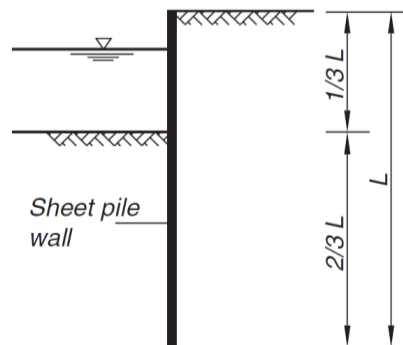


Figure 2.1 – Principle of a cantilever sheet pile structure (Stichting CURNET, 2014)

- Anchored sheet pile structure:** Especially for higher retaining heights, it can be necessary to use anchorage at the upper side of the sheet pile structure. In this way, the anchor can bear horizontal forces and the principle of an anchored sheet pile structure is shown in figure 2.2. In this figure, the anchor is performed as a horizontal anchor. However, anchorage with a grout body is also commonly used in the Netherlands. The anchored wall behaves like a beam with two supports: on the one side the soil and the other side the anchor as support. The soil support can be free or entirely or partly fixed in practice. Anchored combi-wall structures can be applied for retaining heights up to about 20 metres (Rotterdam ((De Gijt, 2010)).

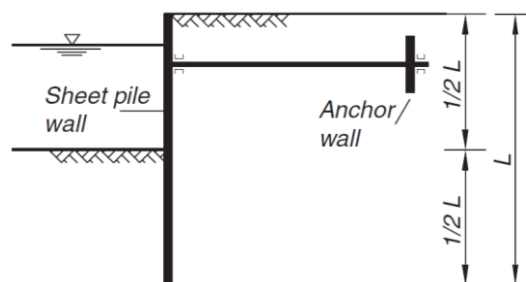


Figure 2.2 – Principle of an anchored sheet pile structure (Stichting CURNET, 2014)

An example of an anchored combi-wall (with MV piles and vibro piles) is constructed in 1992 in the Amazonehaven, Rotterdam and is illustrated in figure 2.3.

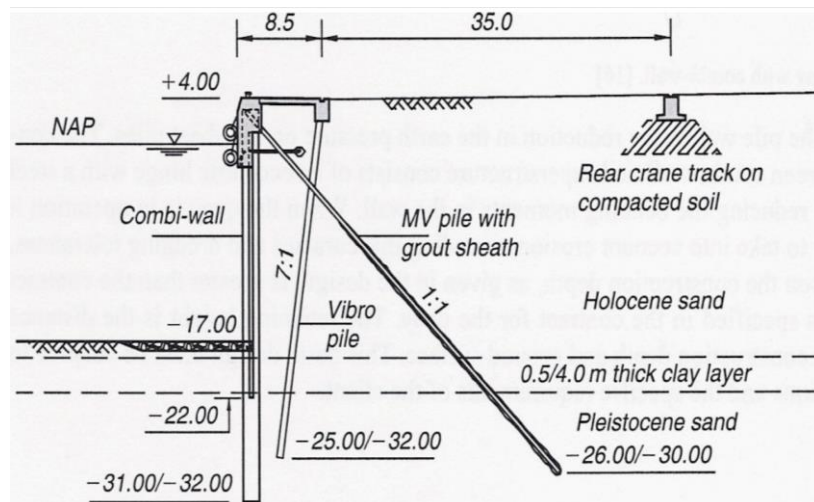


Figure 2.3 – Anchored combi-wall in the Amazonehaven, Rotterdam (De Gijt, 2010)

### 2.1.1.2 Gravity structures

Gravity structures are more complex than sheet pile structures, which obtain stability by the self-weight of the structure. The self-weight of the structure has to be large enough to develop sufficient shear resistance in the soil. Gravity structures are mainly used when the subsoil is not penetrable by or a sheet pile structure, because it consists of rock or very firm sand and when the subsoil has sufficient bearing capacity. From the different gravity types of quay walls reviewed below, only the L-wall and caisson wall are used (little) in the Netherlands and can be relevant for this study. The block wall is also reviewed in order to complete the different gravity type of structures.

Gravity structures often consist of prefabricated elements, and these structures all have shallow foundations, so the bearing capacity of the subsoil is critical. Prefabricated gravity structures can be attractive for the construction of long quays because the high one-off construction costs can be divided over a large number of elements. The most critical failure mechanisms for these types of quay walls are horizontal sliding, overturning or structural failure of the quay wall (De Gijt, 2004). The different types are listed below:

- **Block wall:** This type of gravity structure consists of concrete or natural stone blocks piled on top of each other. Because of the massive weight of the block wall, this type of structure is only possible for subsoil that provides sufficient bearing capacity. Block walls require much building material, and their retaining heights are up to about 20 metres in practice. The principle of a block wall is shown in figure 2.4.

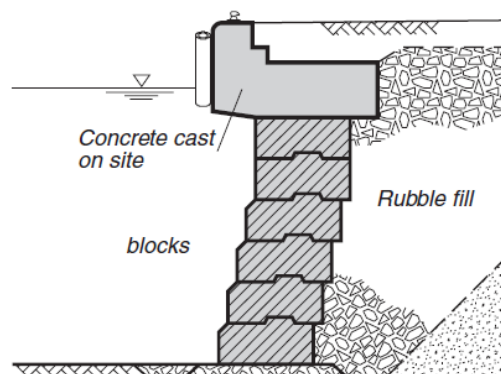


Figure 2.4 – Principle of a block wall (Stichting CURNET, 2014)

An example of a block wall, constructed on top of rubble full in Rijeka, Croatia is depicted in figure 2.5.

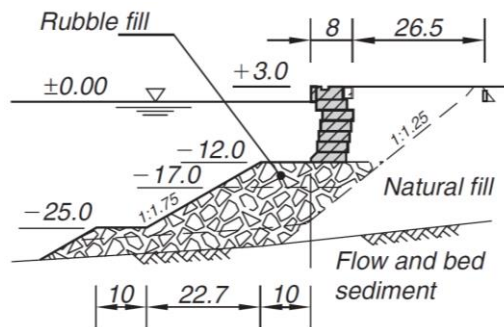


Figure 2.5 – Block wall in Rijeka, Croatia (Stichting CURNET, 2014)

- L-wall:** The L-wall uses their self-weight of the structure, plus the weight of the soil on top of it in order to be stable. Due to this weight, the shear stresses in the subsoil are built up, providing a turning moment in the opposite direction of the moment due to the soil pressure. L-walls can be constructed in a dry building pit (Antwerp, (De Gijt, 2004)) or from the water side (Helsinki, (Boskalis, 2012)). Construction from the water side is possible when the L-walls are prefabricated. The principle of an L-wall is shown in figure 2.6.

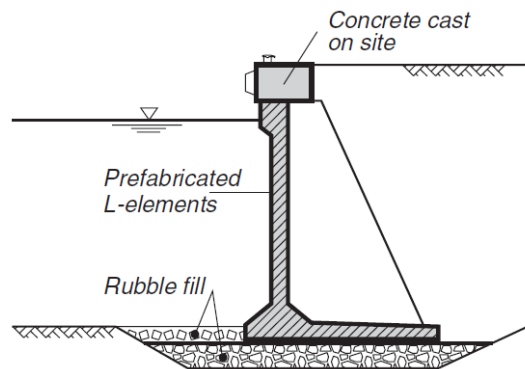


Figure 2.6 – Principle of an L-wall (Stichting CURNET, 2014)

An example of an L-wall, constructed for a container dock in Antwerp, Belgium is depicted in figure 2.7. It is questionable if a dry building pit as used in this case in Antwerp is possible in the Netherlands as well.

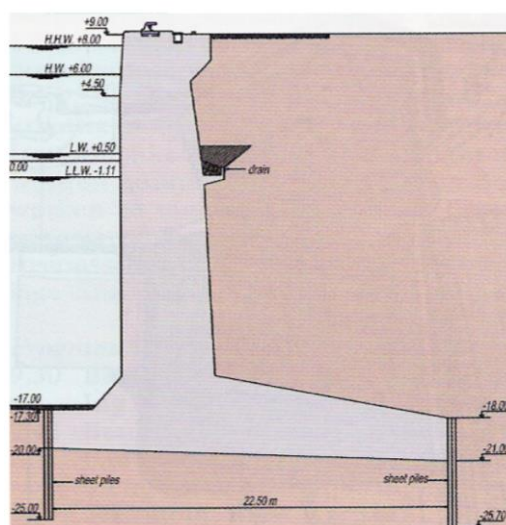


Figure 2.7 – L-wall in Antwerp, Belgium (De Gijt, 2004)

- Caisson wall:** Caissons are large hollow cellular concrete elements, constructed in a construction dock, on a floating pontoon or a Synchro-lift. Thereafter, the caissons are floated to the site and then immersed side by side, thus forming a quay wall. After placing the caissons

can be filled with soil or other material to increase the self-weight, which provides stability. This type of quay wall is economical in material use, but labour is extensive. Caissons are mostly used for major port projects with long quay walls. The principle of a caisson wall is depicted in figure 2.8.

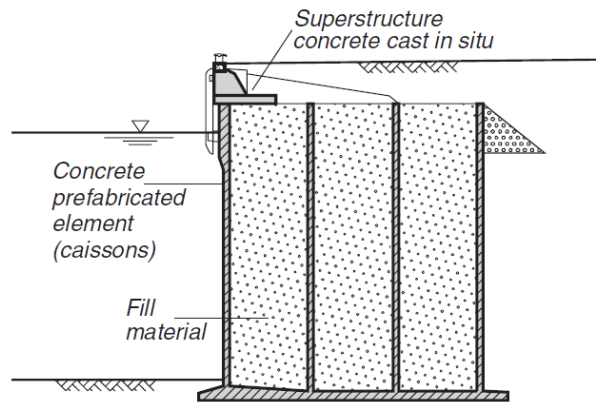


Figure 2.8 – Principle of a caisson wall (Stichting CURNET, 2014)

An example of a caisson wall constructed for the port of Dammam in Saudi Arabia is illustrated in figure 2.9. Here the rear crane track was founded on piles, in general also a shallow foundation is applicable.

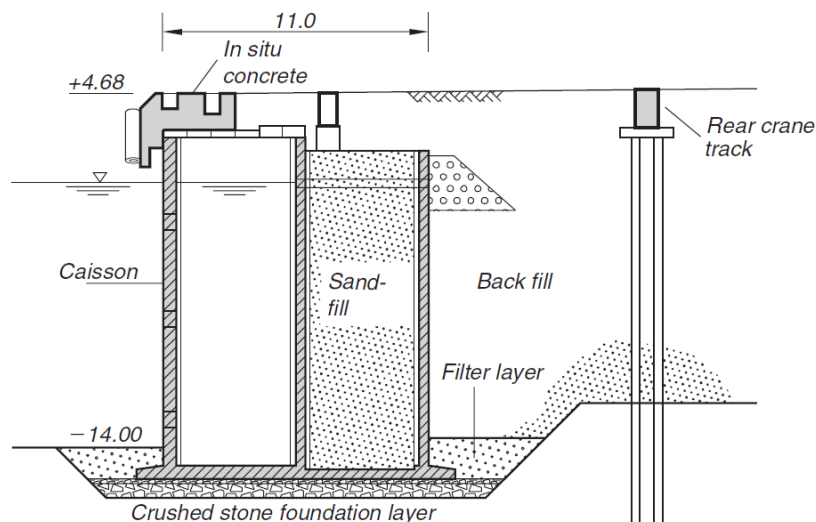


Figure 2.9 – Caisson wall in Dammam, Saudi Arabia (Stichting CURNET, 2014)

- Cellular wall:** Cellular walls consists of vertical web profiles, which are driven straight into the soil. The profiles are forming (partially) cylindrical cells, because they are linked to each other. The cylindrical cells are constructed and filled with sand or other material, resting on the bottom of the port or very little below this level. Relatively little material and limited earthworks is required for this type of quay wall, but the walls are vulnerable to damage when collisions occur. The principle of a cellular wall is shown in figure 2.10.

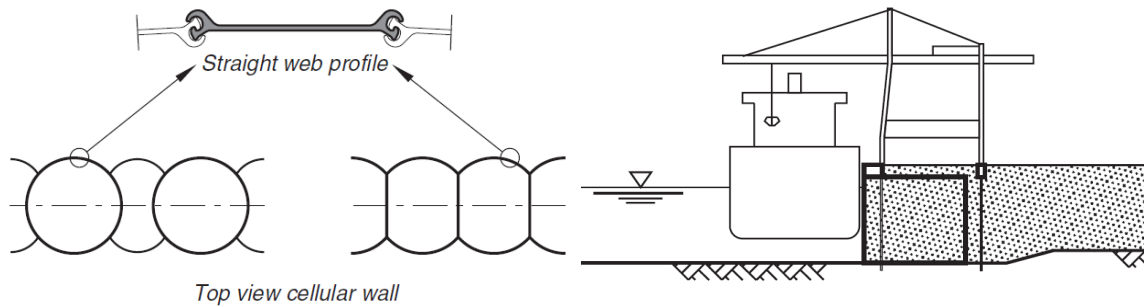


Figure 2.10 – Principle of a cellular wall (Stichting CURNET, 2014)

An example of a cellular wall, constructed as a container quay in Zeebrugge, Belgium is depicted in figure 2.11.

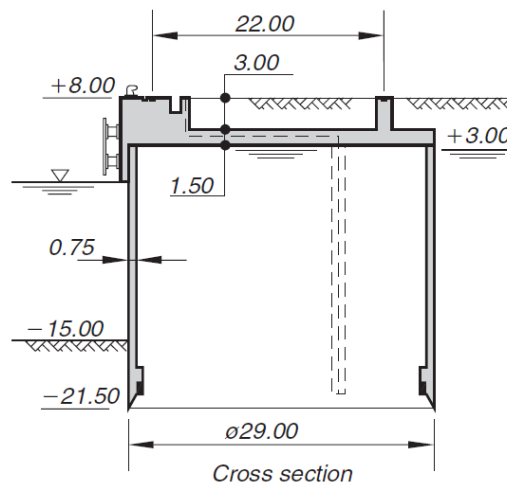


Figure 2.11 – Cellular wall in Zeebrugge, Belgium (Stichting CURNET, 2014)

### 2.1.1.3 Sheet pile structures with a relieving platform

It is also possible to use a complex structure including a relieving platform in combination with a sheet pile structure. Because the relieving platform itself is founded, the horizontal soil pressures on the sheet pile wall are considerably reduced. In this structure, the sheet pile structure is both bearing and soil retaining and the relieving platform is founded with tension and bearing piles. This structure is mainly used for high retaining heights, heavy loads on the site or when high demands in relation to allowable deformations are present. Sheet pile structures with a relieving platform can be applied for retaining heights up to 25 metres or even more (Rotterdam ((Stichting CURNET, 2014))). These types of quay walls are commonly used in the Netherlands and are interesting for this research.

The relieving platform can be installed at various heights, which are distinguished here.

- High relieving platform:** Usually prefabricated concrete elements are used often for the relieving platform. A pile system resists the horizontal soil pressure with tension and bearing piles underneath the superstructure. The high relieving platform usually lies above low water level so that it can be constructed over a slope at low tide. This relieving platform is relatively light and consists of a heavy front wall with moderate bearing pile loads. Construction costs and reliability of quay can depend strongly on these elements. The sheet pile structure can be performed as a combi-wall or diaphragm wall, and the principle of a sheet pile structure with a high relieving platform is shown in figure 2.12. In this figure a slope is present underneath the relieving platform, reducing the horizontal soil pressures and wave reflection. The combi-wall is inclined, which can be necessary constructing a quay wall from land. An important advantage of this inclination is that the combi-wall system now acts as a bearing foundation member and contributes to the stability of the quay wall. Besides this, the inclined combi-wall creates space for the bearing piles as well. However, due to this inclination, the active and passive earth

pressures reduce. The passive earth pressure reduces more than the active earth pressure, thus reducing the stability of the quay wall.

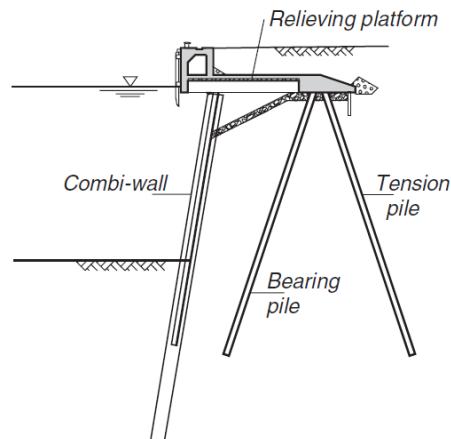


Figure 2.12 – Principle of a sheet pile structure with a high relieving platform (Stichting CURNET, 2014)

An example of a sheet pile structure with a high relieving platform is constructed for the Euromax terminal in the Port of Rotterdam and is depicted in figure 2.13.

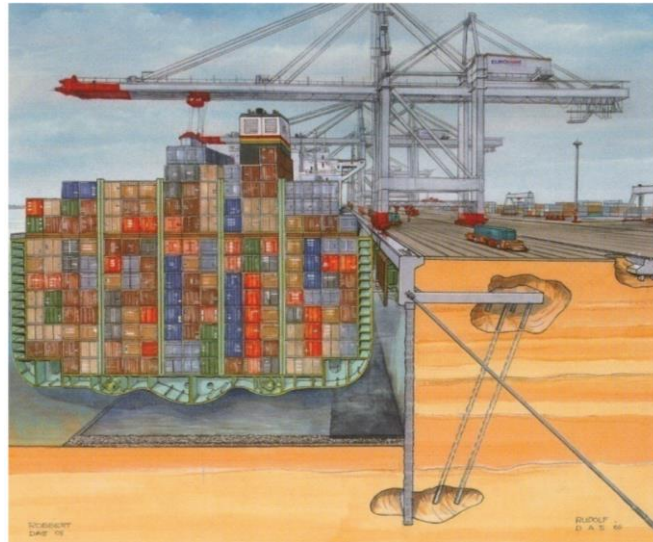


Figure 2.13 – Sheet pile structure with a high relieving platform in the Port of Rotterdam (De Gijt, 2010)

- Low relieving platform:** For high retaining heights a sheet pile structure with a low relieving platform can be used, reducing pile-driving problems. The platform is supported by the retaining and bearing sheet pile structure and one or two rows of prefabricated bearing piles and a row of tension piles. In contrast to the quay wall with a high relieving platform, this platform is relatively heavy, with a light front wall and high bearing pile loads. The principle of a sheet pile structure with a low relieving platform is depicted in figure 2.14.

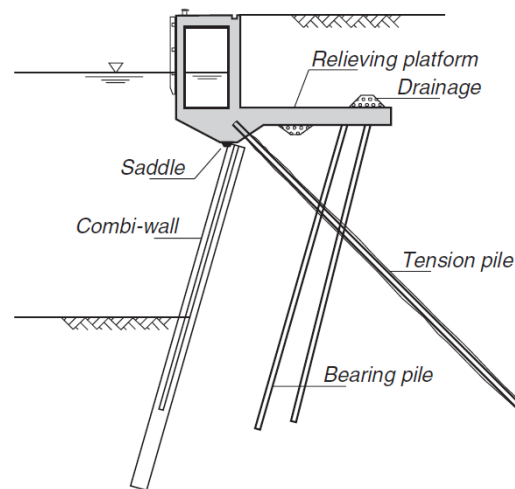


Figure 2.14 – Principle of a sheet pile structure with a deep relieving platform (Stichting CURNET, 2014)

An example of a sheet pile structure with a low relieving platform is constructed at the Maasvlakte in the Port of Rotterdam, the Netherlands and is shown in figure 2.15.

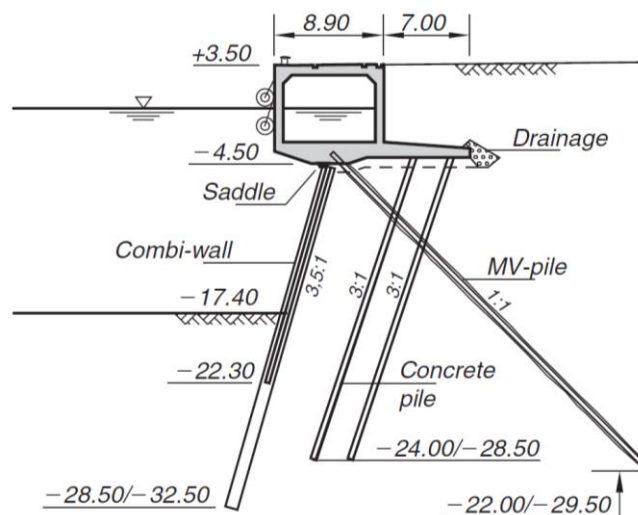


Figure 2.15 – Sheet pile structure with a deep relieving platform in Rotterdam, The Netherlands (Stichting CURNET, 2014)

### 2.1.2 Quay walls in the Netherlands

The most frequently applied types of quay walls in the Netherlands are:

- cantilever sheet pile structure;
- anchored sheet pile structure;
- sheet pile structure with a relieving platform.

Various types of materials, such as wood, steel, concrete and synthetic can be used for the sheet pile structure systems, depending on the retaining height. The quay walls with a relieving platform are often used for greater retaining heights (Stichting CURNET, 2014). Steel is the most applied material in quay structures, which is commonly used for sheet piles or combi-walls. Sheet pile walls also can be performed using wood or synthetic, but this is rather exceptional. Concrete is used for diaphragm walls, cell walls or caissons.

From an engineering point of view, a quay wall design with a relieving platform is more favourable than an anchored sheet pile structure without a relieving platform. This is because this type mostly has smaller displacements and a higher capacity to redistribute loads in case of anchor failure and the design needs smaller elements during construction. From an economic point of view, an anchored sheet pile structure without relieving platform seems to be more favourable (Lopez Gumucio, 2013). This

conclusion has to be checked because some cost aspects were not considered during the cost estimation performed by Lopez Gumucio (2013).

### 2.1.3 Technical failure of quay walls

Technical failure of a structure occurs if one or more of the primary functions of this structure can no longer be fulfilled. For quay walls the following primary functions are distinguished:

- retaining of soil;
- bearing of loads;
- protecting against erosion and groundwater flow.

The failure, or collapse, of a structure can be caused by a loss of overall stability or excessive deformations. When excessive deformations of a quay wall have occurred, it is possible that the structure is not damaged and still includes some residual capacity. An overview of the failure mechanisms can be given in a fault tree, in which they can be linked together as well. In a fault tree, the undesirable events that may lead to failure are given together with their mutual relationships. The failure of the system with the maximum allowable failure probability is placed on top of the fault tree. For each of the failure mechanisms a probability of failure expressed in a reliability index,  $\beta$ , is allocated, which together correspond to the maximum allowable failure probability of the system. Economically, low target probabilities of failure should be allocated to failure mechanisms for which the safety can be improved with relatively little costs, and large target probabilities of failure should be allocated to failure mechanisms for which the costs of achieving a higher margin of safety are relatively high (Wolters, 2012).

The most critical failure mechanisms for a cantilever or anchored sheet pile wall are:

- sheet pile profile fails;
- passive resistance inadequate;
- lack of equilibrium;
- tension member (anchorage) fails.

These failure mechanisms are depicted in figure 2.16 from left to right.

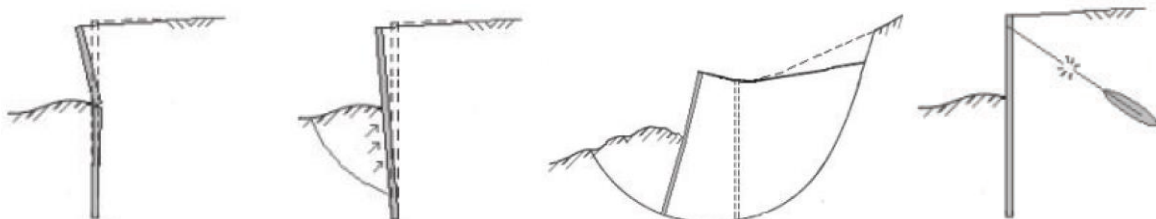


Figure 2.16 – Failure mechanisms cantilever and anchored sheet pile wall (Stichting CURNET, 2014)

For each quay structure, failure trees can be constructed. These are graphical representations of all failure mechanisms. The advantage of this concept is that failure probability can be shown per mechanism. Failure scenarios can be analysed and for each possible scenario a failure probability can be defined. For this end, AND gates and OR gates are defined according to Boolean logic. AND gates yield the value “true” if all of the underlying options are correct. In an AND gate the probabilities of underlying mechanisms are multiplied/added. Besides that, OR gates yield the value “true” if one of the underlying options is correct. In an OR gate the maximum probability of the underlying mechanisms is applied.

As an example, in the first edition of the CUR 211, published in 2003, a fault tree for a sheet pile quay wall and a fault tree of a quay wall with a relieving platform is given and depicted in figure 2.18 and figure 2.19. The top failure mechanisms of this structure are overloading of the quay walls (loss of overall stability) or excessive deformation of the quay wall. In the second edition of the CUR 211, published in 2012, the same fault trees are given, however without the reliability indices per failure mechanism. The events are connected with an AND- or OR-gate, depending on the relationship between the input and output events. In the example, the events are working as a series system with

OR-gates, which means that one of the failure events cause failure of the entire structure. Therefore, the target probability of failure of the failure mechanisms often has a strong dependency. The probability of failure of a system with n components can be calculated with the help of the equations from figure 2.17.

$P_{f,system}$  (with n components):

system	gate	operator	components		
			mutually exclusive	independent	fully dependent
series	 OR	$\cup$	$\sum_{i=1}^n P_i$ (upper bound)	$1 - \prod_{i=1}^n (1 - P_i)$	$\max\{P_i\}$ (lower bound)
parallel	 AND	$\cap$	0 (lower bound)	$\prod_{i=1}^n P_i$	$\min\{P_i\}$ (upper bound)

Figure 2.17 – System failure probability for various OR- and AND-gates (Jonkman et al., 2017)

In the example fault tree for a quay wall with a relieving platform the loss of overall stability of the quay wall is divided into the following failure mechanisms:

- Sheet pile wall fails
- Loss of stability
- Groundwater flow too high
- Superstructure fails
- Bearing pile fails
- Tension member fails

The reliability indices of the failure mechanisms ‘loss of stability’ and ‘groundwater flow too high’ are by far the highest of these five events. This means that the reliability of these failure mechanisms is the highest and the target probability of occurrence of these failure mechanisms are the lowest. The failure mechanisms ‘bearing pile fails’ and, ‘tension member fails’ have a moderate reliability index with a moderate probability of occurrence. Furthermore, the mechanism ‘superstructure fails’ has a lower reliability with a considerable probability of occurrence. The failure mechanism ‘sheet pile wall fails’ contains the lowest target reliability, corresponding to the highest probability of occurrence. Much of attention must be focused on these last failure mechanisms (Stichting CURNET, 2014).

The fault tree for sheet pile structures is introduced in the report ‘veiligheid van damwandconstructies’ (Calle & Spienburg, 1991). In this study, the target reliabilities are allocated for each of the failure mechanisms by expert judgement, which distinguishes between two different reliability levels for each of the failure mechanisms. After that, the fault tree was evaluated and adapted to quay walls in a study of Huijzer (1996). In addition, the distribution of target reliabilities over the failure mechanisms is reviewed in this study. He also concluded that the failure mechanism ‘yielding of the sheet pile’ is the critical failure mechanism, so this one was used to derive the partial factors. In a more detailed study performed by De Grave (2002) these results were validated and he recommended to execute this research more accurately.

Wolters (2012) has evaluated the reliability of the failure mechanisms; ‘profile anchor/tension member fails’, ‘sheet pile profile fails’, ‘soil mechanical failure’ and ‘excessive deformations’. ‘Soil mechanical failure’ can be caused by several failure mechanisms, such as; ‘passive resistance inadequate’, ‘Krantz stability inadequate’ or ‘Bishop stability inadequate’. He concluded that the soil mechanical failure mechanism was most critical. However, these failure mechanisms together includes the highest target reliability. The target reliabilities can be optimised by allocating lower target reliability to the soil mechanical failure mechanism and to increase to target reliabilities of the other mechanisms (Wolters, 2012). Allocating target reliability from the soil mechanical failure to the other reliable failure mechanisms can save investments intended to prevent soil mechanical failure. It is possible that the distribution of the reliability indices per failure mechanism for quay walls can be further optimised.

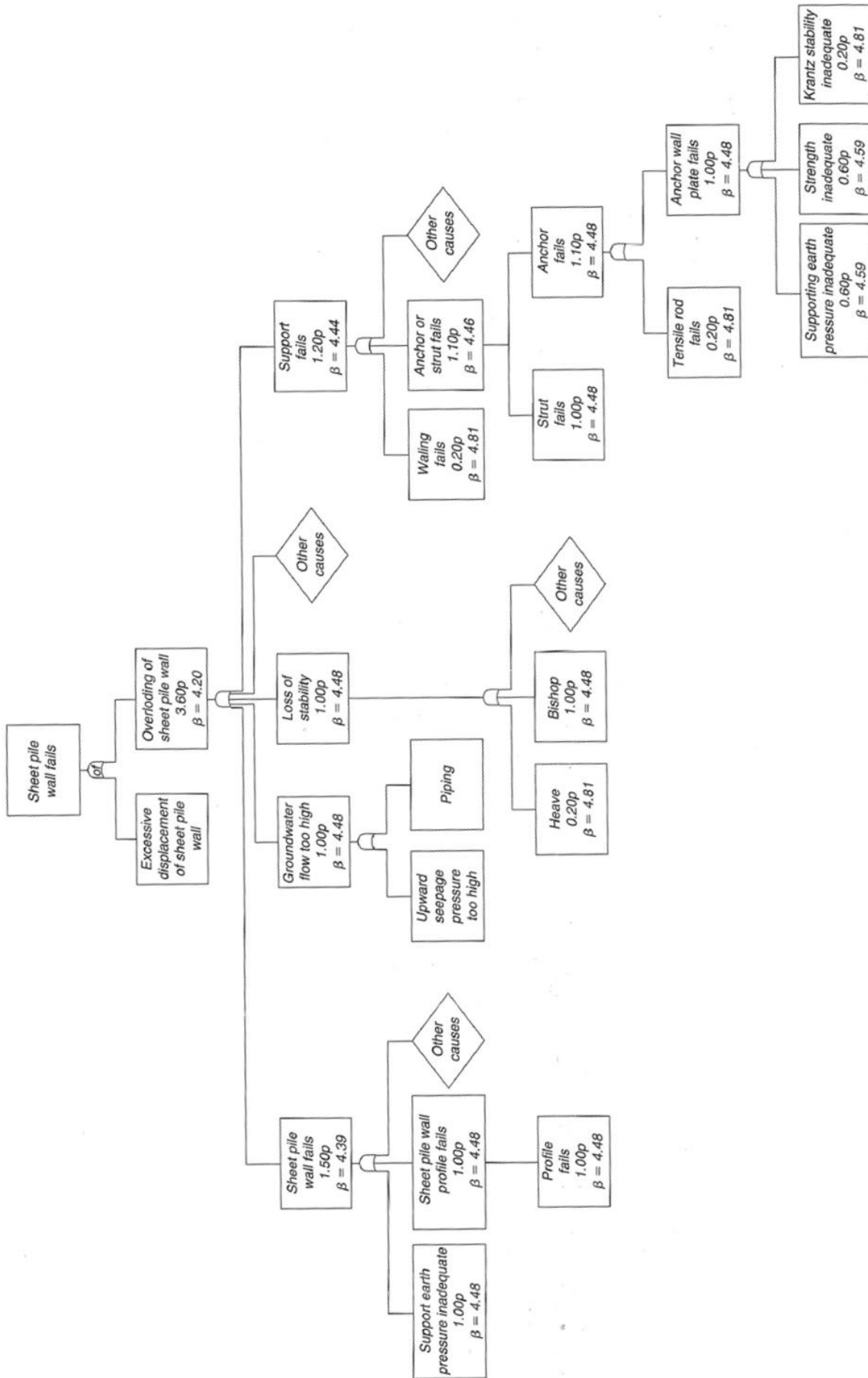


Figure 2.18 – Example of a fault tree for a sheet pile quay wall (CUR, 2005)



## 2.2 Reliability of structures

In this subchapter the general reliability concept of structures is explained, whereby the most frequently used reliability methods are described in detail. Furthermore, the probability of failure and the reliability index, the economic optimum and the limit states are discussed. The reliability theory in this subchapter is generally obtained from the lecture notes of the course Probabilistic Design, written by Jonkman et al. (2017). Besides that, other sources, such as research by Ragi Manoj (2016), is used when the theory or equations are described very clear herein.

The design process of a structure is based on the safety concept. Reliability is the measure of safety of the structure, and this can be assessed by comparing two stochastic quantities: the resistance (R) and the load (or solicitation: S) of the structure. In essence, the resistance of the structure must be larger than the load, in order to obtain a reliable structure:

$$R > S$$

The resistance and load effects are variables that can deviate from their expected values. The loads acting on a structure are varying, both in space and in time and the strength of the applied material is different from element to element. In designing a structure, the probability that a load exceeds a resistance must be smaller than the level defined in the code. This probability is also called the probability of failure of a structure.

### 2.2.1 Probability of failure & reliability index

The probability of failure of a structure is the probability that a load exceeds the resistance. With the help of the probability density functions of resistance and load parameters, the failure probability can be calculated. These functions describe the probability that discrete variables, such as R and S, may take particular values. The failure probability can be calculated as the probability that S is larger than R:

$$P_f = P[S > R]$$

The combination of R and S can also be formulated as a limit state Z, which is a condition beyond which the structure does no longer fulfil its requirements:

$$Z = R - S = g(x)$$

Failure occurs when  $R < S$ , so when  $Z < 0$  or  $g(x) < 0$ . This is depicted in figure 2.20.

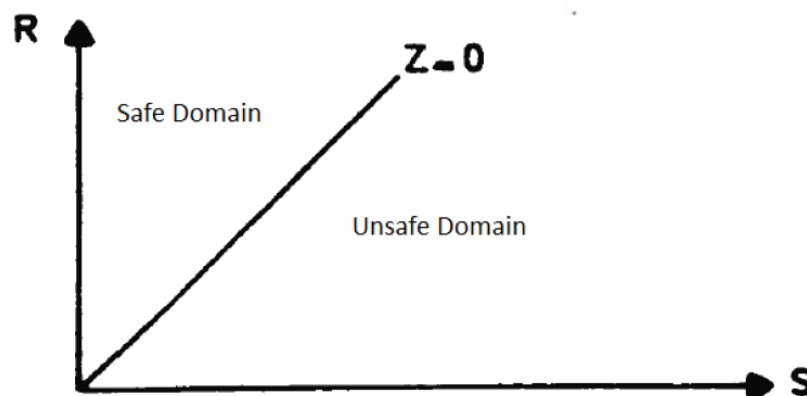


Figure 2.20 – Safe and unsafe domain in case of a linear limit state equation (Jonkman et al., 2017)

The probability of failure is:

$$P_f = P[Z < 0] = P[S > R]$$

An example of the joint probability density function of R and S is shown in figure 2.21. The probability of failure is the integration of the joint probability function over the failure region. So, in this figure, the marked domain represents the unsafe domain and the probability of failure.

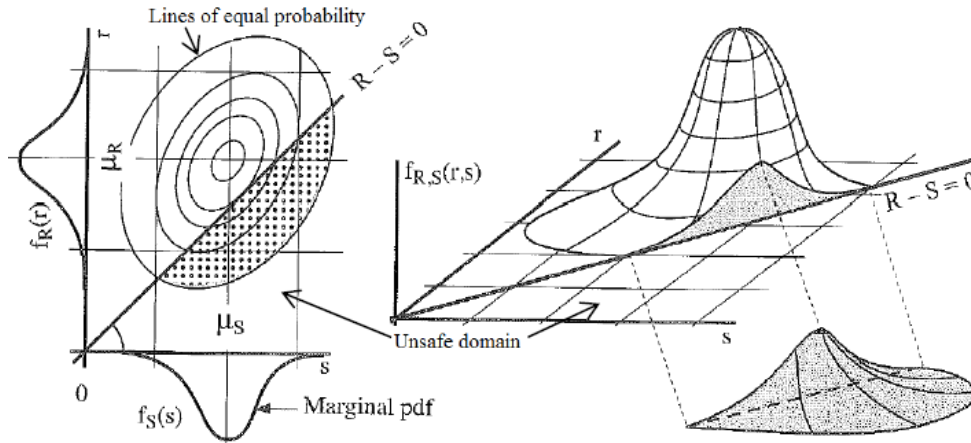


Figure 2.21 – Probability density functions R and S (Jonkman et al., 2017)

The reliability index  $\beta$  is defined as a measure of safety, which is directly related to the failure probability  $P_f$ :

$$P_f = \Phi(-\beta)$$

In which  $\Phi$  is a cumulative normal distribution. The relationship between  $\beta$  and  $P_f$  is listed in table 2.1 and illustrated in figure 2.22. The reliability index is used in codes and guidelines as a measure of safety of a structure. With this level of safety, the partial factors can be determined.

Table 2.1 – Relationship between the probability of failure  $P_f$  and reliability index  $\beta$  (Jonkman et al., 2017)

$P_f$	$10^{-1}$	$10^{-2}$	$10^{-3}$	$10^{-4}$	$10^{-5}$	$10^{-6}$	$10^{-7}$
$\beta$	1.28	2.32	3.09	3.72	4.27	4.75	5.20

In codes and design guidelines, target values for the reliability index are defined, among others,  $\beta$  depends on the reference period ( $t_{ref}$ ) of the structure. The reference period corresponds to the design lifetime of the structure. The following relationship can be used to convert  $\beta$ -values corresponding to different reference periods:

$$\Phi(\beta_n) = [\Phi(\beta_1)]^n$$

in which  $\beta_n$  is the reliability index for  $t_{ref} = n$  years, and  $\beta_1$  is the reliability index for a design life of  $t_{ref} = 1$  year. This relationship can be rewritten as follows:

$$\Phi(\beta_n) = P_{s,n}$$

$$P_{f,n} = 1 - P_{s,n} = 1 - P_{s,1}^n = 1 - (1 - P_{f,1})^n$$

in which  $P_{s,n}$  is the probability of survival over the lifetime  $t_{ref} = n$  years. However, this equation is valid only if reliability problems are largely time-variant. This means that the relation should be used carefully when the dominant stochastic variables of quay walls are time-independent (Roubos et al., 2018). The above relationship is shown in figure 2.22. This figure can be used to convert from the reliability index to the failure probability and the other way around.

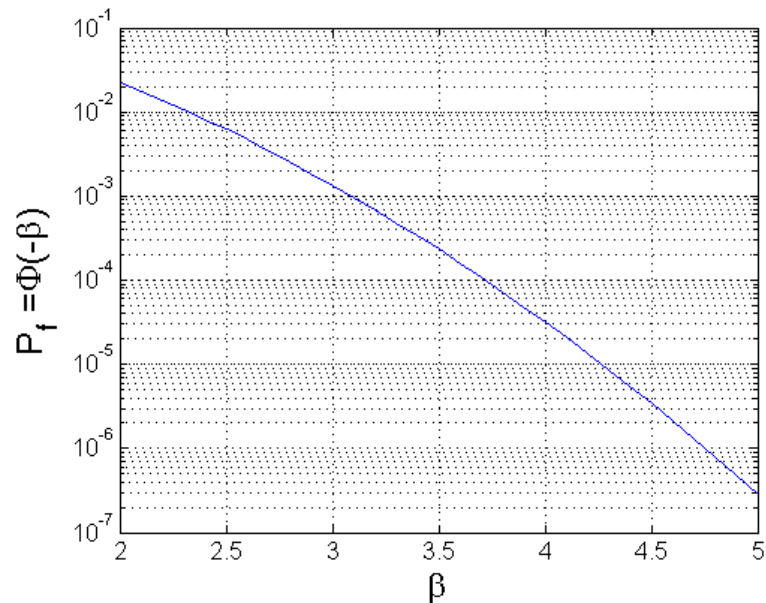


Figure 2.22 – Probability of failure  $P_f$  against reliability index  $\beta$  (Jonkman et al., 2017)

$P_f$  can be calculated analytically in case of a one-dimensional problem with a simple probability density function. However, in practice mostly the limit state is influenced by multiple variables, making it difficult or even impossible to determine the failure probability exact. Therefore, several reliability methods are available for reliability analysis.

### 2.2.2 Reliability methods

There are several ways of determining the reliability of a structure, using one of the reliability methods. Generally, these methods can be divided into the following five groups:

- **Level 0 method:** Level 0 methods are deterministic methods using deterministic values of the design parameters of a structure. Hereby the load is directly compared with the resistance of the design.
- **Level I method:** Level I methods are semi-probabilistic based, in which partial factors are used for modelling the uncertain parameters. The methods are semi-probabilistic based because partial factors are determined by level II calculations.
- **Level II method:** Level II methods are approximating the probability of failure of designs by modelling the uncertain parameters using the mean values, standard deviations and correlation coefficients. The probability of failure is based on the design point of the limit state function, where failure is most probable.
- **Level III method:** Level III methods are using analytical formulations, numerical integration or Monte Carlo simulations by which the probability of failure of the design can be determined. In this method the probability of failure is calculated exactly, that is why this method is time-consuming.
- **Level IV method:** Level IV methods are risk-based because in these methods the risk is used as a measure of the reliability of a design. The risk is determined by multiplying the probabilities and consequences of failure. Eventually, these risks, costs and benefits of the designs are monetarised and compared in order to find the economical optimal design.

The reliability of a structure used to be based on a deterministic reliability method in the past, in which a margin between the characteristic values of resistance and loads was implemented. At present, the European standards are based on a semi-probabilistic method (level I method). However, generally the codes give the designer freedom to use level II to level IV methods.

In the following several levels I and II methods are treated, because in this study level III methods are avoided, because of their calculation time.

2.2.2.1 Level I: Semi-probabilistic reliability method

The semi-probabilistic reliability method is a practical method in which complex probabilistic analyses are avoided. These probabilistic analyses have been carried out already on the limit states of the structure and have yielded a set of partial factors. The principle of this reliability method is that for each limit state the design value of the loads,  $S_d$ , must be compared with the design value of the resistance,  $R_d$ , of (part of) the structure.

$$R_d > S_d$$

The design values are obtained by dividing the (in general lower) characteristic values of the resistance by a partial factor,  $\gamma_R$ , and the particular characteristic values of the loads are multiplied by a partial factor,  $\gamma_S$ .

$$R_d = \frac{R_k}{\gamma_R}$$

$$S_d = \gamma_S S_k$$

Characteristic values of loads and resistance which are normally distributed can be generally calculated with:

$$R_k = \mu_R + k_R \sigma_R$$

$$S_k = \mu_S + k_S \sigma_S$$

In which  $k_R$  will be negative and  $k_S$  can be positive or negative, depending on the load is favourable or unfavourable. For material properties often  $R_k$  is defined as that value that has a probability of non-exceedance of 5% and in that case  $k_R = -1.64$ . Partial factors are depending on the dispersion of the parameter and influence of the parameter on failure of the structure.

This concept is shown graphically in figure 2.23, in which the probability density functions with the variations in load (red) and resistance (green) are shown. The design load and resistance have to be chosen in such a way that the structure has a sufficiently low probability of failure. The probability of failure is proportional to the overlapping area of the two curves. Codes and guidelines provide information on the partial factors  $\gamma$ 's and how to use these.

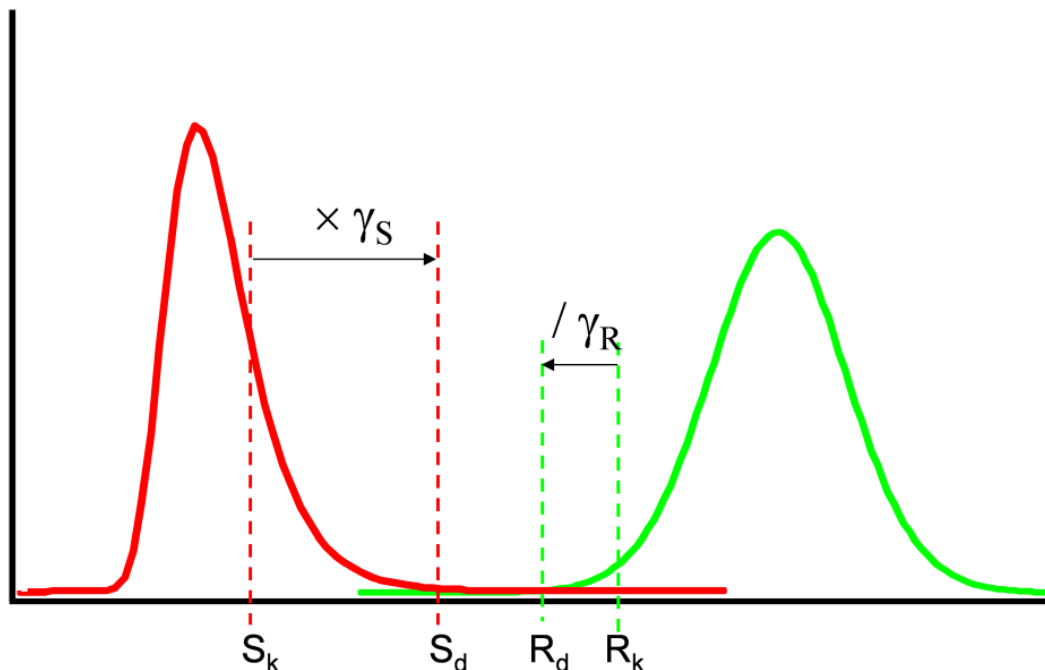


Figure 2.23 – Probability density functions of the load (red) and resistance (green) (Jonkman et al., 2017)

### 2.2.2.1.1 Derivation of partial factors

The partial factors are either determined using deterministic methods or using probabilistic calculations. These methods to determine the partial factors are depicted in figure 2.24. The deterministic methods include historical methods and empirical methods, in which experience based partial factors are calibrated with representative structures.

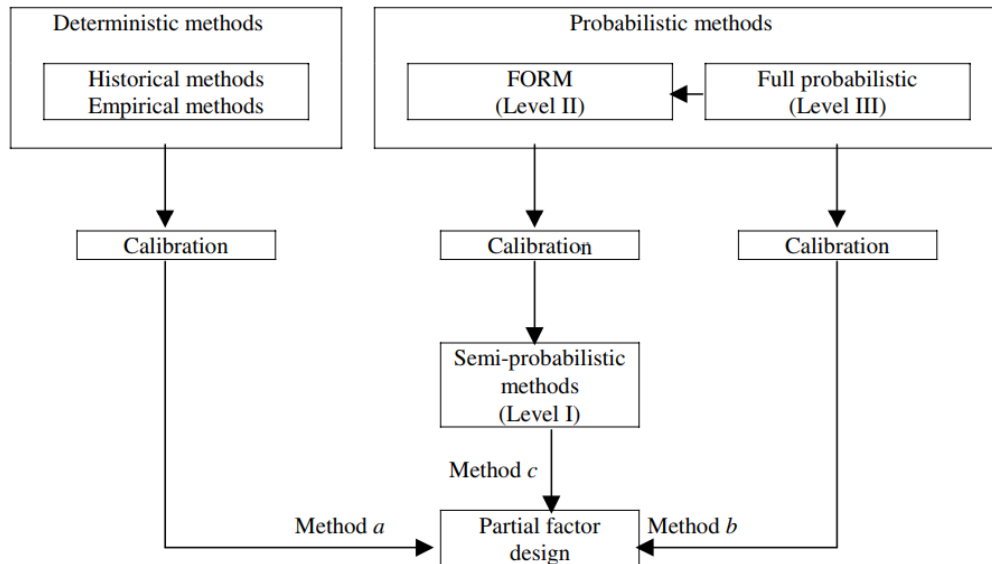


Figure 2.24 – Methods to determine partial factors (The Netherlands Standardisation Institute, 2002)

Using probabilistic calculations, partial factors are derived by the point in the failure space with the greatest joint probability density of the resistance and the load. This point is also called the design point and can be determined using level II calculations. It is therefore plausible that when failure occurs, the values of the resistance and load are close to the values for the design point. In these calculations also the influence of every variable of the design is determined. With normally distributed variables these points are:

$$r^* = \mu_R - \alpha_R \beta \sigma_R = \mu_R (1 - \alpha_R \beta V_R)$$

$$s^* = \mu_S + \alpha_S \beta \sigma_S = \mu_S (1 + \alpha_S \beta V_S)$$

Following in the equation for a partial resistance factor:

$$\gamma_{R,d} = \frac{R_k}{r^*} = \frac{\mu_R (1 + k_R V_R)}{\mu_R (1 - \alpha_R \beta V_R)} = \frac{1 + k_R V_R}{1 - \alpha_R \beta V_R}$$

In the same way, the partial factor for a load parameter can be determined:

$$\gamma_{S,d} = \frac{s^*}{S_k} = \frac{\mu_S (1 + \alpha_S \beta V_S)}{\mu_S (1 + k_S V_S)} = \frac{1 + \alpha_S \beta V_S}{1 + k_S V_S}$$

The partial factors are prescribed slightly conservative, in order to guarantee that the target reliability index is reached minimally for all the different intended structures. When the structure is considerably different from the calibrated structure, the values of the partial factors can be doubtful.

### 2.2.2.2 Level II: First Order Reliability Method

The First Order Reliability Method (FORM) is a level II method to determine the failure probability of the limit state function. FORM is considered as a good alternative of level III methods because it requires less mathematical computations, but generally gains accurate results. FORM uses the introduced limit state function:

$$Z = R - S = g(X) = g(X_1, X_2, \dots, X_n)$$

in which  $X_1, X_2, \dots, X_n$  represents the stochastic variables. The stochastic parameters can be loads, strength and geometric parameters for example. Hasofer and Lind introduced in 1974 two approaches to derive the reliability index for linear and non-linear limit state functions, which are still commonly applied in structural reliability analyses.

### Linear limit state functions

For linear limit state functions the expected value and standard deviation of this function can be determined using the following equations:

$$Z = a_1X_1 + a_2X_2 + \dots + a_nX_n + b$$

$$\mu_Z = a_1\mu_{X_1} + a_2\mu_{X_2} + \dots + a_n\mu_{X_n} + b$$

$$\sigma_Z = \sqrt{\sum_{i=1}^n \sum_{j=1}^n a_i a_j \text{Cov}(X_i, X_j)}$$

$$g'_i = \frac{dZ}{dX_i} = a_i$$

$$\mu(X) = E(X)$$

$$\sigma^2(X) = E[\{Y - \mu(Y)\}^2]$$

$$\text{Cov}(X, Y) = E[(X - E(X))(Y - E(Y))]$$

Furthermore, the mean and standard deviation of the limit state function has to be normalised according to:

$$U_i = \frac{X_i - \mu_i}{\sigma_i}$$

For normalised stochastic variables  $U_i$  it holds that  $\mu_U=0$  and  $\sigma_U=1$ . If both R and S are assumed as normally distributed random variables, Z can be considered as a normally distributed random variable as well. The probability of failure can then be defined as:

$$P_f = P(Z < 0) = \Phi\left[\frac{0 - \mu_Z}{\sigma_Z}\right] = \Phi\left[\frac{0 - (\mu_R - \mu_S)}{\sqrt{\sigma_R^2 + \sigma_S^2}}\right] = \Phi[-\beta]$$

This probability of failure is obtained in the design point, which is: 'the shortest distance from the origin to the surface described by  $g(U)=Z(U)=0$  in the space of the normalised variables'. It is the point with the highest probability density, so failure is most probably in this point. This is depicted in figure 2.25.

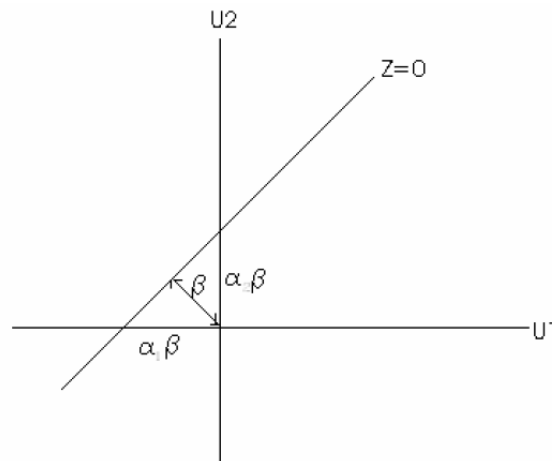


Figure 2.25 – Design point and reliability index (Wolters, 2012)

Each of the stochastic variables has a certain influence on the reliability index, expressed in an influence coefficient. With a linear limit state function, the influence coefficients are given by:

$$\alpha_i = \frac{-a_i \sigma_{xi}}{\sigma_Z}$$

### Nonlinear limit state function

In case of a non-linear limit state function, the function can be approximated using a Taylor series expansion around the mean:

$$g(X) = Z \cong g(\mu_1, \dots, \mu_n) + \sum_{i=1}^n \frac{\partial g(\mu_i)}{\partial X_i} (X_i - \mu_i)$$

The mean value and standard deviation of the limit state function can be approximated as follows:

$$\mu_Z \cong g(\mu_1, \dots, \mu_n)$$

$$\sigma_Z \cong \sqrt{\sum_{i=1}^n \sum_{j=1}^n \frac{\partial g(\mu)}{\partial X_i} \frac{\partial g(\mu)}{\partial X_j} Cov(X_i, X_j)}$$

However, linearisation in different points leads to different values for the approximation of the reliability index. This problem can be overcome by executing the linearisation in the design point. In figure 2.26 two examples of linearisation of the limit state function is depicted. In the left-hand figure, the limit state function is linearised in the mean value and in the right-hand figure in the design point. From the figure follows that the linearisation of the limit state function in the design point gives a much better approximation of the failure probability.

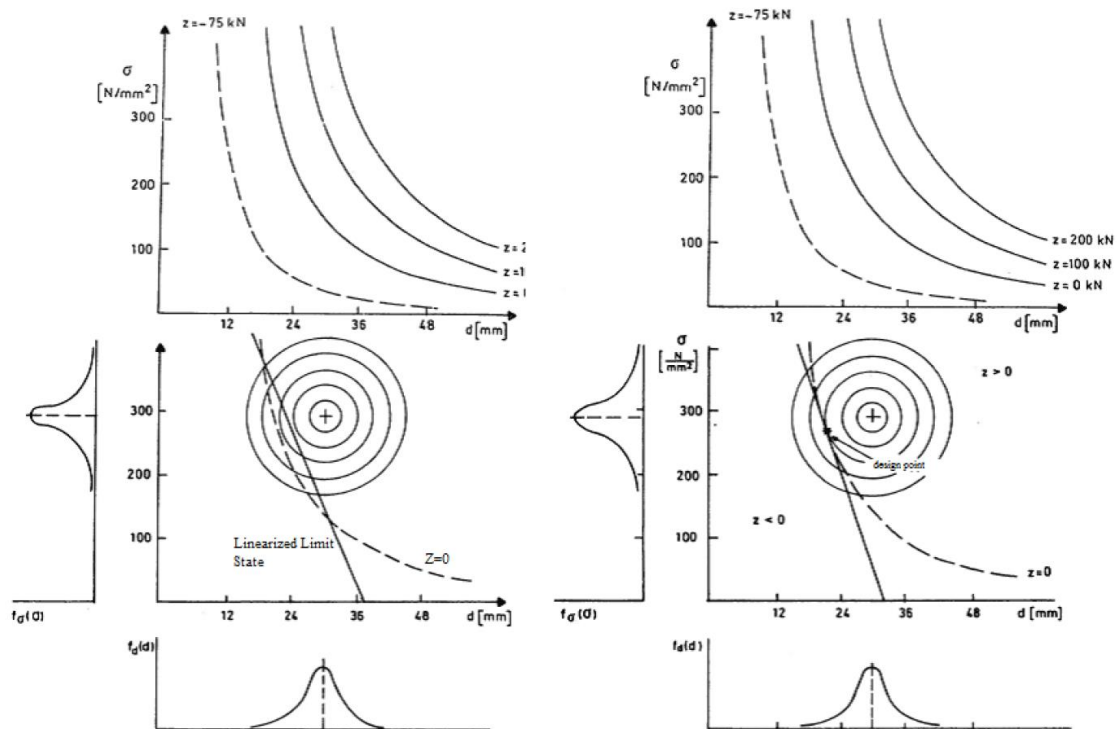


Figure 2.26 – Examples of linearisation of the probability density function (Jonkman et al., 2017)

The reliability index is still defined the same and can be calculated as follows:

$$\beta = \min_{Z=0} \left( \sqrt{U_1^2 + U_2^2} \right)$$

The design point can be found using an iterative process. The design point is first guessed to be the mean value for instance and the obtained  $\beta$ -value is used to determine a new point, in which the limit state function is linearised. In this case, the influence coefficients can be calculated as follows:

$$\alpha_i = \frac{\frac{\partial}{\partial X_i} g(X^*) \sigma_{xi}}{\sqrt{\sum_{j=1}^n (\frac{\partial}{\partial X_j} g(X^*) \sigma_{xj})^2}}$$

$$X_i^* = \mu_i - \alpha_i \beta \sigma_{xi}$$

Once the design point is found after some iterations, also the reliability index can be found.

### 2.2.3 Economic optimum

One way to determine the required reliability index for a system that is yet to be designed is to use the estimated economic optimum. An economic optimisation considers the investment cost of increasing the reliability level and the reduction of risk, expressed in monetary terms. The risk is defined as the product of the potential failure damage and the corresponding failure probability. With these estimations of the reliability for several distinct cases, the graphs of the relationship between investment costs and reliability and between risks and reliability can be drawn, as shown in figure 2.27. In cases where no continuous functions are available, one can consider a limited number of design options and determine the investments, risks and total costs for these options. With these values, the most economically favourable option can be obtained.

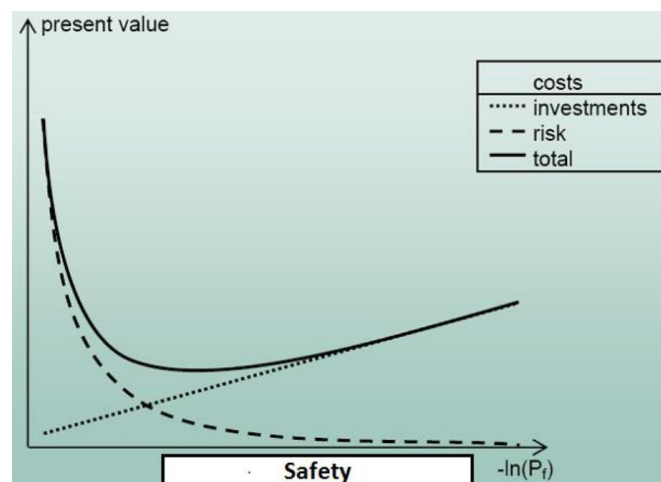


Figure 2.27 – Economic optimum reliability level (Jonkman et al., 2017)

In recent research by Roubos et al. (2018) the target reliability indices for quay walls were derived from various risk acceptance criteria, such as economic optimisation, individual risk, societal risk, the life quality index and the social and environmental repercussion index. The annual and lifetime target reliability indices for failure modes of commercial quay walls found were lower than the target reliabilities defined in the Eurocodes. For the purpose of the economic optimisation, a first estimation of the marginal safety investments for quay walls was determined. The findings included that the marginal safety investments for quay wall are quite low. Thorough research is required in order to determine the marginal safety investments for quay walls.

### 2.2.4 Limit states

The requirements for the design are formulated in the limit states, which are conditions beyond which the structure does no longer fulfil its requirements. When a (part of a) structure no longer fulfils one or more desired objectives, this is known as failure. So, the limit state, or the state of failure, is reached when the state of the structure changes from normal operation and this can be reached through different failure mechanisms. For each of the requirements of the structure, one or more limit states can be formulated. In practice, two types of limit states are distinguished, namely the serviceability limit state (SLS) and the ultimate limit state (ULS).

SLS refers to the requirements with respect to the functionality of a quay wall. The verification of SLS is related to deformations, vibrations and damages, which can be reversible or irreversible. The deformations, vibrations and damages can influence the visual aspects, the comfort of users and the functionality of the structure.

ULS focuses on the safety of persons and/or structural safety or the protection of the content of a quay wall. In this state the ultimate bearing capacity of the structure is defined, exceeding this state failure or collapse of the structure occurs.

## 2.3 Design guidelines

In this subchapter the most frequently used different design guidelines in the Netherlands: NEN 9997-1, CUR 166, CUR 211 are treated and compared. The design guidelines have a lot of differences, such as safety approach, calculation method or partial factors. The differences in reliability classes, design approach and partial factors of the design guidelines are discussed below. First, the standards and rules defined in the Eurocodes are treated, where after the specifications of each of the design guidelines are discussed.

Quay walls can be designed using different design guidelines, with their own design rules. These guidelines are all based on the European standards of the Eurocodes, which are introduced in order to standardise all the existing different design guidelines. The Eurocodes cover the general design standards, with some room for specific differences. Different international institutes have developed their design guidelines which all consider different design methods. There are various codes and guidelines currently applied to design quay walls, amongst other the following are mentioned, which are used in The Netherlands (Stichting CURNET, 2014):

- NEN 9997-1: Eurocode for geotechnical design;
- CUR 166: Manual for sheet pile structures;
- CUR 211: Manual for quay walls;
- BS 6349: British Standard for Maritime Works;
- EAU 2012: German Recommendations of the committee for Waterfront structures, Harbours and Waterways.

The German and British guidelines are already specially developed for maritime infrastructure. This standard includes their own, well-substantiated approach regarding the reliability validation and not only uses the classification as described in the Eurocode. Combining the methods and approaches of these, but possibly also from other international standards and guidelines could lead to a more suitable, generally accepted classification (Smit, 2016). The BS 6349 and EAU 2012 and a comparison of these five design guidelines are treated in Appendix A-3.

### 2.3.1 Eurocodes

The structural design standards for building structures in Europe are harmonised in a number of codes EN 1990:1999. Each Member State of Europe can add a National Annex (NA) in which specific parameters can be stipulated within the degree of freedom indicated in the code. The National Annex cannot change or modify the content of the Eurocode text in any way. Otherwise, the design will not be called 'design according to the Eurocodes' (Schuppener, 2007). The set of Eurocodes together with the Dutch Annexes are called the NEN-EN-standards (Eurocode), and the following are available:

- Eurocode 0 NEN-EN 1990 Basis of Structural Design
- Eurocode 1 NEN-EN 1991 Actions on structures
- Eurocode 2 NEN-EN 1992 Design of concrete structures
- Eurocode 3 NEN-EN 1993 Design of steel structures
- Eurocode 4 NEN-EN 1994 Design of composite steel and concrete structures
- Eurocode 5 NEN-EN 1995 Design of timber structures
- Eurocode 6 NEN-EN 1996 Design of masonry structures
- Eurocode 7 NEN-EN 1997 Geotechnical design
- Eurocode 8 NEN-EN 1998 Design of structures for earthquake resistance
- Eurocode 9 NEN-EN 1999 Design of aluminium structures

The NEN-EN 1990 describes the principles and requirements for safety, serviceability and durability of structures which forms the basis for structural design. NEN-EN 1997-1 considers the design aspects of retaining structures, such as quay walls. During the past years, different amendments and Dutch Annexes are made of this code. In order to increase the usability of these codes, in the Dutch standard NEN 9997-1 a collection of these is prepared for structural geotechnical calculations (The Netherlands Standardisation Institute, 2017). However, the CUR 166 and CUR 211 are more detailed concerning quay wall design. For instance, partial factors are derived for different types of quay walls in the CUR 166 and CUR 211.

### 2.3.1.1 Ultimate limit state

In the ULS the following can be considered according to the Eurocodes, if relevant (The Netherlands Standardisation Institute, 2017):

- Equilibrium (EQU): failure of the structure itself or a part of it, considered as a rigid body, where the soil strength is irrelevant;
- Structural (STR): internal failure of the structure, exceptional deformations of the structure or structural elements including shallow and pile foundations, where the strength of the building materials of the structure is leading;
- Geotechnical (GEO): failure or exceptional deformations of the subsoil at which the strength of the soil is leading for the resistance to be provided;
- Fatigue (FAT): deals with the failure of the structure or structural elements because of fatigue;
- Uplift (UPL): failure of the structure or subsoil, because of upward forces by water pressure or other vertical loads;
- Hydraulic soil failure (HYD): failure of the structure because of internal erosion by concentrated groundwater flow (piping) in the subsoil because of hydraulic gradients.

All the different limit states can be relevant for quay structures, depending on the type of quay wall. For the two most frequently applied types of quay walls (anchored sheet pile structure and sheet pile structure with a relieving platform), the limit states STR, GEO and HYD are most important limit states.

### 2.3.1.2 Reliability classes

In the Eurocodes three reliability classes (RC), or consequence classes (CC) are defined based on the potential consequences of failure. For each reliability class, a level of safety is defined, which depends on a maximum allowable probability of failure, or margin of safety, of the structure. An overview of the different reliability classes is given in table 2.2. Depending on the type of structure and the decisions made during the design and calculation, specific structural elements may be classified in another reliability class than the one that applies to the entire structure.

Table 2.2 – Consequence classes according to the Eurocodes (The Netherlands Standardisation Institute, 2002)

CC	Description		Examples
	Consequences with respect to loss of human lives	Economic, social and environmental consequences	
CC3	High	Very large	Tribunes, public buildings with high consequences of failure (concert hall, ...)
CC2	Moderate	Considerable	Home and office buildings, public buildings with moderate consequences of failure (offices, ...)
CC1	Low	Small or negligible	Agricultural building where people do not normally enter (depositories, greenhouses, ...)

The three reliability classes RC1, RC2 and RC3 correspond to the three consequence classes CC1, CC2 and CC3, respectively. For each of the reliability classes, a target value for  $\beta$  is defined. In table 2.3 the recommended minimum values for  $\beta$  in ULS are given.

Table 2.3 – Recommended minimum values for  $\beta$  in ULS (The Netherlands Standardisation Institute, 2002)

Reliability class	$t_{ref} = 1$ year	$t_{ref} = 50$ years
RC3	5.2	4.3
RC2	4.7	3.8
RC1	4.2	3.3

This reliability classification is originally developed for the design of bridges and buildings and is often considered as not appropriate. Research has shown that the terminology and reference figures of the classification contain a certain subjectivity. Possible future development of a specific standard for maritime infrastructure can influence the acceptance of a new reliability classification (Smit, 2016).

### 2.3.1.3 Design approaches for the limit states STR and GEO

In the Eurocodes are for the structural (STR) and geotechnical (GEO) ULS three different design approaches introduced. The approaches differ in the way the partial factors are distributed over the loads and load effects (A), soil properties (M) and resistances (R). These differences are partly caused by the way the approaches are dealing with uncertainties in the modelling of the load effects and resistances (The Netherlands Standardisation Institute, 2017). National Annexes specify the selected design approach and lay down the values of the partial factors.

Below, the essence of the design approaches 1 to 3 will be reviewed.

#### 2.3.1.3.1 Design approach 1

In design approach 1 there are two checks required for two different combinations of partial factors. When it is clear that one of these combinations is normative for the design, no calculation needs to be performed for the other combination. In combination 1 the partial factors are applied to the load(s) (effects), so this combination aims to provide safety against unfavourable deviations of the loads. Combination 2 contains partial factors (mostly) applied to the soil parameters, so this combination aims to provide safety against uncertainties in the calculation model (Schuppener, 2007).

Non-axial loaded piles or anchors:

Combination 1: A1 + M1 + R1

Combination 2: A2 + M2 + R1

Axial loaded piles or anchors:

Combination 1: A1 + M1 + R1

Combination 2: A2 + (M1 or M2) + R4

in which “+” means: “in combination with”.

#### 2.3.1.3.2 Design approach 2

In design approaches 2 only one check is required for one particular combination of partial factors. The partial factors are applied to the load or the load effects and the resistance in design approach 2.

Combination: A1 + M1 + R2

#### 2.3.1.3.3 Design approach 3

In design approaches 3 a check is required for one particular combination of partial factors. The partial factors are applied to the load or the load effects and to the soil parameters in design approach 3. In this approach, structural and geotechnical loads need to be distinguished.

Combination: (A1\* or A2\*\*) + M2 + R3

\* for structural loads

\*\* for geotechnical loads

So, Eurocode 7 contains a number of possibilities for the national standards, such as three design approaches for the verification of geotechnical and structural ultimate limit states which influences the partial factors. On the one hand, this may be regarded as a shortcoming for the code, but on the other hand, the code is adaptable, and the openness of the implementation can be attractive. In this way, a

gradual evolution of national design codes that co-existed in the pre-Eurocode era into the unified Eurocode approach was facilitated.

The possible design approaches with characteristics of the partial factors are given in table 2.4.

Table 2.4 – Design approaches with characteristics of the partial factors (Van Seters & Jansen, 2011)

Design Approach	Load/ Load effect A - Action	Material-Factor M- Material	Factor total Resistance R - Resistance
DA 1.1	> 1,0	= 1,0	= 1,0
DA 1.2	= 1,0 > 1,0 (q - last)	> 1,0	= 1,0
DA 2	> 1,0	= 1,0	> 1,0
DA 3	> 1,0	> 1,0	= 1,0

#### 2.3.1.4 Execution classes steel structures

In the NEN-EN 1090-2 several execution classes are defined, which specify a classified set of requirements for the execution of the general works as a whole or individual components (The Netherlands Standardisation Institute, 2018). These requirements are specified in order to ensure adequate levels of mechanical resistance and stability, serviceability and durability. Four execution classes 1 to 4, denoted EXC1 to EXC4, are given, for which requirement strictness increases from EXC1 to EXC3 with EXC4 being based on EXC3 with further project specific requirements. The requirements are related to constructor’s documentation, traceability, cutting, welding, etc. and further explained in the NEN-EN 1090-2. A shortlist of these requirements per execution class is given in annex A.3 in NEN-EN 1090-2.

The required execution class is determined according to table C.1 of NEN-EN 1993-1 - design of steel structures (The Netherlands Standardisation Institute, 2016), depicted in table 2.5. There are a few exceptions to this table, namely;

If EXC1 is determined for a structure, EXC2 must be applied for the following structural components:

- welded parts manufactured from steel products with a steel grade of S355 or higher;
- welded parts which are fundamental to the structural integrity and are assembled by welding on the construction site;
- welded parts of lattice girders which consist of round tube profiles for which a profiled adaptation at the end is required;
- parts which are thermoformed or heat-treated during manufacture.

Table 2.5 – Determination of the execution class (The Netherlands Standardisation Institute, 2016)

Reliability Class (RC) or Consequences Class (CC)	Type of loading	
	Static, quasi-static or seismic DCL <sup>a</sup>	Fatigue <sup>b</sup> or seismic DCM or DCH <sup>a</sup>
RC3 or CC3	EXC3 <sup>c</sup>	EXC3c
RC2 or CC2	EXC2	EXC3
RC1 or CC1	EXC1	EXC2

<sup>a</sup> Seismic ductility classes are defined in EN 1998-1: Low = DCL; Medium = DCM; High = DCH.  
<sup>b</sup> See EN 1993-1-9.  
<sup>c</sup> EXC4 may be specified for structures with extreme consequences of structural failure.

### 2.3.2 NEN 9997-1

NEN 9997-1 is the Dutch standard for the geotechnical design of structures. The general rules and parameters derived from the Eurocodes and the Dutch Annexes are collected in the NEN 9997-1, in order to increase the usability of these codes (The Netherlands Standardisation Institute, 2017).

#### 2.3.2.1 Reliability classes

In NEN 9997-1 the reliability indices from table 2.3 have been declared mandatory for all Dutch guidelines.

#### 2.3.2.2 Design approach

In line with NEN 9997-1, design approach 3 has to be applied for the geotechnical calculations. This means that the partial factors are applied to the load or the load effects and the soil parameters, with a distinction between structural and geotechnical loads (The Netherlands Standardisation Institute, 2017). A schematisation of design approach 3 for a quay wall is shown in figure 2.28. Here, for convenience, we also recall design approach 3: (A1\* or A2\*\*) + M2 + R3.

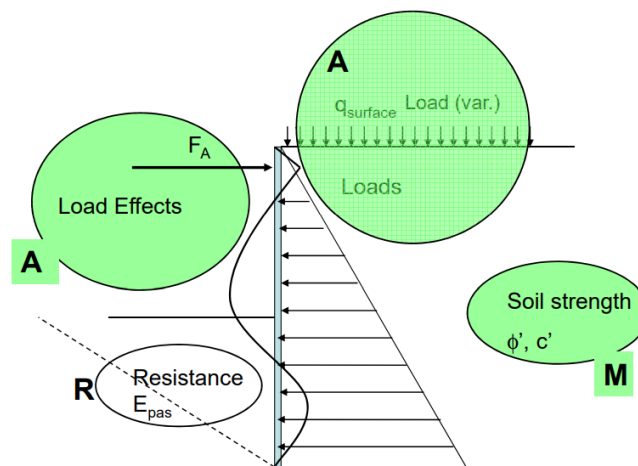


Figure 2.28 – Schematisation of principle of design approach 3 for a quay wall

### 2.3.3 CUR 166

The guideline CUR 166 provides a basis for the design and construction of sheet pile structures (Stichting CURNET, 2012a). It treats all types of sheet pile structures, especially the steel sheet pile wall. It contains a stepwise design guideline which can be used for the design of sheet pile walls, such as a building pit as well as for the design of a quay wall. Furthermore, a lot of information is given about driving piles and other construction works (Meijer, 2006).

The CUR 166 uses a stepwise design approach, expressed in phases. These main phases are shown in figure 2.29.

Phases in the design calculation:

Phase 1: Determine the leading starting points

Phase 2: Determine the characteristic values of the parameters

Phase 3: Determine the design values of the parameters

Phase 4: Choose calculation scheme A or B

Phase 5: Determine minimum embedding depth

Phase 6: Make a dimensioning calculation

Phase 7: Check the bending moment

Phase 8: Check the shear force and normal force

Phase 9: Check the anchorage forces

Phase 10: Check the deformations

Phase 11: Check the others mechanism, if applicable

Phase 11.1: Verify the resistance of the ground slice with the Kranz method

Phase 11.2: Verify the mechanism piping

Phase 11.3: Verify total stability

Phase 11.4: Verify the vertical bearing capacity

Phase 12: Determine the influence of building aspects on the design

Phase 13: Verify choice

Figure 2.29 – Main phases of the design calculation of sheet pile (quay) walls (Stichting CURNET, 2012a)

### 2.3.3.1 Reliability classes

The sixth edition of the CUR 166 matches with Eurocode 7, including the reliability classes with their reliability index.

The former editions of the CUR had defined their own CUR Classes as safety classes:

- CUR Class I: relatively simple structures, no individual safety risks, relatively small failure damage; for instance, a camp shedding;
- CUR Class II: considerable failure damage, small individual safety risks; for instance, a building pit, a sheet pile wall along an inland waterway and a quay wall of a seaport;
- CUR Class III: extensive failure damage and/or considerable individual safety risks; for instance, unique structures.

The reliability indices corresponding to these classes are given in table 2.6, and these are related to the current reliability classes of Eurocode 7. The difference between the  $\beta$ 's are small, therefore acceptable. In the figure also the safety classes, defined in the former standards NEN 6700 are given (Stichting CURNET, 2012b).

Table 2.6 – Overview of the ULS  $\beta$ -factors for a reference period of 50 years (Stichting CURNET, 2012b)

CUR-systeematiek		NEN 6700 (vervallen)		NEN-EN 1990	
klasse	$\beta$	klasse	$\beta$	klasse *)	$\beta$
I	2,5				
		1	3,2	RC1	3,3
II	3,4	2	3,4		
		3	3,6	RC2	3,8
III	4,2			RC3	4,3

\*) RC staat voor *Reliability Class*, die in één verband mag worden gezien met de *Consequence Class (CC)*

Some variation exists between the reliability classes of various guidelines. The former Dutch standards NEN 6700 defined three classes, from which class 1 and 2 correspond to RC1, and class 3 corresponds to RC3 from the Eurocode. The CUR classification also defined one extra lower class, relative to the other two classifications.

### 2.3.3.2 Design approach

According to Eurocode 7, design approach 3 have to be applied for the geotechnical calculations. The CUR 166 uses the same partial factors as Eurocode 7.

### 2.3.4 CUR 211

The CUR 211 is a Dutch manual concerning the design and construction of quay structures with a relieving platform. This design guideline is prepared because quay structures with a relieving platform differ so significantly from that of a simple sheet pile wall, so it demands specific approach (Stichting CURNET, 2014).

#### 2.3.4.1 Reliability classes

The CUR 211 defined the reliability index  $\beta$  and design life in years of the reliability classes RC1 to RC3 as the Eurocodes. However, the distinction between the reliability classes is different, and the description of the classes is more extensive. The reliability classes with their descriptions are illustrated in table 2.7. The prescribed risk of danger to life and economic damage for each of the reliability classes are different comparing with the Eurocode. Furthermore, quay walls with a retaining height until 5 m are classified in RC1 and quay walls with a retaining height more than 5 m in at least RC2. (Stichting CURNET, 2014).

Table 2.7 – Reliability classes according to CUR 211 (Stichting CURNET, 2014)

Description of reliability classes	Reliability index $\beta$	Design life in years	Example
RC 1/CC 1 Consequences of failure – Risk of danger to life negligible – Risk of economic damage low	$\beta = 3.3$	50	Simple sheet pile structure/quay wall for small barges. Retaining height till 5 m
RC 2/CC 2 Consequences of failure – Risk of danger to life negligible – Risk of economic damage high	$\beta = 3.8$	50	Conventional quay wall for barges and seagoing vessels. Retaining height > 5 m
RC 3/CC 3 Consequences of failure – Risk of danger to life high – Risk of economic damage high	$\beta = 4.3$	50	Quay wall in flood defence/ LNG-plant or nuclear plant (hazardous goods)

#### 2.3.4.2 Design approach

According to Eurocode 7, design approach 3 has to be applied for the geotechnical calculations. However, the CUR 211 defines somewhat different partial factors than CUR 166 and Eurocode 7. This guideline considers different safety design methods and safety approaches for two types of structures:

- Type A: relatively complex quay walls with a relieving platform;
- Type B: simple quay walls without relieving platforms.

The partial factors of the effective angle of internal friction ( $\phi$ ) and effective cohesion ( $c'$ ) for type A structures are different than for type B structures. Because of the complexity of type A structures, they should be designed using a finite element method, also following the design phases of figure 2.29. However, the partial factors for soil parameters of sheet walls are based on probabilistic analyses of type B structures. Additional probabilistic analyses revealed that the partial factors on soil parameters should be higher for type A structures than for type B structures.

## 2.4 Calculation methods

The European design guidelines allow the use of different design methods and calculation methods, defining loading conditions on the structural elements of hydraulic structures, such as quay walls. In the past various calculation methods for quay walls are developed, which are empirical, analytical or a combination of both. The most commonly used calculation methods are described in this subchapter, namely the Blum Method, the subgrade reaction method and the finite element method (FEM). The Blum method used to be generally applied in the Netherlands, but this method is a greatly simplified model of reality and is currently mainly used for checking purposes. The other two methods are generally accepted and commonly used nowadays as part of the design of quay walls (Stichting CURNET, 2012b).

### 2.4.1 Blum Method

The Blum Method is a calculation method, intended to be used for analytical (hand)calculations of a sheet pile wall as a first rough estimate. In this calculation method, the statically indeterminate beam and soil around is schematised as a statically determined system, because the sheet pile is modelled fixed in the ground. Hereby only the soil strength influences the system, in contrast to the deformation behaviour of the soil and the sheet pile stiffness. Furthermore, it is assumed that local displacement of the sheet pile wall will result in immediate yielding of the soil, instead of a gradual development of shear stress in the soil. Therefore, large soil deformations and maximum shear stresses in the soil can develop. So, this means that minimum soil stresses at the active side and maximum soil stresses at the passive side will occur. The assumption of this calculation method that no elastic deformation occurs is shown in figure 2.30, in which the simplification of the horizontal soil pressure is shown in red (Vrijling et al., 2015).

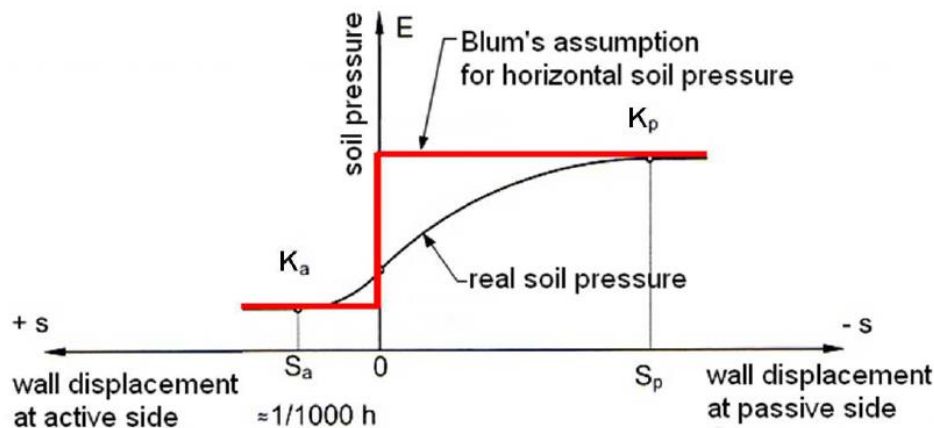


Figure 2.30 – Stress-strain diagram of soil according to the Blum Method (Vrijling et al., 2015)

Based on the determined load distribution, the required embedding depth and length and the type of sheet pile can be determined. The length of the wall should be long enough to provide balance in horizontal pressures, as well as a moment equilibrium to prevent turning over of the wall. The deflection of the sheet pile wall can be obtained from the moment line, but these displacements are not realistic. This method is not taking soil-structure interaction into account (Stichting CURNET, 2012b) since it just looks at equilibrium of the sheet pile itself.

### 2.4.2 Subgrade reaction method

The subgrade reaction method is based on the principle that the soil is schematised by a system of uncoupled springs in which by the term uncoupled is meant to express that fact that the springs, hence the soil layers, do not influence each other. Soil springs can be modelled elastically or elastoplastically. This means that nonlinear deformations of the soil only can develop according to the deformation of the soil retaining structure, instead of immediate yielding of the soil in the Blum Method. In between passive and active yielding of the soil, a linear transition of the soil pressure and displacement is applied, shown in figure 2.31. When the deformation of the structure is sufficient, minimum active soil pressures or maximum passive soil resistance occur. On the other hand, the soil pressure is neutral if there is no displacement of the structure. Furthermore, this calculation method uses the assumption of Bernoulli, namely that cross-sections of the beam (retaining structure) remain straight and perpendicular to the beam axis. Because the soil pressure depends on the deformation of the quay wall, the calculation follows an iterative process, and this process is completed when the results have converged.

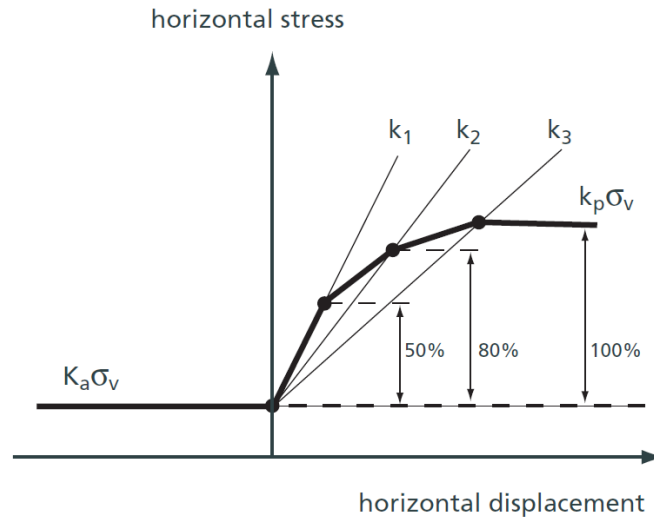


Figure 2.31 – Stress-strain diagram soil according to the subgrade reaction method (Deltares, 2017)

One of the consequences using this calculation method is, because the problem is statically indeterminate to a high degree, the number of variables is high. Therefore, computer software is needed to find a solution. Another consequence is that this method requires the bending stiffnesses of soil (Stichting CURNET, 2012b). Furthermore, in this calculation method soil deformations behind and in front of the quay wall are not considered.

There is many software available that offer this calculation method. In the Netherlands, a very commonly used software to use this calculation method is D-Sheet Piling, developed by Deltares. D-Sheet Piling is a tool used to design sheet pile walls, diaphragm walls and horizontally loaded piles. Different structural elements and loads can be added to the design model, such as anchors, struts, surcharges, forces and moments. Construction staging can be taken into account (Deltares, 2017).

### 2.4.3 Finite element method

Finite element method (FEM) is based on the spatial discretisation of the partial differential equation for equilibrium. The FEM introduces integration of the behaviour of the soil and the structure, in which the properties of soil are generally defined using non-linear stress-strain relations (Stichting CURNET, 2014).

The structure and the soil are divided into finite elements. Each of these elements is defined from:

- Interpolation of the displacement field between the nodes and determination of the strains in the elements by taking the derivative of the displacement field.
- Constitutive behaviour of the material in the elements (stress-strain behaviour = material model).
- Equilibrium in which the stresses in the elements are lumped into nodal forces.

By combining all finite elements into one system and solving it, the deformations in the model are found, as well as stresses, strains and state variables. The method can be used to investigate the distribution of soil stresses and strains, in which structural elements, such as sheet pile walls, anchor rods or anchor walls are included. Soil-structure interaction is possible to model with this method. Furthermore, this method can be used to compute specific sectional forces in structural elements and the global stability and deformations of a quay wall. It is possible to set up two- or three-dimensional finite element models, in order to for example investigate the distribution of soil pressures over the primary piles and intermediate sheet piles in a combined wall, part of a quay wall. Quay structures modelled by a FEM can not only be loaded by static loads but by dynamic loads as well.

Because of the large number of degrees of freedom, the system can only be solved with a finite element software on a computer (e.g. Plaxis or Diana). An example of the input of a two double anchored sheet pile wall in Plaxis is illustrated in figure 2.32.

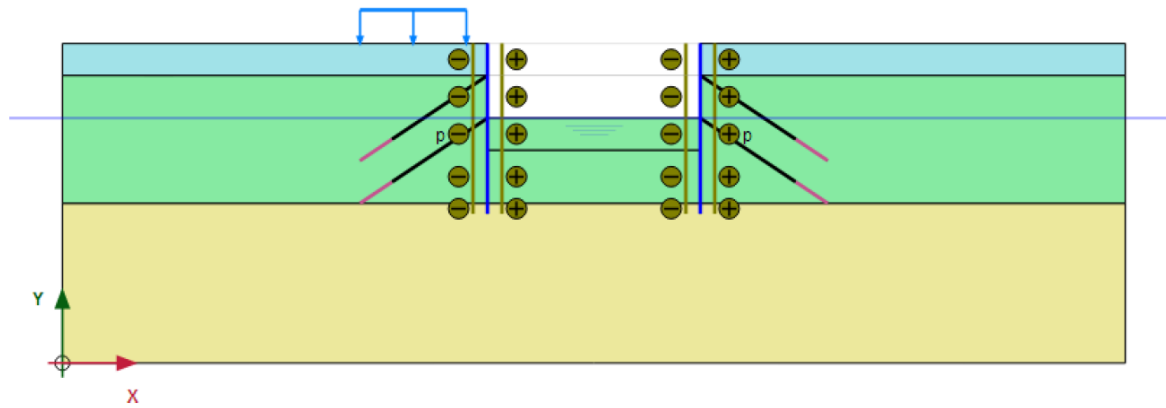


Figure 2.32 – Example of the input of two double anchored sheet pile wall in Plaxis (Plaxis bv, 2017)

The subgrade reaction method and FEM are compared, with the help of D-sheet and Plaxis, for quay wall designs with or without relieving platform in a recent study. It concluded that the type of calculation method could influence the results and design of quay walls. The calculated bending moments for both of the methods not differ much, as well as the calculated anchor force for quay walls without relieving platform. However, for quay wall design with a relieving platform, the differences in the calculated anchor forces can be more significant. Probably this difference is found because D-sheet determines the horizontal pressure on the wall with the help of simplified strip loads with an equation after Boussinesq (Lopez Gumucio, 2013).

## 2.5 Cost of quay walls

In this subchapter an overview is given of the different cost components of a structuring during the entire lifetime, the most important factors influencing the construction costs of a quay wall and the cost development of quay walls in time. Furthermore, cost estimation of projects is discussed.

Especially for decision makers and clients, the cost of quay walls is very important to evaluate the feasibility of a project or to determine the most economic, technical option. The cost of a structure during the entire lifetime can be distinguished into the following costs or investment components: planning, design and engineering costs, construction costs, maintenance costs and demolition costs. The planning, design, engineering and construction costs relate to the initial phase of the project. Maintenance costs are spread over the whole lifetime of the structure, and the demolition costs appear when the structure has to be removed.

The Port of Rotterdam indicated that the construction costs are leading and that the other types of costs vary evenly based on these. Based on experience the Port of Rotterdam developed a relationship between the construction costs and the other types of costs of quay walls and these are shown in table 2.8 (De Gijt & Vinks, 2011).

Table 2.8 – Relationship between the construction costs and the other types of costs of quay walls (De Gijt & Vinks, 2011)

Type of cost	Amount of construction costs [%]
Planning, design & engineering costs	4 – 8
Maintenance costs	0.5 – 1.5 (per year)
Demolition costs	15 – 20

Furthermore, the Port of Rotterdam indicated from experience that the construction costs of a quay wall are determined for 75% by the retaining height and 25% by other factors, as shown in figure 2.33.

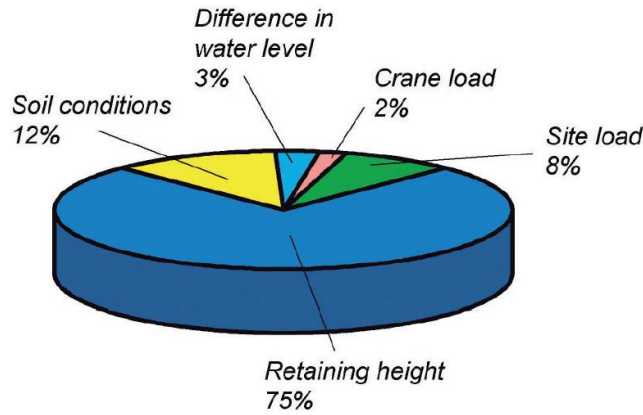


Figure 2.33 – Analysis of factors driving the construction costs of quay walls in Rotterdam (De Gijt, 2010)

The construction costs per running metre versus retaining height for various quay walls around the world are illustrated in figure 2.34 (De Gijt, 2010). The retaining height is defined as the difference between the design depth and the height of the ground surface behind the quay structure. As the figure shows, the retaining height and cost are strongly related. However, the bandwidth in which the cost of quay walls vary, is considerable because the construction costs of quay walls differ for different types of quay walls.

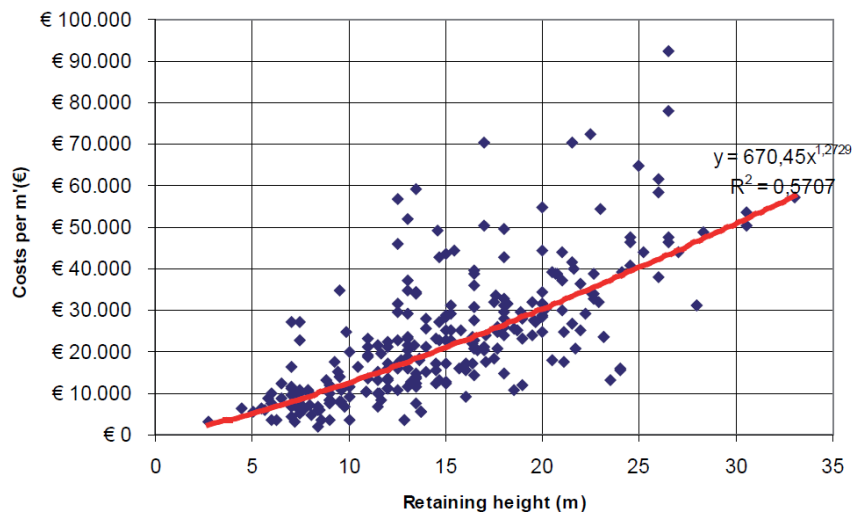


Figure 2.34 – Construction costs (2008 values) of quay walls worldwide as a function of the retaining height (De Gijt, 2010)

In the same research by De Gijt (2010) into the history of quay walls, also the construction costs of sheet piles and piled structures worldwide as a function of the retaining height is discussed and shown in figure 2.35. Piled structures can represent sheet pile structures with a relieving platform, for instance. The bandwidth in which the cost of these structures vary is smaller in figure 2.35 compared with figure 2.34 because figure 2.35 includes less types of quay walls. Figure 2.34 can be used in this study, to compare the construction costs of a double anchored combi-wall and a combi-wall with a relieving platform.

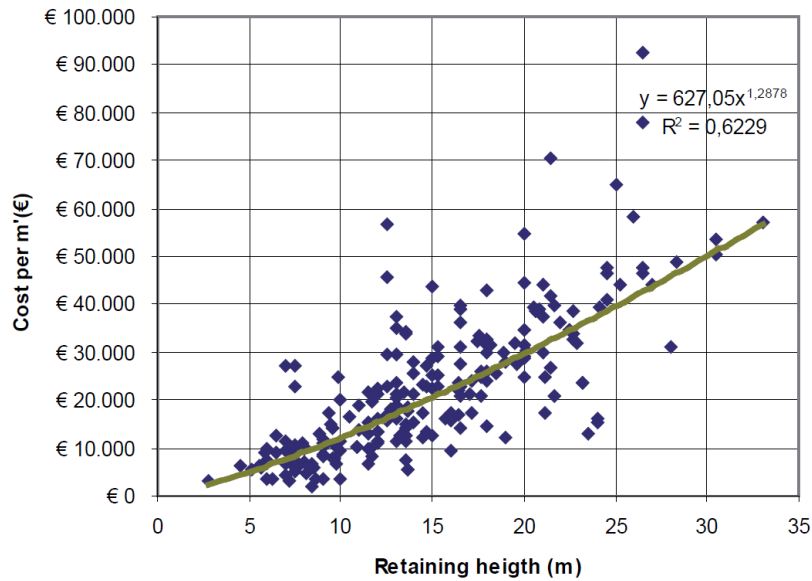


Figure 2.35 – Construction cost (2008 values) of sheet piles and piled structures worldwide as a function of the retaining height (De Gijt, 2010)

### 2.5.1 Indexing

Indexing of cost can be used to obtain a normalised average of price relatives for a given type of goods or services, during a given interval of time. Index numbers are used to present the price changes in time of these type of goods or services. This method is useful for cost specialists or researchers to compare different prices in time, originating from the past or future (De Gijt & Vinks, 2011). Dutch index values from the past can be obtained from various recourses, such as CBS, CPI/IBOI or BDB. For future costs, prognoses of the index values should be used (CROW, 2010). In this study, the CPI-values, determined by CBS (2019), are used by indexing the present construction costs of the considered quay walls to 2008 values to compare them with figure 2.35 from research by De Gijt (2010)

### 2.5.2 Cost estimation

Costs can be estimated for all different stages of the project. In feasibility studies, indices are used for a first rough estimation of the project costs. During the development of a project the uncertainty and so, the bandwidth of the cost estimation becomes smaller and smaller. When more details of the project are known, the costs can be estimated based on quantities, such as the use of equipment, production, formwork, etc. A distribution of construction costs for a combi-wall with a concrete relieving platform is depicted in figure 2.36 (Stichting CURNET, 2014).

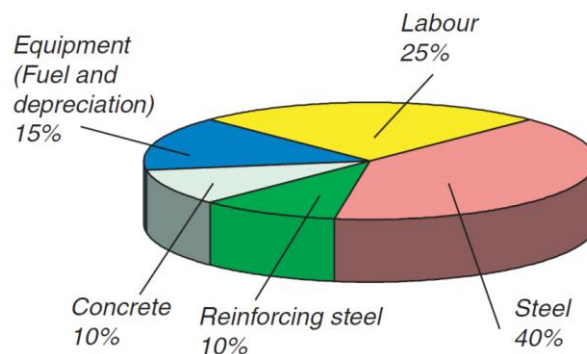


Figure 2.36 – Distribution of construction costs for combi-wall with a concrete relieving platform (Stichting CURNET, 2014)

CROW (2010) developed a cost estimate system for civil engineering projects named standard cost estimate system (standaardsystematiek voor kostenramingen - SSK). This cost estimate system is most accepted within this sector in the Netherlands. A distinction is made between construction costs, real estate costs, engineering costs and additional costs. The system includes a guide to control the cost

development of the project and to prepare the cost estimation using calculation models. Furthermore, it is possible to consider the risks and uncertainties of the project.

Project risks and uncertainties must be adequately stated and can be translated into cost. The most important uncertainties of projects are future scope amendments and price developments, so mostly an amount is reserved for these uncertainties. This method, including assumptions for quantities, prices and risks of the project, is called deterministic cost estimating. Construction costs can also be estimated probabilistically. In a probabilistic cost estimation, probabilistic distributions are used to determine the price and quantities statistically. Based on this, well-founded statements can be made about bandwidth, probabilities of exceedance and the largest uncertainties in the cost estimation. A drawback of probabilistic estimation is that the probabilistic distributions of the parameters must be determined and this can be difficult and time-consuming.

## 2.6 Conclusion

This chapter contains descriptions and evaluations of relevant literature about this subject, which is obtained in the literature study of this research. In the literature study, different sources were consulted in order to collect general information and define underlying theories, such as guidelines, standards, books, lecture notes, reports, etc. This literature together forms the theoretical framework of this research. Furthermore, different papers and theses are used to obtain previous and latest research developments. The objective of the literature study is to treat previous studies about this subject and find the essential missing gaps in this subject in order to provide a starting point for this research. Based on these findings the most important starting points for this research are described below.

Following the Eurocodes, quay walls are designed according to a particular reliability class, corresponding to a maximum allowable failure probability of the structure. Three reliability classes are defined, intended to cluster quay walls with different potential consequence of failure. The differences between the maximum allowable failure probabilities of the reliability classes are known, but the differences between the construction costs of quay walls designed with different reliability classes (reliability indices) are not known. In recent research by Roubos et al. (2018), it is suggested that the marginal safety investments for quay walls are quite low. The findings are a first estimation and thorough research is required to investigate this.

Besides that, every maximum allowable failure probability of the reliability classes corresponds to a target reliability index. The target reliability indices per failure mechanism are allocated by expert judgement in the past, and these are evaluated and adapted using validation studies in the following years. So, the influence of the failure mechanisms on the construction costs are only estimated by expert judgement, but thorough research is required. The validation studies mainly consisted of probabilistic calculations of several failure mechanisms. From these studies also the influence of every stochastic parameter on the failure probability is obtained, but their influence on the cost of the quay walls is currently unknown. These missing gaps in literature are investigated in this research.

## 3 Starting points

In this chapter two benchmark quay walls are introduced, and the starting points of these cases are treated. The starting points form the basis of the design- and reliability calculations, from which the results are presented in the next chapters. In order to become familiar with these design- and reliability calculations, three fictional cases are designed consecutively, using stepwise refinement. The starting points and results of these fictional cases are presented in Appendix B. With the help of these fictional cases several design- and reliability methods are compared and based on these results the methods to be used are decided. In the designs, the normative verifications are considered, and corrosion of the steel components in the structure is regarded.

### 3.1 Benchmark 1: double anchored combi-wall

Benchmark 1 represents a double anchored combi-wall with a retaining height of about 17 m, from which the final design in RC2 was already performed by the designer. In this subchapter, the benchmark is introduced and the boundary conditions and starting points of the design- and reliability calculations are presented. Most of the design starting points are following from the design report of benchmark 1 (Arcadis, 2017).

#### 3.1.1 Introduction of benchmark 1

The Port of Rotterdam is redeveloping the Waalhaven, because of its strategic location for logistics, industrial, maritime and business service providers. Part of this strategy is the realisation of the new quay wall benchmark 1, located at a vessel repair company. The total quay wall length is 365.5 m, which is divided into two sections and the maximum mooring width is 37 m.

#### 3.1.2 Project location

The project location of benchmark 1, together with the Port of Rotterdam, is depicted in figure 3.1 within the red circle. The Waalhaven is part of the Port of Rotterdam and is accessible via the river the Nieuwe Maas. In the current situation, the terminal bank is performed as a slope 1:1 using soil improving mattresses.



Figure 3.1 – Project location of benchmark 1

### 3.1.3 Boundary conditions

The boundary conditions of benchmark 1, including the surface levels, hydraulic conditions, geotechnical conditions, loads and load combinations are collected in Appendix C. In this subchapter, only the critical soil profile of benchmark 1 is given in table 3.1. The corresponding soil characteristics are derived from NEN 9997-1, which are summed up in Appendix D, and these are collected for the soil profile of benchmark 1 in Appendix C.

Table 3.1 – Soil profile of section B-B' (Arcadis, 2017)

#	Type of soil	Waterside (DKM21) Top level layer [m NAP]	Landside (DKM42) Top level layer [m NAP]
1	Sand, loosely packed	-	+3.6
2	Clay, clean, weak	-	-7.5
3	Peat, weak	-	-8.5
4	Sand, loosely packed	-13.35	-
5	Clay, clean, weak	-14.0	-9.8
6	Sand, moderately packed	-17.5	-17.5

### 3.1.4 Existing design of benchmark 1

The designer of benchmark 1 had determined that the following main configuration of the quay wall, has to be used:

- diameter tubular pile: about 1420 mm;
- sheet pile: 3x PU 22;
- system length: about 3.27 m;
- anchoring: 2 grout injection anchors per tubular pile;
- concrete capping beam from NAP-1.0 m.

The optimal anchoring level is NAP+1.0 m. A lower anchoring level will lead to higher anchor forces which is undesirable because of the already heavy anchors. Even higher anchoring level is also inefficient, because in this case, the bending moments will increase very fast. The anchors will be performed at an angle of 40° and 45° with the horizon, taking into account the future pile foundations of the adjacent companies. The level of the top of the grout body is one meter below the bottom of the weak layer, at NAP-18.5 m. Besides that, bed protection is required in front of the quay wall. This bed protection is not designed in this research but performed as a uniform load in the design model. The principle geometry of benchmark 1 is given in figure 3.2.

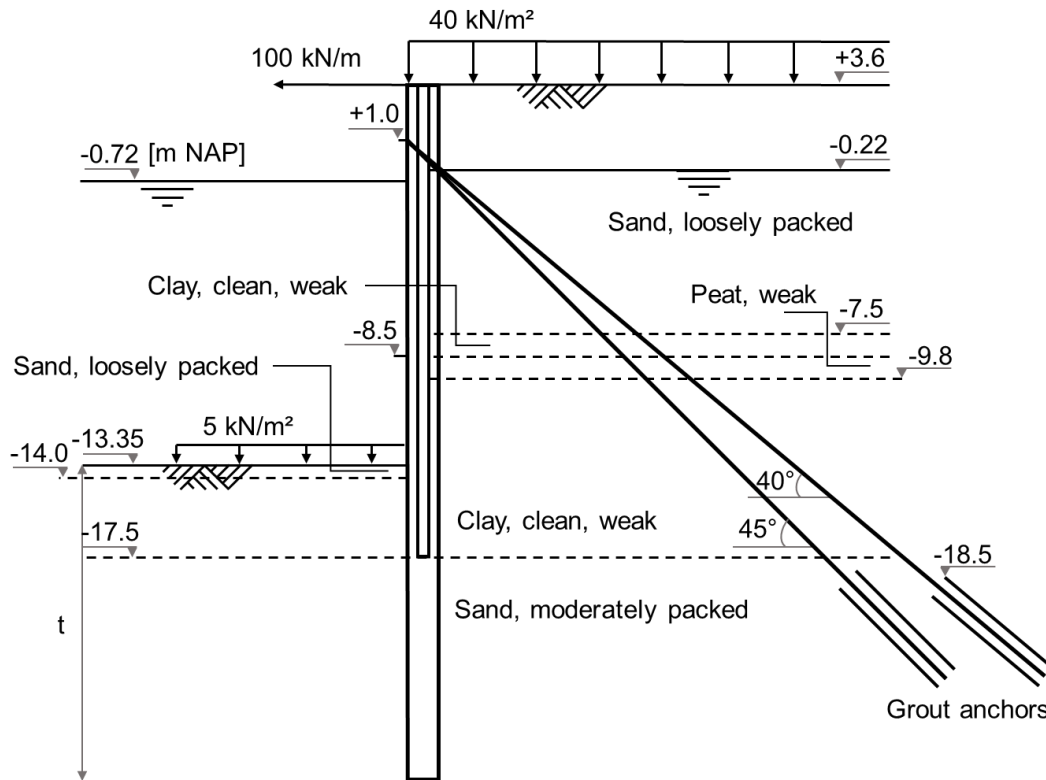


Figure 3.2 – Principle geometry of benchmark 1

### 3.1.5 Partial factors of semi-probabilistic design

In this research, the quay wall is designed semi-probabilistic in several reliability classes, corresponding to different partial factors. The concerning partial factors for sheet pile walls are defined the same in the NEN 9997-1, CUR 166 and CUR 211 and the relevant partial factors for benchmark 1 are given in table 3.2. In these guidelines, the partial factors are influencing the loads and soil parameters.

Notable is that in the design verification of local buckling, the surface load can be interpreted as geotechnical load instead of structural load (The Netherlands Standardisation Institute, 2017). This means that in this verification  $\gamma_Q$ -values of A2 are used. On the other hand, the surface and bollard load in the design verification of vertical bearing capacity  $\gamma_Q$ -values of A1 are used. Besides that, the factors of the geometry modification in D-Sheet Piling, influencing the retaining height and phreatic lines, are not taken into account. Following the CUR 211, the increase of the retaining height should not be used in the design of quay walls (Stichting CURNET, 2014). In the determination of the construction depth, all the required tolerances are including. Therefore, the construction depth is an extreme value, which should not be further reduced by geometrical modification factors. In the final design of the quay wall in RC2, these values were set to zero manually in D-Sheet Piling by the designers, as for the other designs of benchmark 1 in this study.

In order to investigate the influence of the angle of internal friction on the construction costs, benchmark 1 is also designed in SLS with the values of angles of internal friction increased with 10%. This increase of the angle of internal friction in combination with SLS is only applied in this research. The influence of increased angles of internal friction is investigated, because it is suggested that the values of these angles are (significantly) larger in reality than defined in the Dutch standards, such as the NEN 9997-1.

Table 3.2 – Overview of used partial factors for semi-probabilistic design of benchmark 1

Parameter		Symbol	Partial factors					
Design Approach	Reliability class		Design Approach 3					
			RC1	RC2	RC3	RC1	RC2	RC3
Loads (A)	Permanent	Unfavourable	1.215 <sup>bc</sup>	1.35 <sup>bc</sup>	1.485 <sup>bc</sup>	A2 <sup>a</sup> (sheet pile wall)		
		Favourable	0.90	0.90	0.90	1.00	1.00	1.00
	Variable	Unfavourable	1.35	1.50	1.65	1.00	1.10	1.25
		Favourable	0.00	0.00	0.00	0.00	0.00	0.00
Soil properties (M)	Angle of internal friction <sup>d</sup>	$\gamma_{\phi}$	1.15	1.175	1.20	-	-	-
	Effective cohesion	$\gamma_c$	1.15	1.25	1.40	-	-	-

<sup>a</sup>: The partial safety factors A1 have to be applied in case structural loads are considered whereas the factors A2 have to be applied in case of geotechnical loads.

<sup>b</sup>: Only with small variable loads this value is normative (eq. 6.10a in NEN-EN 1990+A1+A1/C2:2011. Otherwise eq. 6.10b)

<sup>c</sup>: With fluid pressure with a physically limit value may be sufficient; RC1: 1.08, RC2: 1.2, RC3:1.32

<sup>d</sup>: Influencing  $\tan(\phi)$

### 3.1.6 Reliability calculations

For this benchmark quay wall the reliability index of the following failure mechanisms can be calculated with the help of D-Sheet Piling:

- passive resistance inadequate;
- sheet pile profile fails;
- tension member anchorage fails.

These failure mechanisms are corresponding to ‘support earth pressure inadequate’, ‘sheet pile wall profile fails’, and ‘tensile rod fails’ of the fault tree for a sheet pile quay wall from the CUR 211 (CUR, 2005). This example of a fault tree is depicted in figure 3.3 with the specific failure mechanisms encircled.

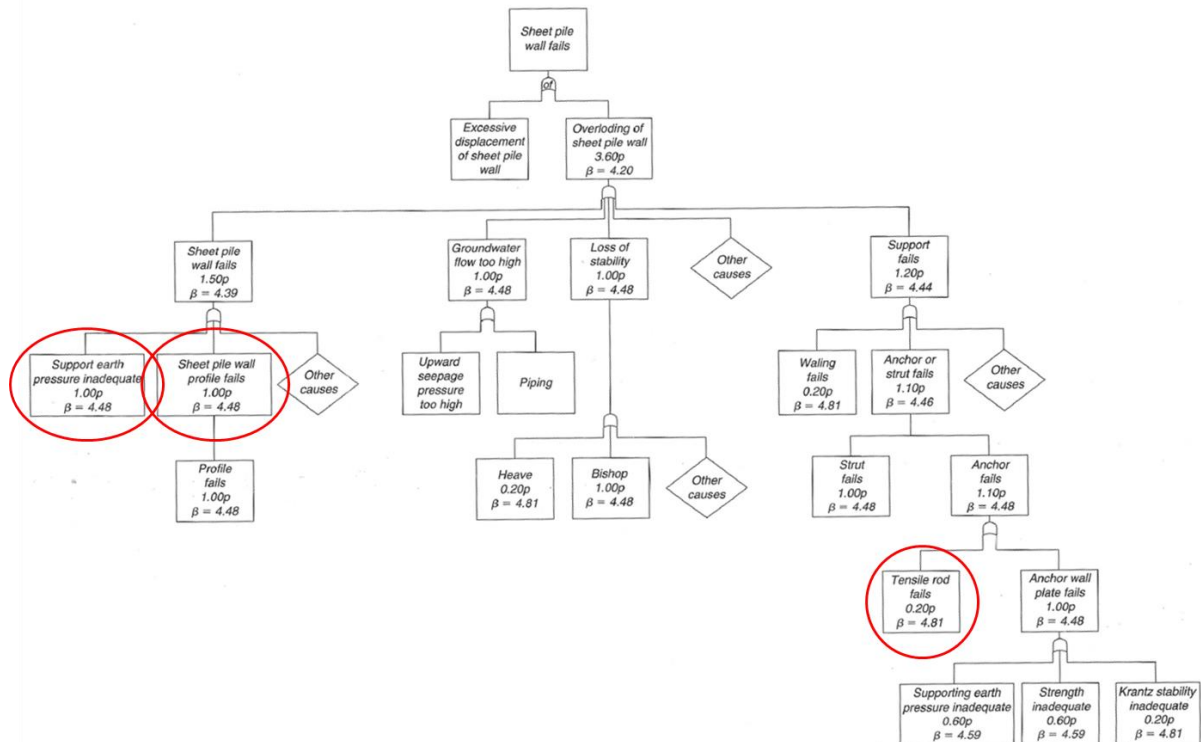


Figure 3.3 – Example of a fault tree for a sheet pile wall (CUR, 2005)

This fault tree originates from 2005 when the Eurocodes were not applied yet. Therefore, the overall  $\beta$  of the structure (overloading of sheet pile wall) of 4.2 is not corresponding to one of the overall target  $\beta$ 's defined for the reliability classes in the Eurocodes. The example fault tree is based on a distribution of failure probability per failure mechanism, expressed in  $p$ . This distribution of  $p$  is estimated and calibrated by expert judgement. The allowable probability of failure  $p$  per failure mechanism for the example fault tree is also given in figure 3.3. With the help of this distribution of failure probabilities per failure mechanism, these failure probabilities and  $\beta$ 's are adapted to the overall  $\beta$  of 3.8 in RC2. An overview of the failure probabilities and  $\beta$ 's of the considered failure mechanisms for RC2 is also given in table 3.3.

Table 3.3 – Allowable probability of failure per failure mechanism for a sheet pile quay wall in RC2 (CUR, 2005)

Failure mechanism	Allowable $p$	CUR 2005		RC2	
		Pf	$\beta$	Pf	$\beta$
Overloading of sheet pile wall	3.6p	1.335E-05	4.200	7.235E-05	3.800
Support earth pressure inadequate	1.0p	3.707E-06	4.481	2.010E-05	4.106
Sheet pile wall profile fails	1.0p	3.707E-06	4.481	2.010E-05	4.106
Tensile rod fails	0.2p	7.414E-07	4.814	4.019E-06	4.464

Using the distribution of failure probabilities per failure mechanism, these failure probabilities and  $\beta$ 's are also adapted to the overall  $\beta$  of 3.3 in RC1 and 4.3 in RC3. An overview of the failure probabilities and  $\beta$ 's of the considered failure mechanism for RC1 and RC3 is also given in table 3.4

Table 3.4 – Allowable probability of failure per failure mechanism for a sheet pile quay wall in RC1 and RC3 (CUR, 2005)

Failure mechanism	Allowable p	RC1		RC3	
		Pf	$\beta$	Pf	$\beta$
Overloading of sheet pile wall	3.6p	4.834E-04	3.300	8.540E-06	4.300
Support earth pressure inadequate	1.0p	1.343E-04	3.644	2.372E-06	4.576
Sheet pile wall profile fails	1.0p	1.343E-04	3.644	2.372E-06	4.576
Tensile rod fails	0.2p	2.686E-05	4.039	4.744E-07	4.902

Using the reliability analyses module of D-Sheet Piling, the following parameters can be chosen as stochastic:

- soil parameters  $\phi'$  and  $c'$ ;
- water levels;
- uniform- and surface loads;
- surface levels.

So, in the reliability analyses module of D-Sheet Piling, it is not possible to implement other stochastic variables, such as the saturated volumetric weight or modulus of subgrade reaction of the soil or steel characteristics. The modulus of subgrade reaction is related to the stiffness parameters of the soil, which can dominate reliability calculations of sheet pile failure (Schweckendiek et al., 2007). Therefore, the influence of the subgrade reaction of the soil on the reliability results will be investigated using a small sensitivity analysis.

Each stochastic variable is characterised by a mean value and standard deviation and a normal or log-normal distribution can be chosen. From the soil properties of NEN 9997-1 (Appendix D), it follows that the coefficient of variation (CoV) of  $\phi'$  is 0.10 and for  $c'$  is 0.20. With the help of this CoV, the mean values of the soil properties following from the NEN 9997-1 can be calculated as the following example of sand, moderately packed (The Netherlands Standardisation Institute, 2017):

$$\mu_i = \frac{X_{k,i}}{1 - 1.64 \cdot V_i} = \frac{32.5}{1 - 1.64 \cdot 0.10} = 38.88$$

in which  $X_{i,k}$  is the characteristic value of a parameter. The CoV is the ratio of the standard deviation and the mean, so the standard deviation can be calculated as follows:

$$\sigma_i = \mu_i \cdot V_i = 38.88 \cdot 0.10 = 3.89$$

The soil parameter  $c'$  is chosen to be lognormally distributed, in order to prevent the values from becoming negative, but the  $\phi'$ -values are normally distributed. This is because negative values of the concerned combinations of the mean and standard deviation of  $\phi'$  are not possible. On the other hand, the surface- and water levels are normally distributed.

The surface load of 40 kN/m<sup>2</sup> is an extreme value, but for the reliability calculations, an average value has to be considered. It is assumed that this extreme value is the characteristic value of the load, which means that there is a 5% probability that the value is higher. Using this assumption, the average load can be calculated in the same way as for the soil parameters (The Netherlands Standardisation Institute, 2017):

$$\mu_i = \frac{X_{k,i}}{1 + 1.64 \cdot V_i} = \frac{40}{1 + 1.64 \cdot 0.30} = 26.81$$

For the distribution and CoV of the surface loads, the researches by Havinga and Wolters are used. From research by Wolters (2012) follows an overview of the standard deviation or coefficient of variance of the retaining height, water level difference and surface load for an anchored sheet pile wall benchmark. These values are based on research by Havinga (2004), and an overview of these stochastic variables is shown in table 3.5.

Table 3.5 – Stochastic variables with standard deviation or coefficient of variance (Wolters, 2012)

Parameter	$\mu$	$\sigma$ / CoV
Retaining height [m]	12	0.25 ( $\sigma$ )
Water level difference [m]	2	0.20 ( $\sigma$ )
Surface load [kN/m <sup>2</sup> ]	30	0.30 (CoV)

The standard deviations of retaining height and water level difference are independent of its mean, so these values are used in this case. However, these values can differ due to different dredging tolerances or tidal characteristics for instance. Only the surface- and water level on the waterside of the sheet pile wall are stochastic variables because it is physically not possible to raise the surface- and (ground)water level above the combi-wall and the values from table 3.5 are defined considering level difference instead of both levels separately. Correlations between parameters are not considered, because it is not possible to implement these in the reliability analyses module of D-Sheet Piling. The stochastic variables with their standard deviation and distribution are listed in table 3.6.

Table 3.6 – Stochastic variables benchmark 1

Type	Name	Distribution	Mean value	Coefficient of variance	Standard deviation
$\phi'$ [°]	Sand, loosely packed	Normal	35.89	0.10	3.59
$\phi'$ [°]	Clay, clean, weak	Normal	28.35	0.10	2.83
$\phi'$ [°]	Peat, weak	Normal	21.89	0.10	2.19
$\phi'$ [°]	Sand, moderately packed	Normal	38.88	0.10	3.89
$c'$ [kN/m <sup>2</sup> ]	Clay, clean, weak	Lognormal	10.12	0.20	2.02
$c'$ [kN/m <sup>2</sup> ]	Peat, weak	Lognormal	6.70	0.20	1.34
Surface level [m NAP]	Surface, waterside	Normal	-13.35	-	0.25
Water level [m NAP]	Water, waterside	Normal	-0.72	-	0.20
Surface load [kN/m <sup>2</sup> ]	Surface load	Normal	26.81	0.30	8.04

From the design calculations of benchmark 1 follows, that for the failure mechanisms 'passive resistance inadequate' and 'sheet pile profile fails', load combination I is normative. For the failure mechanism 'tension member anchorage fails' load combination III is normative. Reliability calculations are performed in the normative load combination of the particular failure mechanism.

### 3.2 Benchmark 2: combi-wall with a relieving platform

Benchmark 2 represents a combi-wall with a relieving platform, from which also the final design in RC2 was already performed by the designer. In the following, the benchmark quay wall is introduced, and the corresponding boundary conditions and starting points of the design- and reliability calculations are presented. Most of the design starting points are following from the design report of benchmark 2 (Arcadis, 2016).

#### 3.2.1 Introduction of benchmark 2

In the Maasvlakte 1 of the Port of Rotterdam, a rise in throughput is expected for a particular terminal. Therefore, the Port of Rotterdam is planning to realise a new quay wall benchmark 2 at this location. Benchmark 2 has a total length of about 246 m and must be an elongation of the existing adjacent quay walls. Besides that, benchmark 2 must be able to be used by seagoing- and inland vessels.

### 3.2.2 Project location

The project location of benchmark 2 is located in the Maasvlakte 1 of the Port of Rotterdam and is depicted in figure 3.4 within the red circle. The Maasvlakte 1 is accessible via the river the Beerkanaal and in the current situation, the terminal bank of benchmark 2 is performed as a slope of about 1:5.

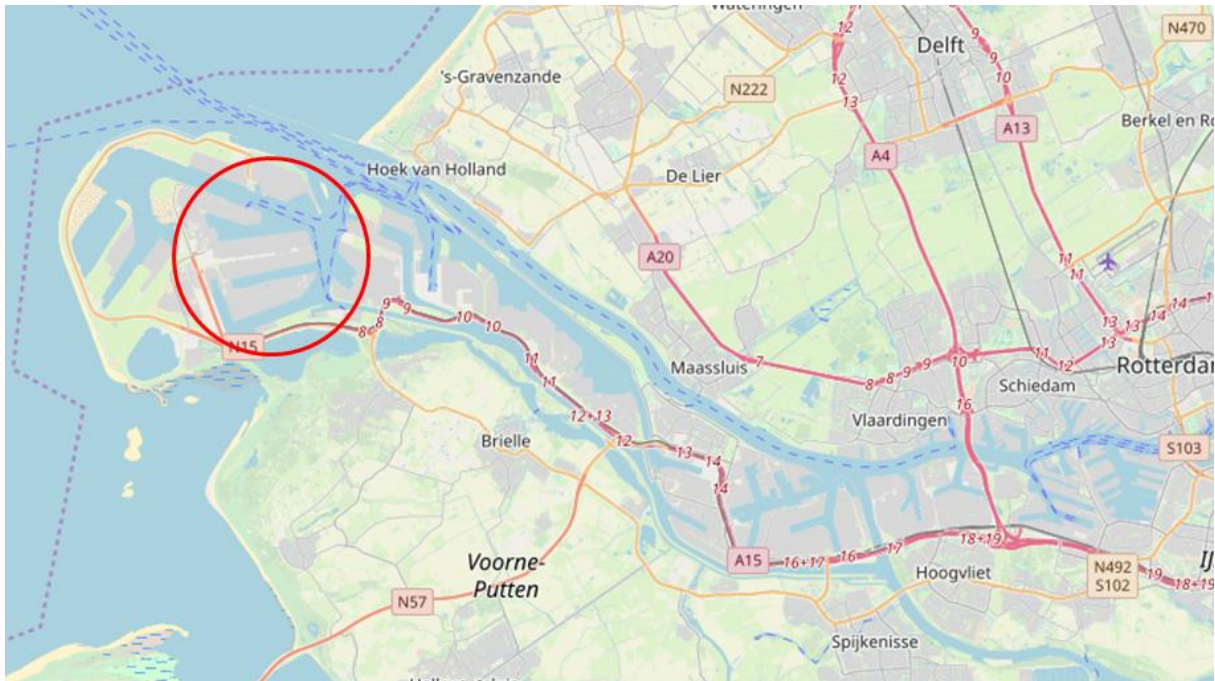


Figure 3.4 – Project location of benchmark 2

### 3.2.3 Boundary conditions

The boundary conditions of benchmark 2, including the surface levels, hydraulic conditions, geotechnical conditions, loads and load combinations are collected in Appendix E. In this subchapter, only the critical soil profile of benchmark 2 is given in table 3.7. The corresponding soil characteristics are derived from NEN 9997-1, which are summed up in Appendix D, and these are collected for the soil profile of benchmark 2 in Appendix E.

Table 3.7 – Soil profile of section B-B' (Arcadis, 2016)

#	Type of soil	Top level layer [m NAP]
1	Sand, loosely packed	+5.0
2	Clay, slightly sandy, moderately packed	+0.0
3	Sand, moderately packed	-0.5
4	Clay, very sandy	-6.4
5	Sand, moderately packed	-8.2
6	Sand, strongly packed	-10.0
7	Sand, slightly silty, clayey	-12.2
8	Sand, loosely packed	-14.2
9	Clay, slightly sandy, moderately packed	-20.5
10	Sand, moderately packed	-22.1
11	Sand, strongly packed	-25.0
12	Sand, slightly silty, clayey	-37.5
13	Sand, strongly packed	-43.0

### 3.2.4 Existing design of benchmark 2

The design of benchmark 2 is based on the already adjacent quay walls. Therefore, the main dimensions of benchmark 2 are the same as the adjacent quay walls. Benchmark 2 is performed as a combi-wall with a concrete relieving platform. The height of the platform is about 6 meters, and the platform is about 16.5 meters wide. The relieving platform is founded on top of the combi-wall and two bearing piles, vibro piles. The relieving platform is connected to the combi-wall with a saddle

construction as a hinge. Furthermore, the relieving platform is anchored, using grout injection anchors. The main dimensions of the quay wall are as follows:

- diameter tubular pile: about 1422 mm;
- sheet pile: 3x AU 23;
- combi-wall oblique about 5:1;
- system length: about 3.73 m;
- anchoring: grout injection anchor about every 2.735 m;
- relieving platform from about NAP+5.0 m till NAP-1.0 m;
- vibro piles every 2.565 m, alternately oblique 3:1 and 6:1.

The tubular piles, vibro piles and anchors are designed for each of the different CPTs along the quay wall. The anchors are designed using a different set of CPTs, located close by the anchoring. Most of the grout bodies of the anchoring are designed in between NAP-3.3 m and NAP -5.5 m. These angles are performed at an angle of 12°. The anchors are performed from the level of the relieving platform. Furthermore, there is no bed protection required in front of the quay wall. The principle geometry of benchmark 2 is given in figure 3.5.

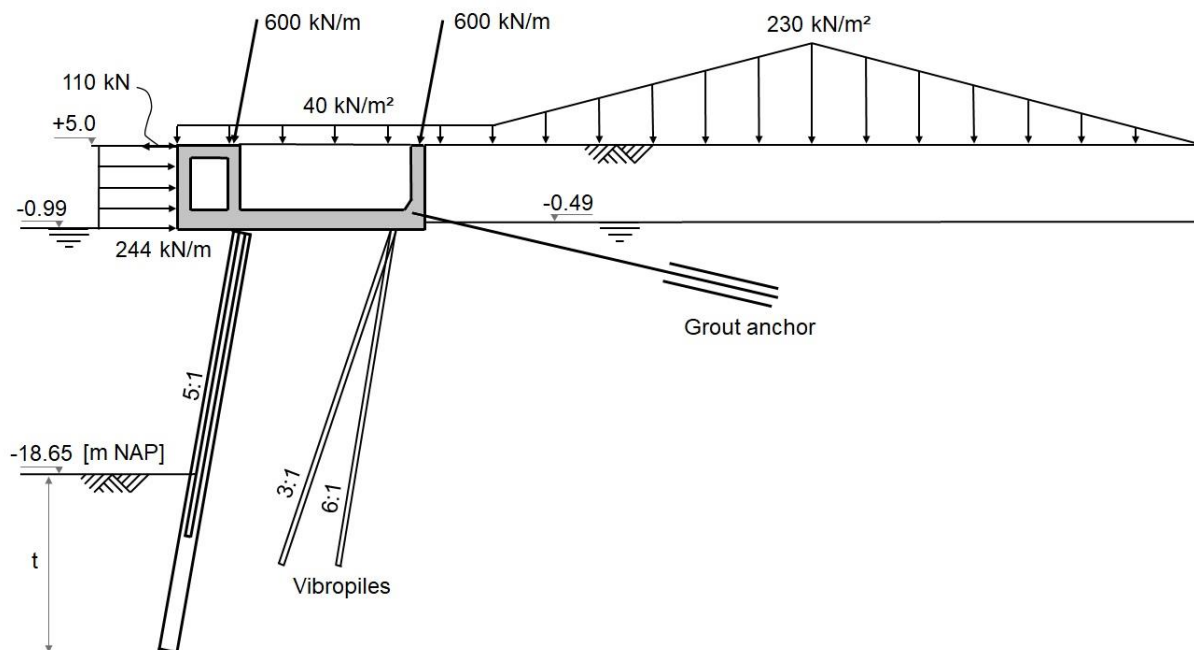


Figure 3.5 – Principle geometry of benchmark 2

### 3.2.5 Partial factors of semi-probabilistic design

In this research, the quay wall is designed semi-probabilistic in several reliability classes, corresponding to different partial factors. In the CUR 211, partial factors are defined uniquely for quay walls with a relieving platform. The partial factors of the variable, unfavourable loads are different for the live load on the superstructure, horizontal load on the superstructure and loads behind the superstructure. Besides that, the partial factors of the soil parameters are somewhat increased. The partial factors of benchmark 2 are given in table 3.8.

Just like benchmark 1, the factors of the geometry modification, influencing the retaining height and phreatic lines, are not taken into account. Following the CUR 211, the increase of the retaining height should not be used in the design of quay walls (Stichting CURNET, 2014). In the determination of the construction depth, all the required tolerances are including. Therefore, the construction depth is an extreme value, which should not be further reduced by geometrical modification factors.

Table 3.8 – Overview of used partial factors for semi-probabilistic design of benchmark 2 (Stichting CURNET, 2014)

Design Approach	Reliability class	Parameter	Symbol	Partial factors		
Loads (A)	Permanent	Unfavourable	$\gamma_G$	RC1		
		Favourable		RC2		
	Variable	Unfavourable	Live load on superstructure	$\gamma_Q$	RC3	
					Horizontal load on superstructure	A1 <sup>a</sup>
		Favourable	Loads behind superstructure	$\gamma_Q$		1.215 <sup>bc</sup>
					1.485 <sup>bc</sup>	
	Soil properties (M)	Angle of internal friction <sup>d</sup>	Unfavourable	$\gamma_\alpha$	0.90	
					Favourable	1.35
		Effective cohesion	Unfavourable	$\gamma_\phi'$	M2 (overall stability & quay wall with relieving platform on piles)	1.17
						Favourable
Effective cohesion	Favourable	$\gamma_{c'}$	M2 (overall stability & quay wall with relieving platform on piles)	1.00		
				0.00		
				1.20		
				1.25		
				1.30		
				1.45		
				1.60		

<sup>a</sup>: The partial safety factors A1 have to be applied in case structural loads are considered whereas the factors A2 have to be applied in case of geotechnical loads.  
<sup>b</sup>: Only with small variable loads this value is normative (eq. 6.10a in NEN-EN 1990+A1+A1/C2:2011. Otherwise eq. 6.10b)  
<sup>c</sup>: With fluid pressure with a physically limit value may be sufficient; RC1: 1.08, RC2: 1.2, RC3:1.32  
<sup>d</sup>: Influencing tan ( $\phi$ )

### 3.2.6 The plaxis model of benchmark 2

The Plaxis model is used for the geotechnical design calculations of the substructure of the quay wall. In Plaxis, the combi-wall can be modelled inclined, and the relieving platform can be modelled. From this model the internal forces of the combi-wall, vibro piles and anchors can be obtained, and the soil mechanical failure verification can be reviewed. The Hardening Soil Small Strain model (HSSS) is applied, in which the soil stiffness can be described extensively. At small strains, an increased soil stiffness is allocated, resulting in reliable deformations.

In this subchapter, the most important starting points of the Plaxis model are described. The Plaxis model of benchmark 2, which is prepared by designers, forms the basis of the Plaxis model of this study. This model is described in the design report of benchmark 2 (Arcadis, 2016). In the Plaxis model the history of the subsoil, the construction of the quay wall and the future loads of the load combinations are included in the phasing of construction. The phasing of this model is summed up in table 3.9.

Table 3.9 – Phasing of benchmark 2 in Plaxis

Phase	Description
1. Initial phase	Determine initial stresses in soil
2. Preloading subsoil	Preloading of 15 kPa, because the area is loaded in the past
3. Insert sheet pile wall, excavate and drain construction pit	Excavation till NAP-1.0 m
4. Construct combi-wall and vibro piles	
5. Construct relieving platform	
6. Apply soil behind relieving platform	
7. Preloading anchors	$F_{\text{preloading}} = 400 \text{ kN/anchor}$
8. Apply soil in relieving platform	
9. Remove sheet pile wall of construction pit	
10. Dredging till construction depth	Construction depth is NAP-18.65 m
11. LCI – LCII – LCIV – LCVIII – LC Kranz	SLS + ULS + phi-c reduction (only the normative LCs for the design verifications are considered)

In the Plaxis model, the soil layers are inserted, and the quay structure consists of plates, embedded pile rows and anchors. The combi-wall is modelled as a plate, with the sectional area (A) and moment of inertia (I) depending on the type of tubular- and sheet piles. The vibro piles and grout bodies modelled as uncracked embedded pile rows. Therefore, for the vibro piles an elasticity modulus (E) of 20,000 kN/m<sup>2</sup> and the grout bodies 2,500 kN/m<sup>2</sup> is used. In the existing design, the E of cracked concrete for the vibro piles of 10,000 kN/m<sup>2</sup> is also considered. It appears that in this case, the internal forces of the combi-wall and anchors are larger than in the model with uncracked vibro piles. The differences in the results are quite small, so cracked vibro piles are not considered in this study. At the tip of the combi-wall and vibro piles a point spring is added, with characteristics based on the displacement of these structures.

The combi-wall is hinged connected to the relieving platform using a cast iron saddle that is placed on the front flange of the tubular piles. In Plaxis this connecting is modelled as a steel plate with very high stiffness, resulting in an eccentric normal force at the location of the connection of the plate and the platform. The vibro piles (and anchors) are fixed into the platform. In figure 3.6 the Plaxis model of benchmark 2 is depicted.

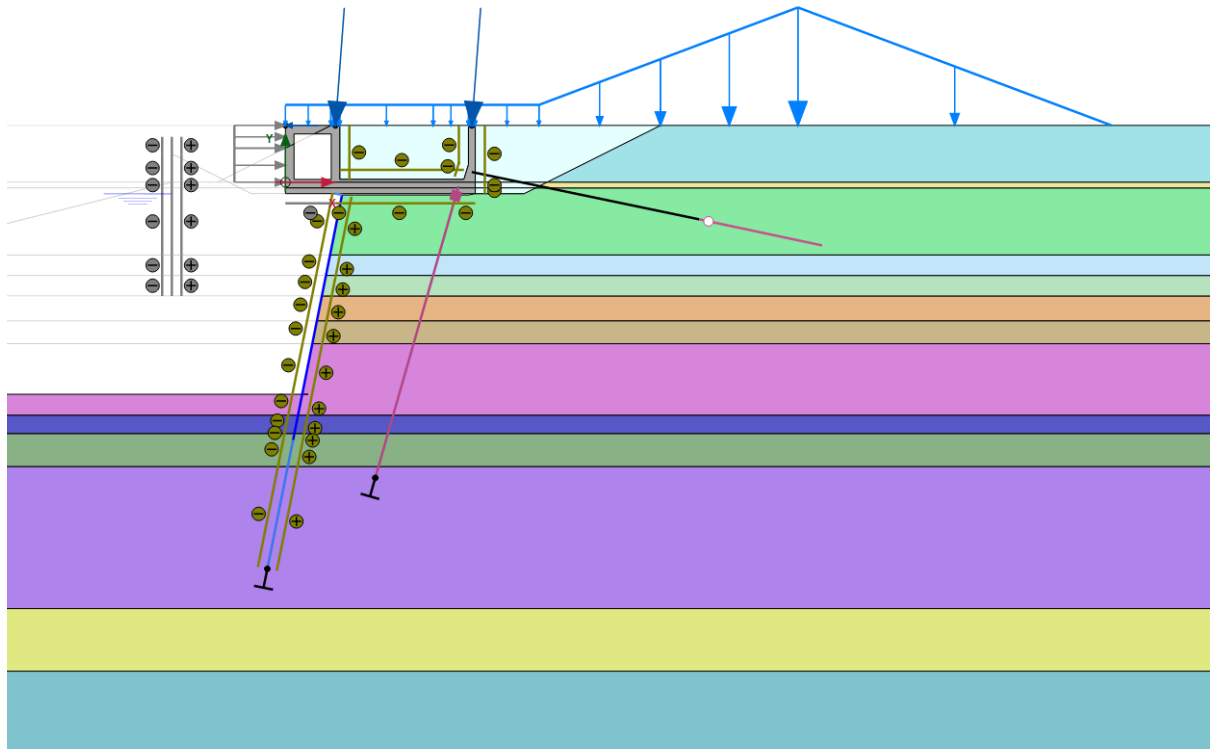


Figure 3.6 – Plaxis model of benchmark 2

# 4 Results benchmark 1: double anchored combi-wall

In this chapter, the design- and reliability calculations and construction costs estimations of the benchmark 1 quay wall are performed, and the results are obtained. In figure 4.1 a flow diagram of the research steps of this chapter is given. Firstly, the design principles of the benchmark quay wall are treated in chapter 4.1. Thereafter, the benchmark is designed semi-probabilistic in RC1, RC2 and RC3 in chapter 4.2 and the construction cost differences between these designs are obtained in chapter 4.3. In chapter 4.4 reliability calculations of these designs are performed, in order to validate the target reliability index per failure mechanism. Furthermore, the influence of partial factors on the construction costs are estimated in chapter 4.5 by performing a sensitivity analysis, in which these factors are varied alternately. Sensitivity analyses are also performed in chapter 4.6 and 4.7. The sensitivity of the construction costs to the dimensions of several structural components is estimated in chapter 4.6 and the sensitivity of the reliability index  $\beta$  to the dimensions of these structural components is estimated in chapter 4.7. In chapter 4.7 these sensitivities are combined to obtain the influence of the corresponding failure mechanisms on the construction costs in chapter 4.7. Reliability calculations are executed in chapter 4.7 in order to find the sensitivity of the reliability index to the dimensions of the structural components. This chapter ends with a conclusion of the most important results of benchmark 1 in chapter 4.8.

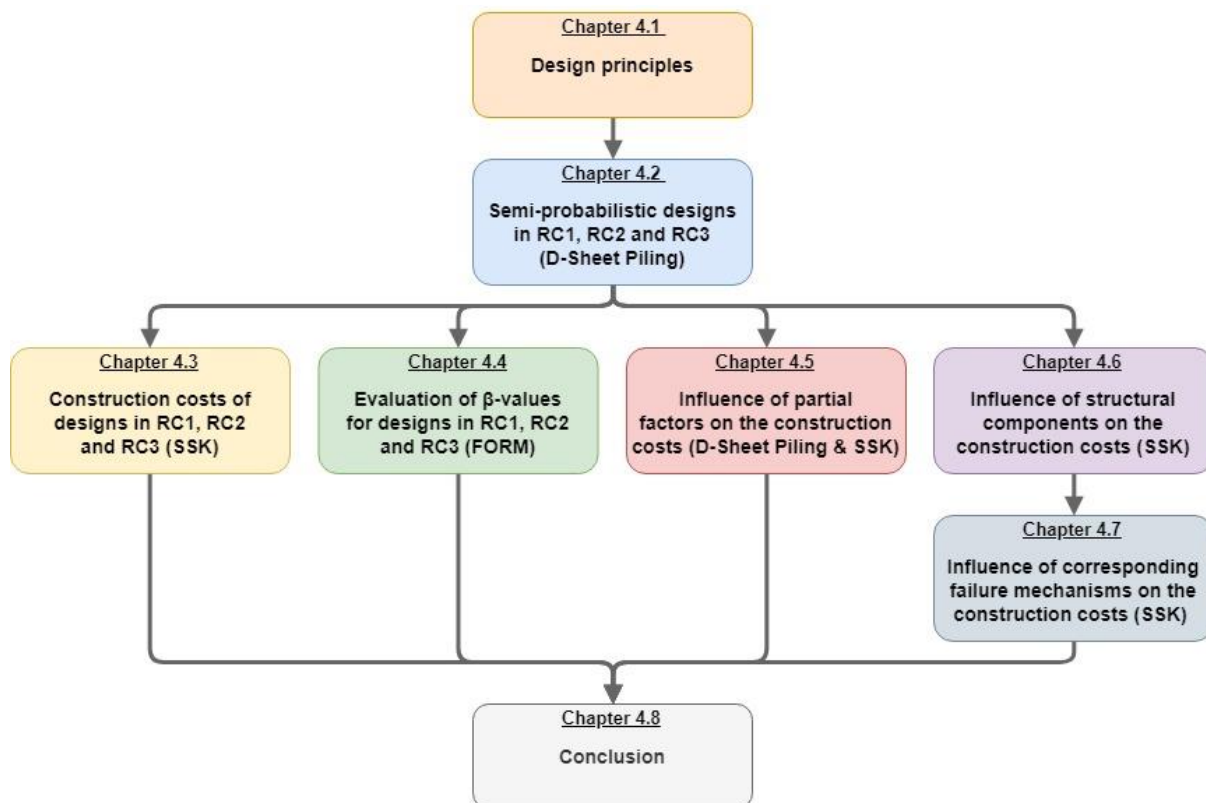


Figure 4.1 – Flow diagram of research steps of chapter 4

## 4.1 Design principles

The final semi-probabilistic design of benchmark 1 in RC2 was already performed by designers and described in a design report (Arcadis, 2017). From the starting points, the quay wall is designed, and several verifications are performed:

- check overall stability of the quay wall;
- check capacity combi-wall and sheet piles;
- check and design anchoring;

- check vertical bearing capacity of the tubular piles;
- check deformation of the quay wall.

Analysing the existing design report, it follows that the capacity of the combi-wall, anchoring and vertical bearing capacity are normative for the design of the quay wall. The capacity of the sheet piles is reviewed in this stage, and it appears that the RC has no influence on the required sheet pile profile for benchmark 1. In the existing design, the overall stability of the quay wall is guaranteed very well, so it can be assumed that this verification is satisfied in all the designs of benchmark 1 in this research. Therefore, only the normative verifications are considered in this research. Benchmark 1 is designed using the subgrade reaction method of D-Sheet Piling and several calculation sheets on behalf of the particular design verifications.

In this research the benchmark is designed for different reliability levels, using different partial factors. For these designs, most of the starting points are constant in order to be able to compare the reliability level and construction costs of these designs. Only the following structural elements, which are directly related to the considered design verifications, are adaptable in the different designs:

- diameter of the tubular piles;
- thickness of the tubular piles;
- toe level of the tubular piles;
- length of the grout body of the anchors.

The thickness of the anchor rod and type of intermediate sheet piles are constant in the different designs, because these structural elements are not normative for the stability of the quay wall. Besides that, the thickness of the grout body is constant because the thickness of the grout body in the design in RC2 is already the maximum value of the standard grout injection anchors of Jetmix (Jetmix, 2016). The toe level of the intermediate sheet piles is constant in the designs because it is assumed that the zero level of the resulting stress on the quay wall is constant over the different designs.

Varying the diameter and thickness of the tubular piles, the standard available dimensions of tubular pipes can be taken into account. In the standard available dimensions of the spirally welded steel pipes of ArcelorMittal, the diameter is varying with about 50 mm and the thickness with 1 mm. An overview of these standard available dimensions of spirally welded steel pipes of ArcelorMittal is attached in Appendix F. When the standard available dimensions of these pipes are used in the several designs, the stability- and structural design verifications cannot be optimised. Therefore, in this subchapter, the benchmark is designed based on the required section modulus, which is called the optimised design in this study. Besides that, benchmark 1 is designed based on the standard available dimensions of tubular pipes and these are treated in Appendix G. In the optimised design it is assumed that every combination of diameter and thickness of the tubular pipes can be used.

In order to avoid the repetition, only the design calculations of benchmark 1 of the optimised design in RC1 are presented in Appendix H of this report. The other designs of benchmark 1 in different reliability classes and the sensitivity analysis are performed in the same way as this optimised design in RC1. From the other designs of benchmark 1 a summary of the design results is given.

#### 4.1.1 Optimised design

In the optimised design the quay wall is designed by varying the toe level with 10 cm, the grout body with 1 cm and varying the section modulus of the tubular piles of the combi-wall. The section modulus is depending on the cross-section of beams or flexural members, like tubular piles, and is also indicated as the moment of resistance in some literature (Vrijling et al., 2015). The cross-section of a hollow pile is schematised in figure 4.2, and the section modulus of hollow piles can be calculated as follows:

$$W_{eff,y} = \frac{\pi(D_o^4 - D_i^4)}{32 \cdot D_o}$$

$$D_i = D_o - 2 \cdot t$$

in which  $D_i$  is the inner diameter,  $D_o$  the outer diameter and  $t$  the thickness of the pile. So, the section modulus of tubular piles depends on the outer diameter and the thickness of the pile. In order to relate

the different designs with different reliability levels to the section modulus of the piles, the ratio  $D_o/t$  is constant in the optimised designs. The ratio  $D_o/t$  of the existing design in RC2 is chosen as the constant ratio, namely  $1420/16 = 88.75$ .

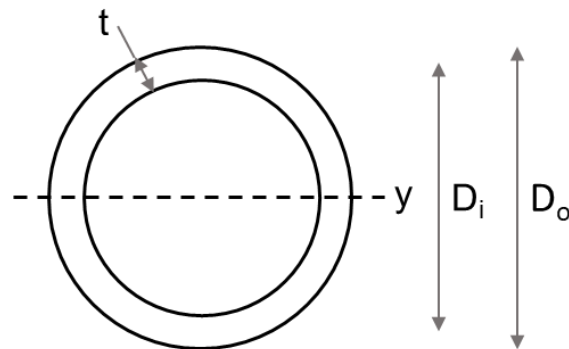


Figure 4.2 – Cross-section of hollow pile

With the help of iteration between the different verifications, a design for every reliability level is found. First, in the D-Sheet Piling design, the stability of the quay wall and the maximum bending moment of the combi-wall are checked. In the iteration, the benchmark is designed until the verifications are just right. The local buckling verification is just right when the unity check for local buckling is in between 0.99 and 1.0. The vertical bearing capacity verification is just right when the unity check is first below 1.0 when the toe level of the tubular piles is lowered. Furthermore, the anchor resistance verification is just right, when the unity check is first below 1.0 when the length of the grout body is decreased.

## 4.2 Semi-probabilistic design results

First, the optimised design of benchmark 1 in RC1 is performed, from which the design calculations are presented in Appendix H. The designs of benchmark 1 in RC2 and RC3 are found in the same way as the optimised design of benchmark 1 in RC1. In order to avoid the repetition of these steps, only a summary of the design results is given. So, the results of the structural dimensions of the optimised semi-probabilistic designs of benchmark 1 in RC1, RC2 and RC3 are collected in table 4.1.

Table 4.1 – Structural dimension of optimised semi-probabilistic designs of benchmark 1 in RC1, RC2 and RC3

Structural characteristics	RC1	RC2	RC3
<b><math>D_o</math> piles [mm]</b>	1360	1400	1450
<b>t piles [mm]</b>	15.32	15.77	16.34
<b><math>D_o / t</math> [-]</b>	88.75	88.75	88.75
<b>Section width combi-wall [m]</b>	3.21	3.25	3.30
<b><math>W_{eff,y}</math> piles [mm<sup>3</sup>/m]</b>	6,703,875	7,222,956	7,903,224
<b>Toe level piles [m NAP]</b>	-27.0	-27.1	-27.8
<b>Length grout body [m]</b>	7.66	7.68	8.73

It is checked that the extended grout bodies are still located in the sand layer. In these calculations, only the section modulus of the tubular piles, length of the tubular piles and length of the grout body of the anchors are varied. The required section modulus, together with the  $D_o$  and  $t$  of the piles, increases almost equally with the partial factors of the RC's.

However, the required toe level of the piles is almost the same for RC1 and RC2, but significantly lower for RC3. This is due to the bearing capacity of the normative CPT DKM23. An indication of the bearing capacity of CPT DKM23 (without excavation) is depicted in figure 4.3. In the design calculation, the bearing capacity is a combination of the unexcavated and the excavated situation. A representative value of the normal forces of the different RC's and the required toe levels are added in the figure. The bearing capacity in RC1 satisfies from a depth of NAP-27.0 m and in RC2 from NAP-27.1 m. From the figure follows that in between NAP-27.2 m and NAP-27.7 m the bearing capacity slightly reduces, due to a local low conus resistance ( $q_c$ ). Therefore, the bearing capacity in RC3 satisfies only from a depth of NAP-27.8 m. So, the vertical bearing capacity is not only depending on the partial factors of the RC, but also on the local soil characteristics.

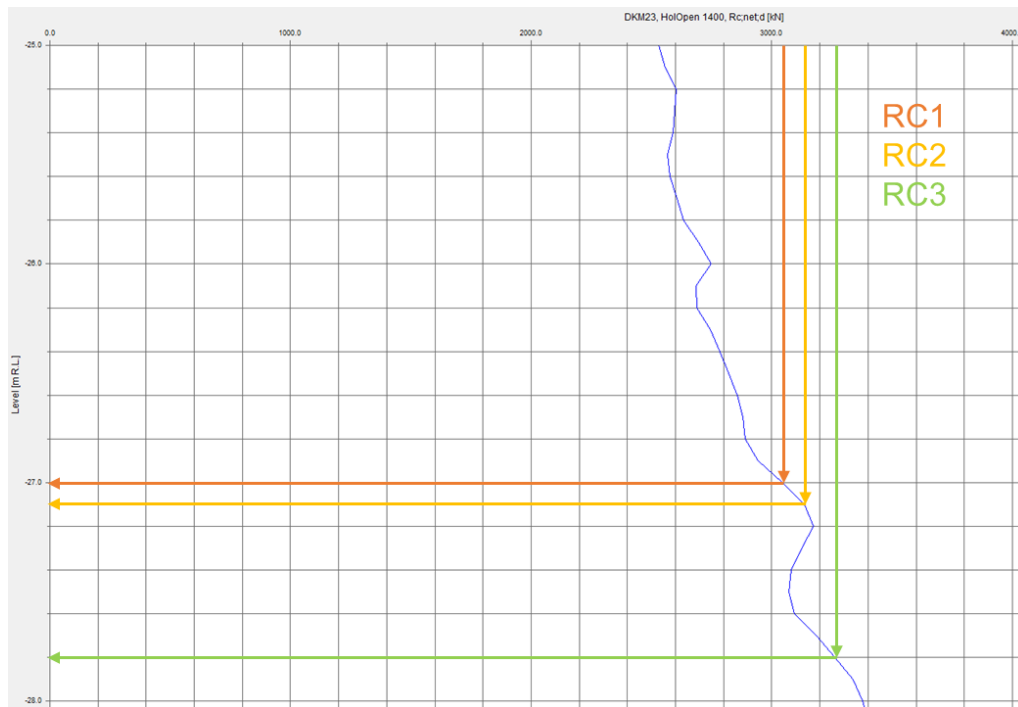


Figure 4.3 – Indication of the bearing capacity of CPT DKM23 (without excavation)

Besides that, also the required grout body lengths of RC1 and RC2 are similar, in contrast to RC3. This is, because the normative design check for the anchor forces is in SLS, in which the anchor forces are multiplied by a factor. The required design checks are defined in NEN 9997-1 and performed in the D-Sheet Piling verification (The Netherlands Standardisation Institute, 2017). The SLS results of the designs in RC1, RC2 and RC3 are almost equal, but the multiplication factor differs for RC3. In RC1 and RC2 this factor is 1.2, and in RC3 this factor is 1.35. Therefore, the normative anchor forces are similar for RC1 and RC2, but larger in RC3 and the required length of the grout body is larger as well.

From benchmark 1 is also an optimised design in SLS with 10% increased  $\phi'$  and the results are shown in Appendix I. This design is performed, because it is suggested that the  $\phi'$  values of the standards CUR 211 and NEN 9997-1 are significantly lower than in reality. Using this design, a first insight into the influence of the  $\phi'$  on the design and the construction costs is obtained.

### 4.3 Construction costs estimation

In this subchapter, the construction costs of benchmark 1 are determined and discussed. Besides that, the execution classes of the steel structures of benchmark 1 and the assumptions regarding these classes are treated. Only the direct construction costs of the defined quay wall structure and the cost influenced by the RC are considered. The quay wall is defined as the retaining wall, including its possible anchoring, pile foundation, relieving platform, bollards and fenders. This means that the cost of the pavement of the terminal and the bed protection in front of the quay wall are not taken into account. Cost of preparation proceedings, such as the property and preparation of site and decommissioning of existing structures, are not taken into account as well. Besides that, costs of planning, design, engineering, maintenance, demolition, insurance and one-off costs, such as profit, risks and general costs, are not considered, because they do not depend on the RC of the quay wall. The construction costs of benchmark 1 only consist of the following cost components:

- soil work;
- drainage;
- construction pit;
- combi-wall;
- anchors;
- concrete work;
- joints;

- fenders and bollards;
- dredging work;
- cathodic protection.

The construction costs of benchmark 1 are considered for the optimised design and the design based on standard available dimensions of tubular pipes in RC1, RC2 and RC3. The construction costs of the design based on standard dimensions are collected in Appendix G. The cost are estimated deterministic using the standard cost estimate system (standaardsystematiek voor kostenramingen - SSK). In the existing design of benchmark 1, an SSK calculation sheet was prepared by cost specialists. In this calculation sheet, the activities accompanying to the cost components above were collected and expressed per unit of length, area, volume, number or weight. The cost of these activities are estimated using unit prices, which are based on standard prices and prices of previous quay wall projects. This calculation sheet is validated using construction costs unit prices of the Port of Rotterdam (Koene, 2018). The activities in the calculation sheet consist of the supply of materials and construction of structures, including labour- and equipment costs. It is emphasised that the construction cost calculation sheet is based on present (2016) unit prices, which can deviate in the future. Besides that, model uncertainties of the design and project risks are not considered in the construction costs. So, these results give a reasonable first insight into the construction costs.

#### 4.3.1 Construction costs estimation of optimised designs

In this subchapter the construction costs estimations of the optimised semi-probabilistic designs of benchmark 1 in RC1, RC2, RC3 are treated. First, the construction costs of the designs are estimated per cost component, and the total construction costs are determined. Benchmark 1 has a length of about 365.5 m, so the in order to compare different quay walls, the construction costs are estimated per running meter. Besides that, the relative increase in the construction costs compared to the design in RC1 is estimated as well. In table 4.2 an overview of the construction costs estimation of benchmark 1, excluding Value Added Tax (VAT), is given.

The construction costs of the designs in RC1, RC2 and RC3 deviate as the differences of the structural dimensions of the designs. Variation of the diameter, thickness and length of the tubular piles and length of the anchors influence the required amount of steel. The diameter of the piles also influences the section width of the combi-wall, which influences the required supply and construction amount of tubular piles or the required amount of cathodic protection.

In the determination of the construction costs, it is assumed that the width of the capping beam is decreased in compliance with the decrease of the diameter of the tubular piles. This reduction of the width of the capping beam leads to a decrease in the formwork-, concrete- and reinforcement costs of the capping beam. In the estimations, the reinforcement costs are based on an estimated reinforcement ratio of 150 kg/m<sup>3</sup> in the capping beam and 120 kg/m<sup>3</sup> in the front wall. In the structural design calculations of the capping beam, the accidental load combination vessel collision is normative. An accidental load combination is based on SLS values of the partial factors, which means that this ratio will not change, changing the RC.

Table 4.2 – Construction costs overview of semi-probabilistic optimised designs

Reliability class	Construction costs (€/m)	Relative increase compared to RC1
RC1	€ 17,380.-	0.00%
RC2	€ 17,570.-	1.08%
RC3	€ 17,980.-	3.42%

The relative cost increase between the designs in RC1 and RC2 is about 1.1%, and the relative cost increase between the designs in RC1 and RC3 is about 3.4%. The relative increase in the construction costs of the designs in RC2 and RC3 compared to RC1 is plotted against the target  $\beta$ -values of the RC's in figure 4.4.

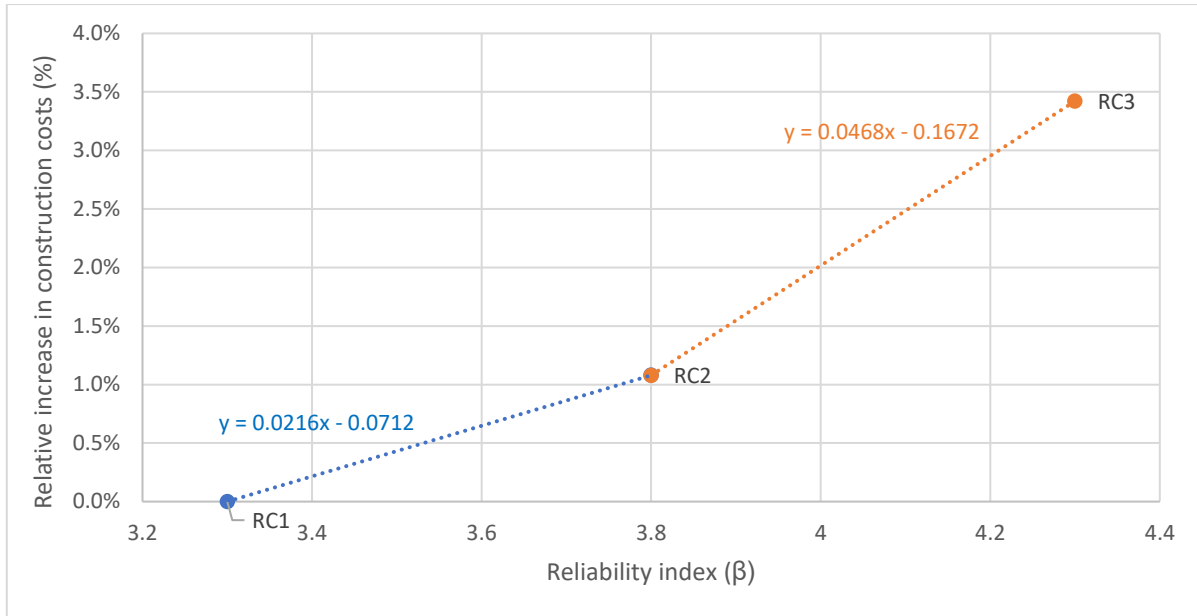


Figure 4.4 – Construction cost increase of quay walls designed semi-probabilistic in RC1, RC2 and RC3

From figure 4.4 the ratio  $\Delta C/\Delta\beta_{\text{target}}$  can be obtained as the slope number of the linear trendlines. So, the ratio  $\Delta C/\Delta\beta_{\text{target}}$  between RC1 and RC2 is about 2.2% and between RC2 and RC3 about 4.7%. These values are lower than estimations of 5-10% by Roubos et al. and Schweckendiek et al. (Roubos et al., 2018). It is emphasised that these ratios are a first estimation because the fraction  $\Delta\beta_{\text{target}}$  is based on the target  $\beta$ -values defined in the Eurocodes and may differ per design.

So, the relative costs difference between the designs in RC1 and RC2 is significantly smaller than the cost difference between the designs in RC2 and RC3. This is the case because of the larger structural differences between the designs in RC2 and RC3, instead of the designs in RC1 and RC2. These larger differences are due to the lower required toe level of the tubular piles, and longer required length of the grout body in the design in RC3, relative to the designs in RC1 and RC2. It is emphasised the results are cost estimations and give a reasonable first insight into the construction costs considering the functionality of benchmark 1. An overview of the relative construction costs comparison of the different cost components of the optimised designs of benchmark 1 is given in figure 4.5.

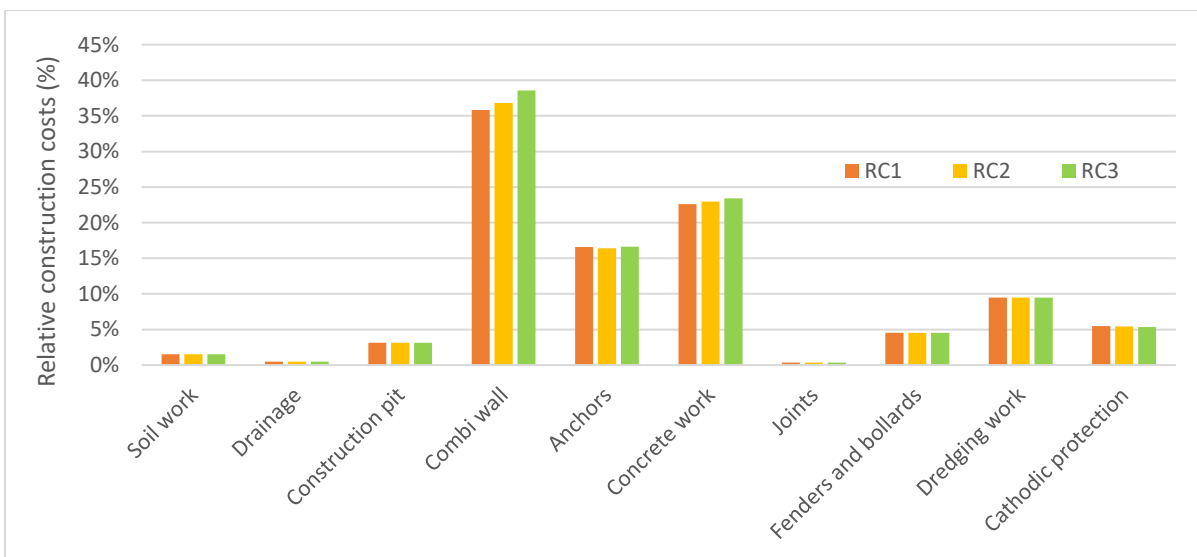


Figure 4.5 – Relative construction costs comparison of optimised designs of benchmark 1

From the cost estimation follows that only the construction costs of the combi-wall, anchors, concrete work and cathodic protection differ between the designs in RC1, RC2 and RC3. Therefore, the relative

cost increase compared to the design in RC1 of these cost components are shown in figure 4.6. The cost components; soil work, drainage, construction pit, joints, fenders and bollards and dredging works are independent of the RC. The construction costs of the combi-wall increase in compliance with the increase of the diameter, thickness and length of the tubular piles. Also, the construction costs of the concrete work, which mainly contains the capping beam, increase together with the increase of the diameter of the piles. Besides that, the construction costs of the anchors show an unusual result. The construction costs of anchors in the design in RC1 are more expensive than the anchors of the design in RC2 and almost equal to the anchors of the design in RC3. This is because the normative anchor forces and the anchor designs are similar in RC1 and RC2, but the anchor forces and the anchor designs are larger for RC3. The centre to centre distances between the anchors increases with the RC, so more anchors are required in RC1 than in RC2, so the construction costs of the anchors are lower in RC2 than in R1. The anchor design in RC3 is larger, but less anchors are required, which almost equals the construction costs of the anchors in RC1 and RC3. Furthermore, the cost of cathodic protection decreases also decreasing the number of tubular piles in the designs in RC2 and RC3.

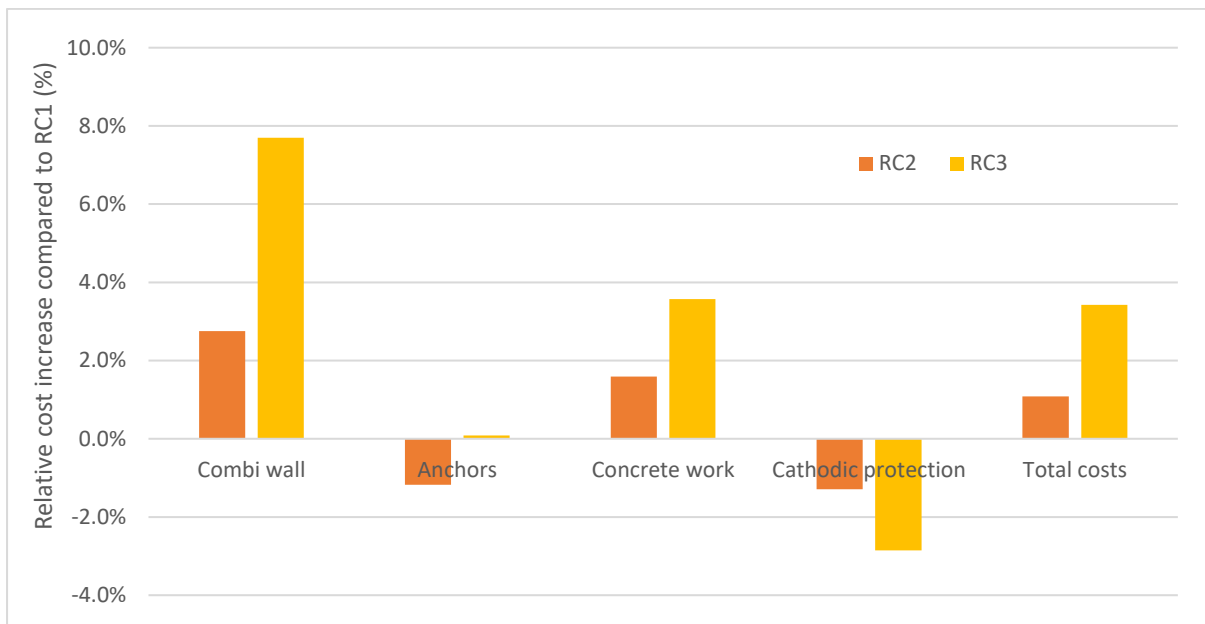


Figure 4.6 – Relative cost increase compared to the design in RC1

### 4.3.2 Execution classes steel structures

For each of the designs, the execution class have to be determined, which specify a classified set of requirements for the execution of the works related to the quay wall construction. These requirements are specified in order to ensure adequate levels of mechanical resistance and stability, serviceability and durability and are further explained in chapter 2.3.1.4.

The execution class is determined following table 2.5 and some exceptions. In the design of benchmark 1, the type of loading is static, and fatigue is not applicable. So, according to table 2.5 RC1 corresponds to EXC1, RC2 to EXC2 and RC3 to EXC3. One exception to that is that for welded parts manufactured from steel products with a steel grade of S355 or higher EXC2 must be applied. For the tubular piles, sheet piles, anchor rods, bollards and fenders of benchmark 1 this is the case. So, the design of benchmark 1 in RC1 EXC2 is applicable. An overview of the execution classes of the different designs is collected in table 4.3.

Table 4.3 – Execution classes per RC of benchmark 1

Reliability class	Execution class
RC1	EXC2
RC2	EXC2
RC3	EXC3

For both execution classes, EXC2 and EXC3 several requirements are defined. The requirements are related to constructor’s documentation, traceability, cutting, welding, etc., which is further explained in the NEN 1090-2. In annex A.3 of the NEN-EN 1090-2 a shortlist of these requirements per execution class is given, and it is notable that the requirements of EXC2 to EXC3 strongly increase. For instance, in EXC3 the steel needs to be fully traceable instead of partly in EXC2 and in EXC3 the amount of welding control is at least twice as large as in EXC2. In this study, it is assumed that the construction costs are not influenced by these EXC’s. In reality, the construction costs of the designs in RC2 and RC3 will differ more.

#### 4.4 Reliability results

In the reliability calculations of benchmark 1, it is essential to consider the section width of the combi-wall. The limit values of the failure mechanisms ‘sheet pile profile fails’ and ‘tension member anchorage fails’ must be considered per section width, instead of per meter. In the designs of benchmark 1 in RC1, RC2 and RC3, the anchor rod is not changed, because this component is not normative. Therefore, the design yield force of the anchors is equal in the different designs. Considering a corrosion layer of 1.5 mm, corresponding to a design life of 50 years, the design yield force of the anchor rod is about 2108 kN. Furthermore, the degree of mobilisation for which the passive resistance is inadequate is determined by iteration for each of the designs. The  $\beta$ ’s calculated are compared with the  $\beta$ ’s defined in the CUR 211 originating from 2005, depicted in figure 2.18.

For the optimised design in RC1, the maximum allowable moment of the combi-wall is equal to about 12030 kNm/section. Furthermore, the combi-wall in RC2 contains a maximum allowable moment of about 12991 kNm/section and in RC3 of about 14271 kNm/section. The results of the reliability calculations for the optimised design in RC1 are shown in table 4.4.

Table 4.4 – Reliability results of the optimised design of benchmark 1 in RC1, RC2 and RC3

Failure mechanism	Limit value	$\beta$ calculated [-]	$\beta$ CUR 211 [-]
<b>RC1</b>			
Passive resistance inadequate	100%	9.20	3.64
Sheet pile profile fails	12030 kNm / section	7.46	3.64
Tension member anchorage fails	2108 kN / anchor	8.35	4.04
<b>RC2</b>			
Passive resistance inadequate	100%	9.25	4.11
Sheet pile profile fails	12991 kNm / section	7.81	4.11
Tension member anchorage fails	2108 kN / anchor	8.20	4.46
<b>RC3</b>			
Passive resistance inadequate	100%	9.48	4.58
Sheet pile profile fails	14271 kNm / section	8.37	4.58
Tension member anchorage fails	2108 kN / anchor	8.16	4.90

The  $\beta$ ’s of the failure mechanism ‘passive resistance inadequate’ are estimated at 9.2 in RC1, 9.25 in RC2 and 9.48 in RC3. These values increase in compliance with the increase of the length of the tubular piles of the designs in different RC’s. The  $\beta$ ’s of the failure mechanism ‘sheet pile profile fails’ are estimated at 7.46 in RC1, 7.81 in RC2 and 8.37 in RC3. These values also increase in compliance with the increase of the section modulus of the piles of the designs in different RC’s. The  $\beta$ ’s of the failure mechanism ‘tension member anchorage fails’ are estimated at 8.35 in RC1, 8.2 in RC2 and 8.16 in RC3. These  $\beta$ ’s are very similar, since the anchor rod in the design in RC1, RC2 and RC3 is unchanged. The anchor rod is unchanged because the grout body of the anchors is normative for the design. In the designs in RC2 and RC3, the centre to centre distance between the anchors is increased with respect to the design in RC1, leading to an increased anchor force. Therefore, the reliability indices of ‘tension

member anchorage fails' is even decreasing in RC2 and RC3, with respect to RC1. It is emphasised that the reliability results are first indications and just rough estimations because model uncertainties and stochastic correlations are not considered and limited different stochastic variables are used. For instance, literature states that the modulus of subgrade reaction of the soil can dominate the influence on the reliability results. The influence of this modulus on the  $\beta$  of benchmark 1 in RC2 is evaluated using a small sensitivity analysis. The results are attached in Appendix J, and it follows that the modulus of subgrade reaction is not influencing the  $\beta$  of benchmark 1 a lot. So, modelling the modulus of subgrade reaction as deterministic seems a reasonable estimation.

The calculated  $\beta$ -values are considerably higher than the target  $\beta$ -values of the fault tree in the CUR 211 of 2005. So, if this fault tree is used, the structure will meet the requirements for all these three failure mechanisms more than sufficiently. The calculated  $\beta$ 's are that high because the investigated failure mechanisms are not normative in the design. The normative design verifications are: vertical bearing capacity of tubular piles (instead of passive resistance), local buckling capacity of combi-wall (instead of moment resistance) and the grout body capacity (instead of tension member anchorage capacity) because the UC's of these failure mechanisms are (very) close to 1.0. The unity checks (UC) and  $\beta$  per failure mechanism of benchmark 1 in RC2 are collected in table 4.5. The UC's of 'passive resistance inadequate' and 'sheet pile profile fails' are that low, that high  $\beta$ 's are expected. For the failure mechanism 'tension member anchorage fails' the  $\beta$  is high because the UC is low and in the anchor verification, conform the CUR 166, extra safety is obtained by increasing the anchor force by 1.25. Because these failure mechanisms are not normative, it is not relevant to adapt the design to just meet the target  $\beta$ 's.

Table 4.5 – Unity checks and  $\beta$  of failure mechanisms of benchmark 1 in RC2

Failure mechanism	Limit value	$\beta$ calculated [-]	UC
Passive resistance inadequate	100% mobilisation	9.25	0.41
Sheet pile profile fails	12991 kNm / section	7.81	0.66
Tension member anchorage fails	2108 kN / anchor	8.20	0.86

For the different failure mechanisms, a first estimation of the relationship between the  $\beta$  and the construction costs is estimated by comparing the costs- and reliability results. This is performed in Appendix K.

For each of failure mechanism, a sensitivity factor for each of the stochastic variables can be determined by D-Sheet Piling as the  $\alpha$ -value. The  $\alpha$ -values are a measure of the relative importance of the particular stochastic variable to the reliability index  $\beta$  (Jonkman et al., 2017). The contribution of the stochastic variable to  $\beta$  is expressed in  $\alpha^2$ , because the  $\alpha^2$ -values of all the stochastic variables per failure mechanism together is 100%. An overview of the  $\alpha^2$ -values of the design in RC2 is given in table 4.6.  $\phi'$  dominates the contributions to the  $\beta$  of all three considered failure mechanisms. Besides that, the surface load has significant contribution to the  $\beta$  of the failure mechanisms 'sheet pile profile fails' and 'tension member anchorage fails'. The contribution of the  $c'$ , water level and surface level on  $\beta$  is for all failure mechanisms very low. Due to rounding errors, the  $\alpha^2$ -values of all stochastic variables together per failure mechanism is not 100% exactly.

Table 4.6 – Contribution of stochastic variables to the  $\beta$  of three failure mechanisms of benchmark 1 in RC2

Stochastic variable	$\alpha^2$ (%)		
	Passive resistance inadequate	Sheet pile profile fails	Tension member anchorage fails
$\phi'$ [°]	92.2%	78.1%	78.1%
$c'$ [kN/m <sup>2</sup> ]	1.2%	3.4%	0.3%
Surface level [m NAP]	3.2%	5.0%	0.5%
Water level [m NAP]	0.9%	3.1%	1.4%
Surface load [kN/m <sup>2</sup> ]	2.2%	10.3%	19.6%

## 4.5 Influence of partial factors on the construction costs

In this subchapter, the influence of the partial factors on the construction costs of benchmark 1 is investigated. The influence of the partial factors on the construction costs is determined by performing a sensitivity analysis by increasing the partial factors from the optimised design in RC1 alternately. So, the optimised design in RC1 forms the basis of this analysis. For every situation in the sensitivity analysis, an optimised design of benchmark 1 is performed, and the design meets the requirements when, after several iterations, all the design verifications are just right. For every situation the design calculations are performed in the same way as the optimised design of benchmark 1 in RC1, presented in Appendix H. In order to avoid the repetition of these steps, only a summary of the design results and construction costs is given. For this analysis the sensitivity of the construction costs to the following partial factors are determined:

- $\gamma_{\phi}$  (of sand, loosely packed; sand, moderately packed; clay, clean, weak and all);
- $\gamma_c$  (of clay, clean, weak);
- $\gamma_Q$  (of surface load and bollard load).

The influence of these partial factors is investigated, because only these partial factors are depending on the RC. In this sensitivity analysis the partial factors of the angle of internal friction and cohesion of peat, weak are not considered, because the thickness of this soil layer is only 1.3 m and it is expected that the influence of these partial factors on the construction costs is negligible. The values of the considered partial factors in RC1, RC2 and RC3 are collected in table 4.7.

Table 4.7 – Partial factors in RC1, RC2 and RC3

Partial factor	RC1		RC2		RC3	
			Relative increase compared to RC1		Relative increase compared to RC1	
$\gamma_{\phi}$	1.15	1.175	2.2%	1.20	4.3%	
$\gamma_c$	1.15	1.25	8.7%	1.40	21.7%	
$\gamma_Q$ (Unfavourable, A1)	1.0	1.10	10.0%	1.25	25.0%	
$\gamma_Q$ (Unfavourable, A2)	1.35	1.50	11.1%	1.65	22.2%	

In table 4.7, also the relative increase in the partial factors compared to RC1 are given. Based on these values, the partial factors in the sensitivity analysis are increased by 10% and 20%. For the partial factors of cohesion and variable, unfavourable load these increases are comparable with the increases of the partial factors in RC2 and RC3 with respect to the partial factor in RC1. However, the partial factor of the angle of internal friction in RC3 increases by only 4.3% compared to RC1. Therefore, for these partial factors also the influence on the construction costs is investigated for an increase of the partial factor of 4.3%. An overview of the evaluated situations in the sensitivity analysis is given in table 4.8. In the sensitivity analysis, the partial factors of the angle of internal friction are increased separately, but also simultaneously in order to investigate the influence of the whole partial factor.

Table 4.8 – Partial factors of the sensitivity analysis of benchmark 1

Partial factor	Sensitivity analysis		
	Increase 1 (Relative increase compared to RC1)	Increase 2 (Relative increase compared to RC1)	Increase 3 (Relative increase compared to RC1)
$\gamma_{\phi}$	1.20 (+4.3%)	1.265 (+10%)	1.38 (+20%)
$\gamma_c$	-	1.265 (+10%)	1.38 (+20%)
$\gamma_Q$ (Unfavourable, A1)	-	1.10 (+10%)	1.38 (+20%)
$\gamma_Q$ (Unfavourable, A2)	-	1.485 (+10%)	1.38 (+20%)

In table 4.9 the results of the structural dimensions of the situations of the sensitivity analysis are given.

Table 4.9 – Structural dimensions of design situations of sensitivity analysis of benchmark 1

Situation	D <sub>o</sub> piles [mm]	t piles [mm]	W <sub>eff,y</sub> [mm <sup>3</sup> / m]	Toe level piles [m NAP]	Length grout body [m]
RC1	1360	15.32	6,703,875	-27.0	7.66
Y <sub>φ',SLP</sub> +4.3%	1370	15.44	6,831,562	-27.0	7.78
Y <sub>φ',SLP</sub> +10%	1380	15.55	6,960,636	-27.1	7.99
Y <sub>φ',SLP</sub> +20%	1395	15.72	7,156,854	-27.1	8.37
Y <sub>φ',SMP</sub> +4.3%	1365	15.38	6,767,546	-27.0	7.70
Y <sub>φ',SMP</sub> +10%	1375	15.49	6,895,926	-27.0	7.67
Y <sub>φ',SMP</sub> +20%	1385	15.49	6,895,926	-27.0	7.67
Y <sub>φ',CCW</sub> +4.3%	1375	15.49	6,895,926	-27.0	7.76
Y <sub>φ',CCW</sub> +10%	1390	15.66	7,091,100	-27.0	7.84
Y <sub>φ',CCW</sub> +20%	1415	15.94	7,423,357	-27.0	8.07
Y <sub>c',CCW</sub> +10%	1365	15.38	6,767,546	-27.0	7.63
Y <sub>c',CCW</sub> +20%	1365	15.38	6,767,546	-27.0	7.69
Y <sub>Q,SL</sub> +10%	1375	15.49	6,895,926	-27.0	7.83
Y <sub>Q,SL</sub> +20%	1390	15.66	7,091,100	-27.1	8.02
Y <sub>Q,BL</sub> +10%	1360	15.32	6,703,875	-27.0	7.73
Y <sub>Q,BL</sub> +20%	1360	15.32	6,703,875	-27.1	7.73
Y <sub>φ',all</sub> +4.3%	1390	15.66	7,091,100	-27.0	7.68
Y <sub>φ',all</sub> +10%	1435	16.17	7,695,459	-27.0	7.82
Y <sub>φ',all</sub> +20%	1500	16.90	8,618,728	-27.1	8.65

In which:

- SLP = sand, loosely packed;
- SMP = sand, moderately packed;
- CCW = clay, clean, weak;
- SL = surface load;
- BL = bollard load.

Using these structural dimensions, the construction costs are estimated for each of the situations to determine the influence of the partial factor on the construction costs of benchmark 1. In figure 4.7 the results of the sensitivity analysis are depicted, with polynomial trendlines between the estimated result points starting in the value of the partial factor in RC1. The trendlines are a first estimate of the influence of the partial factors on the construction costs of benchmark 1.

In figure 4.7 vertical lines are drawn, showing the values of the partial factors in RC3. For  $\gamma_{\phi}$ -factors the sensitivity analysis is performed using values larger than the values in the RC's. These values are used to compare the influence of the partial factor of the angle of internal friction on the construction costs with the other partial factors. The trendlines of some of the influence of the partial factors on the construction costs of benchmark 1 are extrapolated to reach the partial factor value in RC3.

The slopes of the trendlines are a first estimate of the influence of the partial factor on the construction costs. From figure 4.7 follows that  $\gamma_{\phi',CCW}$  has the largest influence on the construction costs, followed by  $\gamma_{\phi',SLP}$ ,  $\gamma_{Q,SL}$  and  $\gamma_{\phi',SMP}$ . The partial factors  $\gamma_{c',CCW}$  and  $\gamma_{Q,BL}$  clearly have the least influence on the construction costs. The  $\gamma_{\phi',CCW}$  and  $\gamma_{\phi',SLP}$  have the largest influence on the construction costs, because the combi-wall is retaining these soil layers. The angle of internal friction of soil influences the active soil coefficient  $K_{y,a}$ , which determines the geotechnical loading on the combi-wall. This loading is important for the design and the construction costs of the combi-wall. The influence of  $\gamma_{\phi',CCW}$  on the construction costs is the largest, because  $K_{y,a}$  of clay, clean, weak is larger than for sand, loosely packed.  $\gamma_{\phi',SMP}$  influences the  $K_{y,p}$ , which determines the geotechnical passive resistance of the tubular piles. It is expected that this partial factor is also significantly influencing the construction costs, but for benchmark 1 the passive resistance of the tubular piles is not normative. The tubular piles are

significantly longer than required for this failure mechanism, so the partial factor  $\gamma_{\phi', SMP}$  influences the construction costs not that much. Furthermore, an important partial factor is  $\gamma_{Q, SL}$ .

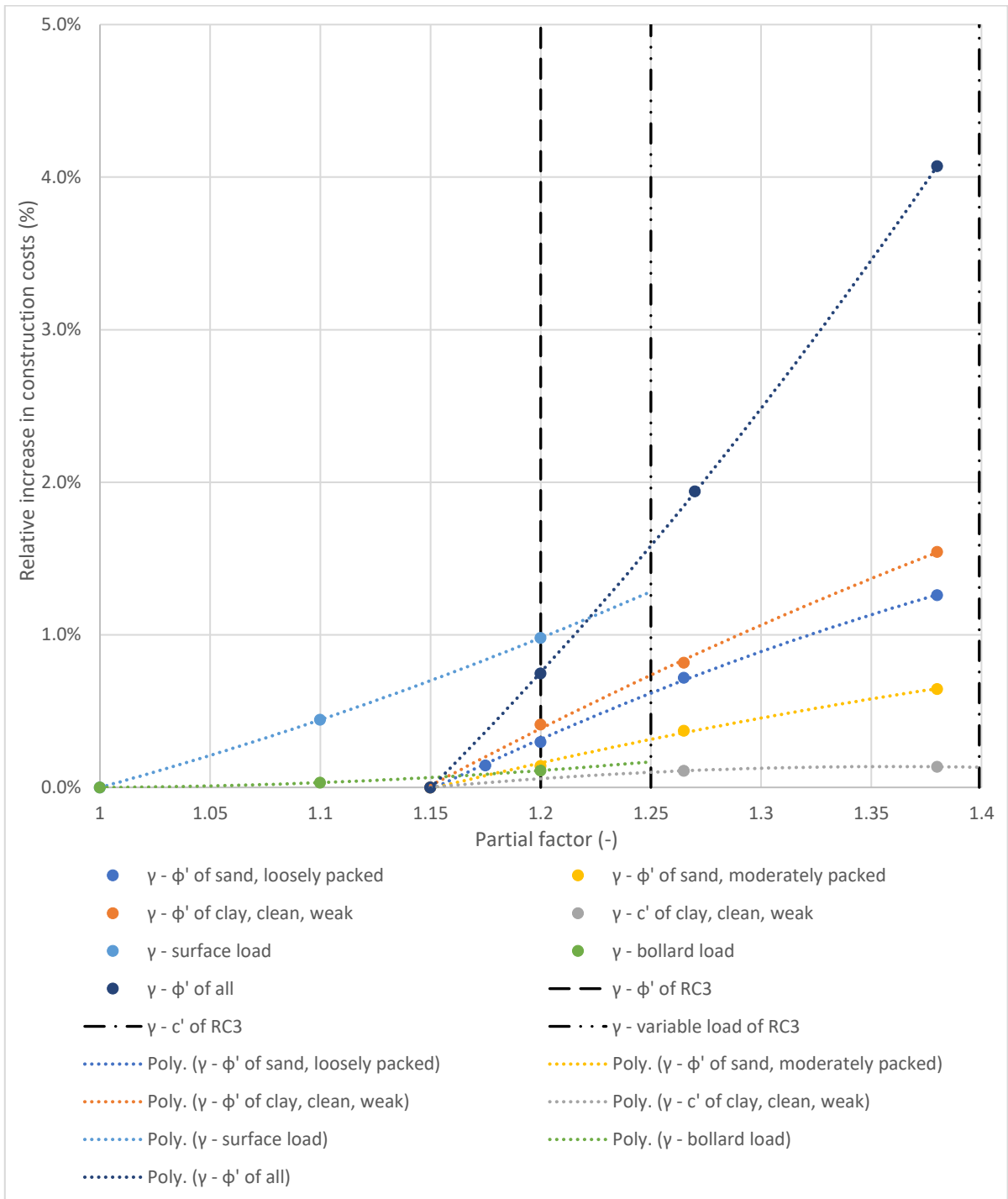


Figure 4.7 – Influence of the partial factors on the construction costs of benchmark 1

The influence of the partial factors on the construction costs can be expressed in the fraction  $\Delta C/\Delta\gamma$ , in which  $\Delta C$  is the change in construction costs and  $\Delta\gamma$  the change in partial factor value. It follows that the  $\gamma_{\phi'}$  clearly has the largest influence on the construction costs of benchmark 1, namely  $\Delta C/\Delta\gamma_{\phi'}$  is about 17%. Besides that, the  $\gamma_Q$  has an influence of  $\Delta C/\Delta\gamma_Q$  of about 5% and  $\gamma_c$  has an influence of  $\Delta C/\Delta\gamma_c$  of about 1%.

In the design calculations in RC1, RC2 and RC3 the partial factors defined in the Eurocodes have to be used. In figure 4.7 vertical lines are drawn, showing the values of the partial factors in RC3. In RC3  $\gamma_{\phi'}$

is 1.2, compared to 1.25 for  $\gamma_Q$ . So, taken into account the partial factors of the RC's, the influence of  $\gamma_Q$  on the construction costs is larger than  $\gamma_\phi$ .

#### 4.6 Influence of structural components on the construction costs

In this subchapter, the influence of several structural components on the construction costs of benchmark 1 is estimated. The influence of the structural components on the construction costs is determined by performing a sensitivity analysis by changing the dimensions of the structural components from the optimised design in RC2 alternately. So, the optimised design in RC2 forms the basis of this analysis. For this analysis the following structural components are considered:

- length of tubular piles [m];
- section modulus of tubular piles ( $W_{eff,y}$ ) [ $mm^3/m$ ];
- steel area of anchor rod [ $mm^2$ ].

These structural components are considered because these components are directly related to the normative design verifications and the following failure mechanisms:

- passive resistance inadequate;
- sheet pile profile fails;
- tension member anchorage fails.

The influence of these failure mechanisms on the construction costs are obtained in subchapter 4.7. In the sensitivity analysis, the dimensions of the structural components are varied by 10-20%, depending on the difference of the structural components between the optimised designs in RC1 and RC3. The situations in the sensitivity analysis changing the length and  $W_{eff,y}$  of the piles are chosen in such a way that the components are just transcending the designs in RC1 and RC3. The steel area of the anchor rod is changed by using a lighter and a heavier type of anchor rod of Jetmix (Appendix L) in the sensitivity analysis. In this analysis, the anchors Jetmix 82.5 x 20.0 mm and Jetmix 101.6 x 22.2 mm are considered. An overview of the structural components in the sensitivity analysis is shown in table 4.10.

Table 4.10 – Structural components of the sensitivity analysis

Structural component	RC2	Change 1 (Relative change compared to RC2)	Change 2 (Relative change compared to RC2)
Length of piles [m]	28.65	25.785 (-10%)	31.515 (+10%)
Section modulus of piles [ $mm^3/m$ ]	7,222,956	6,500,660 (-10%)	7,945,251 (+10%)
Steel area of anchor rod [ $mm^2$ ]	4,578	3,888 (-15.1%)	5,510 (+20.4)

First, the influences of the structural components on the construction costs are determined. For every situation, the construction costs are estimated, and the result points are plotted in figure 4.8. In between these points, polynomial trendlines are drawn. The trendlines are a first estimate of the influence of the structural components on the construction costs of benchmark 1.

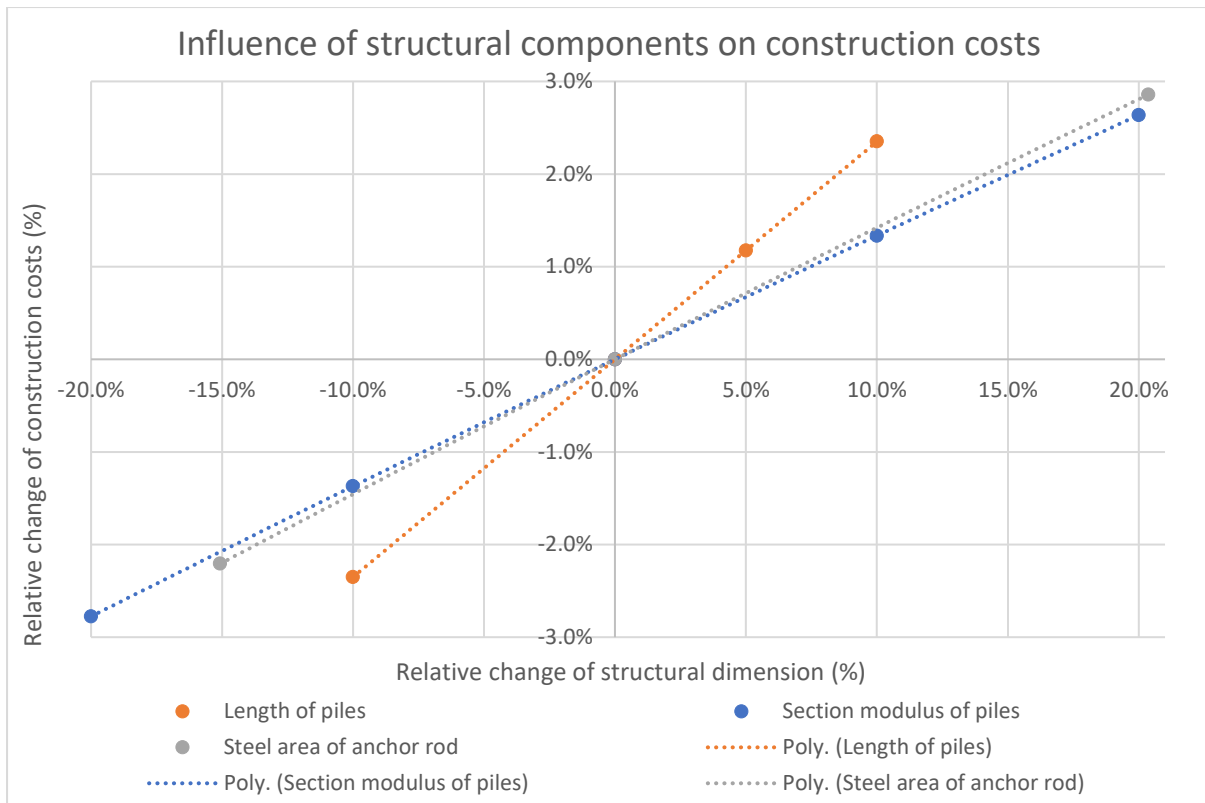


Figure 4.8 – Influence of structural components on construction costs of benchmark 1

From figure 4.8 follows that the length of the tubular piles has the most significant influence on the construction costs of benchmark 1. The length of the tubular piles influences the construction costs about 1.6 times more than the section modulus of the piles and the steel area of the anchor rod. The influence of the section modulus of the piles and the steel area of the anchor rod on the construction costs of benchmark 1 are almost equal.

#### 4.7 Influence of failure mechanisms on the construction costs

In this subchapter, the influence of three failure mechanisms on the construction costs of benchmark 1 is estimated. Previously, the influence of the corresponding structural components on the reliability index  $\beta$  is determined by performing a sensitivity analysis by changing the dimensions of the structural components from the optimised design in RC2 alternately. For this analysis, the same structural components and failure mechanisms as defined in chapter 4.6 are considered. The influence of the failure mechanisms on the construction costs can be obtained by combining the influences of the structural components on the construction costs and  $\beta$ .

The influence of the structural components on the  $\beta$  of three failure mechanisms is determined by performing reliability calculations using the reliability analyses module in D-Sheet Piling. The reliability calculations are based on the starting points of chapter 3.1.6. In the reliability calculations of benchmark 1, the limit values of the failure mechanisms 'sheet pile profile fails' and 'tension member anchorage fails' must be considered per section width, instead of per meter. The degree of mobilisation for which the passive resistance is inadequate is determined by iteration for each of the designs. The maximum allowable moment of the combi-wall changes, varying the  $W_{eff,y}$  of the piles and the design yield force of the anchor rod varying the steel area of the anchor rod. The results of the reliability calculations of the sensitivity analysis varying structural components are shown in table 4.11.

Table 4.11 – Reliability results of the sensitivity analysis varying structural components

Situation	Failure mechanism	Limit value	$\beta$ calculated
RC2	Passive resistance inadequate	100%	9.25
RC2	Sheet pile profile fails	12991 kNm / section	7.81
RC2	Tension member anchorage fails	2108 kN / anchor	8.20
$L_{piles}$ -10%	Passive resistance inadequate	100%	7.87
$L_{piles}$ -10%	Sheet pile profile fails	12991 kNm / section	7.19
$L_{piles}$ -10%	Tension member anchorage fails	2108 kN / anchor	7.92
$L_{piles}$ +5%	Passive resistance inadequate	100%	9.75
$L_{piles}$ +10%	Sheet pile profile fails	12991 kNm / section	8.44
$L_{piles}$ +10%	Tension member anchorage fails	2108 kN / anchor	8.25
$W_{eff,y}$ -10%	Passive resistance inadequate	100%	9.22
$W_{eff,y}$ -10%	Sheet pile profile fails	11659 kNm / section	7.35
$W_{eff,y}$ -10%	Tension member anchorage fails	2108 kN / anchor	8.37
$W_{eff,y}$ +10%	Passive resistance inadequate	100%	9.27
$W_{eff,y}$ +10%	Sheet pile profile fails	14352 kNm / section	8.25
$W_{eff,y}$ +10%	Tension member anchorage fails	2108 kN / anchor	8.09
$A_{rod}$ -15.1%	Passive resistance inadequate	100%	9.24
$A_{rod}$ -15.1%	Sheet pile profile fails	12991 kNm / section	7.81
$A_{rod}$ -15.1%	Tension member anchorage fails	1775 kN / anchor	6.84
$A_{rod}$ +20.4%	Passive resistance inadequate	100%	9.26
$A_{rod}$ +20.4%	Sheet pile profile fails	12991 kNm / section	7.83
$A_{rod}$ +20.4%	Tension member anchorage fails	2554 kNm / anchor	9.64

In which:

- $L_{piles}$  = length of tubular piles;
- $W_{eff,y}$  = section modulus of tubular piles;
- $A_{rod}$  = steel area of anchor rod.

The reliability calculation for 'passive resistance inadequate' for  $L_{piles} + 10\%$  is not possible with the used software, because the  $\beta$  for this situation is too large. Therefore, for this situation the  $\beta$  for  $L_{piles} + 5\%$  is determined. The calculated  $\beta$ 's are high values, like the reliability results in chapter 4.4. A possible explanation of the high  $\beta$ -values is that the investigated failure mechanisms are not normative in the design. Besides that, the partial factors of the Eurocodes are defined such that about 90% of the designs are more reliable than defined. So, extra reliability the design is expected. It is emphasised that the reliability results are first indications and just rough estimations because model uncertainties and stochastic correlations are not considered and limited different stochastic variables are used. These reliability results are elaborated and reviewed in Appendix K. From these results follows that the length of the tubular piles has a large influence on the  $\beta$  of 'passive resistance inadequate', the section modulus of the tubular piles has a significant influence on the  $\beta$  of 'sheet pile profile fails' and the steel area of the anchor rod has a large influence on the  $\beta$  of 'tension member anchorage fails'.

Now, the influence of the structural components on the construction costs and the  $\beta$  of these particular failure mechanisms are compared. By comparing these influences, the influence of the different failure mechanisms on the construction costs can be obtained. This is done, by plotting these particular reliability results against the relative increase in the construction costs in figure 4.9. The linear trendlines of these results indicates a first estimation of the relationship between the construction costs and  $\beta$  per failure mechanism. This influence of the failure mechanism can be expressed in the fraction  $\Delta C / \Delta \beta$ , in which  $\Delta C$  is the relative change in construction costs (%) and  $\Delta \beta$  the absolute change in reliability index

(-). From the figure follows that the failure mechanism ‘sheet pile profile fails’ has the largest influence on the construction costs, with a fraction  $\Delta C/\Delta\beta$  of about 3%. The influences of the failure mechanisms ‘sheet pile profile fails’ and ‘tension member anchorage fails’ are comparable, with a fraction  $\Delta C/\Delta\beta$  of about 1.8%. So, according to these results, the  $\beta$  of the quay wall can be increased in an economically attractive manner by increasing the length of the piles or the steel area of the anchor rod. It is emphasised that these results are first estimations and can differ for normative failure mechanisms.

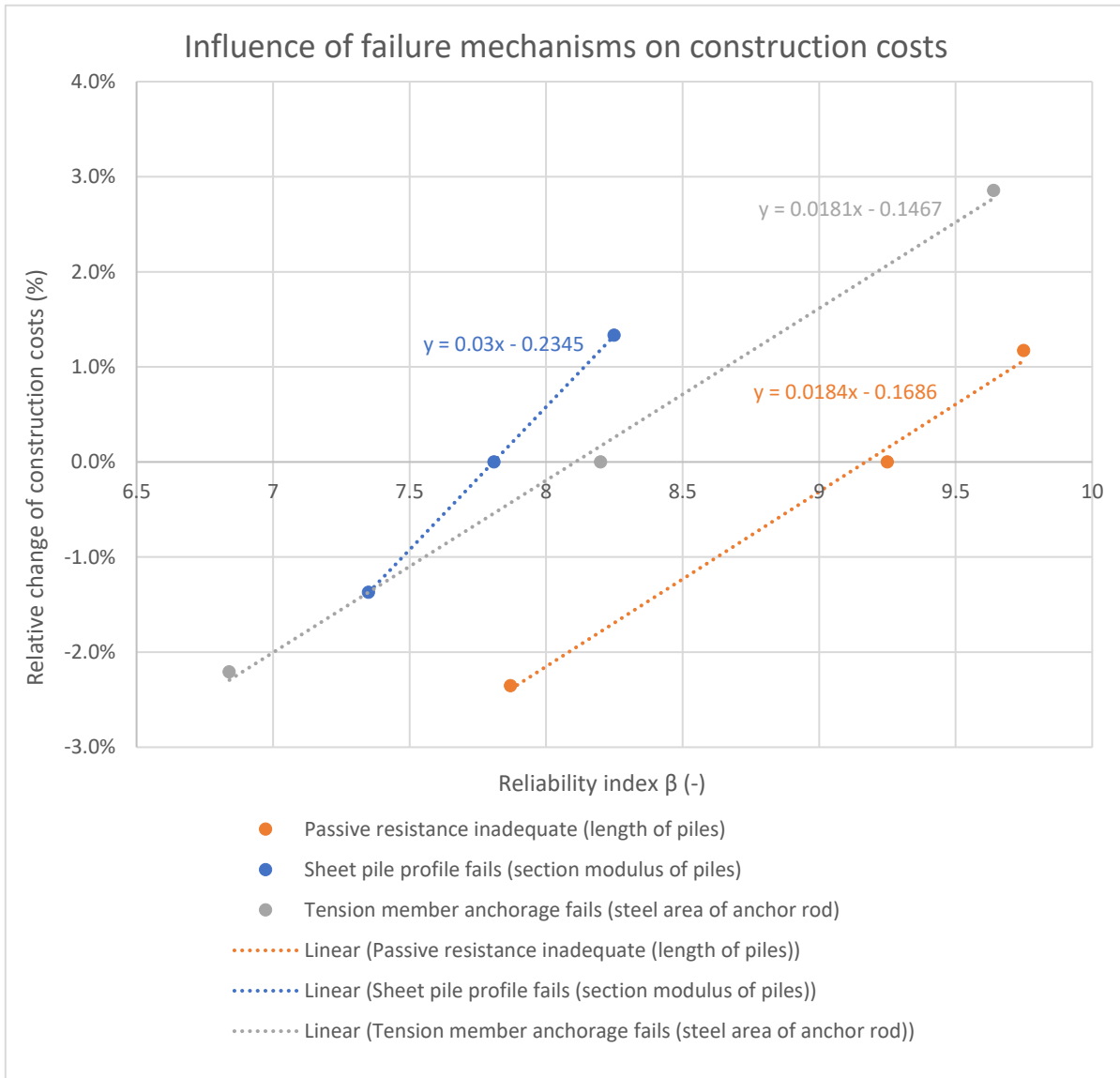


Figure 4.9 – Influence of failure mechanisms on construction costs

### 4.8 Conclusion

In this chapter, the optimised designs of benchmark 1 are performed in RC1, RC2 and RC3. The optimised designs are based on the required section modulus and in these designs, it is assumed that every combination of diameter and thickness of the tubular pipes can be used. It is notable that the differences between the design results of benchmark 1 in RC1, RC2 and RC3 are relatively small. The required toe level of the tubular piles in order to satisfy the vertical bearing capacity verification varies within one meter, and the required length of the grout body of the anchors within about 1.1 meters (14%). The section modulus of the combi-wall of the different designs varies within 18%. However, the section modulus differences do not influence the construction costs that much because the section modulus also influences the section width of the combi-wall. Construction costs differences between the designs in RC1, RC2 and RC3 are only about 1-3%. The construction costs of the combi-wall, anchors, concrete work and cathodic protection vary between the designs.

Furthermore, the influence of the different partial factors on the construction costs are determined. The influence of the partial factors on the construction costs can be expressed in the fraction  $\Delta C/\Delta\gamma$ , in which  $\Delta C$  is the change in construction costs and  $\Delta\gamma$  the change in partial factor value. It follows that the  $\gamma_\phi$  clearly has the largest influence on the construction costs of benchmark 1, namely  $\Delta C/\Delta\gamma_\phi$  is about 18%. Besides that, the  $\gamma_\alpha$  has an influence of  $\Delta C/\Delta\gamma_\alpha$  of about 5% and  $\gamma_c$  has an influence of  $\Delta C/\Delta\gamma_c$  of about 1%. Taken into account the defined values of the partial factors in the RC's, the  $\gamma_\alpha$  has the largest influence on the construction costs, followed by the  $\gamma_\phi$  and the  $\gamma_c$  thereafter.

From the reliability calculations also follow  $\alpha^2$ -values, representing the contribution of the stochastic variables to the  $\beta$  per failure mechanism. The stochastic variables are also the variables which are influenced by the partial factors. Therefore, the influence of the partial factors on the construction costs can be compared to their influence on the  $\beta$  per failure mechanism. It follows that the  $\phi'$  dominates the contribution to the  $\beta$  of all three failure mechanisms and the influence of the surface load on the  $\beta$  of the failure mechanisms 'sheet pile profile fails' and 'tension member fails' is reasonable. Besides that, the contribution of  $c'$  to the  $\beta$  of the three considered failure mechanisms is very low. These influences of the partial factors on the construction costs are comparable to their influences on the  $\beta$ . It can be concluded that in the initial phase of a quay wall design, the determination of  $\phi'$  strongly influences the construction costs and the  $\beta$  of the quay wall, in contrast to  $c'$ .

Besides that, the influence of some failure mechanisms on the construction costs is investigated, by performing a sensitivity analysis with the corresponding structural components. The sensitivity of the construction costs and reliability index  $\beta$  for these structural components is obtained. The obtained  $\beta$ -values of the failure mechanisms 'passive resistance inadequate', 'sheet pile profile fails' and 'tension member anchorage fails' are estimated very high for these designs. The most important reason for this is that the investigated failure mechanisms are not normative in the design verifications. For benchmark 1 the following failure mechanisms are normative; 'bearing capacity of tubular piles inadequate', 'local buckling of combi-wall' and 'soil mechanical failure of tension member'.

From the sensitivity analysis follows that the length of the piles has the largest influence on the costs, followed by the steel surface of the anchor rod and the section modulus of the piles. Combining these results with the  $\beta$ -values, it seems that the failure mechanism 'sheet pile profile fails' has the largest influence on the construction costs, with a fraction  $\Delta C/\Delta\beta$  of about 3%. The influences of the failure mechanisms 'sheet pile profile fails' and 'tension member anchorage fails' are comparable, with a fraction  $\Delta C/\Delta\beta$  of about 1.8%. So, according to these results, the  $\beta$  of the quay wall can be increased in an economically attractive manner by increasing the length of the piles or the steel area of the anchor rod.

# 5 Results benchmark 2: combi-wall with a relieving platform

The design calculations and construction costs estimations of the benchmark 2 quay wall are performed, and the results are presented in this chapter. In figure 5.1 a flow diagram of the research steps of this chapter is given. Firstly, the design principles of the benchmark quay wall are treated in chapter 5.1. This benchmark is designed semi-probabilistic in RC1, RC2 and RC3 in chapter 5.2 and the construction costs of these designs are estimated and compared in chapter 5.3. The influence of partial factors on the construction costs is estimated in chapter 5.4 by performing a sensitivity analysis in which these factors are varied alternately. Besides that, in chapter 5.5 the influence of several structural components on the construction costs is estimated. There are no reliability calculations performed for these designs because the considered failure mechanisms are not normative in the design. So, for this benchmark, the influence of failure mechanisms on the construction costs is not considered. This chapter ends with a conclusion of the most important results of benchmark 2 in chapter 5.6.

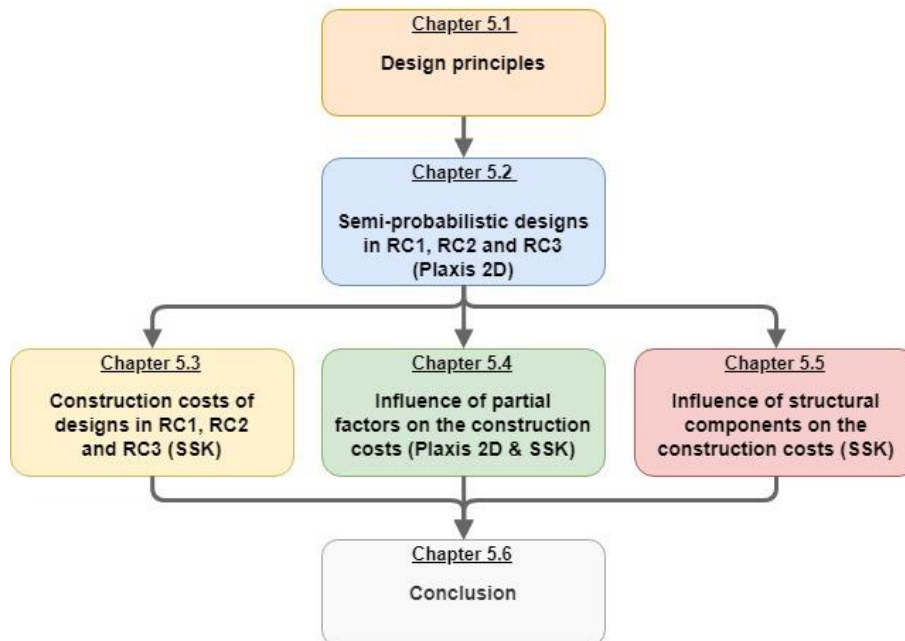


Figure 5.1 – Flow diagram of research steps of chapter 5

## 5.1 Design principles

The final semi-probabilistic design of benchmark 2 in RC2 was already performed by designers and is described in a design report (Arcadis, 2016). From the starting points the combi-wall, vibro piles and anchoring are designed, and several verifications are performed:

- check overall stability of the quay wall;
- check capacity combi-wall and sheet piles;
- check and design vibro piles;
- check and design anchoring;
- check vertical bearing capacity of the tubular piles;
- check deformation of the quay wall.

From the design report of benchmark 2 follows that the capacity of the combi-wall, vibro piles, anchoring and the vertical bearing capacity of the tubular piles are normative for the design of the quay wall. Therefore, only these verifications are considered in this study. The overall stability of the quay wall is checked in the design model of benchmark 2 and the capacity of the sheet piles is reviewed in this

stage. It appears that the RC has no influence on the required sheet pile profile for benchmark 2, so the capacity of the sheet piles is satisfied in all different designs. Furthermore, the requirements for the deformation of the quay wall are easily satisfied in the existing. Therefore, a reasonable assumption is that the deformations of the other designs also satisfy. Benchmark 2 is designed using the FEM of Plaxis 2D and several calculation sheets on behalf of the particular design verifications.

In this research the benchmark is designed for different reliability levels, using different partial factors. For these designs, most of the starting points are constant in order to be able to compare the reliability level and construction costs of these designs. Only the following structural elements, which are directly related to the considered design verifications, are adaptable in the different designs:

- diameter of the tubular piles;
- thickness of the tubular piles;
- toe level of the tubular piles;
- toe level of the vibro piles;
- length of the grout body of the anchors.

The thickness of the anchor rods is constant in the different designs because this structural element is not normative in the anchor design. Besides that, the thickness of the grout body is constant, because it is sufficient to increase the change of the grout bodies. The toe level of the intermediate sheet piles is constant in the designs, because it is assumed that the zero level of the resulting stress on the quay wall is constant over the different designs.

For benchmark 2 the optimised design and the design based on standard available dimensions of tubular piles are performed, just like benchmark 1. In this chapter, the optimised designs of benchmark 2 are presented, and the designs based on standard dimensions of benchmark 2 are treated in Appendix M. In the optimised design, the design is based on the required section modulus, and it is assumed that every combination of diameter and thickness of the tubular pipes can be used. Further explanation about the difference between the optimised design and the design based on standard dimensions is elaborated in chapter 4.1.

The final design based on standard dimensions of benchmark 2 in RC2 was already performed by designers and the other designs, in the other reliability classes, are performed in this study. In order to avoid the repetition, only the design calculations of the optimised design of benchmark 2 in RC1 are presented in Appendix N of this report. From the other designs of benchmark 2 a summary of the design results is given.

### 5.1.1 Optimised design

The optimised design of benchmark 2 is obtained by an iterative process, varying the toe level of the tubular piles and vibro piles and the length of the grout body with 10 cm. Besides that, the section modulus of the tubular piles of the combi-wall is varied. The section modulus is depending on the cross-section of the tubular piles, so both the outer diameter  $D_o$  and thickness  $t$  is influencing the section modulus. In the design principles of benchmark 1 in chapter 4.1.1, the section modulus is further explained. In order to relate the different designs with different reliability levels to the section modulus of the piles, the ratio  $D_o/t$  is constant in the optimised designs. The ratio  $D_o/t$  of the existing design in RC2 is chosen as the constant ratio, namely  $1422/21 = 67.72$ .

In the iterative design process, the different verifications are considered until all verifications are just right. First, the quay wall is modelled in Plaxis in which the geotechnical stability of the structure is checked. The local buckling verification is just right when the unity check for local buckling is in between 0.99 and 1.0. The vertical bearing capacity verifications are just right when the unity check is first below 1.0 when the toe level of the tubular piles or vibro piles is lowered. Furthermore, the anchor resistance verification is just right, when the unity check is first below 1.0 when the length of the grout body is decreased.

## 5.2 Semi-probabilistic design results

The optimised design of benchmark 2 in RC1 is performed first, from which the design calculations are presented in Appendix N. Benchmark 2 is designed in RC2 and RC3 in the same way as the optimised

design of benchmark 2 in RC1. In order to avoid the repetition of these steps, only a summary of the design results is given in this subchapter.

The vertical bearing capacity of the tubular piles of the quay wall is verified conform NEN 9997-1. Since 01-01-2017 the pile class factor for the point resistance ( $\alpha_p$ ) in this verification was modified from 1.0 to 0.7, lowering the vertical bearing capacity. Initially, benchmark 2 is designed using the bearing capacity verification of pre-2017, containing  $\alpha_p = 1.0$ , as is done in the existing design. Besides that, benchmark 2 is also designed using the bearing capacity verification of post-2016, containing  $\alpha_p = 0.7$ , to be consistent with benchmark 1. The results of the structural dimensions of the optimised semi-probabilistic designs of benchmark 2, using  $\alpha_p = 1.0$ , are collected in table 5.1 and the results using  $\alpha_p = 0.7$ , are collected in table 5.2. In the comparison of both types of benchmark quay walls, the results of the design using the post-2016 bearing capacity verification, containing  $\alpha_p = 0.7$ , have to be used because benchmark 1 is also designed using  $\alpha_p = 0.7$  and this vertical bearing capacity verification is currently used.

Table 5.1 – Structural dimension of optimised semi-probabilistic designs of benchmark 2,  $\alpha_p = 1.0$

Structural characteristics	RC1	RC2	RC3
<b>D<sub>o</sub> piles [mm]</b>	1225	1310	1495
<b>t piles [mm]</b>	18.09	19.35	22.08
<b>D<sub>o</sub> / t [-]</b>	67.72	67.72	67.72
<b>Section width combi-wall [m]</b>	3.54	3.62	3.81
<b>W<sub>eff,y</sub> piles [mm<sup>3</sup> / m]</b>	5,769,546	6,890,141	9,742,977
<b>Toe level tubular piles [m NAP]</b>	-34.5	-33.8	-37.0
<b>Toe level vibro piles [m NAP]</b>	-27.8	-27.8	-27.9
<b>Length grout body [m]</b>	7.3	8.0	9.6

Table 5.2 – Structural dimension of optimised semi-probabilistic designs of benchmark 2,  $\alpha_p = 0.7$

Structural characteristics	RC1	RC2	RC3
<b>D<sub>o</sub> piles [mm]</b>	1225	1300	1475
<b>t piles [mm]</b>	18.09	19.20	21.78
<b>D<sub>o</sub> / t [-]</b>	67.72	67.72	67.72
<b>Section width combi-wall [m]</b>	3.54	3.61	3.79
<b>W<sub>eff,y</sub> piles [mm<sup>3</sup> / m]</b>	5,769,546	6,752,205	9,406,606
<b>Toe level tubular piles [m NAP]</b>	-43.8	-43.5	-40.8
<b>Toe level vibro piles [m NAP]</b>	-27.8	-27.8	-27.9
<b>Length grout body [m]</b>	6.9	7.6	9.3

It is checked that the extended grout bodies are still located in the sand layer. The design results of table 5.1 and table 5.2 are comparable, except for the required toe level of the tubular piles, due to the  $\alpha_p$  used. In the design calculations, only the section modulus of the tubular piles, the length of the tubular piles, the length of the vibro piles and the length of the grout bodies are varied. Notable is that the required section modulus of the tubular piles, the length of the piles and the length of the grout body of the anchors increases more in RC3 with respect to RC2. The required length of the vibro piles in the different designs is almost equal.

From these results can be obtained that the required toe level of the tubular piles in the design of benchmark 2, using  $\alpha_p = 0.7$ , is considerably lower than for the design using  $\alpha_p = 1.0$ . Designing the quay wall using  $\alpha_p = 0.7$ , the section modulus of the tubular piles is lowered until the buckling verification is just right. The section modulus of the piles is lowered by decreasing the diameter and thickness of the piles. When decreasing the diameter of the piles, the tip resistance of the piles decreases, and the vertical bearing capacity of the piles reduces. Therefore, the required toe level of the tubular piles decreases at a higher RC. This is also the case for the optimised design in RC1 and RC2, using  $\alpha_p = 1.0$ . However, in the design of benchmark 2 in RC3, using  $\alpha_p = 1.0$ , the toe level of the tubular piles had to be lowered in order to reduce the internal forces of the combi-wall. Lengthening of the tubular piles is required to fulfil the deformation verification and reduce the bending moment in the combi-wall as well. So, in the optimised designs of benchmark 2 in RC3, using  $\alpha_p = 1.0$ , the toe level of the piles is

chosen based on the internal forces of the combi-wall instead of on the vertical bearing capacity of the piles.

The anchor forces are increasing together with the increased horizontal soil displacements, driven by the increased surface load and decreased soil characteristics. The vertical bearing capacity of the vibro piles are independent of the RC, so the maximal base resistance of the vibro piles is constant in the different Plaxis models. The maximal base capacity is used completely in the design in RC1 already. Therefore, the normal forces in the vibro piles are almost equal in the different designs.

### 5.3 Construction costs estimation

In this subchapter, the construction costs of the semi-probabilistic designs of benchmark 2 are determined and discussed. Besides that, the execution classes of the steel structures of benchmark 2 and the assumptions regarding these classes are treated. The construction costs of benchmark 2 are excluding the same type of costs as for benchmark 1, as described in chapter 4.3. The construction costs of benchmark 2 consist of the following cost components:

- soil work;
- drainage;
- construction pit;
- combi-wall;
- anchors;
- vibro piles;
- relieving platform;
- joints;
- fenders and bollards;
- dredging work;
- cathodic protection.

As for benchmark 1, the construction costs of benchmark 2 are estimated deterministic using the standard cost estimate system (standaardsystematiek voor kostenramingen - SSK). In the existing design of benchmark 2, an SSK calculation sheet was prepared by cost specialists. In this calculation sheet, the activities accompanying to the cost components above were collected and expressed per unit of length, area, volume, number or weight. The cost of these activities are estimated using unit prices, which are based on standard prices and prices of previous quay wall projects. This calculation sheet is validated using construction costs unit prices of the Port of Rotterdam (Koene, 2018). The activities in the calculation sheet consist of the supply of materials and construction of structures, including labour- and equipment costs. It is emphasised that the construction cost calculation sheet is based on present (2016) unit prices, which can deviate in the future. Besides that, model uncertainties of the design and project risks are not considered in the construction costs. So, these results give a reasonable first insight into the construction costs.

#### 5.3.1 Construction costs estimation of optimised designs

The construction costs estimations of the optimised designs of benchmark 2 in RC1, RC2 and RC3 are discussed in this subchapter, for both the designs using the pre-2017- ( $\alpha_p = 1.0$ ) as the post-2016 ( $\alpha_p = 0.7$ ) bearing capacity verifications. These construction costs are estimated per cost component, and thereafter the total construction costs are determined. In order to estimate the construction costs per running meter, the total construction costs are divided by the total length of benchmark 2 of about 246 m. Besides that, the relative increase in the construction costs compared to the design in RC1 is estimated as well. In table 5.3 an overview of the construction costs estimation of benchmark 2, excluding Value Added Tax (VAT), is given.

The construction costs of the designs in RC1, RC2 and RC3 deviate as the differences of the structural dimensions of the designs. Variation of the diameter, thickness and length of tubular piles, the length of the anchors and the length of the vibro piles influence the required amount of steel. Besides that, the diameter of the piles also influences the section width of combi-wall, which influences the required supply and construction amount of tubular piles or the required amount of cathodic protection.

In the determination of the construction costs, it is assumed that the dimensions of the relieving platform are constant in the different designs. Besides that, it is assumed that the required amount of steel used in the relieving platform is also constant. Therefore, the construction costs of the relieving platform are not influenced by the RC in this case. It is expected that this is a reasonable assumption because in the structural design calculations the crack width of the concrete is normative. In the crack width verification, the SLS loads are applied, which means that it is likely that the required amount of steel in the platform is independent of the RC. Differences in the required amount of steel can have a significant influence on the construction costs. A 5% increase in the amount of steel used in the platform would increase the total construction costs by about 1%.

Table 5.3 – Construction costs overview of optimised semi-probabilistic designs

Reliability class	Construction costs (€/m)		Relative increase compared to RC1	
	$\alpha_p = 1.0$	$\alpha_p = 0.7$	$\alpha_p = 1.0$	$\alpha_p = 0.7$
RC1	€ 34,367.-	€ 35,539.-	0.00%	0.00%
RC2	€ 34,715.-	€ 36,017.-	1.01%	1.08%
RC3	€ 36,315.-	€ 36,839.-	5.67%	3.42%

The relative increase in construction costs for the design in RC2 is about 1% for both design principles, in which  $\alpha_p = 1.0$  and  $\alpha_p = 0.7$  are used. For the design principle using  $\alpha_p = 1.0$ , the relative construction costs increase in RC3 is about 5.7%, which is significantly larger than the increase in RC3 using  $\alpha_p = 1.0$ , of about 3.4%. This difference in the relative increase in construction costs between the used  $\alpha_p$ 's in RC3 complies with the difference in the required toe level of the tubular piles. These relative increases in the construction costs of the designs in RC2 and RC3 compared to RC1 are plotted against the target  $\beta$ -values of the RC's, as defined in the Eurocodes, in figure 5.2.

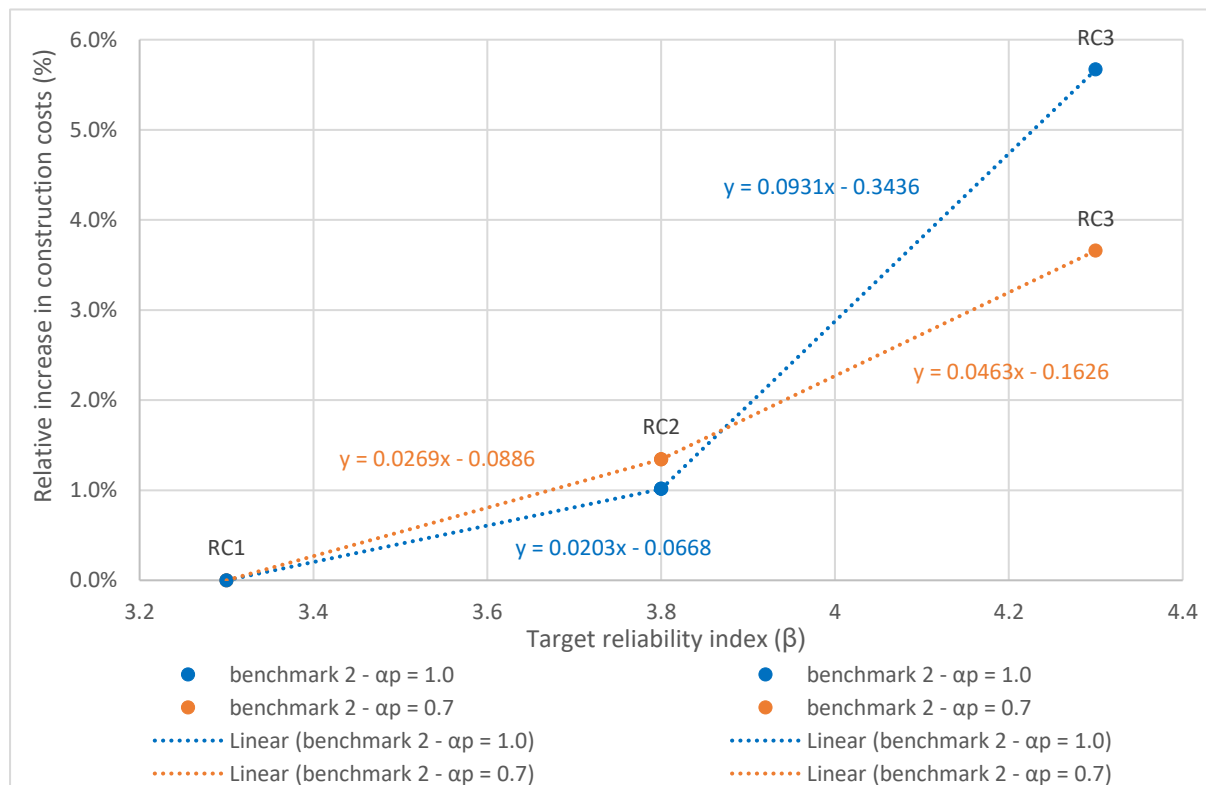


Figure 5.2 – Construction costs increase of quay walls designed semi-probabilistic in RC1, RC2 and RC3

From figure 5.2 follows a first estimation of the ratio  $\Delta C / \Delta \beta_{\text{target}}$  as the slope number of the linear trendlines. So, the ratio  $\Delta C / \Delta \beta_{\text{target}}$  between RC1 and RC2 is about 2.0% using  $\alpha_p = 1.0$  and about 2.7% using  $\alpha_p = 0.7$ . Besides that, the ratio  $\Delta C / \Delta \beta_{\text{target}}$  between RC2 and RC3 is about 9.3% using  $\alpha_p = 1.0$  and about 4.6% using  $\alpha_p = 0.7$ . In the comparison of both types of benchmark quay walls, the results of

the design using the post-2016 bearing capacity verification, containing  $\alpha_p = 0.7$ , have to be used because benchmark 1 is also designed using  $\alpha_p = 0.7$  and this vertical bearing capacity verification is currently used. So, it follows that the ratio  $\Delta C/\Delta\beta_{\text{target}}$  is estimated between about 2.5-5%, which is even lower than the estimations of 5-10% by Roubos et al. and Schweckendiek et al. (Roubos et al., 2018). It is emphasised that these ratios are a first estimation because the fraction  $\Delta\beta_{\text{target}}$  is based on the target  $\beta$ -values defined in the Eurocodes and may differ per design.

From the results follows that the relative costs difference between the designs in RC2 and RC3, is significantly larger than the difference between the designs in RC1 and RC2, for the design principle using  $\alpha_p = 1.0$ . Therefore, the construction costs of these designs are considered below. These differences are in compliance with the structural dimensions of the designs. The design in RC3 contains significantly longer, thicker and larger tubular piles of the combi-wall and longer anchors. It is emphasised the results are cost estimations and give a reasonable first insight into the construction costs considering the functionality of benchmark 2.

An overview of the relative construction costs comparison of the different cost components of the optimised designs of benchmark 2, using  $\alpha_p = 1.0$ , is given in figure 5.3.

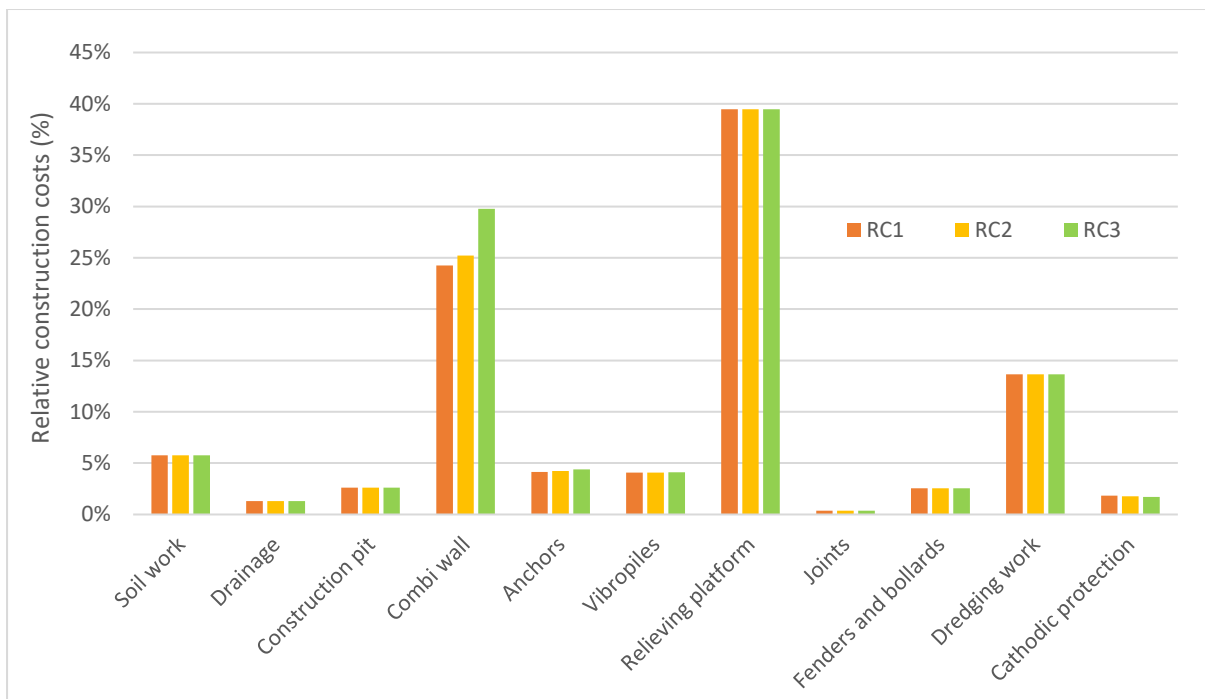


Figure 5.3 – Relative construction costs comparison of optimised designs of benchmark 2,  $\alpha_p = 1.0$

From the construction costs comparison follows that only the costs of the combi-wall, anchors, vibro piles and cathodic protection differ between the designs in RC1, RC2 and RC3. The relative cost increase compared to RC1 of these cost components are depicted in figure 5.4. The construction costs of the combi-wall, anchors and vibro piles increases in compliance with dimensions of these structural components of the quay wall. Furthermore, the cost of cathodic protection decreases together with the required number of sections of the combi-wall in the designs in RC2 and RC3.

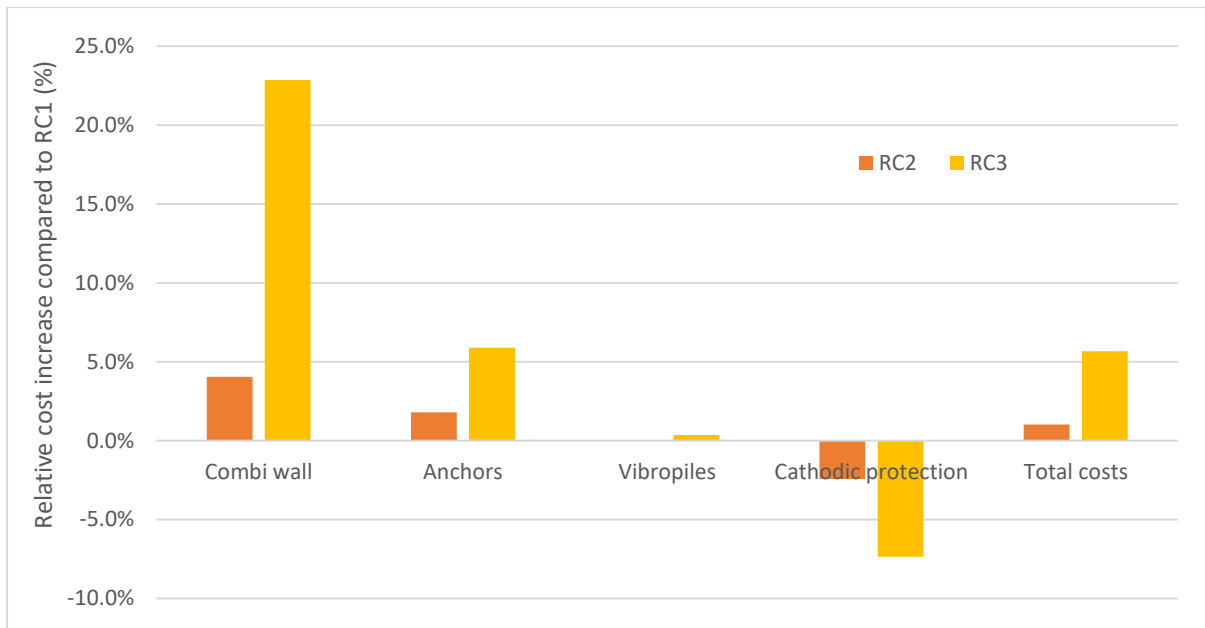


Figure 5.4 – Relative cost increase compared to the design in RC1,  $\alpha_p = 1.0$

### 5.3.2 Execution class steel structures

As for benchmark 1, the execution classes have to be determined for benchmark 2 as well, which specify a classified set of requirements for the execution of the works related to the quay wall construction. These requirements are specified in order to ensure adequate levels of mechanical resistance and stability, serviceability and durability and are further explained in chapter 2.3.1.4.

The execution class is determined in the same way as for benchmark 1, explained in chapter 4.3.2. Besides that, the execution classes for the designs in the reliability classes are equal to benchmark 1, and an overview of these is given in table 4.3. In this study, it is assumed that the construction costs are not influenced by these EXC's. In reality, the construction costs of the designs in RC2 and RC3 will differ more.

### 5.4 Influence of partial factors on the construction costs

The influence of the partial factors on the construction costs of benchmark 2 is investigated performing a sensitivity analysis, as is done for benchmark 1. In the sensitivity analysis, the partial factors from the optimised design in RC1 are increased alternately. So, the optimised design in RC1, forms the basis of this analysis. For every situation in the sensitivity analysis, the optimised design of benchmark 2 is performed, and the design meets the requirements when, after several iterations, all the design verifications are just right. The design calculation is performed in the same way as the optimised design of benchmark 2 in RC1, presented in Appendix N. In order to avoid the repetition of these steps, only a summary of the design results and construction costs is given. For this analysis the sensitivity of the construction costs to the following partial factors are determined:

- $\gamma_\phi$  (of all);
- $\gamma_c$  (of all);
- $\gamma_Q$  (of surface load, crane load bollard load).

The influence of these partial factors is investigated because only these partial factors are depending on the RC. The influence of all angle of internal frictions and cohesion together are investigated, because of the large number of different soil layers. The values of the considered partial factors in RC1, RC2 and RC3 are collected in table 5.4.

Table 5.4 – Partial factors in RC1, RC2 and RC3

Partial factor	RC1		RC2		RC3	
			Relative increase compared to RC1			Relative increase compared to RC1
$\gamma_{\phi'}$	1.2	1.25	4.17%		1.30	8.33%
$\gamma_{c'}$	1.3	1.45	11.54%		1.60	23.08%
$\gamma_Q$ (on top of superstructure: surface / crane)	1.35	1.50	11.1%		1.65	22.2%
$\gamma_Q$ (behind superstructure: surface / coal)	1.0	1.10	10%		1.25	25.0%
$\gamma_Q$ (bollard load)	1.17	1.30	11.1%		1.43	22.2%

In the table above also, the relative increase in the partial factors compared to RC1 are given. Based on these values, the partial factors in the sensitivity analysis are increased by 10% and 20%. The increases of the partial factors of cohesion and load are comparable with the RC's, in contrast to the partial factor of the angle of internal friction. These partial factors are increased with the same values, in order to be able to compare the results. An overview of the evaluated situations in the sensitivity analysis is given in table 5.5.

Table 5.5 – Partial factors of the sensitivity analysis of benchmark 2

Partial factor	Location	Sensitivity analysis	
		Increase 1 (Relative increase compared to RC1)	Increase 2 (Relative increase compared to RC1)
$\gamma_{\phi'}$		1.32 (+10%)	1.44 (+20%)
$\gamma_{c'}$		1.43 (+10%)	1.56 (+20%)
$\gamma_Q$ (surface load)	On top of superstructure	1.485 (+10%)	1.62 (+20%)
	Behind superstructure	1.10 (+10%)	1.20 (+20%)
$\gamma_Q$ (crane load)		1.485 (+10%)	1.62 (+20%)
$\gamma_Q$ (bollard load)		1.287 (+10%)	1.404 (+20%)

In table 5.6 the results of the structural dimensions of the situations of the sensitivity analysis are given.

Table 5.6 – Structural dimensions of design situations of sensitivity analysis of benchmark 2

Situation	$D_o$ piles [mm]	t piles [mm]	$W_{eff,y}$ [mm <sup>3</sup> / m]	Toe level piles [m NAP]	Toe level vibro piles [m NAP]	Length grout body [m]
RC1	1225	18.09	5,769,546	-34.5	-27.8	7.30
$\gamma_{\phi',all}$ +10%	1470	21.71	9,406,606	-33.0	-27.9	9.30
$\gamma_{\phi',all}$ +20%	1700	25.40	13,593,308	-39.0	-27.9	10.20
$\gamma_{c',all}$ +10%	1230	18.16	5,832,233	-34.4	-27.8	7.30
$\gamma_{c',all}$ +20%	1235	18.24	5,895,320	-34.3	-27.8	7.30
$\gamma_{Q,SL}$ +10%	1250	18.46	6,086,993	-34.4	-27.8	7.10
$\gamma_{Q,SL}$ +20%	1300	19.20	6,752,205	-33.5	-27.8	8.30
$\gamma_{Q,CL}$ +10%	1230	18.16	5,832,233	-34.4	-27.8	7.20
$\gamma_{Q,CL}$ +20%	1240	18.31	5,958,809	-35.1	-27.8	7.00
$\gamma_{Q,BL}$ +10%	1230	18.16	5,832,233	-34.4	-27.8	7.30
$\gamma_{Q,BL}$ +20%	1235	18.24	5,895,320	-34.3	-27.8	7.30

In which:

- SL = surface load;
- CL = crane load;
- BL = bollard load.

The construction costs are estimated for each of the situations, based on these structural dimensions. Using these costs, the influence of the partial factor on the construction costs of benchmark 2 can be estimated. In figure 5.5 the results of the sensitivity analysis are depicted, with polynomial trendlines between the estimated result points starting in the value of the partial factor in RC1. The trendlines are a first estimate of the influence of the partial factors on the construction costs of benchmark 2.

In the figure also vertical lines are drawn, showing the partial factor values in RC3. For  $\gamma_\phi$ -factors the sensitivity analysis is performed using values larger than the values in the RC's. These values are considered in order to be able to compare the influence of the partial factor of the angle of internal friction on the construction costs with the influence of the other partial factors. The trendlines of the other partial factors of benchmark 2 are extrapolated, in order to reach the partial factor value in RC3.

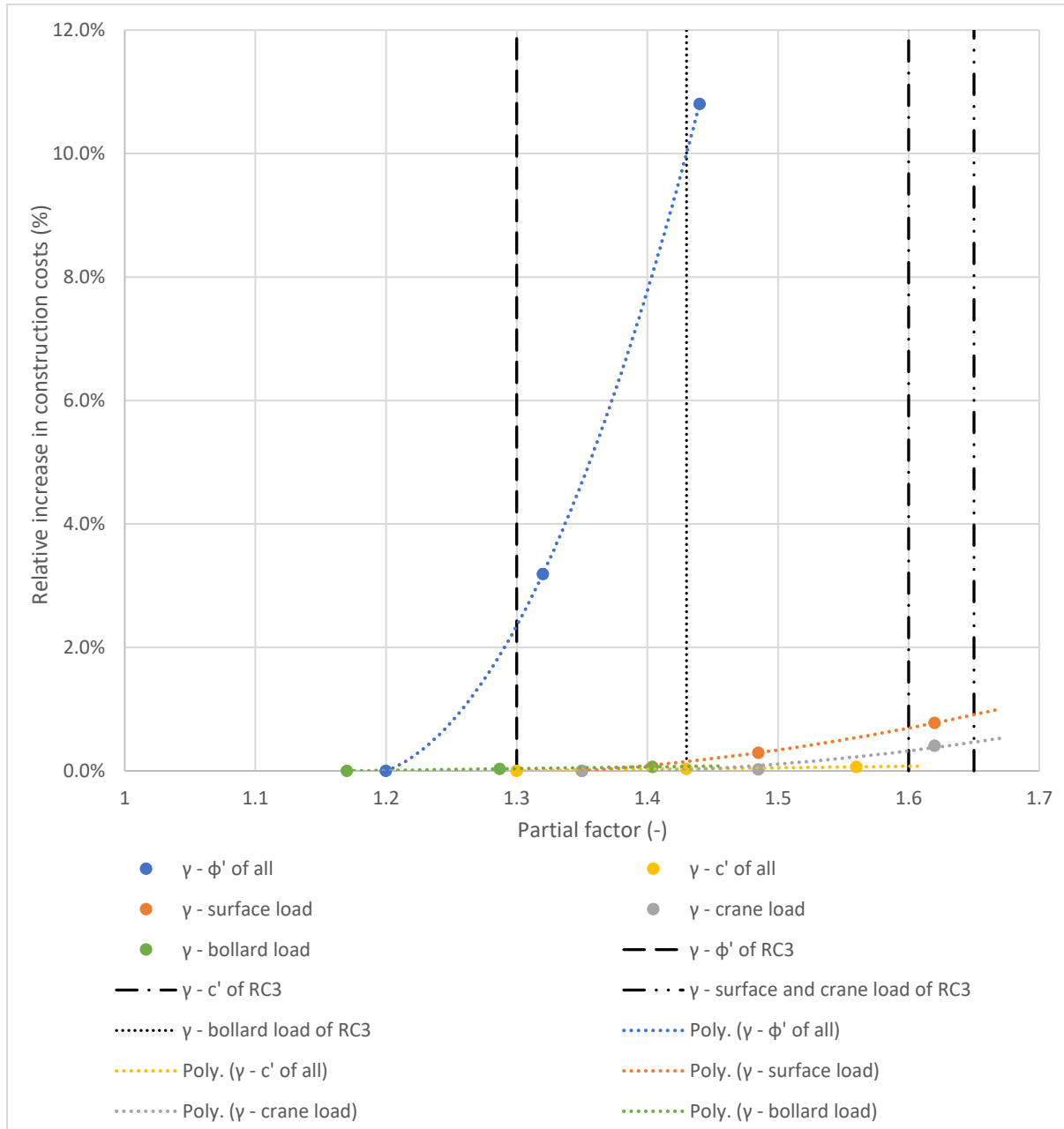


Figure 5.5 – Influence of the partial factors on the construction costs of benchmark 2

The slopes of the trendlines are a first estimate of the influence of the partial factor on the construction costs. From figure 5.5 follows that the influence of  $\gamma_\phi$  on the construction costs of benchmark 2 is obviously the largest and increases for larger  $\gamma_\phi$ -values. The angle of internal friction of soil influences the active soil coefficient  $K_{\gamma,a}$ , which determines the geotechnical loading on the combi-wall. This loading

is dominant for the design and the construction costs of benchmark 2. The influence of the other partial factors is depicted more clearly in figure 5.6, in which the influence of  $\gamma_\phi$  is excluded.

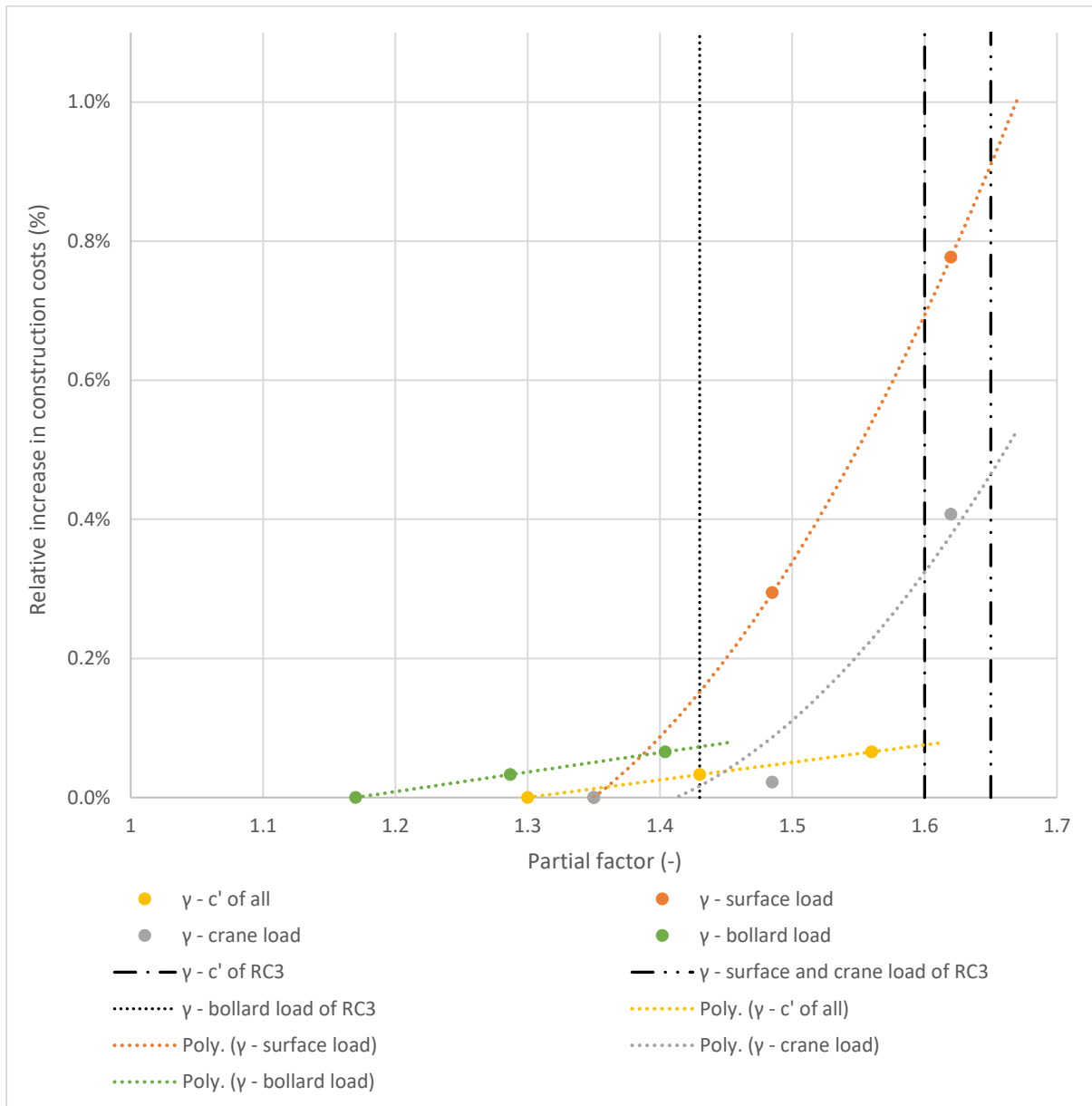


Figure 5.6 – Influence of the partial factors (excluding  $\phi$ ) on the construction costs of benchmark 2

From figure 5.6 follows that the influence of  $\gamma_{c'}$  and  $\gamma_{Q, BL}$  are both very low. Besides that,  $\gamma_{Q, CL}$  has some influence on the construction costs and increases for higher  $\gamma_{Q, CL}$ -values and  $\gamma_{Q, SL}$  has a significant influence on the construction costs. Except for the relieving platform, the combi-wall is the dominating cost component of benchmark 2. The surface load (behind the relieving platform) is the dominant loading and has the largest influence on the construction costs of benchmark 2, because it influences the horizontal loading of the combi-wall. The crane- and bollard load are acting on the relieving platform, which can be partially resisted by the vibro piles vertically and the anchors horizontally. These components are not dominating the construction costs, resulting in less influence on these.

The influence of the partial factors on the construction costs can be expressed in the fraction  $\Delta C/\Delta\gamma$ , in which  $\Delta C$  is the relative change in construction costs (%) and  $\Delta\gamma$  the absolute change in partial factor value (-). This fraction can be estimated using linear trendlines in figure 5.5 and figure 5.6. The trendlines of the influence of  $\gamma_\phi$  and  $\gamma_{Q, BL}$  does not have a linear character, so the fractions are a first estimation. It follows that the  $\gamma_\phi$  clearly has the largest influence on the construction costs of benchmark

2, namely  $\Delta C/\Delta\gamma_\psi$  is about 45%. Besides that, the  $\gamma_Q$  has an influence of  $\Delta C/\Delta\gamma_Q$  of about 5% and  $\gamma_C$  has an influence of  $\Delta C/\Delta\gamma_C$  of about 0.3%, which is negligible.

In figure 5.5 and figure 5.6 vertical lines are drawn, showing the values of the partial factors in RC3. Taken into account the partial factors of RC1, RC2 and RC3 defined in the Eurocodes, the  $\gamma_\psi$  still has the largest influence on the construction costs of benchmark 2, followed by  $\gamma_Q$  and eventually also  $\gamma_C$ .

## 5.5 Influence of structural components on the construction costs

In this subchapter, the influence of several structural components on the construction costs of benchmark 2 is estimated. These influences are determined by performing a sensitivity analysis by changing the dimensions of the structural components from the optimised design in RC2 alternately. So, the optimised design in RC2, forms the basis of this analysis. The following structural components are considered:

- length of tubular piles [m];
- section modulus of tubular piles ( $W_{eff,y}$ ) [ $mm^3/m$ ];
- steel area of anchor rod [ $mm^2$ ];
- length of vibro piles [m].

The influence on the construction costs of these components are also considered for benchmark 1, except for the length of the vibro piles. For benchmark 2 the influence of the structural components on  $\beta$  and the corresponding failure mechanisms on the construction costs is not investigated, because it is expected that it will result in large  $\beta$ -values as for benchmark 1. The influences of the failure mechanisms on the construction costs found for large  $\beta$ -values can differ for  $\beta$ -values close to the defined values in the Eurocodes. Therefore, the influences of the failure mechanisms on the construction costs can be unrealistic for large  $\beta$ -values. In the current reliability analyses module of D-Sheet Piling, reliability calculations can only be performed for three failure mechanisms. The  $\beta$ -values are that high because these failure mechanisms are not normative for the design of benchmark 1, which is also shown by the high UC-values (UC1) in table 5.7. In table 5.7 the UC-values for benchmark 2 (UC2) are also collected. The UC-values of the failure mechanism ‘sheet pile profile fails’ are comparable, and for ‘tension member anchorage fails’ the UC-value of benchmark 2 is even lower than for benchmark 1. For the failure mechanism ‘passive resistance inadequate’, the MSF of benchmark 2 is above 1.20 anyhow. In Plaxis the UC for ‘soil mechanical failure’ of the structure can be obtained by the MSF. ‘Soil mechanical failure’ occurs for  $MSF < 1$  and includes the failure mechanisms ‘passive resistance inadequate’, ‘lack of equilibrium’ and ‘Kranz stability inadequate’. So, the higher MSF-value, the safer the structure, in contrast to the UC-values. From the Plaxis results follows that ‘Kranz stability inadequate’ occurs for an MSF of 1.20, so the failure mechanism ‘passive resistance inadequate’ is not reached yet. Therefore, it is expected that the  $\beta$ -values of benchmark 2 will also be high.

Table 5.7 – Unity checks of failure mechanisms of benchmark 2 in RC2

Failure mechanism	Limit value	UC1	UC2
Passive resistance inadequate	MSF > 1	0.41	MSF > 1.20
Sheet pile profile fails	14,144 kNm / section	0.66	0.72
Tension member anchorage fails	2,108 kN / anchor	0.86	0.68

The dimensions of the structural components are varied by 10-20%, depending on the dimensions of the optimised designs in RC1, RC2 and RC3. The length of the tubular- and vibro piles are varied by 10% and the section modulus of the tubular piles by 20%. The steel area of the anchor rod is changed by using a lighter and a heavier type of anchor rod of Jetmix (Appendix L) in the sensitivity analysis. In this analysis, the anchors Jetmix 82.5 x 20.0 mm and Jetmix 101.6 x 22.2 mm are considered. An overview of the structural components in the sensitivity analysis is shown in table 5.8.

Table 5.8 – Structural components of the sensitivity analysis

Structural component	RC2	Change 1 (Relative change compared to RC2)	Change 2 (Relative change compared to RC2)
Length of tubular piles [m]	33.42	30.08 (-10%)	36.76 (+10%)
Section modulus of piles [mm <sup>3</sup> /m]	6,890,141	5,512,112 (-20%)	8,268,169 (+20%)
Steel area of anchor rod [mm <sup>2</sup> ]	4,578	3,888 (-15.1%)	5,510 (+20.4%)
Length of vibro piles [m]	27.87	25.09 (-10%)	30.66 (+10%)

For every situation of table 5.8 the construction costs of benchmark 2 are determined and the results points are plotted in figure 5.7. In between these points polynomial trendlines are drawn, representing a first estimate of the influence of the structural components on the construction costs of benchmark 2.

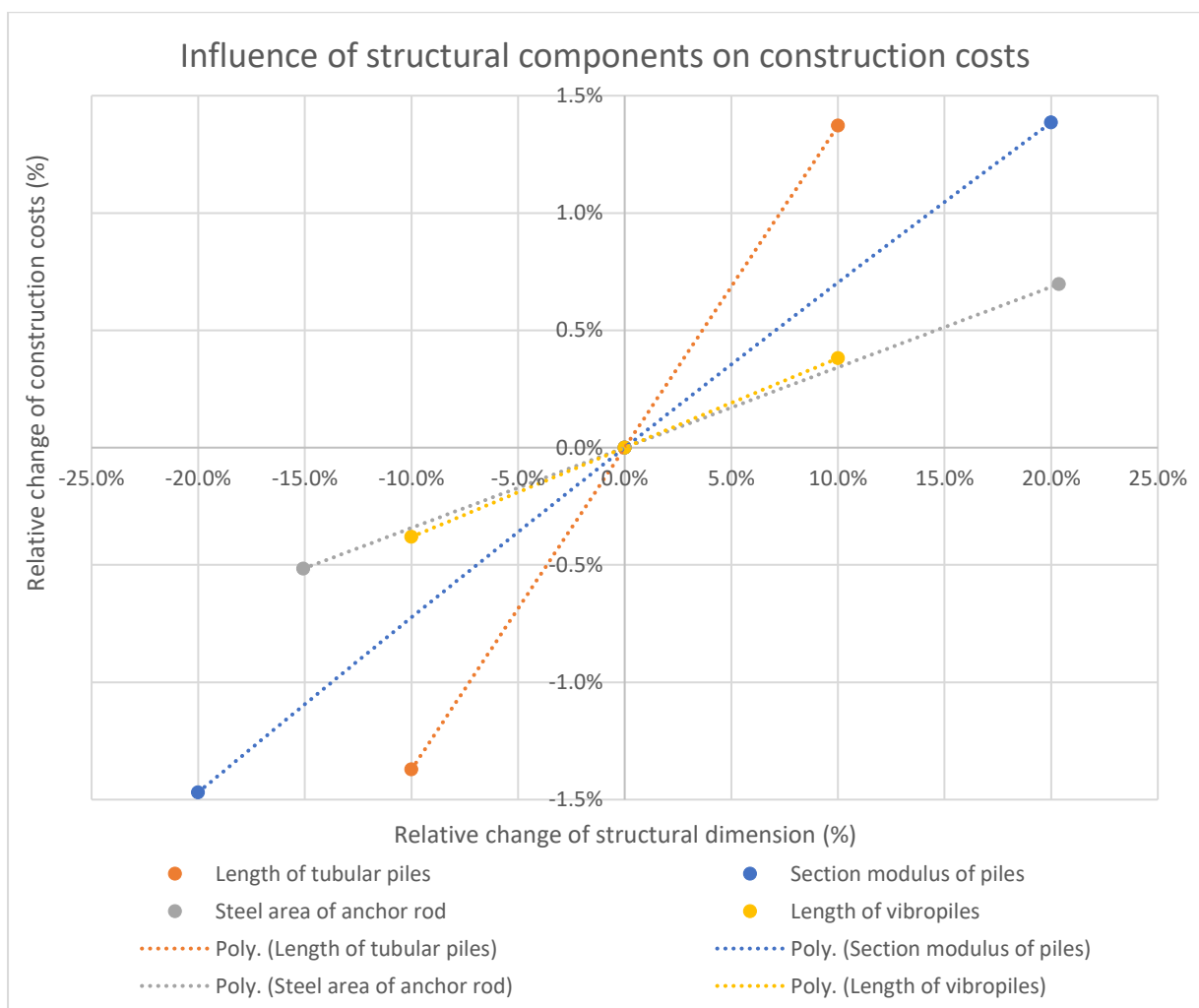


Figure 5.7 – Influence of structural components on construction costs of benchmark 2

From figure 5.7 follows that the length of the tubular piles has the largest influence on the construction costs of benchmark 2, followed by the section modulus of the tubular piles. The influence of the steel of the anchor rod, and the length of the vibro piles on the construction costs are lower and comparable.

## 5.6 Conclusion

In this chapter, the optimised designs of benchmark 2 are performed in RC1, RC2 and RC3. The optimised designs are based on the required section modulus and in these designs, it is assumed that

every combination of diameter and thickness of the tubular pipes can be used. Initially in this study, benchmark 2 is designed using the pre-2017 bearing capacity verification, containing a pile class factor for the point resistance ( $\alpha_p$ ) of 1.0. Thereafter, benchmark 2 is also designed using the post-2016 verification, in order to be consistent with benchmark 1. In the comparison of both benchmarks, the results of the designs using the post-2016 bearing capacity verification, containing  $\alpha_p = 0.7$ , have to be used because this verification is currently being used.

The construction costs differences between the designs in RC1, RC2 and RC3, using the post-2016 bearing capacity verification containing  $\alpha_p = 0.7$ , are rather small, between 1-2.5%. Furthermore, the construction costs differences are also rather small between the designs in RC1 and RC2, using the pre-2017 bearing capacity verification containing  $\alpha_p = 1.0$ , namely about 1%. Only the construction costs of the design in RC3, using the pre-2017 bearing capacity verification, are considerably larger due to the required length of the tubular piles of the combi-wall. The construction costs difference between these designs in RC2 and RC3 is about 5%. In this design in RC3, the embedded depth of the tubular piles of the combi-wall had to be increased additionally to reduce the bending moment in the combi-wall. In the other designs, the embedded depth of the tubular piles is larger due to  $\alpha_p = 0.7$ , and additional lengthening is not required. The construction costs of the combi-wall, anchors, vibro piles and cathodic protection vary between the designs.

The influence of the partial factors on the construction costs is determined by performing a sensitivity analysis. The trendlines in figure 5.5 can be used as a first estimate of their influence on the construction costs, and it follows that the influence of  $\gamma_\psi$  on the construction costs is relatively very large. Besides that, the influence of the different  $\gamma_Q$ 's is significant, except for  $\gamma_{Q, BL}$ . The influence of  $\gamma_C$  on the construction costs is also very low.

For benchmark 2 the influence of the structural components on  $\beta$  and the corresponding failure mechanisms on the construction costs is not investigated, because it is expected that it will result in large  $\beta$ -values as for benchmark 1. In table 5.7 the UC-values of benchmark 2 (UC2) reveals that these corresponding failure mechanisms are not normative for the design and therefore large  $\beta$ -values are expected. However, the influence of the dimensions of the structural components on the construction costs is evaluated. It follows that the length of the tubular piles has the largest influence on the construction costs of benchmark 2, followed by the section modulus of the tubular piles. The influence of the steel is of the anchor rod and the length of the vibro piles on the construction costs are lower and comparable.

## 6 Conclusion and discussion

This chapter contains the conclusions, discussion and recommendations based on the results of this study. The objective of this study was defined as follows:

**Objective:** *Acquire more insight into the relationship between the construction costs and the reliability index  $\beta$  of quay walls.*

It is emphasised that this relationship is considered as the marginal costs of safety investments, given specific functionality and boundary conditions of a quay wall. The marginal costs of safety investments are directly influenced by the partial factors defined in the Eurocodes, which distinguish the different reliability classes.

### 6.1 Conclusions

The main research question, corresponding to the research objective was formulated as follows:

**Main question:** What is the relationship between the construction costs and the reliability index  $\beta$  of quay walls?

Three research questions were set up in order to answer the main question, and in the following, these research questions will be answered using the findings of this study. The answers to these research questions together form the answer to the main question. Besides that, the answers contain additional more general conclusions found during this study. The research questions are answered based on the design of two most frequently used types of quay walls in the Port of Rotterdam, the Netherlands;

1. Benchmark 1: a double anchored combi-wall;
2. Benchmark 2: a combi-wall with a relieving platform.

The double anchored combi-wall has a retaining height of about 17 m and is located in the Waalhaven. The combi-wall with a relieving platform has a retaining height of about 24 m and is located in the Maasvlakte 1.

**Research question 1:** What are the construction cost differences between quay walls designed with a different reliability index  $\beta$ ?

For the two types of quay walls an optimised design and a design based on standard available dimensions of tubular pipes is performed for three different reliability classes (RC), each corresponding to a specific target reliability index ( $\beta$ ) defined in the Eurocodes. The optimised semi-probabilistic designs are based on the required section modulus of the tubular piles and in these designs, it is assumed that every combination of diameter and thickness of the tubular pipes can be used. Thereafter, the construction costs of these quay walls are estimated and these results are collected in table 6.1. The increases in construction costs for the optimised semi-probabilistic designs compared to RC1 are depicted in figure 6.1. The influence of the reliability class on the construction costs can be expressed in the fraction  $\Delta C / \Delta \beta_{\text{target}}$ , in which  $\Delta C$  is the relative change in construction costs (%) and  $\Delta \beta_{\text{target}}$  the absolute change in target reliability index (-). The target reliability indices are defined in the Eurocodes. These fractions follow from the slope of the linear trendlines between the result points of figure 6.1 and are also collected in table 6.1.

Designing the quay walls, the vertical bearing capacity of the tubular piles of the combi-walls has been verified conform the NEN 9997-1. Since 01-01-2017 the pile class factor for the point resistance ( $\alpha_p$ ) in this verification was modified from 1.0 to 0.7, lowering the vertical bearing capacity. The double anchored combi-wall is designed using the post-2016 vertical bearing capacity verification, containing  $\alpha_p = 0.7$ . Initially in this study, the combi-wall with a relieving platform is designed using the pre-2017 bearing capacity verification, containing  $\alpha_p = 1.0$ . Thereafter, the combi-wall with a relieving platform is also designed using the post-2016 verification, in order to be consistent with the double anchored combi-wall. In the comparison of both types of quay walls, the results of the designs using the post-2016 bearing capacity verification, containing  $\alpha_p = 0.7$ , have to be used because this verification is currently being used.

Table 6.1 – Construction costs and fraction  $\Delta C/\Delta\beta_{target}$  estimations of semi-probabilistic designs

Type of quay wall	$\alpha_p$	Construction costs			$\Delta C/\Delta\beta_{target}$ (%)	
		RC1	RC2	RC3	RC1 – RC2	RC2 – RC3
Double anchored combi-wall	0.7	€ 17,380.-	€ 17,570.-	€ 17,980.-	2.2%	4.7%
Combi-wall with a relieving platform	1.0	€ 34,367.-	€ 34,715.-	€ 36,315.-	2.0%	9.3%
Combi-wall with a relieving platform	0.7	€ 35,539.-	€ 36,017.-	€ 36,839.-	2.7%	4.6%

From table 6.1 follows that fraction  $\Delta C/\Delta\beta_{target}$  estimations of both quay walls for RC1 – RC2 and RC2 – RC3 are generally comparable and relatively low. The estimated fractions of the designs, using the vertical bearing capacity verification of the tubular piles containing  $\alpha_p = 0.7$ , are even lower than the suggested value of 5–10% by Roubos et al. (2018). These differences in construction costs between the reliability classes are in the same order of magnitude of the uncertainty of the estimate of the construction costs. Besides that, the fraction  $\Delta C/\Delta\beta_{target}$  estimation increases for RC2 – RC3, suggesting that the relationship between the construction costs and  $\beta$  increases for higher  $\beta$ -values.

The increase in construction costs of designs in higher reliability classes is dominated by the enlarged tubular piles of the combi-wall. Especially due to the local buckling verification of the combi-wall, the diameter and thickness of the tubular piles have to increase in designs in higher reliability classes. Only for the combi-wall with a relieving platform, designed in RC3 using  $\alpha_p = 1.0$ , the vertical bearing capacity verification of the tubular piles of the combi-wall also influences the construction costs significantly.

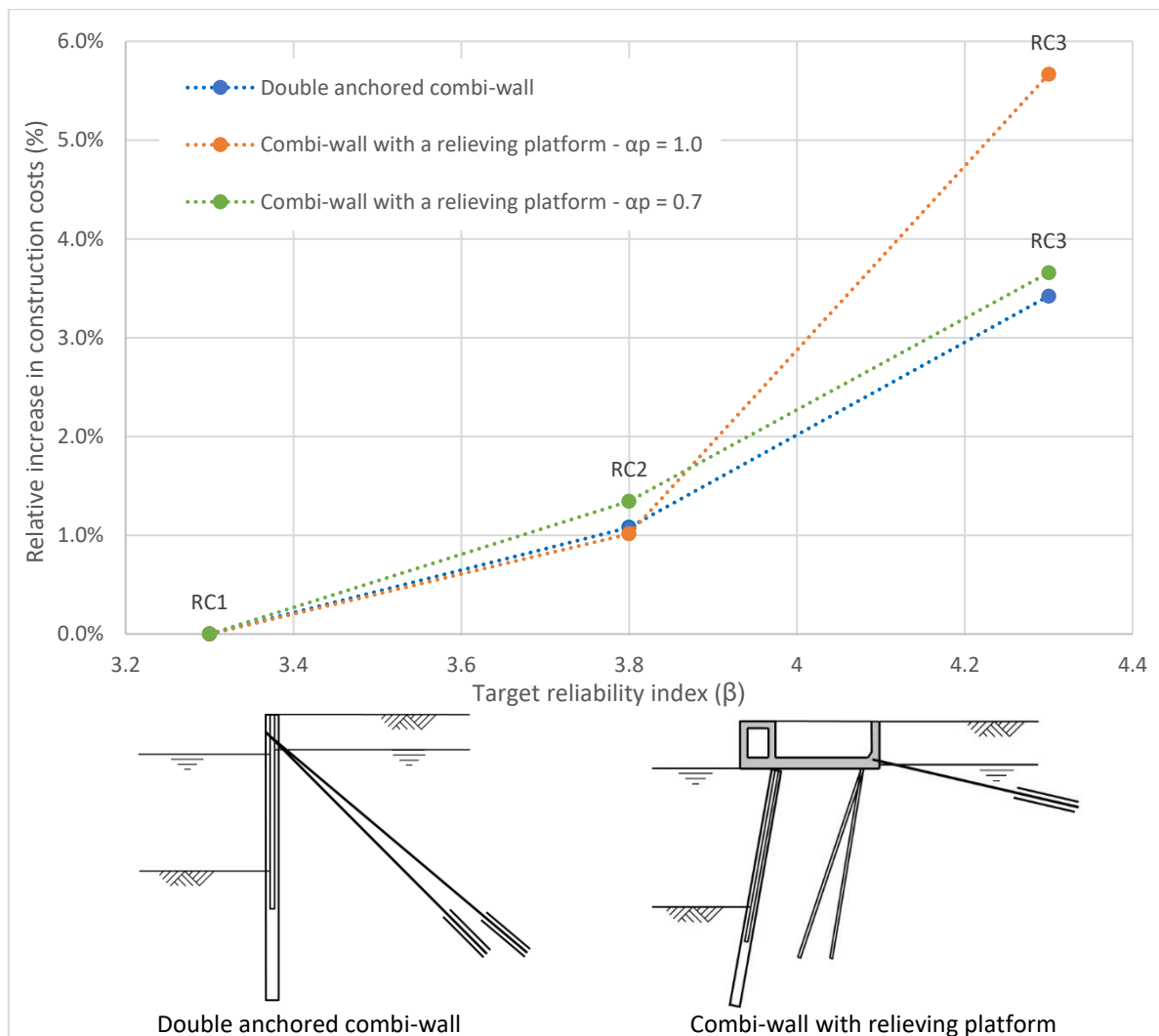


Figure 6.1 – Construction cost increase of quay walls designed semi-probabilistic in RC1, RC2 and RC3

The construction costs of the design of the combi-wall with a relieving platform in RC3, using  $\alpha_p = 1.0$ , are considerably larger due to the required length of the tubular piles of the combi-wall. In this semi-probabilistic design in RC3, the embedded depth of the tubular piles of the combi-wall had to be increased additionally to reduce the bending moment in the combi-wall. In the other designs, the embedded depth of the tubular piles is larger due to  $\alpha_p = 0.7$ , and additional lengthening is not required. Therefore, the fraction  $\Delta C/\Delta\beta_{\text{target}}$  estimation for RC2 – RC3 of the combi-wall with a relieving platform, designed using  $\alpha_p = 1.0$ , is considerably higher than for the other designs. However, in the comparison of both types of quay walls, the results using  $\alpha_p = 0.7$  have to be used.

Due to the relatively low marginal cost of safety investments of quay walls, the reliability level of a quay wall can be upgraded with relatively low investment costs. Besides that, in the determination of the reliability class, it is advised to consider the potential consequences carefully, because the expected benefits considering a lower reliability class, are quite low. For instance, mitigation of the potential damage to the reputation of a terminal or port because of failure of the quay wall, can transcend the cost benefit easily.

In figure 6.2 the construction costs of sheet piles and piled structures in practice worldwide are presented, together with the construction costs of the double anchored combi-wall and the combi-wall with a relieving platform, both considered in this study. For the quay walls considered in this study, the construction costs of the semi-probabilistic designs in RC1, RC2 and RC3 are depicted. Before the construction costs results of this study are implemented in the figure, these values were indexed from 2016- to 2008-values. The construction costs results of this study are reduced by 8.9%, based on CPI-values determined by CBS (2019). From this figure follows that the differentiation in construction costs between the reliability classes is about one order of magnitude less than the differentiation in construction costs between quay walls in practice. Therefore, it seems that the current reliability classes and the corresponding set of partial factors, as defined in the Eurocodes and CUR 211, are non-functional for quay walls.

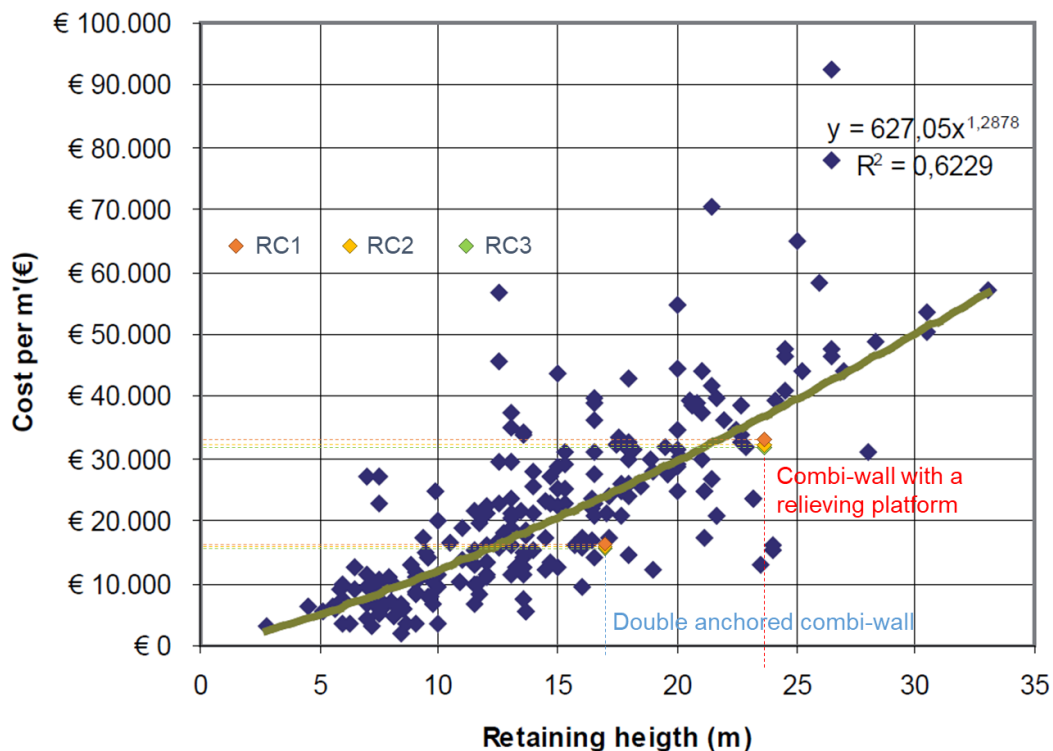


Figure 6.2 – Construction costs of sheet piles and piled structures worldwide and of the quay walls considered in this study designed in RC1, RC2 and RC3, as a function of the retaining height (De Gijt, 2010)

From the reliability results of the double anchored combi-wall in RC1, RC2 and RC3 it is notable that the differentiation between the reliability classes is minor. However, differentiation in reliability between the reliability classes is important, because of the large variety in reliability for quay walls in practice. It

appeared that the reliability differentiation between the reliability classes in practice is smaller than defined in the Eurocodes. Only the differentiation in the calculated  $\beta$ -values of the failure mechanism ‘sheet pile profile fails’ approximately complies with the differentiation as defined in the Eurocodes because this failure mechanism is strongly correlated to the normative failure mechanism ‘local buckling of combi-wall’. Recent research by Van der Wel (2018) already suggested that the steps between the current partial factors defined in the Eurocodes are too small. The small differentiation between the construction costs of quay walls corresponds to these findings. It is questionable whether the current set of partial factors, as defined in the Eurocodes and CUR 211, is corresponding to their defined target  $\beta$ -values for RC1 and RC3. The partial factors are validated to their target  $\beta$  of RC2, in contrast to RC1 and RC3. Therefore, it is advised to validate and possibly adjust the partial factors for designs in RC1 and RC3 also.

**Research question 2:** What are the influences of the partial factors on the construction costs of quay walls?

Partial factors distinguish the different reliability classes, which are defined in the Eurocodes and used in research question 1. Through a sensitivity analysis the sensitivity of the construction costs of the quay walls to every partial factor is determined, representing the influence of each factor. The influence of the partial factors on the construction costs can be expressed in the fraction  $\Delta C/\Delta \gamma$ , in which  $\Delta C$  is the relative change in construction costs (%) and  $\Delta \gamma$  the absolute change in partial factor value (-). An overview of the fractions  $\Delta C/\Delta \gamma$  is given in table 6.2.

Table 6.2 – Influence of partial factors on the construction costs of quay walls

Y	$\Delta C/\Delta \gamma$ (%)	
	Double anchored combi-wall	Combi-wall with a relieving platform
$\gamma_{\phi'}$	17.8%	45.0%
$\gamma_{c'}$	0.6%	0.3%
$\gamma_{Q, \text{ surface}}$	5.0%	2.9%
$\gamma_{Q, \text{ bollard}}$	0.6%	0.3%
$\gamma_{Q, \text{ crane}}$	-	1.5%

For the double anchored combi-wall, reliability calculations are performed evaluating the  $\beta$ -values of three of the critical failure mechanisms; ‘passive resistance inadequate’, ‘sheet pile profile fails’ and ‘tension member anchorage fails’. The  $\beta$ -values are estimated using the reliability analyses module of D-Sheet Piling, which is based on the probabilistic level II, the First Order Reliability Method (FORM). The reliability analyses module of D-Sheet Piling can perform reliability calculation for these three failure mechanisms. From the reliability calculations follow  $\alpha^2$ -values, representing the contribution of the stochastic variables to the  $\beta$  per failure mechanism. In table 6.3  $\alpha^2$ -values of the stochastic variables are given, which follow from the reliability results of the double anchored combi-wall in RC2. Due to rounding errors, the  $\alpha^2$ -values of the variables together per failure mechanism is not 100% exactly.

From the results of table 6.2 and table 6.3 follows that the  $\gamma_{\phi'}$  greatly affects the construction costs, just like  $\phi'$  dominates the contribution to the  $\beta$  of all three failure mechanisms. The influence of  $\gamma_{Q, \text{ surface}}$  on the construction costs is reasonable, and comparable to the contribution of the surface load to the  $\beta$  of the failure mechanisms ‘sheet pile profile fails’ and ‘tension member fails’. Besides that, the  $\gamma_{c'}$  influences the construction costs very little, as is the contribution of  $c'$  to the  $\beta$  of the three considered failure mechanisms is very low. It can be concluded that in the initial phase of a quay wall design, the determination of  $\phi'$  strongly influences the construction costs and the  $\beta$  of the quay wall, in contrast to  $c'$ .

Table 6.3 – Contribution of stochastic variables to the  $\beta$  of three failure mechanisms of the anchored combi-wall in RC2

Stochastic variable	$\alpha^2$ (%)		
	Passive resistance inadequate	Sheet pile profile fails	Tension member anchorage fails
$\phi'$ [°]	92.2%	78.1%	78.1%
$c'$ [kN/m <sup>2</sup> ]	1.2%	3.4%	0.3%
Surface load [kN/m <sup>2</sup> ]	2.2%	10.3%	19.6%
Water level [m NAP]	0.9%	3.1%	1.4%
Surface level [m NAP]	3.2%	5.0%	0.5%

**Research question 3:** What are the influences of failure mechanisms on the construction costs of quay walls?

The influence of failure mechanisms on the construction costs of quay walls is evaluated by combining the results of two sensitivity analyses, in which the dimensions of several structural components are varied. In these analyses the sensitivities of both the construction costs and the reliability index  $\beta$  to the dimensions of structural components are determined.

The  $\beta$ -values are also estimated using the reliability analyses module of D-Sheet Piling for three of the critical failure mechanisms, from which their corresponding structural components are used in the sensitivity analyses. The considered failure mechanisms, together with their corresponding structural components, are listed in table 6.4.

Table 6.4 – Considered failure mechanisms with their corresponding structural component

Structural component	Failure mechanism
Length of tubular piles [m]	Passive resistance inadequate
Section modulus of piles [mm <sup>3</sup> / m]	Sheet pile profile fails
Steel area of anchor rod [mm <sup>2</sup> ]	Tension member anchorage fails

The results of the relative construction costs increase due to dimension of the structural components, can be expressed by the dimensionless fraction  $\Delta C/\Delta D$ , in which  $\Delta C$  is the change in construction costs (%) and  $\Delta D$  the change in structural dimension (%). In table 6.5 an overview of the fractions  $\Delta C/\Delta D$  of the different structural components for both types of quay walls is given, together with the absolute cost increase for a 10% increase of the dimensions of the structural components.

Table 6.5 – Influence of structural components on the construction costs of the quay walls

Type of quay wall	Structural component	Relative cost increase, $\Delta C/\Delta D$	Cost increase for $\Delta D = +10\%$ (€ / m)
Double anchored combi-wall	Length of tubular piles [m]	23.5	€ 413.-
	Section modulus of piles [mm <sup>3</sup> / m]	13.5	€ 238.-
	Steel area of anchor rod [mm <sup>2</sup> ]	14.3	€ 251.-
Combi-wall with a relieving platform	Length of tubular piles [m]	13.7	€ 476.-
	Section modulus of piles [mm <sup>3</sup> / m]	7.1	€ 248.-
	Steel area of anchor rod [mm <sup>2</sup> ]	3.4	€ 119.-
	Length of vibro piles [m]	3.8	€ 132.-

From table 6.5 follows that the influence of the structural components on the absolute construction costs for both quay walls is comparable. The fractions  $\Delta C/\Delta D$  for the combi-wall with a relieving platform are lower in general because the total construction costs of this type of quay wall are larger. For both type of quay walls the length of the tubular piles is very important for the construction costs of quay walls, followed by the section modulus of the piles. The influence of the steel area of the anchor rod is larger for the double anchored combi-wall, because the relative number of anchors is larger for this quay wall.

For the double anchored combi-wall the influences of the structural dimensions on the  $\beta$  are estimated and combined with their influences on the construction cost. The influences of the failure mechanisms are found by plotting the reliability results against the relative increase in the construction costs in figure 6.3. The linear trendlines in figure 6.3 indicate a first estimation of the influences of the failure mechanisms on the construction costs. The influences can be expressed in the fraction  $\Delta C/\Delta\beta$ , and these results are collected in table 6.6, together with the target  $\beta$ -values for RC2 defined in the CUR 211.

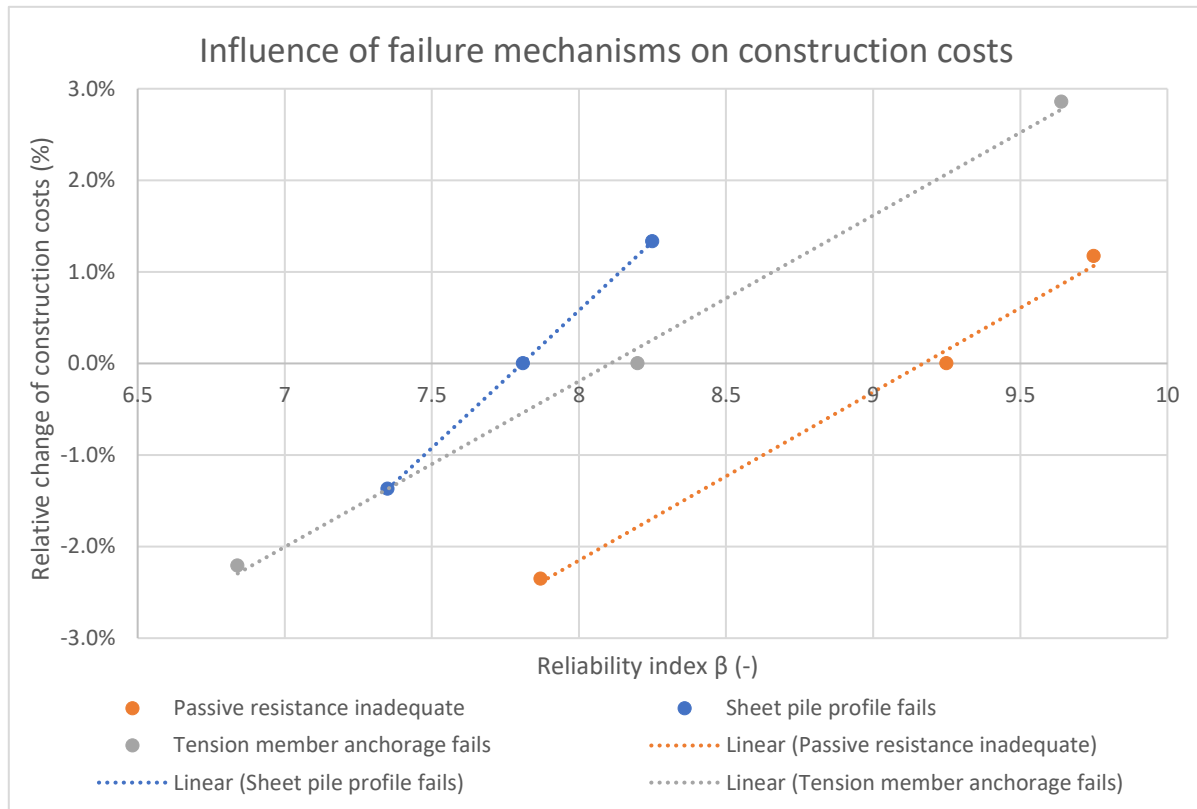


Figure 6.3 – Influence of failure mechanisms on construction costs of the double anchored combi-wall

Table 6.6 – Influence of failure mechanisms on the construction costs of the double anchored combi-wall,  $\Delta C/\Delta\beta$ , compared to the target  $\beta$ -values of RC2, defined in CUR 211

Failure mechanism	$\Delta C/\Delta\beta$ (%)	$\beta_{\text{target}}$ (RC2) CUR 211 [-]
Passive resistance inadequate	1.8%	4.11
Sheet pile profile fails	3.0%	4.11
Tension member anchorage fails	1.8%	4.46

From figure 6.3 and table 6.6 follows that the influence of the mechanism ‘sheet pile profile fails’ on the construction costs is the largest with a fraction  $\Delta C/\Delta\beta$  of about 3%. The influences of the failure mechanisms ‘passive resistance inadequate’ and ‘tension member anchorage fails’ are comparable with a fraction  $\Delta C/\Delta\beta$  of about 1.8%. According to these results, the  $\beta$  of the quay wall can be increased in an economically attractive manner by increasing the length of the piles or the steel area of the anchor rod. From the reliability results follow that the  $\beta$  of the other failure mechanisms also increases significantly by increasing the length of the tubular piles.

Comparing the influences of the failure mechanisms on the construction costs with the target  $\beta$ -values for RC2, defined in the CUR 211, it is notable that this distribution of influences not correspond to the distribution of target  $\beta$ -values between the failure mechanisms. Therefore, economic optimisation in the probabilistic design of quay walls is possible. It is economically attractive to use a smaller target  $\beta$  for a failure mechanism which is relatively inexpensive to improve. In this case, it is advised to increase the

target  $\beta$  of the failure mechanism 'passive resistance inadequate' and decrease the target  $\beta$  of 'sheet pile profile fails'.

## 6.2 Discussion

Throughout this research, several assumptions and simplifications have been made, which can influence the interpretation of the results, and the most important ones are discussed in this subchapter. Besides that, the findings of this study are compared with statements from other research.

### 6.2.1 Execution class

In the determination of the construction costs, the influence of the execution classes (EXC) is neglected in this study. The EXC's specify a classified set of requirements for the execution of the works related to the quay wall construction. The requirements of the EXC's are specified in order to ensure adequate levels of mechanical resistance and stability, serviceability and durability.

For both quay walls, the designs in RC1 and RC2 correspond to EXC2 and the design in RC3 to EXC3. In annex A.3 of the NEN-EN 1090-2 a shortlist of these requirements per EXC is given, and it is notable that the requirements of EXC2 to EXC3 strongly increase. Considering the influence of the EXC's on the construction costs, the construction costs of the designs in RC2 and RC3 will differ more.

### 6.2.2 Fraction $\Delta C/\Delta\beta_{\text{target}}$ estimations

The influence of the reliability class on the construction costs is expressed in the fraction  $\Delta C/\Delta\beta_{\text{target}}$ , in which  $\Delta C$  is relative the change in construction costs (%) and  $\Delta\beta_{\text{target}}$  absolute the change in target reliability index (-). In this fraction, it is assumed that the target  $\beta$ -values, defined in the Eurocodes for the reliability classes, correspond to the quay wall designs. The target  $\beta$ -values of the Eurocodes are intended as lower limit values to guarantee the safety of the structures. Therefore, it is very likely that the real  $\beta$  of the quay wall designs differs from the target  $\beta$ -values. Reliability calculations have to be performed to determine the real  $\beta$ -values of the quay walls. These calculations are performed for three failure mechanisms of the double anchored combi-wall in chapter 4.4, finding fraction  $\Delta C/\Delta\beta$  estimations per failure mechanism.

### 6.2.3 Fraction $\Delta C/\Delta\beta$ estimations

The influence of three failure mechanisms on the construction costs is estimated for the double anchored combi-wall. This influence of the failure mechanism can be expressed in the fraction  $\Delta C/\Delta\beta$ , in which  $\Delta C$  is relative the change in construction costs (%) and  $\Delta\beta$  absolute the change in reliability index (-). The fraction  $\Delta C/\Delta\beta$  estimations of this study are very low, even lower than the estimations of 5-10% by Roubos et al. (2018) and Schweckendiek et al. (2007). The estimated  $\beta$ 's are very high ( $\geq 7$ ) and it is uncertain whether the fraction  $\Delta C/\Delta\beta$  estimations are comparable for lower  $\beta$ 's.

The most important reason for the high  $\beta$ -values is that the investigated failure mechanisms are not normative in the design verifications because their UC-values are much less than their maximum value of 1.0. However, it is expected that the fraction  $\Delta C/\Delta\beta$  estimations of the considered failure mechanisms will be comparable when these failure mechanisms are normative. This is because the critical variables of these failure mechanisms are also critical variables for the normative failure mechanisms. The influences of the normative failure mechanisms of the considered quay walls on the construction costs are unknown.

Therefore, in the development of probabilistic design of quay walls, it is essential that reliability calculations can be performed for the normative failure mechanisms at least, such as; 'bearing capacity of tubular piles inadequate', 'local buckling of combi-wall' or 'soil mechanical failure of tension member'. It is expected that these failure mechanisms are normative for most of the quay walls. In the reliability analyses module of D-Sheet Piling, these failure mechanisms cannot be considered yet. Probabilistic calculations are also possible using Plaxis (with the help of the software ProbAna), but nowadays only for the failure mechanisms; 'soil mechanical failure', 'sheet pile profile fails', 'tension member anchorage fails' and 'excessive displacements of sheet pile wall'. So, the normative failure mechanisms cannot be considered using Plaxis either.

## 6.3 Recommendations

In this subchapter, recommendations for science and recommendations for practice, resulting from this study are treated.

### 6.3.1 Recommendations for science

In the following, recommendations for further research are given:

- In this study, the relationship between the construction costs and the reliability index  $\beta$  is mainly focused on quay walls in the Port of Rotterdam, the Netherlands. Both evaluated quay walls and their soil characteristics are specific for the Port of Rotterdam and therefore not immediately applicable for other ports in the Netherlands. Further research needs to validate the findings of this study by analysing more quay wall designs located outside Rotterdam, in the Netherlands. Besides that, it is required to investigate the relationship between the construction costs and the reliability index  $\beta$  for other types of quay walls as well.
- From the reliability results of the double anchored combi-wall followed that the reliability differentiation between the reliability classes in practice is smaller than defined in the Eurocodes. Recent research by Van der Wel (2018) already suggested that the steps between the current partial factors defined in the Eurocodes are too small. It is questionable whether the current set of partial factors, as defined in the Eurocodes and CUR 211, is corresponding to their defined target  $\beta$ -values for RC1 and RC3. The partial factors are validated to their target  $\beta$  of RC2, in contrast to RC1 and RC3. Therefore, it is advised to validate and possibly adjust the partial factors for designs in RC1 and RC3.
- The estimated influences of the failure mechanisms on the construction costs do not correspond to the distribution of target  $\beta$ -values between the failure mechanisms, defined in the CUR 211. Therefore, it is possible that redistribution of the target  $\beta$ -values of the fault tree of the CUR 211, leads to economic optimisation in the probabilistic design of quay walls. In this case, it is possible that the cost of the quay wall decreases, but the overall  $\beta$  of the quay wall remains constant. From this study follows that it is attractive to increase the target  $\beta$  of the failure mechanism 'passive resistance inadequate' and decrease the  $\beta$  of 'sheet pile profile fails'. Further research would be required in order to determine the optimised target  $\beta$ 's, considering other critical failure mechanisms as well.
- From this study follows that the length of the tubular piles of the combi-wall is essential for the construction costs of quay walls. The required length of the tubular piles is determined by the vertical bearing capacity verification. Recently, the vertical bearing capacity verification conform NEN 9997-1 is adapted (The Netherlands Standardisation Institute, 2017). Therefore, thorough research into this verification conform the NEN 9997-1 can be interesting.
- The relationship between the construction costs and reliability index  $\beta$  is expressed in fraction  $\Delta C/\Delta\beta$  estimations per failure mechanism. It appeared that reliability calculations are not possible yet for the normative failure mechanisms using the reliability analyses module of D-Sheet Piling or the probabilistic module ProbAna of Plaxis. A failure mechanism is considered as normative when the corresponding UC-value (almost) has reached its maximum value of 1.0. Therefore, the overall fraction  $\Delta C/\Delta\beta$  estimation of the quay walls and the influence of the of the normative failure mechanisms on the construction costs is still unknown. It is crucial that probabilistic software for quay walls extend their possibilities to perform reliability calculations for other (normative) failure mechanisms. In this study the following failure mechanisms are normative for both quay walls; 'bearing capacity of tubular piles inadequate', 'local buckling of combi-wall' and 'soil mechanical failure of tension member'.
- Reliability calculations are performed using the reliability analyses module of D-Sheet Piling, which is based on the probabilistic level II analysis, the First Order Reliability Method (FORM). In level II methods, the failure probabilities are approximated and in the reliability analyses module of D-Sheet Piling it is not possible to include correlations between parameters. Besides that, not all parameters can be chosen as stochastic. Therefore, reliability calculations should ideally be performed using a level III method, in which correlations are included, all critical parameters can be chosen as stochastic, and the probability of failure is calculated more exactly.

### 6.3.2 Recommendations for practice

In the following, recommendations for quay wall design in practice are given:

- The estimated construction cost differences between the different designs in RC1, RC2 and RC3 are rather small, especially between the designs in RC1 and RC2. For both quay walls, the construction costs of the design in RC1 and RC2 differ only about 1%. This study can contribute to the consideration of decision makers of the required reliability class of quay walls, before the start of the design process. Besides that, the reliability class of quay walls can be upgraded to a higher reliability class relatively inexpensive.
- In this study, the influence of the partial factors on the construction costs is evaluated. From this analysis followed that the  $\gamma_{\phi'}$  greatly affects the construction costs, followed by the  $\gamma_{Q, \text{surface}}$  and the  $\gamma_{Q, \text{crane}}$ . Besides that, for both quay walls the influence of  $\gamma_{c'}$  and the  $\gamma_{Q, \text{bollard}}$  is very small. It can be concluded that in the initial phase of a quay wall design, the determination of  $\phi'$  strongly influences the construction costs and the  $\beta$  of the quay wall, in contrast to  $c'$ .
- In this study, the influence of failure mechanisms on the construction costs of quay walls is estimated. It is possible to optimise quay wall designs economically by comparing these influences with the distribution of target  $\beta$ -values between these failure mechanisms. It is economically attractive to use a smaller target  $\beta$  for a failure mechanism which is relatively inexpensive to improve. This principle is comparable to the failure probability distribution for flood defences.
- Reliability calculations were performed using the reliability analyses module of D-Sheet Piling, for which it was possible to obtain the reliability index  $\beta$  and sensitivity factors  $\alpha$  for three failure mechanisms. The reliability indices can be used for probabilistic design of quay walls and the sensitivity factors to extend the geotechnical investigation of a specific soil layer.

# References

- Arcadis. (2016). *Final design of benchmark 2*
- Arcadis. (2017). *Final design of benchmark 1*
- ArcelorMittal. (2016). *Spirally welded steel pipes*
- Boskalis (Producer). (2012). Project sheet - Construction of a completely new harbor in Finland.
- British Standards Institution. (2007). UK National Annex to Eurocode 7: Geotechnical design - Part 1: general rules
- British Standards Institution. (2010). Maritime works - Part 2 - Code of practice for the design of quay walls, jetties and dolphins.
- Calle, E. O. F., & Spierenburg, S. E. J. (1991). *Veiligheid van damwandconstructies - Onderzoeksrapportage deel I*
- CBS. (2019). *Consumentenprijzen; prijsindex 2015=100*.
- Committee for Waterfront Structures of the Harbour Engineering and the German Society for Soil Mechanics and Foundation Engineering. (2012). Recommendations of the Committee for Waterfront Structures Harbours and Waterways EAU 2012 (11th edition).
- Construction Innovations (UK) Ltd. (2005). *Review international procurement*
- CROW. (2005). *Handboek Zandboek*.
- CROW. (2010). *Standaardsystematiek voor kostenramingen - SSK-2010 - Handreiking voor kostenmanagement en kostenramen*.
- CUR. (2005). CUR-publication 211E 'Handbook Quay walls'.
- De Gijt, J. G. (2004). *Structures in Hydraulic Engineering - Lecture notes on Port Infrastructure CT5313*.
- De Gijt, J. G. (2010). *A History of Quay Walls*. TU Delft,
- De Gijt, J. G. (2015). The Importance of Hydraulic Structures for Society: Quay Walls and Dikes in the Netherlands.
- De Gijt, J. G., & Vinks, R. (2011). Cost of quay walls including life cycle aspects
- De Grave, J. G. (2002). *Validatie van partiële factoren uit "Probabilistische analyse damwandconstructies"*.
- Deltares. (2017). *D-Sheet Piling, User Manual*
- Havinga, H. (2004). *Dossier Probabilistische berekeningen, onderdeel 7.1*
- Havinga, H. (2018) *Limit value mobilisation in reliability module of D-Sheet Piling/Interviewer: R. Wesstein*.
- Huijzer, G. P. (1996). *Eindrapport probabilistische analyse damwandconstructies*
- Jetmix. (2016). *Groutinjectieankers*

- Jonkman, S. N., Steenbergen, R. D. J. M., Morales-Napoles, O., Vrouwenvelder, A. C. W. M., & Vrijling, J. K. (2017). *Probabilistic Design: Risk and Reliability Analysis in Civil Engineering (4th edition)*.
- Koene, K. J. (2018) *Construction costs of quay walls/Interviewer: R. Wesstein*.
- Lesny, K. (2011). *Implementation of Eurocode 7 in Germany and Consequences for Practical Design*
- Lopez Gumucio, J. P. (2013). *Design of Quay Walls using the Finite Element Method*.
- Meigh, & Corbett. (1997). *Cone penetration testing, methods and interpretation*
- Meijer, E. (2006). *Comparative analysis of design recommendations for Quay Walls*. TU Delft,
- Plaxis bv. (2017). *PLAXIS 2017*
- Ragi Manoj, N. (2016). *First - order Reliability Method: Concepts and Application - Additional Graduation Thesis*
- Roubos, A. A., Steenbergen, R. D. J. M., Schweckendiek, T., & Jonkman, S. N. (2018). Risk-based target reliability indices for quay walls.
- Schuppener, B. (2007). Eurocode 7: Geotechnical design - its implementation in the European Member states.
- Schweckendiek, T., Courage, W. M. G., & Van Gelder, P. H. A. J. M. (2007). Reliability of Sheet Pile Walls and the Influence of Corrosion - Structural Reliability Analysis with Finite Elements - .
- Smit, M. (2016). *Differentiatie in betrouwbaarheid van kadeconstructies*.
- Stichting CURNET. (2012a). CUR-publicatie 166 deel 1 (6th edition) Damwandconstructies.
- Stichting CURNET. (2012b). CUR-publicatie 166 deel 2 (6th edition) Damwandconstructies.
- Stichting CURNET. (2014). CUR-publication 211E (2nd edition) Quay walls.
- The Netherlands Standardisation Institute. (2002). NEN-EN 1990 (en) - Basis of structural design.
- The Netherlands Standardisation Institute. (2016). NEN-EN 1993-1-1 (nl) - Eurocode 3: Design of steel structures - Part 1-1: General rules and rules for buildings.
- The Netherlands Standardisation Institute. (2017). NEN 9997-1 Geotechnical design - Part 1: General rules.
- The Netherlands Standardisation Institute. (2018). NEN-EN 1090-2 (en) Execution of steel structures and aluminium structures - Part 2: Technical requirements for steel structures.
- UNCTAD/RMT. (2015). *Review of maritime transport*
- Valley, B., & Kaiser, P. K. (2010). Consideration of uncertainty in modelling the behaviour of underground excavations.
- Van der Wel, T. J. (2018). *Reliability based Assessment of Quay Walls*.
- Van Seters, A., & Jansen, H. (2011). *Safety concepts and calibration of partial factors in European and North American codes of practice*
- Vrijling, J. K., Bezuyen, K. G., Kuijpers, H. K. T., Van Baars, S., Molenaar, W. F., & Voorendt, M. Z. (2015). *Manual Hydraulic Structures*.

Wolters, H. J. (2012). *Reliability of Quay Walls*.

# Appendices

## Appendix A Additional theoretical framework

### Appendix A-1 Importance of quay walls

Since mankind exists, one wants to improve the quality of life and engineers have an important role in this development. Hydraulic structures are one of the means to strive for this objective, for instance by stimulating the shipping at rivers, canals or over the sea. Different continents are connected with the rest of the world more than ever and transport by water is still growing. Quay walls play an important role in the transshipment of freight. The design and construction of quays is no simple matter and the value of the quay structures is immense, thus requires attention (De Gijt, 2015).

### Appendix A-2 Level II reliability method: Point estimate method

The point estimate method is also a level II method and a relatively simple method to evaluate the reliability index of a structure. So, this method is able to estimate the reliability index of a structure using probabilistic calculations with several assumptions. With the help of input of the mean and the coefficient of variation, the parameter distributions are simplified by equivalent distributions. This is done by allocating three points from the original parameter distribution to the assumed equivalent distribution. For these points commonly the mean value and the two values which deviate one standard deviation from the mean value are used. This results in  $2^n$  calculations, in which  $n$  is the number of included stochastic variables.

The outcomes of the point estimate method consist of a probability density function with a mean and coefficient of variation. In contrast to level I methods, the exact shape of the output distribution is not known using the point estimate method. Even when the distributions of the input parameters are similar and known, the output distribution can be different. Therefore, several studies have been done to give better insight into the uncertainties of this model. Valley and Kaiser performed a study into the consideration of uncertainty in modelling the behaviour of underground excavations and Kamp evaluated the outcomes of the point estimate method with the level I Monte Carlo method. Both studies concluded that this method proves to be an efficient method to include uncertainty.

From research by Valley and Kaiser (2010) followed that the uncertainty in the output distribution increases for increasing non-linearity compared to level I Monte Carlo computations. When for instance both elastic and plastic soil behaviour is involved in finite element analysis, non-linearity and uncertainty in the output distribution increases. This concept is illustrated in Figure A.1. The study from Valley and Kaiser recommend investigating these effects. It is possible to use a limited number of stochastic parameters at a time, use different parameters and compare the outcomes of these calculations.

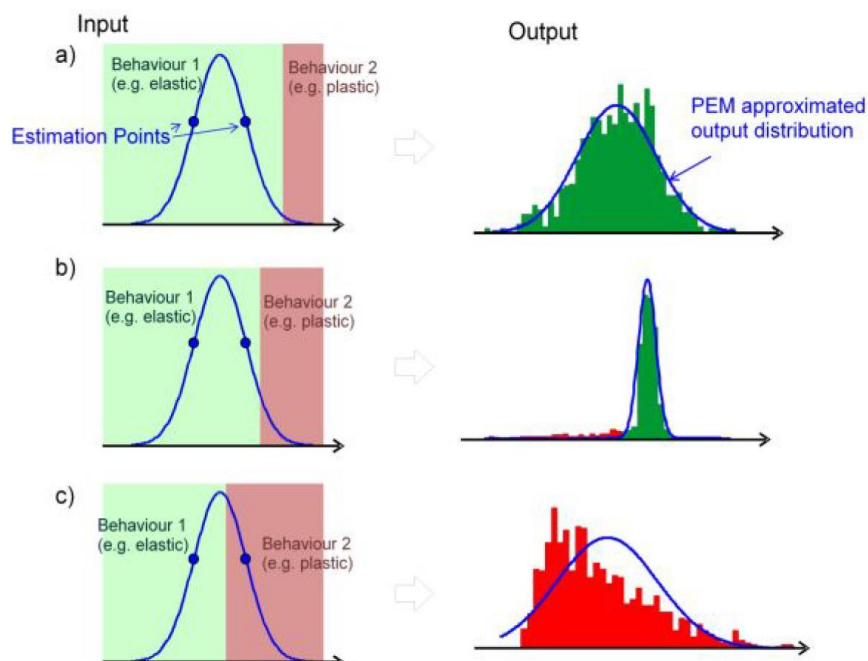


Figure A.1 – Differences in uncertainties in the outcomes of the point estimate method for three situations with differences in the input due to combinations of elastic and plastic soil behaviour (Valley & Kaiser, 2010)

Kamp concluded in his research that the point estimate method provides a straightforward and economic method to obtain reliability indices for complex design situations. This study evaluated the outcomes of the point estimate method for different types of benchmarks; slope stability, shallow foundation and cantilever retaining wall. It followed that for relative less complicated problems, such as slope stability problems, the results from the point estimate method are very similar to the result from the Monte Carlo method. The results are less accurate for problems where stiffness properties and soil-structure interactions play role, as for quay walls. Still satisfactory results are obtained for all analysed benchmarks. Important is that an indication of an overview of the dominant uncertain properties is required for this method. It is crucial to only assume parameters as stochastic when they are uncertain and dominant in the design. This overview can be determined using a sensitivity analysis, which indicates the influence of each of the parameters on the results. It is advised to control of the results additionally by comparing the outcomes of deterministic calculations with the determined mean, characteristic and design value of the point estimate method. This is especially recommended for problems with non-linear behaviour in finite element methods.

So, advantages of this method are that it requires only little probabilistic knowledge and input parameters and no long computation times are needed. From the method valuable information of the possible spread of the output parameters and an estimation of the reliability index can be obtained. However, it produces less extended results than level I methods and output uncertainty can be larger. The results are valuable, but it is not recommended to use this method on its own for the design of geotechnical structures yet.

### Appendix A-3 Design guidelines

In this subchapter the different design guidelines: BS 6349 and EAU 2012 are treated and these guidelines, together with the NEN 9997-1, CUR 166 and CUR 211 are compared.

#### **BS 6349**

In the BS 6349, the code of practice for the design of quay walls, jetties and dolphins is included, which is based on the Eurocodes. As a code of practice, this part of the British Standards takes the form of guidance and recommendations.

The BS 6349 has no reliability differentiation, such as defined in the Eurocodes.

The design of quay walls and jetties, including earth retaining structures, foundations and suspended decks, should be determined using the limit state design techniques set out in the Eurocodes. National choice is permitted in the use of design approach for the structural and geotechnical limit states. According to the BS 6349, only design approach 1 is to be used in this design guideline. Design of structural members not involving geotechnical actions should be verified using the design approach Set B. Design of structural members (footings, piles, basement walls etc.) should be verified by calculating using the least favourable of the effects from Set B and Set C. The partial factors to be used are defined in the National Annexes of the BS 6349 (British Standards Institution, 2010) and the National Annexes of Eurocode 7 (British Standards Institution, 2007).

#### **EAU 2012**

The EAU 2012 has been developed in order to collect the publications and recommendations of Waterfront structures, Harbours and Waterways as part of the European harmonisation of the regulations with respect to quay walls. The previous versions are published in 1996 and 2004, which were still based on experience gained over many years. (Schuppener, 2007).

The EAU 2012 does not use the reliability classes defined in the Eurocodes, but defined a unique classification, based on design situations. Each of the design situations, determines the partial factors and combination coefficients. There are three different design situations defined, namely:

- BS-P (Permanent)
- BS-T (Transient)
- BS-A (Accidental)

In addition, the design situation BS-E (Earthquake) for earthquakes was introduced. In this design situation no partial factors are applied (Committee for Waterfront Structures of the Harbour Engineering and the German Society for Soil Mechanics and Foundation Engineering, 2012).

The ultimate limit states, defined in the Eurocode, are also used in EAU2012, but it divides the geotechnical GEO limit state into two parts. GEO-2 is used for failure or very large deformation of the subsoil and GEO-3 is used as limit state of loss of overall stability (Lesny, 2011).

According to EAU 2012, design approach 2 (2\*) is to be used for geotechnical verification of the limit states STR and GEO-2, and design approach 3 for verification of the limit state GEO-3. Design approach 2\* specifies that the characteristic or representative stresses (lateral forces, bearing forces, bending moments, stresses in the relevant sections through the structure and in contact surfaces between the structure and ground) are determined first, whereas the partial factors have to be applied. The partial factors are defined in table E 0-1 until E 0-3 in EAU 2012 (Committee for Waterfront Structures of the Harbour Engineering and the German Society for Soil Mechanics and Foundation Engineering, 2012).

### **Comparison of the considered design guidelines**

The treated design guidelines can have different reliability classes and most of them differ in design approach. The reliability levels of the reliability classes of the Dutch guidelines NEN 9997-1, CUR 166 and CUR 211 correspond to the Eurocode, but the distinction between the classes is different for CUR 211 and the British Standard 6349. In CUR 211 the prescribed risk of danger to life and economic damage for each of the reliability classes is different comparing with the Eurocode. The EAU 2012 uses a completely different safety approach. Besides that, the design guidelines contain several design approaches, which influence the partial factors. The British Standard 6349 doesn't include a reliability differentiation at all. An overview of the design guidelines, with design approach and partial factors are given in Figure A.2 and Figure A.3.

E. Meijer compared the design guidelines CUR 166 (4<sup>th</sup> edition), CUR 211 (1<sup>st</sup> edition) and EAU 2004 in a study, executed in 2006. He concluded that it is important to use safety factors from only one design guideline, because otherwise it is possible that the target reliability level of the structure is not reached. The study recommends using CUR 211 for designing quay walls, because it is straightforward to apply, it deals with fundamental and special load combinations, it gives a clear description of the calculation of a superstructure and a clear description of the design philosophy is available. It must be noted that this study was performed with old design guidelines, which are now replaced. The results of this study can be changed by now (Meijer, 2006).

Design Approach	Reliability class	Parameter	Symbol	NEN 9997 & CUR 166						CUR 211						
				Design Approach 3						Design Approach 3						
				RC1	RC2	RC3	RC1	RC2	RC3	RC1	RC2	RC3	RC1	RC2	RC3	
				A1 <sup>a</sup>						A2 <sup>a</sup> (sheet pile wall)						
Loads (A)	Permanent	Unfavourable	$\gamma_G$	1.215 <sup>bc</sup>	1.35 <sup>bc</sup>	1.485 <sup>bc</sup>	1.00	1.00	1.00	1.215	1.35	1.485	1.00	1.00	1.00	
		Favourable		0.90	0.90	0.90	1.00	1.00	1.00	0.90	0.90	0.90	1.00	1.00	1.00	1.00
	Variable	Unfavourable	$\gamma_Q$	1.35	1.50	1.65	1.00	1.10	1.25	1.35	1.50	1.65	1.00	1.10	1.25	1.25
		Favourable		0.00	0.00	0.00	0.00	0.00	0.00	0.00	0.00	0.00	0.00	0.00	0.00	0.00
				M2 (sheet pile wall)						M2 <sup>e</sup> (sheet pile wall)						
Soil properties (M)	Angle of internal friction <sup>d</sup>		$\gamma_{\phi'}$	1.15	1.175	1.20	-	-	-	1.15	1.175	1.20	1.20	1.25	1.30	
	Effective cohesion		$\gamma_c'$	1.15	1.25	1.40	-	-	-	1.15	1.25	1.40	1.30	1.45	1.60	
	Undrained shear strength		$\gamma_{cu}$	1.50	1.60	1.65	-	-	-	1.50	1.60	1.65	1.50	1.75	2.00	
	Unconfined strength		$\gamma_{qu}$	1.50	1.60	1.65	-	-	-	1.50	1.60	1.65	1.50	1.75	2.00	
	Weight density		$\gamma_t$	1.00	1.00	1.00	-	-	-	1.00	1.00	1.00	1.00	1.00	1.00	
					R3 (retaining structures)						R3 (retaining structures)					
Resistance (R)	Bearing capacity		$\gamma_{R,v}$	1.00	1.00	1.00	-	-	-	1.00	1.00	1.00	-	-	-	
	Sliding resistance		$\gamma_{R,h}$	1.00	1.00	1.00	-	-	-	1.00	1.00	1.00	-	-	-	
	Soil resistance		$\gamma_{R,e}$	1.00	1.00	1.00	-	-	-	1.00	1.00	1.00	-	-	-	

a. The partial safety factors A1 have to be applied in case structural loads are considered whereas the factors A2 have to be applied in case of geotechnical loads.

b. Only with small variable loads this value is normative (eq. 6.10a in NEN-EN 1990+A1+A1/C2:2011. Otherwise eq. 6.10b)

c. With fluid pressure with a physically limit value may be sufficient; RC1: 1.08, RC2: 1.2, RC3:1.32

d. Influencing tan ( $\phi'$ )

e. Use M2 (sheet pile wall) for sheet pile walls and M2 (quay wall with relieving floor) for quay walls with a relieving floor

Figure A.2 – Overview of partial factors per design guideline 1 (Own work)

Design Approach Reliability class	Parameter	Symbol	BS 6349						EAU 2012			
			Design Approach 1			Design Approach 2*			BS-P	BS-T	BS-A	
Loads <sup>c</sup> (A)	Permanent	$\gamma_G$	RC1	RC2	RC3	RC1	RC2	RC3	BS-P	BS-T	BS-A	
			Set B <sup>d</sup>			Set C <sup>d</sup>			1.35 <sup>f</sup>	1.20 <sup>f</sup>	1.10 <sup>f</sup>	
	Variable	Unfavourable	1.35	1.35	1.35	1.00	1.00	1.00	1.00	1.00	1.00	
		Favourable	1.00	1.00	1.00	1.00	1.00	1.00	1.00	1.00	1.00	
	Favourable	Unfavourable	1.50 <sup>b</sup>	1.50 <sup>b</sup>	1.50 <sup>b</sup>	1.30 <sup>b</sup>	1.30 <sup>b</sup>	1.30 <sup>b</sup>	1.30 <sup>b</sup>	1.50 <sup>f</sup>	1.30 <sup>f</sup>	1.10 <sup>f</sup>
		Favourable	0.00	0.00	0.00	1.00	1.00	1.00	1.00	0.00	0.00	0.00
Soil properties <sup>c</sup> (M)	Angle of internal friction <sup>a</sup>	$\psi$	M1 <sup>e</sup>			M2 <sup>e</sup>						
	Effective cohesion	$\gamma_c$	1.00	1.00	1.00	1.25	1.25	1.25	1.00	1.00	1.00	
	Undrained shear strength	$\gamma_{cu}$	1.00	1.00	1.00	1.25	1.25	1.25	1.00	1.00	1.00	
	Unconfined strength	$\gamma_{qu}$	1.00	1.00	1.00	1.40	1.40	1.40	1.00	1.00	1.00	
	Weight density	$\gamma_r$	1.00	1.00	1.00	1.40	1.40	1.40	1.00	1.00	1.00	
				R1 (retaining structures)								
Resistance (R)	Bearing capacity	$R_{R,v}$	1.00	1.00	1.00	-	-	-	1.40	1.30	1.20	
	Sliding resistance	$R_{R,h}$	1.00	1.00	1.00	-	-	-	1.10	1.10	1.10	
	Soil resistance	$R_{R,e}$	1.00	1.00	1.00	-	-	-	1.40	1.30	1.20	

<sup>a</sup>: Influencing  $\tan(\phi)$

<sup>b</sup>: Maximum value of partial safety factor, can be lower for specific loads

<sup>c</sup>: Reliability differentiation of BS6349 may also be applied by multiplying the  $K_{FI}$  factors with the soil parameter partial safety factors. However, this is not normally used.

<sup>d</sup>: Design of structural members not involving geotechnical actions should be verified using the design approach Set B. Design of structural members (footings, piles, basement walls etc.) should be verified by calculating using the least favourable of the effects from Set B and Set C.

<sup>e</sup>: In design approach 1 there are two checks required for two different combinations of partial safety factors: A1+M1 and A2+A2

<sup>f</sup>: Maximum value of partial safety factor, can be lower for specific load

Figure A.3 – Overview of partial factors per design guideline 2 (Own work)

## Appendix A-4 Procurement

This chapter clarifies the procurement process and the characteristics of the different types of contracts, such as traditional, mediatorial, integrated, extra-integrated, public-private cooperation. Furthermore, some advantages and disadvantages of these types are given, because it isn't possible to indicate that one of the contracts have the largest cost efficiency and project control.

Whenever a client announces that a project must be executed, it can be decided that the project will be tendered. A tender or procurement is a process of purchasing products or services, which are defined by the client with the help of requirements and wishes. Tendering reduces the costs of the project due to the competition between tenderers and provides equal opportunities for contractors to execute the project.

There are different phases within the procurement process, namely:

- determination of financing method;
- determination type of contract;
- the procurement and determination of contractor.

The project can be financed using own recourses, resources from third parties or market resources. This financing method influences the type of contract between the client and contractor.

### Type of contracts

The Institute Construction Innovations conducted a study into types of contract and the considerations choosing one of them. There are five main types of contracts (Construction Innovations (UK) Ltd, 2005):

- Traditional: separated responsibilities and usually tender on the lowest price for a fully developed design.
- Mediatorial: a specific third party has the responsibility coordinating the tender- and construction process.
- Integrated: one contractor is responsible for the design and construction of the project.
- Extra-integrated: One contractor is responsible for the design, construction and maintenance of the project.
- Public-private cooperation: A cooperation between the government and one or more private companies, which is often responsible for the design, construction and/or maintenance, but often also finance of the project.

One of the advantages of the traditional contract is that it includes a high level of quality certainty, but the separation causes longer design- and construction phases and increasing project risks. Using a mediatorial contract, there can be advise about the design early in the process, resulting in a large flexibility. Disadvantages of this type of contract are that there is no fixed price and the client is responsible for most of the project risks. In case of an (extra-)integrated contract the final budget is certain in an early stage of the project and design, construction and possibly maintenance of the project can be arranged together. However, often the requirements in these contracts are very specific to avoid ambiguity, reducing the flexibility of the design. The last type of contract reduces the public expenses, but this type is not in favour by most of the contractors.

It is not possible to indicate in general which contract form contains the largest cost efficiency and project control. The type of contract is determined by the client and depends on different considerations, such as the complexity and predictability of the project. Furthermore, the extent to which one seeks innovative solutions or wants to keep space for flexibility can influence this choice. The focus of the contracts is slowly shifted in recent years from striving for the lowest possible costs to striving for certainty about costs, delivery time and life cycle costs of the structure. Besides this, the more integrated the project, the more innovation is stimulated (Construction Innovations (UK) Ltd, 2005).

## Appendix B Fictional cases

In this chapter three fictional cases are introduced, the starting points of these cases are treated and design- and reliability results are obtained. These three fictional cases are introduced to become familiar with the research steps and possible results. Therefore, the complexity of these fictional cases is slowly increased, towards the complexity of the double anchored combi-wall of benchmark 1. With the help of these fictional cases several design- and reliability methods are explored, what is used in the decision of the methods to be used for the benchmarks.

This research starts considering fictional case 1 performed as a simple cantilever quay wall, with one type of soil and without any external loading. Fictional case 2 includes a real soil profile and in fictional case 3 also an anchor and a surface load is added to the structure. Fictional case 1 is designed using three calculation methods, again starting with the simplest method, followed by the more complex ones. So, sequentially the used methods used are: the Blum Method, hand calculation and the subgrade reaction method of D-Sheet Piling. The other two fictional cases are designed using the subgrade reaction method of D-Sheet Piling. These fictional cases are non-existing cases, based on realistic starting points. The benchmark quay walls are existing projects, of which all research steps are performed and research results are obtained.

Benchmark 1 and benchmark 2 are designed using the guideline CUR 211, so the fictional cases are designed following these guidelines as well. According to the CUR 211, sheet piles and combined walls should be designed using the stepwise approach of CUR 166 or chapter 9 of NEN 9997-1, showed in figure 2.29 (The Netherlands Standardisation Institute, 2017). For the fictional cases the stepwise approach is performed, except for step 10-12. Corrosion is disregarded in the design of the fictional cases. In this chapter the design- and reliability results are obtained as well.

### Appendix B-1 Starting points of fictional case 1

Fictional case 1 is a fictional simple cantilever quay wall with a retaining height of 5 m. This value is assumed, because cantilevered quay walls are used up to this retaining height (Stichting CURNET, 2012b). Furthermore, the quay wall has to be executed using steel sheet piling. The principle geometry of fictional case 1 is depicted in Figure B.1. The minimal embedded depth of the sheet pile wall has to be calculated and is now indicated as  $t$ .

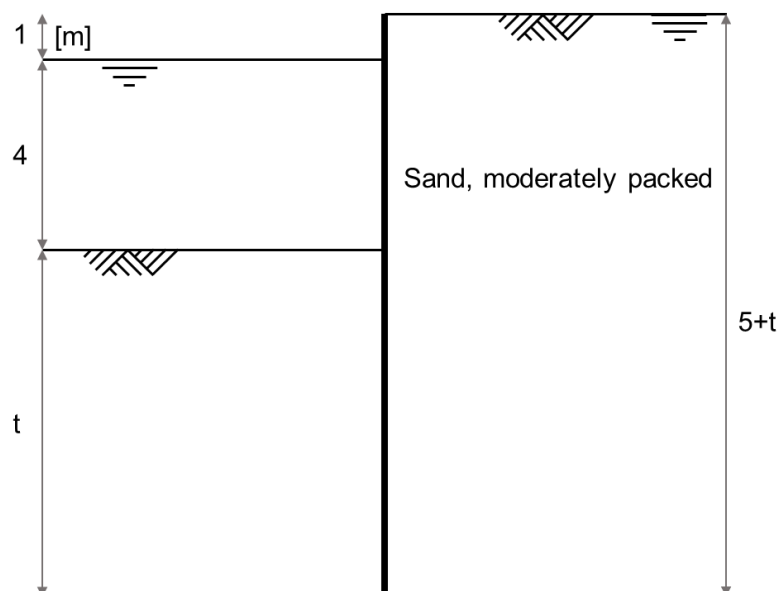


Figure B.1 – Principle geometry of fictional case 1

It is assumed that the soil profile consists of only one type of soil, namely; sand, moderately packed. For the soil properties of this type of soil, the soil properties from final design report of benchmark 1 are used. In this report the soil properties from NEN 9997-1 are used, which are also summed up in Appendix D (The Netherlands Standardisation Institute, 2017). The soil properties of fictional case 1 are collected in Table B.1.

Table B.1 – Soil properties fictional case 1 (Arcadis, 2017)

Type of soil	$\gamma_{dry} / \gamma_{wet}$ [kN/m <sup>3</sup> ]	c [kN/m <sup>2</sup> ]	$\phi$ [°]	$\delta$ [°]	OCR [-]	$k_{h,1}$ [kN/m <sup>3</sup> ]	$k_{h,2}$ [kN/m <sup>3</sup> ]	$k_{h,3}$ [kN/m <sup>3</sup> ]
Sand, moderately packed	18 / 20	0	32.5	21.7	1.0	20,000	10,000	5,000

The moduli of subgrade reaction ( $k_h$ ) are obtained from CUR 166 (Stichting CURNET, 2012a). Furthermore, the specific weight of water ( $\gamma_w$ ) is 10 kN/m<sup>3</sup>.

### Reliability calculations

Reliability calculations are performed with the help of D-Sheet Piling, for fictional case 1 designed in RC2. For this fictional case the reliability index of the following failure mechanisms can be calculated:

- passive resistance inadequate;
- sheet pile profile fails.

Using the reliability analyses module of D-Sheet Piling, the following parameters can be chosen as stochastic:

- soil parameters  $\phi'$  and  $c'$ ;
- water levels;
- uniform- and surface loads;
- surface levels.

From the soil properties of NEN 9997-1 (Appendix D) follows the characteristic values and CoVs of the soil parameters. With the help of these, the mean value and standard deviation of the parameters can be calculated, as is done in chapter 3.1.6. The distributions of the stochastic variables are chosen the same as benchmark 1. The surface- and water level on the waterside of the sheet pile wall are stochastic, because it is physically not possible to raise the surface- and (ground)water level on the landside of the sheet pile wall. Furthermore, the standard deviations of the water- and surface levels are based on research by Havinga (2004), shown in table 3.5. The stochastic variables with their standard deviation and distribution are listed in Table B.2.

Table B.2 – Stochastic variables fictional case 1

Type	Name	Distribution	Mean value	Coefficient of variance	Standard deviation
$\phi'$ [°]	Sand, moderately packed	Normal	38.88	0.10	3.89
Surface level [m NAP]	Surface, waterside	Normal	-5.0	-	0.25
Water level [m NAP]	Water, waterside	Normal	-1.0	-	0.20

### Appendix B-2 Starting points of fictional case 2

In fictional case 2 a real soil profile is added to the simple cantilever sheet pile wall of fictional case 1. For this soil profile, the soil profile of the landside of section B-B' of benchmark 1 is used, because this soil profile is normative for most of the design results of benchmark. This soil profile is shown in Table B.3 and the corresponding soil characteristics are shown in Table B.4.

Table B.3 – Soil profile (Arcadis, 2017)

#	Type of soil	Landside (DKM42) Top level layer [m NAP]
1	Sand, loosely packed	+3.6
2	Clay, clean, weak	-7.5
3	Peat, weak	-8.5
5	Clay, clean, weak	-9.8
6	Sand, moderately packed	-17.5

Table B.4 – Soil characteristics (Arcadis, 2017)

Type of soil	$\gamma_{dry} / \gamma_{wet}$ [kN/m <sup>3</sup> ]	c [kN/m <sup>2</sup> ]	$\phi$ [°]	$\delta$ [°]	OCR [-]	$k_{h;1}$ [kN/m <sup>3</sup> ]	$k_{h;2}$ [kN/m <sup>3</sup> ]	$k_{h;3}$ [kN/m <sup>3</sup> ]
Sand, loosely packed	17 / 19	0	30.0	20.0	1.0	12,000	6,000	3,000
Sand, moderately packed	18 / 20	0	32.5	21.7	1.0	20,000	10,000	5,000
Clay, clean, weak	13.5 / 13.5	6.8	23.7	11.8	1.0	2,000	800	500
Peat, weak	10.5 / 10.5	4.5	18.3	0	1.0	1000	500	250

The moduli of subgrade reaction  $k_h$  are obtained from CUR 166 (Stichting CURNET, 2012a). Furthermore, the specific weight of water ( $\gamma_w$ ) = 10 kN/m<sup>3</sup>.

The principle geometry of fictional case 2 is depicted in Figure B.2. The minimal embedded depth of the sheet pile wall has to be calculated and is now indicated as  $t$ .

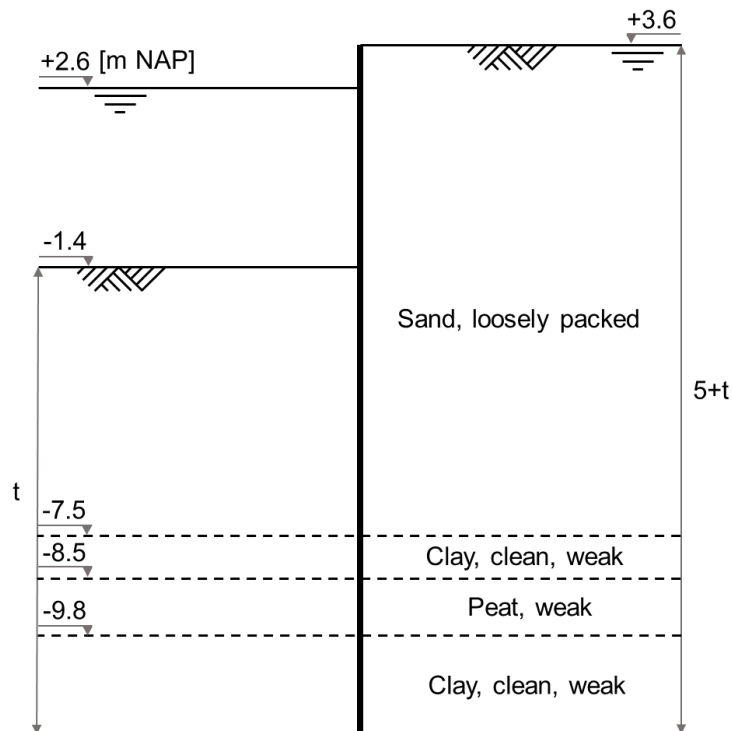


Figure B.2 – Principle geometry of fictional case 2

### Reliability calculations

For fictional case 2 designed in RC2 reliability calculations are performed with the help of D-Sheet Piling. For this fictional case the reliability index of the same failure mechanisms of fictional case 1 can be calculated, namely:

- passive resistance inadequate;
- sheet pile profile fails.

From the soil properties of NEN 9997-1 (Appendix D) follows the characteristic values and CoVs of the soil parameters. With the help of these, the mean value and standard deviation of the parameters can be calculated, as is done in chapter 3.1.6. The distributions of the stochastic variables are chosen the same as benchmark 1. The stochastic variables with their standard deviation and distribution are listed in Table B.5.

Table B.5 – Stochastic variables fictional case 2

Type	Name	Distribution	Mean value	Coefficient of variance	Standard deviation
$\phi'$ [°]	Sand, loosely packed	Normal	35.89	0.10	3.59
$\phi'$ [°]	Clay, clean, weak	Normal	28.35	0.10	2.83
$\phi'$ [°]	Peat, weak	Normal	21.89	0.10	2.19
$\phi'$ [°]	Sand, moderately packed	Normal	38.88	0.10	3.89
$c'$ [kN/m <sup>2</sup> ]	Clay, clean, weak	Lognormal	10.12	0.20	2.02
$c'$ [kN/m <sup>2</sup> ]	Peat, weak	Lognormal	6.70	0.20	1.34
Surface level [m NAP]	Surface, waterside	Normal	-5.0	-	0.25
Water level [m NAP]	Water, waterside	Normal	-3.0	-	0.20

### Appendix B-3 Starting points of fictional case 3

Fictional case 3 is a fictional anchored quay wall with a retaining height of 10 m. With this retaining height an anchor is required. For this case also the soil profile of the landside of section B-B' of benchmark 1 is used. The soil profile is given in Table B.3 and the soil characteristics are given in Table B.4. The principle geometry of fictional case 3 is depicted in Figure B.3. The minimal embedded depth of the sheet pile wall has to be calculated and is now indicated as  $t$ .

In this fictional case a grout anchor is applied every two sheet pile walls. Using an AZ-700 profile of ArcelorMittal the anchors are applied every 2.8 m. The anchorage level is NAP+2.6 m, because just for this level no drainage is required installing them. The anchor is designed in RC2, according to the normal force in the anchor rod. The design of the grout body of the anchor and anchor dropout are not considered in this fictional case.

Besides that, a characteristic value of the surface load of 10 kN/m<sup>2</sup> for quay walls is applied on the landside of the sheet pile wall (Stichting CURNET, 2012a). Furthermore, the specific weight of water ( $\gamma_w$ ) = 10 kN/m<sup>3</sup>.

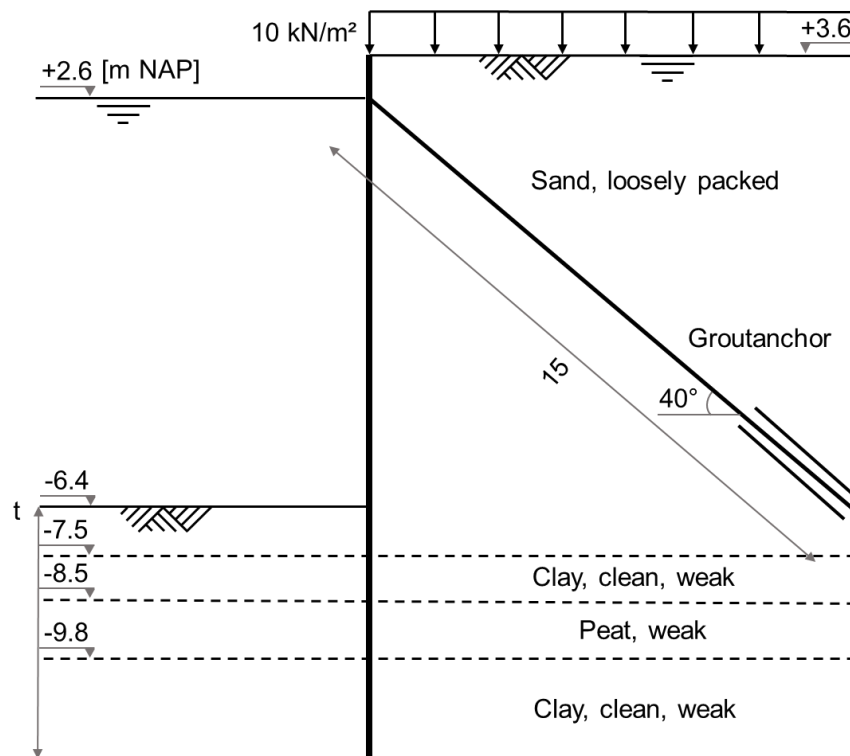


Figure B.3 – Principle geometry of fictional case 3

## Reliability calculations

For this fictional case the reliability index of the following failure mechanisms can be calculated with the help of D-Sheet Piling:

- passive resistance inadequate;
- sheet pile profile fails;
- tension member anchorage fails.

From the soil properties of NEN 9997-1 (Appendix D) follows the characteristic values and CoVs of the soil parameters. With the help of these, the mean value and standard deviation of the parameters can be calculated, as is done in chapter 3.1.6. The distributions of the stochastic variables are chosen the same as benchmark 1. The stochastic variables with their standard deviation and distribution are listed in Table B.6.

Table B.6 – Stochastic variables fictional case 3

Type	Name	Distribution	Mean value	Coefficient of variance	Standard deviation
$\phi'$ [°]	Sand, loosely packed	Normal	35.89	0.10	3.59
$\phi'$ [°]	Clay, clean, weak	Normal	28.35	0.10	2.83
$\phi'$ [°]	Peat, weak	Normal	21.89	0.10	2.19
$\phi'$ [°]	Sand, moderately packed	Normal	38.88	0.10	3.89
$c'$ [kN/m <sup>2</sup> ]	Clay, clean, weak	Lognormal	10.12	0.20	2.02
$c'$ [kN/m <sup>2</sup> ]	Peat, weak	Lognormal	6.70	0.20	1.34
<b>Surface level [m NAP]</b>	Surface, waterside	Normal	-5.0	-	0.25
<b>Water level [m NAP]</b>	Water, waterside	Normal	-3.0	-	0.20
<b>Surface load [kN/m<sup>2</sup>]</b>	Surface load	Normal	6.70	0.30	2.01

### Appendix B-4 Results of fictional case 1

For fictional case 1 the cantilever sheet pile wall is designed using the Blum Method, a hand calculation and the subgrade reaction of D-Sheet Piling. The fictional quay wall is designed using characteristic parameters (without RC) and in reliability class 2 (RC2). Furthermore reliability calculations are performed for the quay wall designed in RC2.

### Design with characteristic parameters

In this subchapter fictional case 1 is designed using characteristic parameters (without RC). First the Blum Method is used, thereafter a hand calculation and eventually the subgrade reaction of D-Sheet Piling is performed. The results of these methods are obtained and differences are discussed.

#### Blum Method

For the Blum Method calculations the manual hydraulic structures, developed by the Delft University of Technology, is used (Vrijling et al., 2015). The Blum Method assumes that the sheet pile wall tends to rotate around a deep point and at this location of the sheet pile the shear force is zero. The sheet pile wall displacement is the result of this rotation and the local deformation of the wall.

At first the required embedded depth  $t$  can be calculated, in order to provide a balance in horizontal stresses and forces, and moment equilibrium. In order to find the required embedded depth the vertical and horizontal soil stresses and water pressures have to be determined. The vertical stresses are determined by the depth and the specific weight of the materials, for the water and the soil separately. An overview of these vertical stresses is depicted in Figure B.4. In this figure the vertical water pressures are illustrated in blue, the vertical soil stresses in brown and the vertical effective stress (the difference between the vertical soil stress and the vertical water pressure) in black. These values are depending on the embedded depth  $t$ .

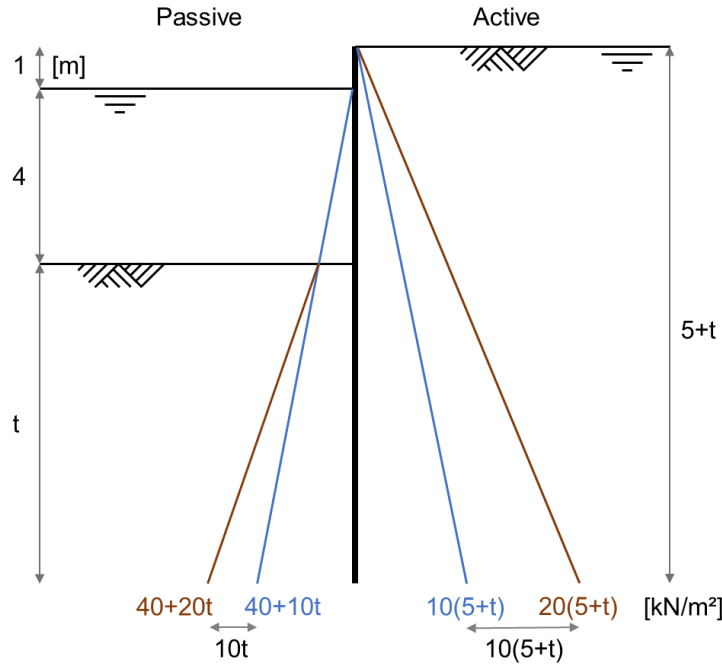


Figure B.4 – Vertical stresses with Blum Method with characteristic values

With the help of the vertical stresses the horizontal stresses can be determined. The horizontal water pressures are equal to the vertical water pressures according to Pascals law. The horizontal soil stresses are determined by the product of the vertical soil stresses and active or passive soil coefficients. Active soil coefficients are applied at the side where the soil becomes less compacted than at rest, due to displacement of the sheet pile wall. At the side where the soil is compressed due to displacement of the sheet pile wall, the passive soil coefficients are applied. So, the active side is at the landside and the passive side at the waterside of the sheet pile wall. These active and passive soil coefficients can be calculated using the Müller-Breslau equations (The Netherlands Standardisation Institute, 2017):

$$\begin{aligned}
 K_{\gamma,a;k} &= \frac{\cos(\varphi'_k + \alpha)^2}{\cos(\alpha)^2 \left( 1 + \sqrt{\frac{\sin(\varphi'_k + \delta_{a;k}) \sin(\varphi'_k - \beta_a)}{\cos(\alpha - \delta_{a;k}) \cos(\alpha + \beta_a)}} \right)^2} \\
 &= \frac{\cos(32.5 + 0)^2}{\cos(0)^2 \left( 1 + \sqrt{\frac{\sin(32.5 + 21.7) \sin(32.5 - 0)}{\cos(0 - 21.7) \cos(0 + 0)}} \right)^2} = 0.25 \\
 K_{\gamma,p;k} &= \frac{\cos(\varphi'_k - \alpha)^2}{\cos(\alpha)^2 \left( 1 - \sqrt{\frac{\sin(\varphi'_k - \delta_{p;k}) \sin(\varphi'_k + \beta_p)}{\cos(\alpha - \delta_{p;k}) \cos(\alpha + \beta_p)}} \right)^2} \\
 &= \frac{\cos(32.5 - 0)^2}{\cos(0)^2 \left( 1 - \sqrt{\frac{\sin(32.5 + 21.7) \sin(32.5 + 0)}{\cos(0 + 21.7) \cos(0 + 0)}} \right)^2} = 7.16
 \end{aligned}$$

The angles used in the equations are illustrated in Figure B.5.

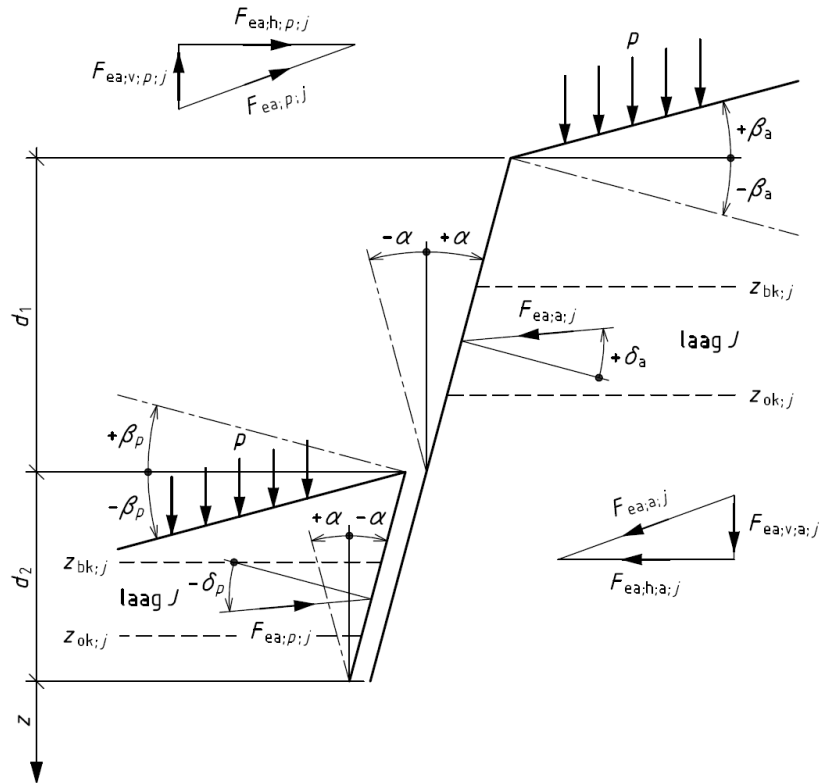


Figure B.5 – Relevant angles for the purpose of Müller-Breslau equations (The Netherlands Standardisation Institute, 2017)

This approach assumes straight sliding surfaces, which is not realistic for angles of internal friction higher than 30°. In these fictional cases this is ignored. With the help of the active and passive soil coefficients the horizontal pressures are determined and these are depicted in Figure B.6. These water and soil stresses can be simplified into four resulting horizontal forces H1, H2, H3 and H4.

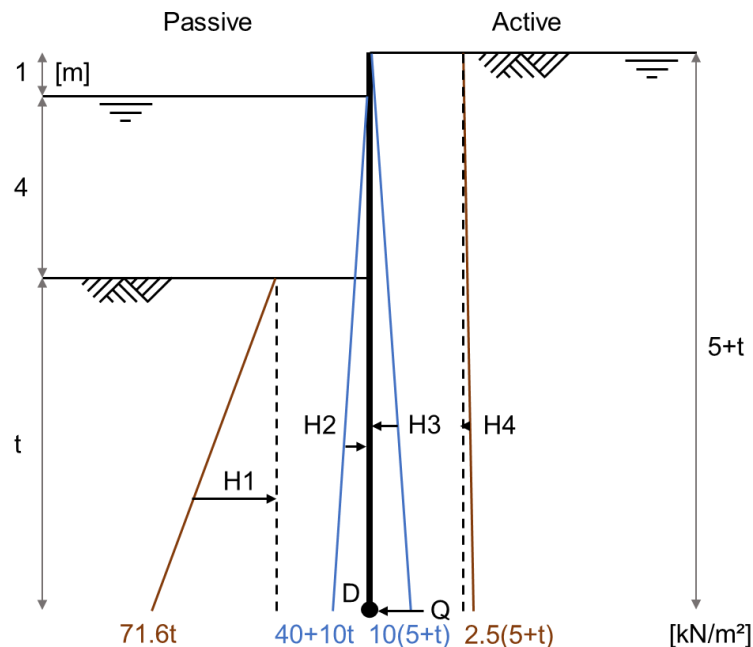


Figure B.6 – Horizontal stresses with Blum Method with characteristic values

The required embedded depth  $t$  can be determined considering an equilibrium of moments around point D. In this schematisation the sheet pile wall inclines to turn around point D and in order to resist the turning of the wall the length of the sheet pile wall is somewhat longer. So, eventually the embedded

depth has to be increased by 20% for cantilever sheet pile walls. Because of this extra length the toe will act as a clamped edge and a passive soil pressure to the left will develop at this extra sheet pile length. The resulting force of this extra passive soil pressure is schematised by a substitute force Q in D.

For the determination of t, first the resulting horizontal forces and their corresponding arm from point D to the work lines of these forces are calculated. These calculations of the moment equilibrium around point D are shown in Table B.7.

Table B.7 – Moment equilibrium around point D

Force [kN/m]	Arm [m]	Moment [kNm/m]
$H1 = \frac{1}{2} \cdot -71.6t \cdot t =$	$-35.8t^2$	$\frac{1}{3}t$
$H2 = \frac{1}{2} \cdot -(40+10t) \cdot (4+t) =$	$-80 - 40t - 5t^2$	$\frac{1}{3}(4+t)$
$H3 = \frac{1}{2} \cdot 10(5+t) \cdot (5+t) =$	$125 + 50t + 5t^2$	$\frac{1}{3}(5+t)$
$H4 = \frac{1}{2} \cdot 2.5(5+t) \cdot (5+t) =$	$31\frac{1}{4} + 12\frac{1}{2}t + 1\frac{1}{4}t^2$	$\frac{1}{3}(5+t)$
$\Sigma H - Q =$	$76\frac{1}{4} + 22\frac{1}{4}t - 34.6t^2$	$\Sigma M_D =$
		$153\frac{3}{4} + 76\frac{1}{4}t + 11\frac{1}{4}t^2 - 11\frac{1}{2}t^3$

So, with the equations from Table B.7, the required embedded depth t, the substitute force Q and the total length of the sheet pile wall L can be calculated:

$$\Sigma M_D = 153\frac{3}{4} + 76\frac{1}{4}t + 11\frac{1}{4}t^2 - 11\frac{1}{2}t^3 = 0 \rightarrow t = 3.72 \text{ m}$$

$$Q = -76\frac{1}{4} - 22\frac{1}{4} \cdot 3.72 + 34.6 \cdot 3.72^2 = 320 \text{ kN/m}$$

$$L = 5 + 1.2 \cdot t = 5 + 1.2 \cdot 3.72 = 9.5 \text{ m}$$

Summarizing the horizontal soil stresses and water pressures on both sides for every depth will give the resulting horizontal stress. The shear force can be found by integrating the equation for the resulting horizontal stress and the bending moment by integrating the equation for the shear force. The results of this calculations are shown in Table B.8. As can be seen, the substitute force Q corresponds approximately to the shear force at a depth of -8.72 m.

Table B.8 – Resulting horizontal stress, shear force and bending moment

Depth [m]	Resulting horizontal stress [kN/m <sup>2</sup> ]	Shear force [kN/m]	Bending moment [kNm/m]
0.00	0.0	0.0	0.0
-1.00	12.5	6.3	3.1
-2.00	15.0	20.0	16.3
-3.00	17.5	36.3	44.4
-4.00	20.0	55.0	90.0
-5.00	22.5	76.3	155.6
-5.33	0.0	79.9	181.0
-5.66	-23.2	76.0	207.1
-6.00	-46.7	64.2	231.0
-6.85	-105.2	0.0	258.0
-7.00	-115.9	-17.2	256.7
-8.00	-185.1	-167.7	164.3
-8.72	-234.9	-318.9	-10.8

With the help of the results of Table B.8, the resulting horizontal stress diagram is depicted in Figure B.7, the shear force diagram in Figure B.8 and the bending moment diagram in Figure B.9.

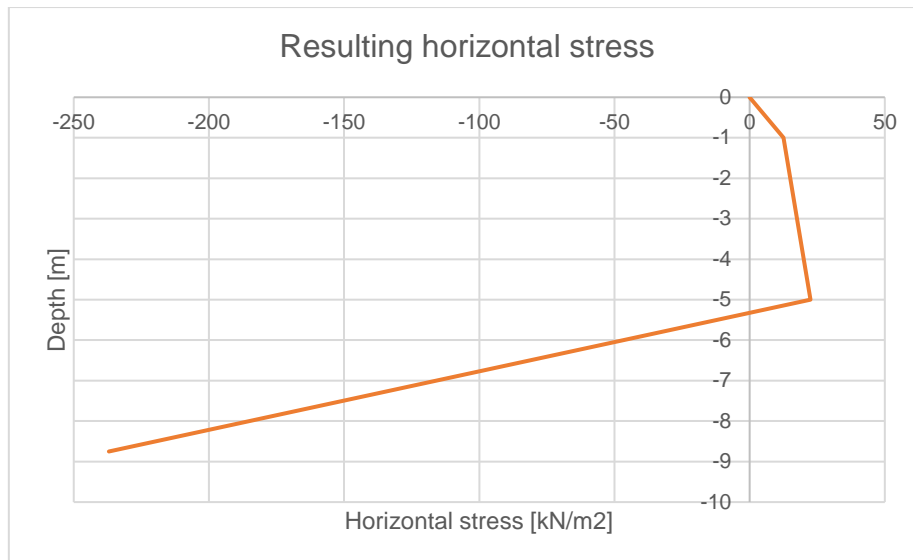


Figure B.7 – Resulting horizontal stress diagram

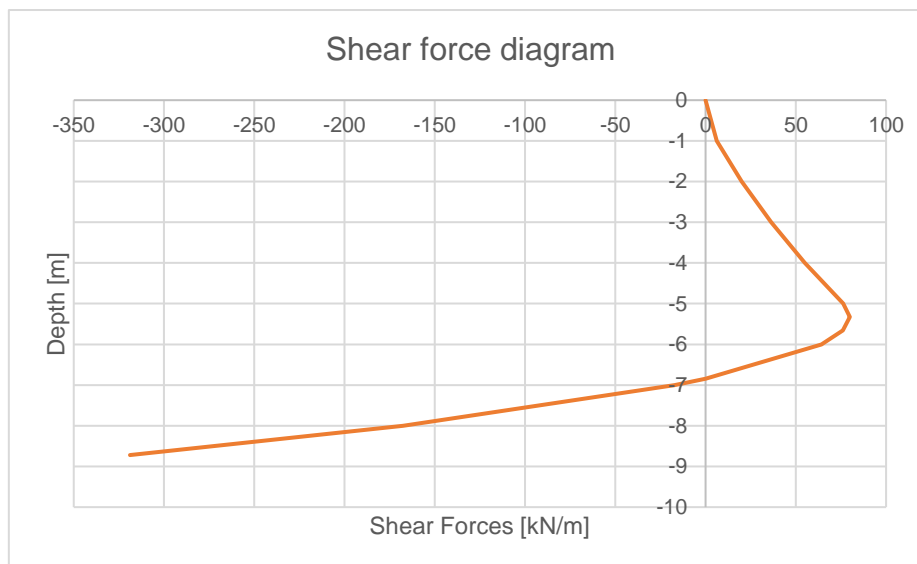


Figure B.8 – Shear force diagram

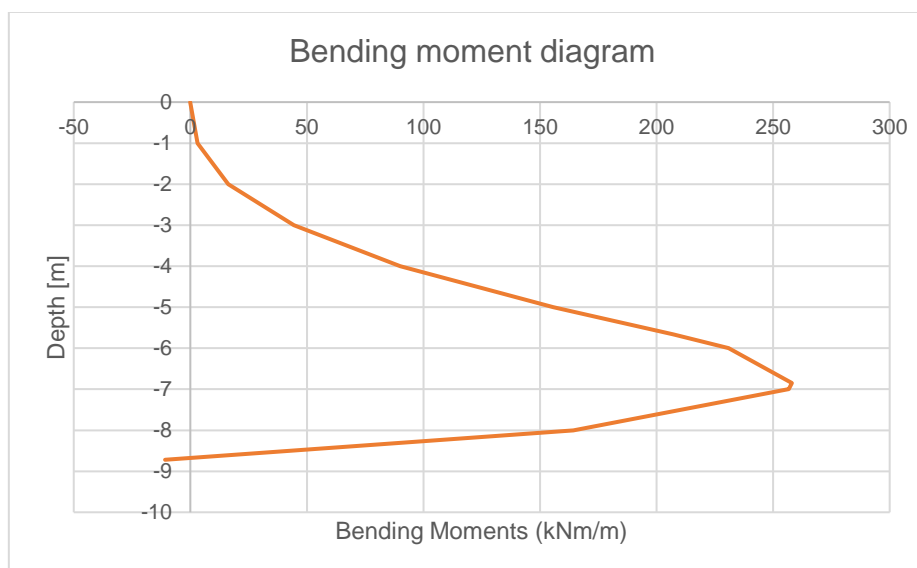


Figure B.9 – Bending moment diagram

So the required embedded depth of fictional case 1 is 3.72 m and the total required length of the sheet pile is 9.5 m. The maximum shear force acts at a depth of -8.72 m and is about -235 kN/m and the maximum bending moment acts at a depth of -6.85 m and is about 260 kNm/m. It is emphasised that this calculation method is a strong schematisation of reality and the results are rough estimations.

The required type of sheet pile profile (for steel quality S240) to resist the maximum bending stresses being determined can be determined by calculating the required elastic section modulus:

$$W_{eff,y} = \frac{M_{max}}{f_{y,d}} = \frac{260 \cdot 10^6}{240} = 1083 \cdot 10^3 \text{ mm}^3/\text{m}$$

The catalog of Z-type sheet pile profiles of ArcelorMittal, shown in Appendix O, can be used in order to determine a sheet pile profile which is able to resist the maximum bending stress. From the catalog follows that sheet pile profile AZ 12-700 (240) is sufficient, because it has an elastic section modulus of  $1205 \cdot 10^3 \text{ mm}^3/\text{m}$ .

### Hand calculation

A cantilever sheet pile wall mechanically is wedged at a depth where the shear force in the sheet pile wall is zero. From Table B.8 in the Blum Method calculation with characteristic values follows that this location is at a depth of -6.85 m.

The maximum displacement of a uniform loaded cantilever can be calculated using the 'vergeet-mij-nietje' of Figure B.10. A 'vergeet-mij-nietje' is collection of basic equations for deflection and displacement of a simple beam, like a cantilever.

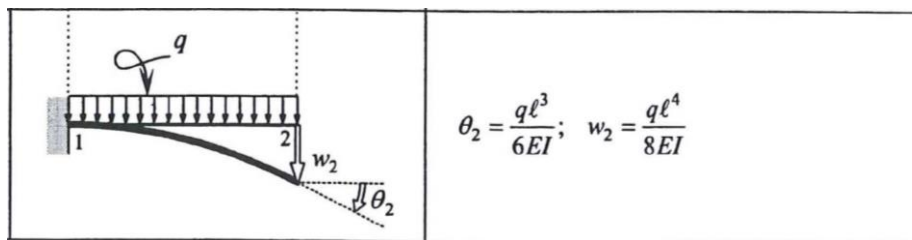


Figure B.10 – 'Vergeet-mij-nietje' uniform loaded cantilever (Vrijling et al., 2015)

The displacement in 2 of the model can be calculated following the equation of  $w_2$  of Figure B.10.  $EI$  is representing the elastic stiffness of the sheet pile profile, which is  $3.96 \cdot 10^4 \text{ kNm}^2/\text{m}$  for the AZ12-700 (S240). The maximum bending moment in 1 of the model can be determined taking the moment equilibrium around point 1:

$$M_1 = \frac{1}{2} ql^2$$

The uniform load  $q$  can be roughly estimated at the unbalance in (ground)water pressure. The (ground)water level difference is 1 m, so the unbalance in (ground)water pressure is 10 kNm/m. This uniform load is a very rough schematisation of reality, because the horizontal water and soil pressure depends on the depth. With the help of the uniform load, the following estimations of the maximum displacement, maximum bending moment and constant shear force can be performed:

$$w_2 = \frac{ql^4}{8EI} = \frac{10 \cdot 6.85^4}{8 \cdot 3.96 \cdot 10^4} = 0.069 \text{ m} = 69 \text{ mm}$$

$$M_1 = \frac{1}{2} ql^2 = \frac{1}{2} \cdot 10 \cdot 6.85^2 = 235 \text{ kNm/m}$$

$$V = ql = 10 \cdot 6.85 = 69 \text{ kN/m}$$

The maximum bending moment in point 1 of Figure B.10 can be compared with the maximum bending moment calculated with the Blum Method. The values are in the same order of magnitude, but both methods are rough estimations. In order to obtain more accurate results, D-Sheet Piling can be used for instance.

### ***D-Sheet Piling***

The results from the Blum Method with characteristic values are used as input for the calculations using D-Sheet Piling. The geometry of Figure B.1 is built and sheet pile profile AZ 12-700 (240) is chosen. First the minimal required sheet pile length in order to be stable is determined, using the 'design sheet piling length' calculation method of D-Sheet Piling. The sheet pile is considered to be unstable if 100% of the mobilised resistance is reached or if the displacement reaches 25% of the sheet piling length. The mobilised resistance is defined as the actual total passive soil reaction divided by the capacity of the total passive soil reaction at full yield (Deltares, 2017).

The minimal required sheet pile length in order to be stable is determined at 9.5 m. For this model the bending moment diagram, the shear force diagram and also the displacements are calculated for the characteristic values. These calculations are performed without reducing the delta friction angle. The results are depicted in Figure B.11.

From the results follows the maximum calculated bending moment does not exceeds the maximum allowable elastic moment. It can be obtained that the maximum calculated bending moment is about 261 kNm/m and the maximum absolute value of the calculated shear force about 166 kN/m. Furthermore the maximum calculated displacement of the sheet pile wall is at the top of the sheet pile wall, which is about 275 mm.

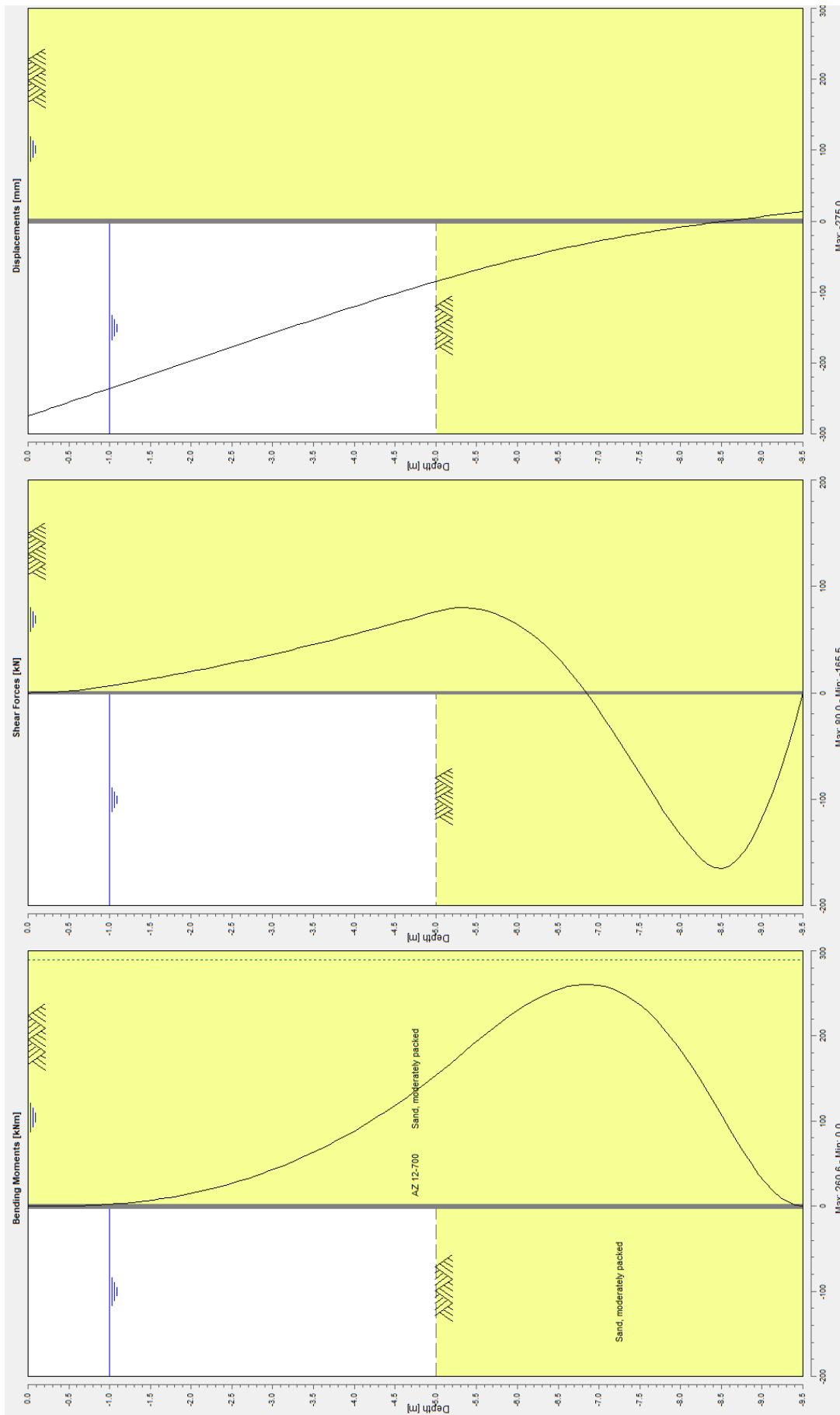


Figure B.11 – Results of fictional case 1 for characteristic values D-Sheet Piling

## Discussion results

The results of the design of fictional case 1 with characteristic parameters are overviewed in Figure B.11.

Table B.9 – Design results of fictional case 1 with characteristic parameters

Structural characteristics	Blum Method	Hand calculation	D-Sheet Piling
Min. sheet pile length [m]	9.5	9.5	9.5
Max. shear force [kN/m]	235	69	166
Max. bending moment [kNm/m]	260	235	261
Max. displacement [mm]	-	69	275
Sheet pile profile (S240)	AZ 12-700	AZ 12-700	AZ 12-700

The minimum sheet pile length calculated with D-Sheet Piling equal to the required length calculated with the Blum Method and a hand calculation. The maximum bending moment calculated using the Blum Method is also very similar to the maximum bending moment calculated with D-Sheet Piling, however it is considerably lower than the maximum bending moment estimated using the ‘vergeet-mij-nietje’. The ‘vergeet-mij-nietje’ is a very rough calculation, which under estimates the bending moment. On the other hand, the maximum shear force calculated with the Blum Method and D-Sheet Piling are very similar, but a lot higher than the maximum shear force calculated with the hand calculation. Furthermore the required sheet pile profile for this fictional case 1 is the same in all three methods.

## Design in RC2

In this subchapter fictional case 1 is designed in RC2, defined in the Eurocodes (The Netherlands Standardisation Institute, 2017). In this calculation the characteristic values of the parameters have to be multiplied by a partial factor. For these calculations in D-Sheet Piling, the model ‘verification (EC7/CUR)’ can be used. In this model, the characteristic values of the soil parameters and loads are multiplied by a chosen set of partial factors and the geometry is modified.

Using the ‘design sheet piling length’ calculation method of D-Sheet Piling, the minimal required sheet pile length in order to be stable is determined as 11.5 m. In this model the maximum allowed elastic moment exceeded, so another sheet profile has to be considered. Now the maximum moment calculated is about 463 kNm/m and based on this moment the sheet pile profile AZ 20-700 (S240) is chosen. Furthermore the maximum absolute value of the calculated shear force is about 255 kNm/m and the maximum calculated displacement of the sheet pile wall is about 711 mm. These results are listed in Table B.10. and depicted in Figure B.12.

Table B.10 – Design results in RC2

Structural characteristics	Structural dimensions
Min. sheet pile length [m]	11.5
Max. shear force [kN/m]	-255
Max. bending moment [kNm/m]	463
Max. displacement [mm]	711
Sheet pile profile	AZ 20-700 (S240)

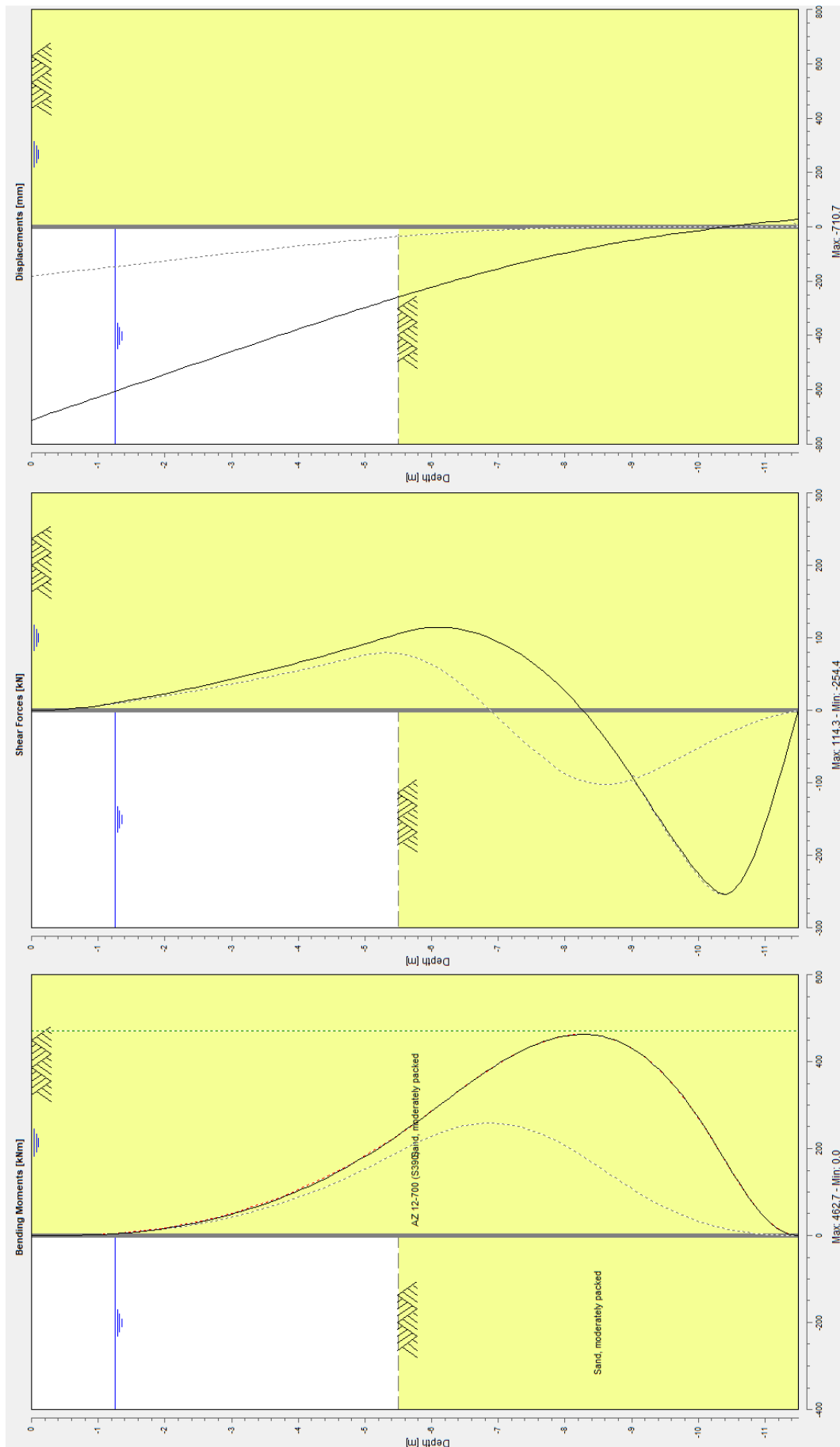


Figure B.12 – Results of fictional case 1 in RC2 D-Sheet Piling

## Reliability results

The results of these reliability calculations are shown in Table B.11.

Table B.11 – Reliability results of fictional case 1

Failure mechanism	Limit value	$\beta$ calculated [-]
Passive resistance inadequate	79%	3.30
Sheet pile profile fails	470 kNm/m	3.30

For the reliability calculations in D-Sheet Piling, an allowable mobilisation, moment or anchor force has to be determined for the different failure mechanisms. This allowable mobilisation, moment or anchor force is also called the limit value. The sheet pile is considered to be unstable if 100% of the mobilised resistance is reached or if the displacement reaches 25% of the sheet piling length (Deltares, 2017). So, the limit value of the mobilisation for the failure mechanism ‘passive resistance inadequate’ is 100%. However, for several models it is not possible to calculate the reliability index for this mobilisation, because the deformation of the sheet pile wall in these calculations is too large and causes numerical problems. For fictional case 1, reliability calculations are possible up to a mobilisation of 79%. So, there is some extra reliability between the 79% and 100% mobilisation, which cannot be calculated by D-Sheet Piling. This extra safety is rather small, because the point of mobilisation till which reliability calculations are possible is very close to failure due to inadequate passive resistance (Havinga, 2018). For the limit value of mobilisation of 79%  $\beta$  is estimated at 3.3. The target  $\beta$  of this failure mechanism for the cantilever sheet pile wall is not known, but this value is already lower than the overall  $\beta$  of RC2 of 3.8. So, this structure will not meet the requirement for the failure mechanism ‘passive resistance inadequate’. It is emphasised that the reliability results are first indications and just rough estimations, because model uncertainties and stochastic correlations are not considered and limited different stochastic variables are used.

The maximum allowable moment of AZ 20-700 (S390) is 470 kNm/m, so this value is used as limit value in the reliability analysis for the failure mechanism ‘sheet pile profile fails’. From calculations followed that the  $\beta$  of the failure mechanism ‘sheet pile profile fails’ is estimated at 3.3. Again, the target  $\beta$  of this failure mechanism for the cantilever sheet pile wall is not known, but this value is already lower than the overall  $\beta$  of RC2 of 3.8. So, this structure will not meet the requirement for the failure mechanism ‘sheet pile profile fails’ as well.

A possible explanation for the relatively low values of  $\beta$  is that these reliability calculations are based on only three stochastic variables, from which only one stochastic variable is a soil parameter. When more soil parameters are stochastic variables, the reliability can be divided over the stochastic variables and the  $\beta$  can be higher. Besides that, the standard deviations of the water- and surface level are relatively high, with respect to the retaining height. Because of the large uncertainty of these two stochastic variables, the  $\beta$  is decreased considerably.

### Appendix B-5 Results of fictional case 2

For fictional case 2 the cantilever sheet pile wall is designed in RC2 and reliability calculations are performed using D-Sheet Piling.

### Design in RC2

In this subchapter fictional case 2 is designed in RC2 using the EC7 verification model in D-Sheet Piling. Using the ‘design sheet piling length’ calculation method of D-Sheet Piling, the minimal required sheet pile length in order to be stable is determined as 13 m. This means that the minimum embedded depth ( $t$ ) is 8 m. The maximum bending moment calculated is about 526 kNm/m and based on this moment the sheet pile profile AZ 14-700 (S390) is chosen. Furthermore the maximum absolute value of the calculated shear force is about 254 kNm/m and the maximum calculated displacement of the sheet pile wall is about 1956 mm. This displacement is very high and probably have to be decreased in case of a real project. These results are listed in Table B.12 and depicted in Table B.11.

Table B.12 – Design results in RC2

Structural characteristics	Structural dimensions
Min. sheet pile length [m]	13
Max. shear force [kN/m]	-254
Max. bending moment [kNm/m]	526
Max. displacement [mm]	1956
Sheet pile profile	AZ 14-700 (S390)

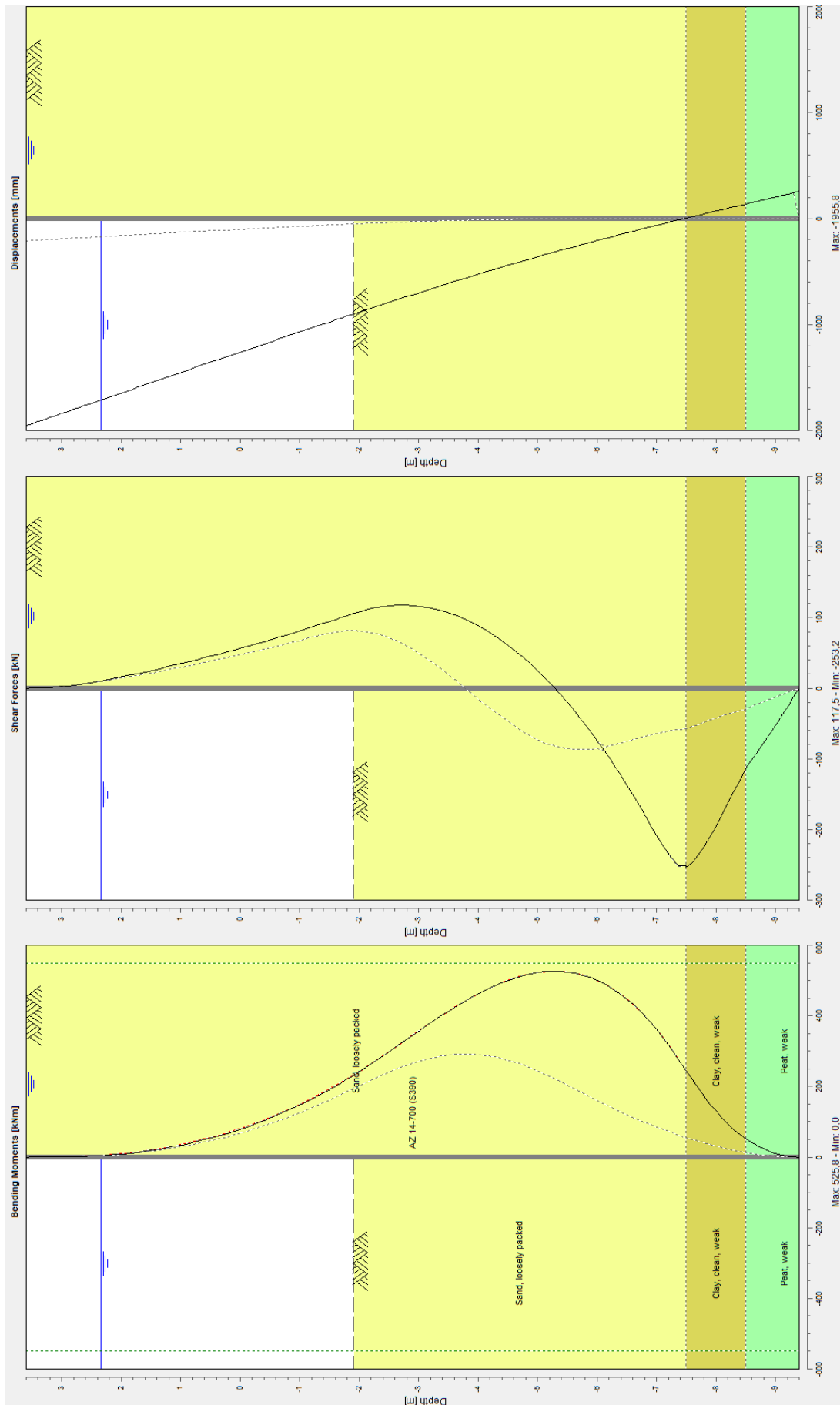


Figure B.13 – Results of fictional case 2 in RC2 D-Sheet Piling

## Reliability results

The results of these reliability calculations are shown in Table B.13.

*Table B.13 – Reliability results of fictional case 2*

Failure mechanism	Limit value	$\beta$ calculated [-]
Passive resistance inadequate	75%	3.30
Sheet pile profile fails	548 kNm/m	3.26

For fictional case 2, reliability calculations are possible up to a mobilisation of 75%. For a limit value of the mobilisation of 75%  $\beta$  is estimated at 3.3. The target  $\beta$  of this failure mechanism for the cantilever sheet pile wall is not known, but this value is already lower than the overall  $\beta$  of RC2 of 3.8. So, this structure will not meet the requirement for the failure mechanism ‘passive resistance inadequate’.

The maximum allowable moment of AZ 14-700 (S390) is 548 kNm/m, so this value is used in the reliability analysis as limit value. From calculations followed that the  $\beta$  of the failure mechanism ‘sheet pile profile fails’ is estimated at 3.26. Again, the target  $\beta$  of this failure mechanism for the cantilever sheet pile wall is not known, but this value is already lower than the overall  $\beta$  of RC2 of 3.8. So, this structure will not meet the requirement for the failure mechanism ‘sheet pile profile fails’ as well. It is emphasised that the reliability results are first indications and just rough estimations, because model uncertainties and stochastic correlations are not considered and limited different stochastic variables are used.

A possible explanation for the relatively low values of  $\beta$  is that these reliability calculations are based on only three stochastic variables again, because only the  $\phi'$  of sand, loosely packed contributes to the reliability calculations. When more soil parameters contribute to the reliability calculations, the reliability can be divided over the stochastic variables and the  $\beta$  can be higher. Besides that, the standard deviations of the water- and surface level are relatively high, with respect to the retaining height. Because of the large uncertainty of these two stochastic variables, the  $\beta$  is decreased considerably.

### Appendix B-6 Results of fictional case 3

For fictional case 3 the anchored sheet pile wall is designed in RC2 and reliability calculations are performed using D-Sheet Piling.

### Design in RC2

In this subchapter fictional case 3 is designed in RC2 using the EC7 verification model in D-Sheet Piling. After a couple of iterations, the minimal required sheet pile length in order to be stable is obtained as 22 m. This means that the minimum embedded depth (t) is 12 m.

The maximum shear force, bending moment and anchor force are calculated for the acting width of 2.8 m and are depicted in Figure B.14. The maximum bending moment is about 1320 kNm/m and based on this moment the sheet pile profile AZ 37-700 (S390) is chosen. Furthermore the maximum calculated shear force is about -273 kNm/m and the maximum calculated displacement of the sheet pile wall is about 316 mm. These results are listed in Table B.14.

*Table B.14 – Design results in RC2*

Structural characteristics	Structural dimensions
Min. sheet pile length [m]	22
Max. shear force [kN/m]	-273
Max. bending moment [kNm/m]	1320
Max. anchor force [kN/m]	376
Max. displacement [mm]	316
Sheet pile profile	AZ 37-700 (S390)

The maximum anchor force is about 1051 kN. Following the CUR 166, this load has to be multiplied by an extra load for the anchor rod of 1.25, so the design anchor force is 1314 kN. An overview of the

available grout injection anchor from Jetmix is given in Appendix L. According to this design anchor force, Jetmix grout injection anchor 7 is chosen (76.5 x 14.2 mm). The characteristics of this grout anchor are listed in Table B.15.

Table B.15 – Characteristics Jetmix grout injection anchor 7 (Jetmix, 2016)

Anchor component	Anchor characteristics
Level [m NAP]	+2.6
E-modulus [kN/m <sup>2</sup> ]	$2.1 \cdot 10^8$
Cross-section [m <sup>2</sup> /m]	$9.67 \cdot 10^{-4}$
Length [m]	15
Angle [°]	40
Design yield force [kN]	1354

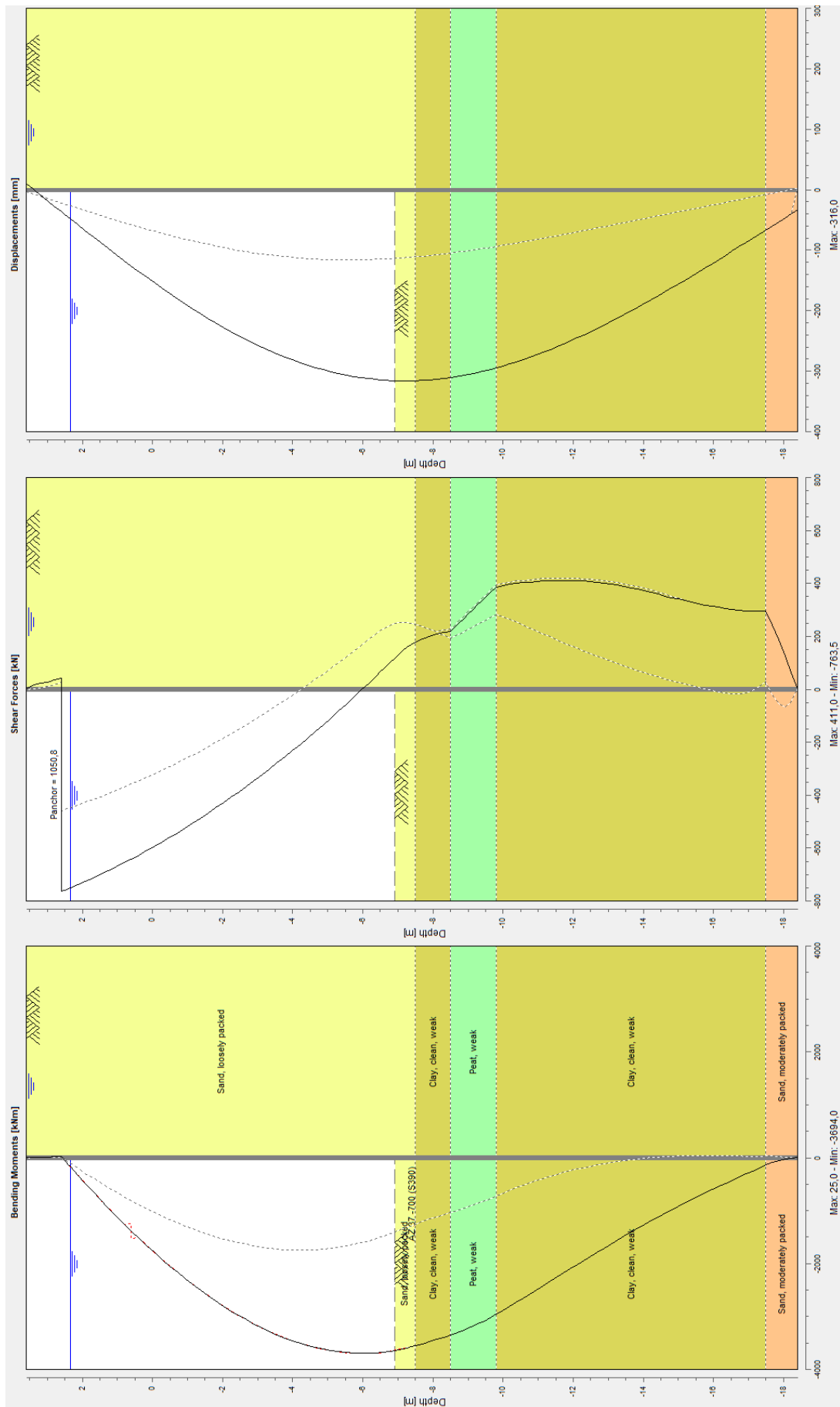


Figure B.14 – Results of fictional case 3 in RC2 D-Sheet Piling

## Reliability results

For fictional case 3 designed in RC2 reliability calculations are performed with the help of D-Sheet Piling and Prob2B.

### D-Sheet Piling

In the reliability calculations of fictional case 3, the centre to centre distance of the anchors of 2.8 m have to be taken into account. Therefore, the limit values of the failure mechanisms ‘sheet pile profile fails’ and ‘tension member anchorage fails’ have to be inserted per section width, in stead of per meter. The maximum allowable moment of AZ 37-700 (S390) is 1445 kNm/m, so this is equal to 4046 kNm/section. The design yield force of the anchor rod is 1354 kN/anchor, so this value is used in the reliability calculations. The results of these reliability calculations are shown in Table B.16. The  $\beta$ 's calculated are compared with the  $\beta$ 's defined in the CUR 211 originating from 2005, depicted in figure 2.18.

Table B.16 – Reliability results of fictional case 3

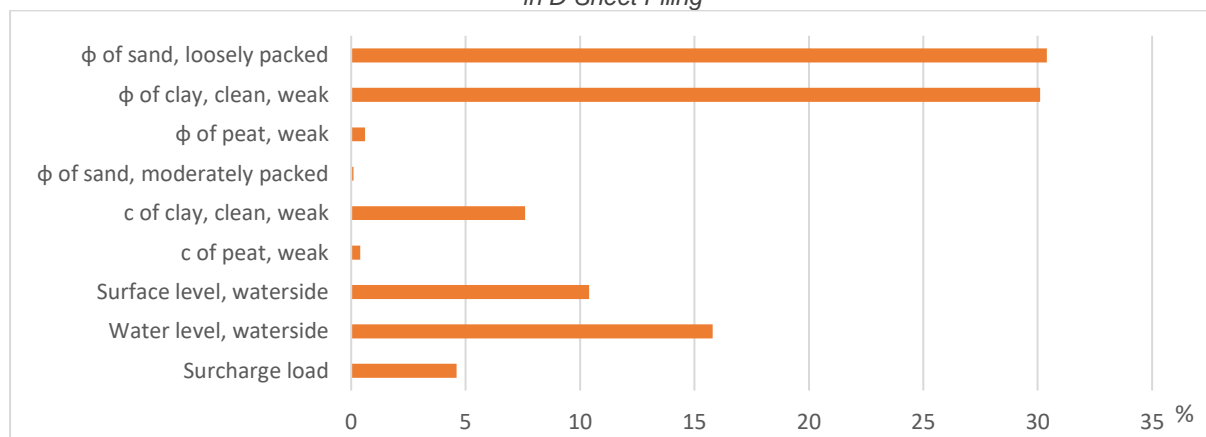
Failure mechanism	Limit value	$\beta$ calculated [-]	$\beta$ CUR 211 (RC2) [-]
Passive resistance inadequate	100%	5.68	4.11
Sheet pile profile fails	4046 kNm / section	6.01	4.11
Tension member anchorage fails	1354 kN / anchor	7.30	4.46

The  $\beta$  of the failure mechanism ‘passive resistance inadequate’ is estimated at 5.68, the  $\beta$  of ‘sheet pile profile fails’ is estimated at 6.01 and the  $\beta$  of ‘tension member anchorage fails’ is estimated at 7.30. These values are significantly higher than the target  $\beta$ 's of the fault tree in the CUR 211 of 2005. So, if this fault tree is used, the structure will meet the requirements for all these three failure mechanisms. It is emphasised that the reliability results are first indications and just rough estimations, because model uncertainties and stochastic correlations are not considered and limited different stochastic variables are used.

The  $\beta$ 's of fictional case 3 are considerably lower than the  $\beta$ 's of fictional case 1 and 2. A possible explanation for the relatively high values of  $\beta$  is that these reliability calculations are depending on almost all stochastic variables, because the sheet pile wall is performed in all the soil layers. When more soil parameters contribute to the reliability calculations, the reliability can be divided over the stochastic variables and the  $\beta$  can be higher. Besides that, the standard deviations of the water- and surface level are now relative lower with respect to the retaining height, comparing to fictional case 1 and 2.

For each of failure mechanism, a sensitivity factor for each of the stochastic variables can be determined by D-Sheet Piling as the  $\alpha$ -value. The contribution of each of the stochastic variables to the failure mechanism ‘tension member anchorage fails’ can be estimated as  $\alpha^2$  and is shown in Table B.17. It appears that the relative contributions are strongly dominated by the  $\phi$ -values.

Table B.17 – Contribution of stochastic variables to the  $\beta$  of ‘tension member anchorage fails’ of fictional case 3 in D-Sheet Piling



### Prob2B

For the purpose of the Prob2B calculation of  $\beta$ , a limit state function has to be defined. The limit state function for the failure mechanism ‘tension member anchorage fails’ is given (Wolters, 2012):

$$Z = f_y - \frac{F_{anchor}}{A_{anchor}}$$

$$A_{anchor} = \frac{1}{4} \cdot \pi \cdot D_{anchor}^2, \text{ so } D_{anchor} = \sqrt{\frac{4 \cdot A_{anchor}}{\pi}}$$

From Table B.15 follows that  $A_{anchor}$  is  $9.67 \cdot 10^{-4} \text{ m}^2/\text{m}$ . Assumed is that every 2.8 meters an anchor is applied, so  $A_{anchor}$  is  $2.7 \cdot 10^{-3} \text{ m}^2$ . The diameter of the anchor rod ( $D_{anchor}$ ) can be calculated:

$$D_{anchor} = \sqrt{\frac{4 \cdot 2.7 \cdot 10^{-3}}{\pi}} = 5.87 \cdot 10^{-2} \text{ m}$$

So, this reliability calculation consists of three stochastic variables, shown in Table B.18. In this table also the distributions and standard deviations are given.

Table B.18 – Stochastic variables fictional case 3 – Prob2B

Parameter	Distribution	Mean value	Coefficient of variance	Standard deviation
$f_y$ [kN/m <sup>2</sup> ]	Normal	$5.00 \cdot 10^5$	0.07	$3.5 \cdot 10^4$
$D_{anchor}$ [m]	Normal	$5.87 \cdot 10^{-2}$	0.032	$1.88 \cdot 10^{-3}$
$F_{anchor}$ [kN]	Normal	632	0.20	126.4

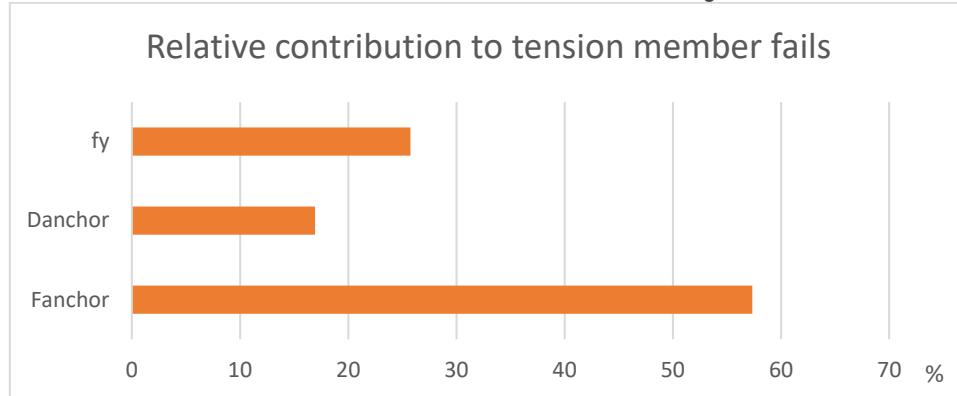
The mean value of the yield stress ( $f_y$ ) and the diameter ( $D_{anchor}$ ) of the anchor follow from the characteristics of the Jetmix grout injection anchor 7, attached in Appendix L (Jetmix, 2016). The coefficient of variance of these stochastic variables follow from research by Wolters (2012), which used a steel producer as recourse for these values. The mean value of the anchor force ( $F_{anchor}$ ) follows from a D-Sheet Piling calculation of fictional case 3 with characteristic parameters. Furthermore the coefficient of variance of the anchor force is estimated at 0.20. This rather high value is chosen, because this parameter is quite uncertain. The standard deviations are calculated by the product of the mean value and the coefficient of variance. The results of the reliability calculation using FORM with Prob2b are shown in Table B.19.

Table B.19 – Reliability results of fictional case 2 – Prob2B

Failure mechanism	$\beta$ calculated [-]	$\beta$ CUR 211 (RC2) [-]
Tension member anchorage fails	4.16	4.46

According to the FORM using Prob2B, the calculated  $\beta$  is somewhat lower than the target  $\beta$  of the fault tree in the CUR 211 of 2005. So, if this fault tree is used, the structure will not meet the requirements for the failure mechanism ‘tension member anchorage fails’. Besides that, this  $\beta$  calculated using Prob2B is lower than the  $\beta$  calculated using D-Sheet Piling. Due to the reduced number of stochastic variables, less spread of reliability over the stochastic variables is possible and  $\beta$  is lower. However, these results are hardly comparable, because they both include a completely different set of stochastic variables. For each of the failure mechanisms, the  $\alpha$ -value of the stochastic variables to the  $\beta$  can be determined by Prob2B as well. The contribution of each of the stochastic variables to the failure mechanism ‘sheet pile profile fails’ is determined as  $\alpha^2$  and is shown in Table B.20. It appears that the anchor force,  $F_{anchor}$ , has the largest contribution to the failure mechanism ‘tension member anchorage fails’. It is emphasised that the reliability results are first indications and just rough estimations, because model uncertainties and stochastic correlations are not considered and limited different stochastic variables are used.

Table B.20 –  $\alpha^2$ -values of stochastic variables to ‘tension member anchorage fails’ of fictional case 3 Prob2B



### Appendix B-7 Conclusion

In this chapter three fictional cases are introduced, the starting points of these cases are treated and design- and reliability results are obtained. These three fictional cases are examined to become familiar with the research steps and possible results. Therefore, the complexity of these fictional cases is slowly increased, towards the complexity of the double anchored combi-wall of benchmark 1. Several design- and reliability methods are explored, what is used in the decision of the methods to be used for the benchmarks.

The first fictional cantilever sheet pile structure is designed using three calculation methods, starting with the simplest method, followed by the more complex ones. So, sequentially the used methods used are: the Blum method, the hand calculation and the subgrade reaction method. The hand calculation is used as a first estimate of the result and the Blum Method is used as validation of the subgrade reaction method. The design results of these methods are comparable and the subgrade reaction method is used for the other fictional cases and for benchmark 1.

The reliability calculations for the fictional cases are performed using the reliability analyses module of D-Sheet Piling. This method is chosen, because of the relatively low computational time and it generally gains accurate results. It followed that this module have some restrictions and is not always able to obtain reliability results. On the one hand, a bug in the script of the module causes these errors. During this study Deltares found and solved this bug. On the other hand, in some cases the deformation of the structure becomes too large, causing numerical problems. Generally, the reliability analyses module of D-Sheet Piling are user friendly, the FORM is accurate and therefore it is used for the reliability calculations of the benchmark quay wall.

## Appendix C Boundary conditions of benchmark 1

In this chapter, the surface levels, hydraulic conditions, geotechnical conditions, loads and load combinations are determined.

### Appendix C-1 Surface levels

The required surface level at the landside of the quay wall is NAP+3.6 m. For the required depth of the quay wall the normative vessel have to be considered. The normative vessel for this quay wall is the Normand Cutter, with a nautical required depth of NAP-9.5 m (Arcadis, 2017) and a nautical required mooring length of 267 m. In consultation with the Port of Rotterdam, it has been decided that the nautical guaranteed depth is NAP-10.65 m instead of the minimal required depth of NAP-9.5 m. This is done, because from a cost comparison in the variants study followed that a reduction of the nautical guaranteed depth will lead to a limited reduction of the investments costs. Furthermore, from the performed variants study followed that a bed protection is desirable. So, considering a maintenance margin, thickness of the bed protection and additional tolerances the construction depth is defined as NAP-13.35 m.

### Appendix C-2 Hydraulic conditions

In this subchapter the considered free- and groundwater levels are given for the design of benchmark 1. The design includes a drainage system which regulates the groundwater level at the landside.

#### Free water levels

The acting water levels, specified by the Port of Rotterdam, are listed in Table C.1.

Table C.1 – Free water levels (Arcadis, 2017)

Water level	Level [m NAP]
Mean High Water (MHW)	+1.17
Mean High Water Spring (MHWS)	+1.32
Mean Low Water (MLW)	-0.38
ALW (Agreed Low Water Level)	-0.72
LW <sub>1</sub> x year	-1.10
LW <sub>1</sub> x 250 years	-1.65

#### Design water levels

The design water levels are defined using CUR 211 (Stichting CURNET, 2014). For practical reasons no distinction is made between the water levels in SLS and ULS. This means that the water levels in SLS are conservative. The situation considering low free water level in combination with unfavourable loads is normative for the design of the quay wall. Thereby in the fundamental load combination it is assumed that an operating drainage is applied at NAP-1.25 m. The extreme water level should be considered as accidental limit state (ALS). For these extreme water levels, two accidental combinations are introduced; extremely low water and drainage failure.

Following the CUR 211, the minimum water level difference between free- and groundwater level in the fundamental combination is 0.5 m. The water level difference between free- and groundwater level in the combination drainage failure is assumed as the difference between MHW and MLW, so 1.55 m. This value has to be minimally 1.0 m, following the CUR 211. This leads to the design water levels as given in Table C.2.

Table C.2 – Design water levels

Situation	Free water level	Groundwater level
<b>Fundamental combination</b>		
SLS / ULS	NAP-0.72 m (ALW)	NAP-0.22 m
<b>Accidental combinations</b>		
Extremely low water	NAP-1.65 m (LW <sub>1</sub> x 250 years)	NAP -0.95 m
Drainage failure	NAP-1.10 m (LW <sub>1</sub> x year)	NAP+0.45 m

### Appendix C-3 Geotechnical conditions

On the basis of the soil investigations the quay wall is divided into three sections, each consisting of a different soil profile. These sections, A-A', B-B' and C-C', are depicted in Figure C.1.

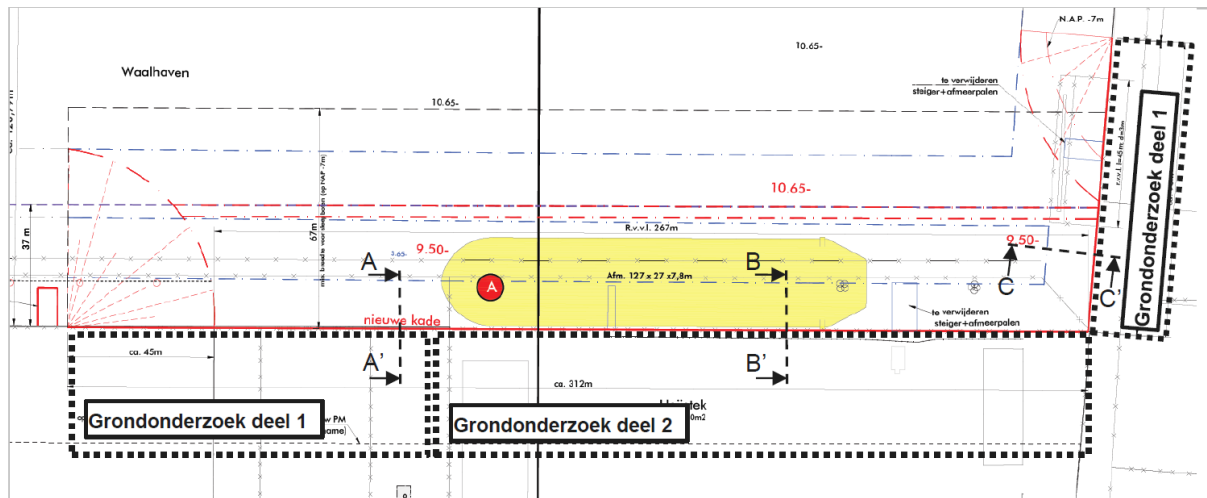


Figure C.1 – Sections quay wall design (Arcadis, 2017)

In this research only the soil profile of section B-B' is considered, because this soil profile is normative for most of the design verifications. The considered soil profile of benchmark 1 is shown in Table C.3 and the soil characteristics are shown in Table C.4. For the soil properties of these types of soil, the soil properties from the final design report of benchmark 1 are used (Arcadis, 2017). In this report the soil properties from NEN 9997-1 are used, which are also summed up in Appendix D (The Netherlands Standardisation Institute, 2017).

Table C.3 – Soil profile of section B-B' (Arcadis, 2017)

#	Type of soil	Waterside (DKM21)	Landside (DKM42)
		Top level layer [m NAP]	Top level layer [m NAP]
1	Sand, loosely packed	-	+3.6
2	Clay, clean, weak	-	-7.5
3	Peat, weak	-	-8.5
4	Sand, loosely packed	-13.35	-
5	Clay, clean, weak	-14.0	-9.8
6	Sand, moderately packed	-17.5	-17.5

Table C.4 – Soil characteristics (Arcadis, 2017)

Type of soil								
<b>Sand, loosely packed</b>	17 / 19	0	30.0	20.0	1.0	12,000	6,000	3,000
<b>Sand, moderately packed</b>	18 / 20	0	32.5	21.7	1.0	20,000	10,000	5,000
<b>Sand, very silty, clayey</b>	18 / 20	0	25.0	16.7	1.0	12,000	6,000	3,000
<b>Clay, mild sandy, weak</b>	16 / 16	1.5	22.5	11.2	1.0	4,000	2,000	800
<b>Clay, clean, weak</b>	13.5 / 13.5	6.8	23.7	11.8	1.0	2,000	800	500
<b>Peat, weak</b>	10.5 / 10.5	4.5	18.3	0	1.0	1000	500	250

### Appendix C-4 Loads

The loads are specified in final design report of benchmark 1 (Arcadis, 2017) and listed below:

- Surface load of 40 kN/m<sup>2</sup> in the front of the quay wall till 30 m.
- Bollard force of 1500 kN/bollard
- Bed protection as uniform load of 5 kN/m<sup>2</sup>

The centre to centre distance between the bollards is 15 m. Forces due to the mooring of vessels and waves are negligible and not considered. The failure of drainage and extremely low water are considered in the load combinations. Furthermore, anchor failure is taken into account designing the quay wall.

#### Appendix C-5 Load combinations and phasing of construction

In the existing design, three fundamental and three accidental loads are treated. The three accidental load combinations are:

- extremely low water;
- drainage failure;
- construction of bed protection (future deepening).

The load combinations, together with their corresponding load- ( $\gamma$ ) and load combination factors ( $\psi$ ) for the design in RC2 are shown in Table C.5.

Table C.5 – Load combinations with their corresponding load- and load combination factors in RC2 (Arcadis, 2017)

Load combinations ULS	Fundamental / accidental	$\gamma_Q$	$\Psi_0$			$\Psi_1$		$\Psi_0$
			I	II	III	IV	V	VI
Fundamental water level difference	Fundamental	1.0	1	1	1			1
Surface load	Fundamental	1.1	1	0.7	1	0.5	0.5	0.5
Bollard load	Fundamental	1.3		1	0.7	0.3	0.3	
Extremely low water	Accidental	1.0				1		
Drainage failure	Accidental	1.0					1	

### Appendix D Characteristic values of soil properties

Grondsoort		Karakteristieke waarde <sup>a</sup> van grondeigenschap												
Hoofd-naam	Bijmengsel	Consistentie <sup>b</sup>	$\gamma^c$ kN/m <sup>3</sup>	$\gamma_{sat}$ kN/m <sup>3</sup>	$q_c^{d,g}$ MPa	$C_p^h$	$C_s$	$C_d/(1+e_0)^g$ [-]	$C_{\sigma^f}$ [-]	$C_{sw}/(1+e_0)^g$ [-]	$E_{100}^{g,h}$ MPa	$\phi^g$ Graden	$c^i$ kPa	$c_u$ kPa
Grind	Zwak siltig	Los	17	19	15	500	$\infty$	0,0046	0	0,0015	45	32,5	0	
	Matig	Matig	18	20	25	1000	$\infty$	0,0023	0	0,0008	75	35,0	0	N.v.t.
	Vast	Vast	19	20	30	1200	1400	0,0019	0	0,0006	90	37,5	0	
Zand	Sterk siltig	Los	18	20	10	400	$\infty$	0,0058	0	0,0019	30	30,0	0	
	Matig	Matig	19	21	15	600	$\infty$	0,0038	0	0,0013	45	32,5	0	N.v.t.
	Vast	Vast	20	21	25	1000	1500	0,0023	0	0,0008	75	35,0	0	
Zand	Schoon	Los	17	19	5	200	$\infty$	0,0115	0	0,0038	15	30,0	0	
	Matig	Matig	18	20	15	600	$\infty$	0,0038	0	0,0013	45	32,5	0	N.v.t.
	Vast	Vast	19	20	25	1000	1500	0,0023	0	0,0008	75	35,0	0	
Leem <sup>e</sup>	Zwak siltig, kleilig		18	19	12	450	650	0,0051	0	0,0017	35	27,0	0	N.v.t.
	Sterk siltig, kleilig		18	19	8	200	400	0,0115	0	0,0038	15	30,0	0	N.v.t.
	Zwak zandig	Slap	19	19	1	25	650	0,0920	0,0037	0,0307	2	27,5	0	50
Klei	Schoon	Matig	17	17	1,0	15	160	0,1533	0,0061	0,0511	2	17,5	5	50
	Matig	Vast	19	20	2,0	25	320	0,0920	0,0037	0,0307	4	17,5	13	100
	Zwak zandig	Slap	15	15	0,7	10	110	0,2300	0,0092	0,0767	1,5	22,5	0	40
Veen	Sterk zandig	Matig	18	18	1,5	20	240	0,1150	0,0046	0,0383	3	22,5	5	80
	Matig	Vast	20	21	2,5	30	400	0,0767	0,0031	0,0256	5	22,5	13	120
	Vast	Vast	18	18	1,0	25	140	0,0920	0,0037	0,0307	2	27,5	0	10
Variatiecoëfficiënt v	Organisch	Slap	13	13	0,2	7,5	30	0,3067	0,0153	0,1022	0,5	15,0	0	10
	Matig	Matig	15	15	0,5	10	40	0,2300	0,0115	0,0767	1,0	2,0	0	25
	Niet voorbelast	Slap	10	10	0,1	5	20	0,4800	0,0230	0,1533	0,2	0,5	1	2,5
Variatiecoëfficiënt v	Matig voorbelast	Matig	12	12	0,2	7,5	30	0,3067	0,0153	0,1022	0,5	1,0	2,5	5
			0,05					0,25				0,10		20

<sup>a</sup> De tabel geeft van de desbetreffende grondsoort de lage, respectievelijk de hoge karakteristieke waarde van gemiddelden. Binnen een gebied, vastgesteld door de rij van het bijmengsel en de kolom van de parameter (een cel), geldt:  
— als een verhoging van de waarde van een van de grondeigenschappen tot een ongunstiger situatie leidt dan de toepassing van de in de tabel gepresenteerde lagere karakteristieke waarde, moet de rechterwaarde op dezelfde regel zijn gebruikt. Is er rechts geen waarde vermeld, dan moet de waarde er recht onder zijn toegepast;  
OPMERKING Dit is bijvoorbeeld het geval bij negatieve kleeft op een paal waar een hogere waarde van  $\phi^g$ ,  $c^i$  en  $c_u$  ook een hogere waarde van de negatieve kleeft oplevert.  
— voor  $C_d/(1+e_0)$ ,  $C_{\sigma}$  en  $C_{sw}/(1+e_0)$  zijn in de tabel de hoge karakteristieke gemiddelde waarden vermeld.

Figure D.1 – Characteristic values of soil parameters, part 1 (The Netherlands Standardisation Institute, 2017)

b	Los: $0 < R_n < 0,33$
	Matig: $0,33 \leq R_n \leq 0,67$
	Vast: $0,67 < R_n < 1,00$
c	De $\gamma$ -waarden zijn van toepassing bij een natuurlijk vochtgehalte.
d	De hier gegeven $q_c$ -waarden (conusweerstand) behoren beschouwd te worden als ingang in de tabel en mogen niet in de berekeningen worden gebruikt.
e	De waarden hebben betrekking op verzadigd leem.
f	De $C_{\sigma}$ -waarden zijn geldig voor een spanningverhogingstraject van ten hoogste 100 %.
g	Voor grind, zand en in beperkte mate ook voor leem en sterk zandige klei zijn $q_c$ , $E_{100}$ , $\phi'$ en de samendrukkingsparameters $C'_p$ , $C'_d/(1+e_0)$ en $C_{sw}/(1+e_0)$ genormeerd voor een effectieve verticale grondspanning $\sigma'_v$ van 100 kPa. Om voor de in het terrein gemeten waarden van $q_c$ een juiste ingang in de tabel te krijgen moeten deze waarden zijn geconverteerd naar het niveau van de effectieve verticale grondspanning $\sigma'_v$ van 100 kPa. In dat kader moet de formule $q_{c,tabel} = q_{c,terrein} \times C_{qc}$ worden gebruikt, waarbij $C_{qc}$ moet zijn ontleend aan $C_{qc} = (100/\sigma'_v)^{0,67}$ . Voor de hoek van inwendige wrijving $\phi'$ en de cohesie $c'$ geldt dat deze afhankelijk zijn van de consistentie van de grond. Dit betekent dat deze conversie ook nodig is voor $\phi'$ en $c'$ . Als $q_{c,tabel}$ groter wordt dan de in de tabel gegeven waarde geldt de onderste regel voor de desbetreffende grondsoort.
h	De elasticiteitsmodulus bij belastingsherhalingen mag zijn aangenomen als zijnde driemaal de aangegeven waarde.

Figure D.2 – Characteristic values of soil parameters, part 2 (The Netherlands Standardisation Institute, 2017)

## Appendix E Boundary conditions of benchmark 2

In this chapter, the surface levels, hydraulic conditions, geotechnical conditions, loads and load combinations are determined.

### Appendix E-1 Surface levels

Benchmark 2 has to be connected to adjacent quay wall with corresponding surface levels. This means that the required surface level of the terminal at the landside of the quay wall is NAP+5.0 m. The normative vessel determines the required depth of the quay wall. The future normative vessel of the terminal is the Lucky Sunday (Panamax vessel), having a draught of about 14.5 m and a nautical required depth of NAP-16.65 m (Arcadis, 2016). Considering a maintenance margin and additional tolerances the construction depth is defined as NAP-18.65 m. This means that the retaining height of benchmark 2 is about 23.65 m.

### Appendix E-2 Hydraulic conditions

In this subchapter the considered free- and groundwater levels are given for benchmark 2. The design includes a drainage system which regulates the groundwater level at the landside.

#### Free water levels

The acting water levels are based on hydro meteo information, collected in the technical program of requirements and listed in Table E.1.

Table E.1 – Free water levels (Arcadis, 2016)

Water level	Level [m NAP]
Mean High Water (MHW)	+1.26
Mean Sea Level (MSL)	+0.06
Mean Low Water (MLW)	-0.71
Lowest Low Water Spring (LLWS)	-0.99
LW <sub>1</sub> x year	-1.50
LW <sub>1</sub> x 250 years	-2.35

#### Design water levels

The design water levels are determined following the CUR 211 (Stichting CURNET, 2014). No distinction is made between the water levels in SLS and ULS, so conservative water levels are used in SLS. The situation considering low free water level in combination with unfavourable loads is normative for the design of the quay wall. In the design calculation two accidental limit states (ALS) are considered, corresponding to two extreme water levels; extremely low water and drainage failure.

Following the CUR 211, the minimum water level difference between free- and groundwater level in the fundamental combination 1 is 0.5 m. Fundamental combination 2 is added, because in some specific cases fundamental combination 1 results in a positive upward water pressure underneath the relieving platform. For the groundwater level in the combination drainage failure, the MSL is used. This leads to the design water levels as given in Table E.2.

Table E.2 – Design water levels

Situation	Free water level	Groundwater level
<b>Fundamental combination 1</b>		
SLS / ULS	NAP-0.99 m (LLWS)	NAP-0.49 m
<b>Fundamental combination 2</b>		
SLS / ULS	NAP-0.99 m (LLWS)	NAP-0.99 m (LLWS)
<b>Accidental combinations</b>		
Extremely low water	NAP-2.35 m (LW <sub>1</sub> x 250 years)	NAP -1.35 m
Drainage failure	NAP-1.50 m (LW <sub>1</sub> x year)	NAP+0.06 m (MSL)

### Appendix E-3 Geotechnical conditions

The representative soil profile for the design of the quay wall is based on the normative CPT along the quay wall, CPT EN387. For this CPT the clay layer is the thickest and least sandy and some sand

layers are most loose. Therefore, it is expected that the least stability will be achieved at this location, what leads to the normative structural dimensions. The representative soil profile of benchmark 2 is defined in the final design report of benchmark 2 and shown in Table E.3.

Table E.3 – Soil profile of section B-B' (Arcadis, 2016)

#	Type of soil	Top level layer [m NAP]
1	Sand, loosely packed	+5.0
2	Clay, slightly sandy, moderately packed	+0.0
3	Sand, moderately packed	-0.5
4	Clay, very sandy	-6.4
5	Sand, moderately packed	-8.2
6	Sand, strongly packed	-10.0
7	Sand, slightly silty, clayey	-12.2
8	Sand, loosely packed	-14.2
9	Clay, slightly sandy, moderately packed	-20.5
10	Sand, moderately packed	-22.1
11	Sand, strongly packed	-25.0
12	Sand, slightly silty, clayey	-37.5
13	Sand, strongly packed	-43.0

The soil characteristics are determined using the soil properties from NEN 9997-1, which are also summed up in Appendix D (The Netherlands Standardisation Institute, 2017). These characteristics are shown in Table E.4. Notable is that the cohesion (c) of the sand layers is 1.0 kPa, in order to prevent numerical problems in the FEM model. These values have no significant influence on the design results. For the interface strength ( $R_{inter}$ ) the value of 2/3 is used as defined in the Plaxis manual (Plaxis bv, 2017) for the cohesive and clayey layers. In clean sand layers  $R_{inter}$  is increased to 0.8 conform the CUR 211 (Stichting CURNET, 2014)

Table E.4 – Soil and interface characteristics (Arcadis, 2016)

#	Type of soil	Drained / undrained	$\gamma_{dry} / \gamma_{wet}$ [kN/m <sup>3</sup> ]	c [kN/m <sup>2</sup> ]	$\phi$ [°]	$\delta$ [°]	$R_{inter}$ [-]
1	Sand, loosely packed	Drained	18 / 20	1	30.0	0	0.8
2	Clay, slightly sandy, moderately packed	Undrained	18 / 18	5	22.5	0	0.67
3	Sand, moderately packed	Drained	18 / 20	1	32.5	2.5	0.8
4	Clay, very sandy	Undrained	18 / 18	1	27.5	0	0.67
5	Sand, moderately packed	Drained	18 / 20	1	32.5	2.5	0.8
6	Sand, strongly packed	Drained	18 / 20	1	35.0	2.5	0.8
7	Sand, slightly silty, clayey	Drained	18 / 20	1	27.0	0	0.67
8	Sand, loosely packed	Drained	18 / 20	1	30.0	0	0.67
9	Clay, slightly sandy, moderately packed	Undrained	18 / 18	5	22.5	0	0.67
10	Sand, moderately packed	Drained	18 / 20	1	32.5	2.5	0.8
11	Sand, strongly packed	Drained	18 / 20	1	35.0	2.5	0.8
12	Sand, slightly silty, clayey	Drained	18 / 20	1	27.0	0	0.67
13	Sand, strongly packed	Drained	18 / 20	1	35.0	2.5	0.8

The stiffness parameters of the sand layers are determined using different correlations. For the sand layers, correlations Lunne & Christofferson (1982) are used (CROW, 2005):

$$E_{oed} = \begin{cases} 4 \cdot q_c & \text{for } q_c < 10 \text{ MPa} \\ 2 \cdot q_c + 20 & \text{for } 10 < q_c < 50 \text{ MPa} \\ 120 & \text{for } q_c > 50 \text{ MPa} \end{cases}$$

$$E_{50} = E_{oed}$$

$$E_{ur} = 3 \cdot E_{50}$$

For clay layers, the following correlations are used (Meigh & Corbett, 1997):

$$E_{oed} = 5 \cdot q_c$$

$$E_{50} = 1.5 \cdot E_{oed}$$

$$E_{ur} = 6 \cdot E_{50}$$

In which:

- $E_{oed}$  = Oedometer stiffness for the reference stress, commonly used  $p_{ref} = 100$  kPa [kN/m<sup>2</sup>]
- $E_{50}$  = Secant soil stiffness, for a shear level that is 50% of the maximum shear stress in a triaxial testing for the reference stress of  $p_{ref} = 100$  kPa. [kN/m<sup>2</sup>]
- $E_{ur}$  = Unloading-reloading stiffness. [kN/m<sup>2</sup>]

The stiffnesses of layer 2 and 9 are somewhat increased, in order to prevent numerical problems in Plaxis. These soil stiffnesses of the soil layers and the other required input parameters for the Hardening Soil small strain-model are presented in Table E.5.

Table E.5 – Stiffness parameters Hardening Soil small strain-model (Arcadis, 2016)

#	Type of soil	$E_{50}$ [kN/m <sup>2</sup> ]	$E_{oed}$ [kN/m <sup>2</sup> ]	$E_{ur}$ [kN/m <sup>2</sup> ]	Power [-]	$G_0$ [kN/m <sup>2</sup> ]	$\nu_{0.7}$ [-]
1	Sand, loosely packed	25.000	25.000	75.000	0.5	70.000	7.9 E-5
2	Clay, slightly sandy, moderately packed	13.500	9.000	27.000	1.0	30.000	4.5 E-4
3	Sand, moderately packed	35.000	35.000	105.000	0.5	100.000	1.6 E-4
4	Clay, very sandy	9.000	6.000	36.000	1.0	45.000	4.5 E-4
5	Sand, moderately packed	35.000	35.000	105.000	0.5	100.000	2.2 E-4
6	Sand, strongly packed	45.000	45.000	135.000	0.5	110.000	2.3 E-4
7	Sand, slightly silty, clayey	18.000	18.000	54.000	0.5	75.000	3.8 E-4
8	Sand, loosely packed	23.000	23.000	69.000	0.5	85.000	3.8 E-4
9	Clay, slightly sandy, moderately packed	10.500	7.000	21.000	1.0	50.000	6.6 E-4
10	Sand, moderately packed	28.000	28.000	84.000	0.5	95.000	4.3 E-4
11	Sand, strongly packed	35.000	35.000	105.000	0.5	100.000	5.1 E-4
12	Sand, slightly silty, clayey	12.000	12.000	36.000	0.5	70.000	8.4 E-4
13	Sand, strongly packed	25.000	25.000	75.000	0.5	95.000	7.3 E-4

#### Appendix E-4 Loads

The relieving platform of the quay wall is divided into 6 sections of about 41 m. In the determination of the loads it is taken into account that the relieving platform can distribute the acting loads over 1 section. The loads are specified in the final design report of benchmark 2 (Arcadis, 2016) and listed below:

- Surface load, consisting of an uniform load of 40 kN/m<sup>2</sup> and a distributing load of a coal hill increasing from 40 kN/m<sup>2</sup> to 230 kN/m<sup>2</sup> at 45.1 m and thereafter decreasing to 0 kN/m<sup>2</sup> at 72.7 m from the waterline.
- Crane load of 600 kN/m for both rails.
- Bollard load distributed over one section, resulting in an uniform load of 110 kN/m.

- Ship collision load on one section, resulting in an uniform load of 244 kN/m.

#### Appendix E-5 Load combination and phasing of construction

The load combinations are determined in the design report of benchmark 2. The load combinations, together with their corresponding load- ( $\gamma$ ) and load combination factors ( $\psi$ ) for the design in RC2 are shown in Table E.6.

Table E.6 – Load combinations with their corresponding load- and load combination factors in RC2 (Arcadis, 2016)

Load combinations ULS	$\gamma_Q$	$\Psi_0$								$\Psi_2$		
		I	II	III	IV	V	VI	VII	VIII	IX	X	XI
Fundamental combination 1	1	1	1	1	1	1	1					
Fundamental combination 2	1							1	1	1		
Extremely low water	1										1	
Drainage failure	1											1
Surface load on top of relieving platform	1.5	1	0.7	0.7				0.7	1		0.3	0.3
Surface load behind relieving platform	1.1	1	0.7	0.7	1	0.7	0.7	0.7	1		0.3	0.3
Coal hill behind relieving platform	1.1	1	0.7	0.7	1	0.7	0.7	0.7	1		0.3	0.3
Crane load landwards	1.5							1	0.6	0.7	0.7	0.7
Crane load seawards	1.5	0.6	1	0.6	0.6	1	0.6					
Bollard load	1.3	0.7	0.7	1	0.7	0.7	1					
Ship collision	1									1		

Because of the high own weight of the crane (load), a load combination factor of 0.7 is applied in load combinations IX, X and XI. Kranz stability is checked separately with a shifted coal hill. Besides that, another accidental load combination anchor dropout is checked using the representative value of the anchor load.

## Appendix F Spirally welded steel pipes of ArcelorMittal

Weight (kg/m pipe)	Wall thickness (mm & inch)															
	mm	12	13	14	15	16	17	18	19	20	21	22	23	24	25	25.4
	mm	inch	0,47	0,51	0,55	0,59	0,63	0,67	0,71	0,75	0,79	0,83	0,87	0,91	0,94	0,98
914	36	267	289	311	333	354	376	398	419	441	462	484	505	527	548	557
965	38	282	305	328	351	374	397	420	443	466	489	512	534	557	580	589
1016	40	297	322	346	370	395	419	443	467	491	515	539	563	587	611	621
1067	42	312	338	364	389	415	440	466	491	516	542	567	592	617	642	652
1118	44	327	354	381	408	435	462	488	515	542	568	595	621	648	674	684
1168	46	342	370	398	427	455	483	510	538	566	594	622	649	677	705	716
1219	48	357	387	416	445	475	504	533	562	591	620	649	678	707	736	748
1270	50	372	403	434	464	495	525	556	586	617	647	677	707	737	768	780
1321	52	387	419	451	483	515	547	578	610	642	673	705	736	768	799	812
1372	54	402	436	469	502	535	568	601	634	667	700	732	765	798	830	844
1422	56	417	452	486	520	555	589	623	657	692	726	760	794	827	861	875
1473	58	432	468	504	539	575	610	646	681	717	752	787	822	858	893	907
1524	60	447	484	521	558	595	632	669	705	742	778	815	851	888	924	939
1575	62	463	501	539	577	615	653	691	729	767	805	843	880	918	956	971
1626	64	478	517	557	596	635	675	714	753	792	831	870	909	948	987	1003
1676	66	492	533	574	614	655	696	736	776	817	857	897	938	978	1018	1034
1727	68	508	550	591	633	675	717	759	800	842	884	925	967	1008	1049	1066
1778	70	523	566	609	652	695	738	781	824	867	910	953	995	1038	1081	1098
1829	72	538	582	627	671	715	760	804	848	892	936	980	1024	1068	1112	1130
1880	74	553	599	644	690	736	781	827	872	917	963	1008	1053	1099	1144	1162
1930	76	568	615	662	708	755	802	849	895	942	989	1035	1082	1128	1175	1193
1981	78	583	631	679	727	775	823	871	919	967	1015	1063	1111	1158	1206	1225
2032	80	598	647	697	746	795	845	894	943	992	1041	1091	1140	1188	1237	1257
2083	82	613	664	714	765	816	866	917	967	1018	1068	1118	1168	1219	1269	1289
2134	84	628	680	732	784	836	888	939	991	1043	1094	1146	1197	1249	1300	1321
2184	86	643	696	749	802	855	909	962	1014	1067	1120	1173	1226	1278	1331	1352
2235	88	658	712	767	821	876	930	984	1038	1093	1147	1201	1255	1309	1363	1384
2286	90	673	729	784	840	896	951	1007	1062	1118	1173	1228	1284	1339	1394	1416
2337	92	688	745	802	859	916	973	1029	1086	1143	1199	1256	1313	1369	1425	1448
2388	94	703	761	820	878	936	994	1052	1110	1168	1226	1284	1341	1399	1457	1480
2438	96	718	777	837	896	956	1015	1074	1133	1193	1252	1311	1370	1429	1488	1511
2489	98	733	794	855	915	976	1036	1097	1157	1218	1278	1338	1399	1459	1519	1543
2540	100	748	810	872	934	996	1058	1120	1181	1243	1305	1366	1428	1489	1551	1575
2591	102	763	827	890	953	1016	1079	1142	1205	1268	1331	1394	1457	1519	1582	1607
2642	104	778	843	907	972	1036	1101	1165	1229	1293	1357	1421	1486	1550	1613	1639
2692	106	793	859	925	990	1056	1121	1187	1252	1318	1383	1449	1514	1579	1644	1670
2743	108	808	875	942	1009	1076	1143	1210	1276	1343	1410	1476	1543	1609	1676	1702
2794	110	823	892	960	1028	1096	1164	1232	1300	1368	1436	1504	1572	1639	1707	1734
2845	112	838	908	977	1047	1116	1186	1255	1324	1393	1463	1532	1601	1670	1739	1766

Figure F.1 – Spirally welded steel pipes of ArcelorMittal (ArcelorMittal, 2016)

## Appendix G Designs based on standard dimensions of benchmark 1

In the design based on standard available dimensions of the tubular pipes of the quay wall is designed following standard available dimensions of spirally welded steel piles of ArcelorMittal, which are attached in Appendix F. Besides that, the toe level of the piles and the length of the grout body are varied with 10 cm. So, in the design based on standard dimensions the ratio  $D_o/t$  changes per pile. Important is that if  $D_o/t < 100$ , the resistance can be increased with a factor 1.13 in the local buckling verification (Stichting CURNET, 2014). As this increase is valuable for the design of the quay wall, this ratio is used as a limit value.

With the help of iteration between the different verifications a design for every reliability class is found. First, in the D-Sheet Piling design, the quay wall can not be unstable and the maximum bending moment of the combi-wall can not be exceeded. In the iteration the benchmark is designed until the verifications are just right. The verifications are just right, when the unity checks are first below 1.0, when the dimension of tubular pile is decreased, the toe level of the pile is lowered and the length of the grout body is decreased.

The design based on standard dimensions in RC2 was already performed by designers. This design in RC2 is optimised in this study and forms the basis of the designs in RC1 and RC3. The design in RC2 is treated first, thereafter the designs in RC1 and RC3 performed in this study. From these designs the results are obtained and differences are discussed.

### Appendix G-1 Design in RC2

At first the design based on standard dimensions of benchmark 1 in RC2 is performed. The design meets the requirements when all the design verifications are just right. The design calculations are performed in the same way as the optimised design of benchmark 1 in RC1, presented in Appendix H. In order to avoid the repetition of these steps, only a summary of the design steps and results is given. In the final design benchmark 1 is designed as double anchored combi-wall, using tubular piles with a toe level of NAP-27.0 m. This means the tubular piles are performed with a length of 28.5 m. The tubular piles have a  $D_o$  of 1420 mm and  $t$  of 16 mm, so the ratio  $D_o/t$  is 88.75. Due to the large retaining height of the quay wall, every tubular pile is provided with two Jetmix 101.6 x 17.5 mm grout anchors (or similar). In the existing design the length of the grout bodies of the anchors are 8.0 m. The structural dimensions of the final design of benchmark 1 is collected in Table G.1 and depicted in Figure G.1

Table G.1 – Structural dimensions of design based on standard dimensions in RC2

<b>Structural characteristics</b>	<b>Structural dimensions</b>
<b><math>D_o</math> [mm]</b>	1420
<b><math>t</math> [mm]</b>	16
<b><math>D_o / t</math> [-]</b>	88.75
<b>Section width [m]</b>	3.27
<b><math>W_{eff,y}</math> [mm<sup>3</sup> / m]</b>	7,490,857
<b>Toe level piles [m NAP]</b>	-27.0
<b>Length grout body [m]</b>	8.0

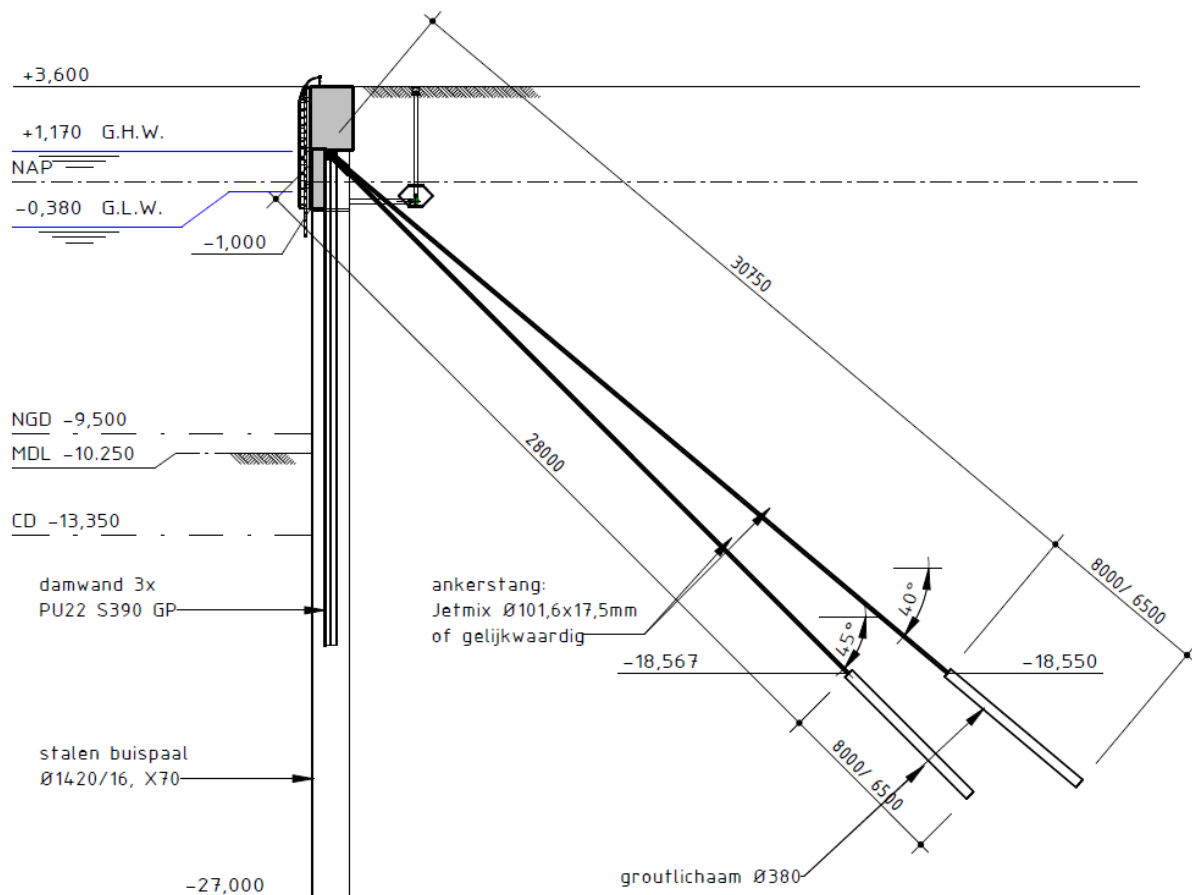


Figure G.1 – Final design of benchmark 1 (Arcadis, 2017)

## Appendix G-2 Design in RC1

After analysing the design based on standard dimensions of benchmark 1 in RC2, the design based on standard dimensions of benchmark 1 is performed in RC1. The design meets the requirements when all the design verifications are just right. The design calculations are performed in the same way as the optimised design of benchmark 1 in RC1, presented in Appendix H. In order to avoid the repetition of these steps, only a summary of the design steps and results is given.

Decreasing the tubular pile thickness to 15 mm, can have a significant influence on the construction costs. With this thickness the maximum  $D_o$  of the tubular pile is 1470 mm in order to fulfil the limit value of  $D_o/t$ . From design calculations follows that this design does not satisfies the verification of local buckling. So, the thickness of the tubular piles of benchmark 1 in RC1 must be 16 mm also. From several design iterations follows that for the local buckling verification, the  $D_o$  of the tubular piles have to be 1220 mm minimally. However, for this design the required toe level of the piles in the vertical bearing capacity verification is significantly lower. Longer tubular piles will increase the construction costs considerably, so it is desirable to prevent this. It follows that the tubular piles with a  $D_o$  of 1320 mm must have a toe level of NAP-27.0 m, so this  $D_o$  is chosen. Furthermore from the anchor verification follows that for this design the required grout body length is 8.0 m. The results of the structural dimensions of the design based on standard dimensions in RC1 are collected in Table G.2.

Table G.2 – Structural dimensions of design based on standard dimensions in RC1

Structural characteristics	Structural dimensions
$D_o$ [mm]	1320
$t$ [mm]	16
$D_o / t$ [-]	82.5
Section width [m]	3.17
$W_{eff,y}$ [mm <sup>3</sup> / m]	6,660,009
Toe level piles [m NAP]	-27.0
Length grout body [m]	8.0

### Appendix G-3 Design in RC3

Thereafter the design based on standard dimensions of benchmark 1 in RC3 is performed. The design meets the requirements when all the design verifications are just right. The design calculations are performed in the same way as the optimised design of benchmark 1 in RC1, presented in Appendix H. In order to avoid the repetition of these steps, only a summary of the design steps and results is given again.

Having the tubular pile thickness unmodified, can have a significant influence on the construction costs. With this thickness the maximum  $D_o$  of the tubular pile is 1575 mm in order to fulfill the limit value of  $D_o/t$ . From design calculations follows that this design does not satisfies the verification of local buckling. So, the thickness of the tubular pile of benchmark 1 in RC1 must be at least 17 mm. From several design iterations follows that for the vertical bearing capacity verification the  $D_o$  must be minimally 1420 mm, in order to fulfill for a toe level of about NAP-27.9 m. Decreasing the  $D_o$ , would significantly lower the required toe level of the piles and increase the construction costs of the design considerably. This is not desirable, so the  $D_o$  have to be 1420 mm and the toe level NAP-27.9 m. Furthermore, from the anchor verification follows that for this design the required grout body length is 8.7 m. The results of the structural dimensions of the design based on standard dimensions in RC3 are collected in Table G.3.

Table G.3 – Structural dimensions of design based on standard dimensions in RC3

Structural characteristics	Structural dimensions
$D_o$ [mm]	1420
t [mm]	17
$D_o / t$ [-]	83.53
Section width [m]	3.27
$W_{eff,y}$ [mm <sup>3</sup> / m]	7,942,175
Toe level piles [m NAP]	-27.9
Length grout body [m]	8.7

### Appendix G-4 Discussion of the results

The results of the structural dimensions of the designs based on standard dimensions in RC1, RC2 and RC3 are collected in Table G.4. As for the optimised designs, the required  $W_{eff,y}$ , together with the  $D_o$  and t of the piles, increases almost equally with the partial factors of the RC's. The required toe levels of the piles in RC1 and RC2 are comparable, in contrast to the required toe level of the piles in RC3. This is, as for the optimised design, due to the normative CPT DKM23, from which the  $q_c$  decreases locally and is depicted in figure 4.3. Besides that, also the required grout body lengths of RC1 and RC2 are similar, in contrast to RC3. This is, also as for the optimised design, due to a different multiplication load factor in RC1 and RC2 and RC3. So, in general the structural dimension differences between the designs of benchmark 1 in RC1 and RC2 are less different than structural dimension differences between the designs in RC2 and RC3.

Table G.4 – Structural dimension of designs based on standard dimensions of benchmark 1 in RC1, RC2 and RC3

Structural characteristics	RC1	RC2	RC3
$D_o$ piles [mm]	1320	1420	1420
t piles [mm]	16	16	17
$D_o / t$ [-]	82.5	88.75	83.53
Section width combi-wall [m]	3.17	3.27	3.27
$W_{eff,y}$ piles [mm <sup>3</sup> / m]	6,660,009	7,490,857	7,942,175
Toe level piles [m NAP]	-27.0	-27.0	-27.9
Length grout body [m]	8.0	8.0	8.7

It is checked that the extended grout bodies are still located in the sand layer.

### Appendix G-5 Construction costs estimation of designs based on standard dimensions

The construction costs of the designs based on standard available dimensions of tubular pipes in RC1, RC2 and RC3 are also estimated and the results are collected in Table G.5. The construction costs estimations are comparable with the construction costs estimations from the optimised designs.

However, these results are based on available tubular pile dimensions, so the construction costs of these piles differ abruptly and are somewhat higher. Therefore, the relationship between these construction costs and RC is less reliable.

Table G.5 – Construction costs overview of designs based on standard dimensions

Reliability class	Construction costs (€/m)	Relative increase compared to RC1
RC1	€ 17,560.-	0.00%
RC2	€ 17,650.-	0.49%
RC3	€ 18,120.-	3.17%

The relative cost increase between the designs in RC1 and RC2 is about 0.5% and the relative cost increase between the designs in RC1 and RC3 is about 3.2%. So, the costs difference between RC1 and RC3 of the designs based on standard dimensions, are larger than for the optimised designs. An overview of the relative construction costs comparison of the different cost components of the designs based on standard dimensions of benchmark 1 is given in Table G.2.

It is emphasised the results are cost estimations and give a reasonable first insight into the construction costs considering the functionality of benchmark 1.

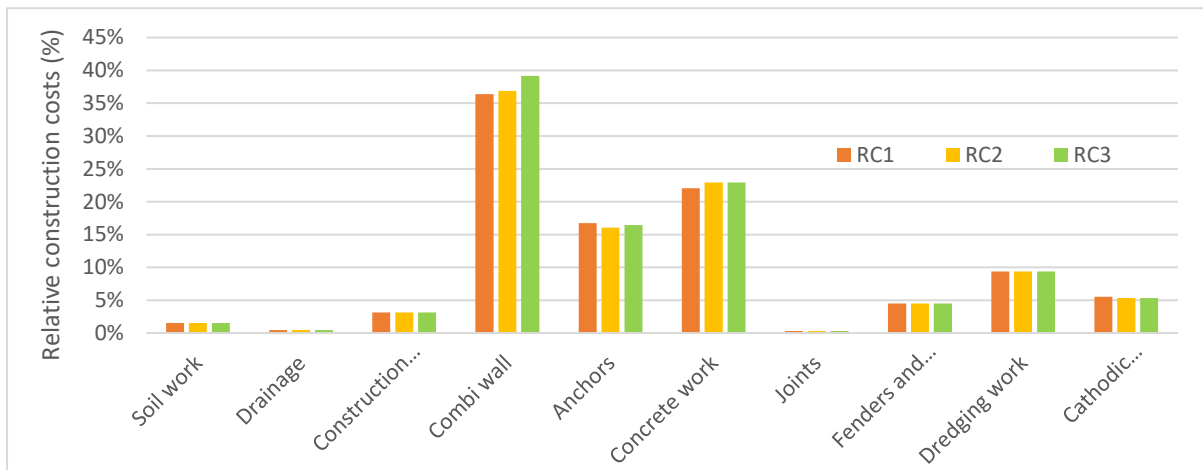


Figure G.2 – Relative construction costs comparison of designs based on standard dimensions of benchmark 1

From the cost estimation follows, that again only the construction costs of the combi-wall, anchors, concrete work and cathodic protection differ between the designs in RC1, RC2 and RC3. Therefore, the relative cost increase compared to the design in RC1 of these cost components are shown in Figure G.3. The difference between the construction costs of the combi-wall of the designs in RC1 and RC2 is lower and the difference between the construction costs of the designs in RC2 and RC3 is larger for the designs based on standard dimensions. This is due to the abrupt design differences between the RC's. For these designs the construction costs of the anchors in the design in RC2 are less than for the designs in RC1 and RC3, because the amount of required anchors is higher in the design based on standard dimensions in RC3 than the optimised design in RC3. Besides that, the construction costs of the concrete work and the cathodic protection of the designs in RC2 and RC3 are equal, because the diameter of the tubular piles is not changed. Generally, the difference between the construction costs of the designs of benchmark 1 in RC1 and RC2 is lower and the difference between the construction costs of these designs in RC2 and RC3 is larger for these designs based on standard dimensions.

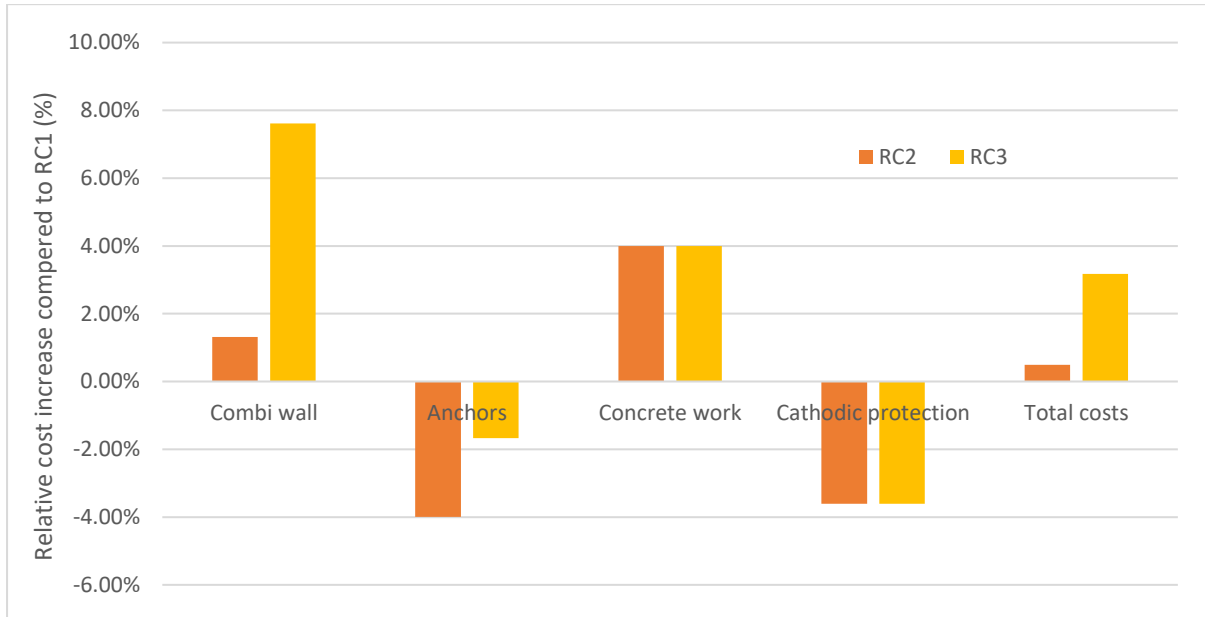


Figure G.3 – Relative cost increase compared to the design in RC1

Appendix H Design calculations of optimised design of benchmark 1 in RC1  
 First, the optimised design of benchmark 1 is performed in RC1. After several iterations all the design verifications of the optimised design in RC1 are just right and the design meets the requirements. The results of the structural dimensions of the optimised design in RC1 are collected in Table H.1.

Table H.1 – Structural dimensions of optimised design in RC1

Structural characteristics	Structural dimensions
D <sub>o</sub> piles [mm]	1360
t piles [mm]	15.32
D <sub>o</sub> / t [-]	88.75
Section width combi-wall [m]	3.21
W <sub>eff,y</sub> piles [mm <sup>3</sup> / m]	6,703,875
Toe level piles [m NAP]	-27.0
Length grout body [m]	7.66

In the optimised design iterations, the section modulus of the piles is decreased, until the design meets the local buckling verification. The required section modulus of the piles is about 6,703,900 mm<sup>3</sup>/m and this value is reached with tubular piles with D<sub>o</sub> of 1360 mm and thickness of about 15.32 mm. With this geometry of the structure, the required toe level of the piles and the length of the grout body is determined using a calculation sheet, used in the existing design. The required toe level of the piles is about NAP-27.0 m and the length of the grout body about 7.66 m.

#### Appendix H-1 Internal- and anchor forces

With the help of this geometry the internal- and anchor forces of the quay wall can be determined using the verification module of D-Sheet Piling. From this D-Sheet Piling calculation in RC1 already follows that the quay wall is stable and the maximum bending moment is not exceeded. The verification report with the input variables and design calculations of this D-Sheet Piling calculation is attached in Appendix P. An overview of the internal and anchor forces is given in Table H.2.

Table H.2 – Internal and anchor forces of optimised design in RC1

Force	Unity	LC I (SLS / ULS)	LC II (SLS / ULS)	LC III (SLS / ULS)	LC IV (ALS)	LC V (ALS)	LC VI (SLS / ULS)
S <sub>ED</sub>	[kN]	<b>1361 / 1633</b>	1322 / 1587	1354 / 1625	1367	1378	1364 / 1637
M <sub>ED</sub>	[kNm]	<b>6515 / 7905</b>	6373 / 6791	6432 / 7718	6545	6662	6561 / 7873
F <sub>anchor,1</sub>	[kN]	1158 / 1390	1205 / 1446	<b>1210 / 1453</b>	1183	1192	1178 / 1413
F <sub>anchor,2</sub>	[kN]	1154 / 1385	1200 / 1440	<b>1205 / 1447</b>	1179	1187	1173 / 1408

From these results follows that load combination (LC) I is normative for the internal forces in the combi-wall and LC III for the anchor forces.

#### Appendix H-2 Capacity combi-wall

The capacity of the combi-wall is checked by means of a local buckling verification at the location of the maximum bending moment. This verification is performed following the CUR 211, using a calculation sheet in Mathcad, used in the existing design. The required input variables consist of, among others, the maximum normal force and the maximum bending moment in the combi-wall. In stead of the maximum normal force, the normal force at the location of the maximum bending moment should have been used, but this difference is negligible. The maximum normal force consists of the vertical resulting force and an extra surface load on top of the capping beam of 40 kN/m<sup>2</sup>. The surface load on top of the capping beam can be calculated as follows:

$$F_{d,surface} = \gamma_Q \cdot F_{surface} \cdot w_{capping\ beam} \cdot c.t.c.\ piles = 1.0 \cdot 40 \cdot 2.05 \cdot 3.21 = 263\ kN/pile$$

In which  $w_{capping\ beam}$  is the width of the capping beam and c.t.c. piles is the centre to centre distance between the tubular piles. Furthermore it is assumed that corrosion has not affected the combi-wall, because the combi-wall is performed including cathodic protectors. From the D-Sheet Piling calculation follows that the maximum resulting vertical force is 2842 kN and the maximum bending moment in the combi-wall is 7905 kNm. It is assumed that the piles are filled with sand with a relative density of 70%

and a  $q_c$  above 4 MPa. The verification report with the input variables and design calculations of this verification is attached in Appendix P. The result of this verification is as follows:

$$UC = \frac{M_{ed}}{M_{Rd}} + \left(\frac{N_{ed}}{N_{Rd}}\right)^{1.7} = \frac{7905}{8231} + \left(\frac{3105}{23271}\right)^{1.7} = 0.993$$

$0.993 \leq 1.0$ , so the structure satisfies

### Appendix H-3 Anchoring

The anchoring is designed following the CUR 166, using a calculation sheet, used in the existing design. The verification report with the input variables and design calculations of this verification is attached in Appendix P. In this verification, the anchor forces are increased with extra load factors described in CUR 166; the load factor for the grout body is 1.1, the load factor for the anchor rod is 1.25. These load factors are independent of the RC. In the design it is assumed that the shaft friction,  $\alpha_t$ , is 0.015 and 100% of the installed anchors is tested. The c.t.c. distance between the anchors is equal to the c.t.c. distance between the tubular piles, 3.21 m. The normative anchor forces are following from the D-Sheet Piling calculation in LC III and are showed in Table H.3.

Table H.3 – Normative anchor forces in RC1

Anchor	LC	$F_{a,rep}$ [kN]	$F_{a,max}$ [kN]	$F_{a,max;gr;d}$ [kN]	$F_{s;A;rod;d}$ [kN]
1	III	1210	1453	1598	1815
2	III	1205	1447	1592	1808

In this verification, corrosion of the anchor rod is considered, because cathodic protectors cannot be applied to anchors. Conform CUR 166 a corrosion layer of 1.5 mm (contaminated soil, stirred soil), corresponding to a design life of 50 years, is taken into account. In the design calculation also the situation is checked that both two anchors of a tubular pile are dropped out. In this situation the adjacent anchors have to accommodate extra anchor forces. So, in the calculation the c.t.c. distance between anchors becomes 4.82 m in stead of 3.21 m. In this ALS the representative anchor loads are used and the extra load factors from the CUR 166 are not applied. The results of the verification of the anchor rod are listed in Table H.4.

Table H.4 – Anchor rod check in RC1

Anchor	Tube	Type	Length [m]	Angle [°]	$F_{r;A;rod;d}$ [kN]	$UC_{rod}$	$UC_{dropout}$
1	Grout anchor rod	Jetmix 101.6 x 17.5	27.6	45	2108	0.86	0.86
2	Grout anchor rod	Jetmix 101.6 x 17.5	30.4	40	2108	0.86	0.86

Furthermore the grout body of the anchor is checked and the results of this verification are showed in Table H.5. From this verification followed that the steel anchor rod is sufficient and the grout body with a diameter of 380 mm must be minimally 7.7 m.

Table H.5 – Grout body check in RC1

Anchor	Tube	Diameter [m]	Length [m]	$F_{r;A;gr;rep}$ [kN]	$F_{r;A;gr;d}$ [kN]	$UC_{grout}$	$UC_{dropout}$
1	Grout anchor rod	380	7.7	1930	1609	0.99	0.94
2	Grout anchor rod	380	7.7	1930	1609	0.99	0.94

### Appendix H-4 Vertical bearing capacity

The vertical bearing capacity is verified conform NEN 9997-1, using D-Foundation. For the optimised design of benchmark 1, the vertical bearing capacity verification of post-2016 is used, which means that that  $\alpha_p = 0.7$ . In D-Foundation the concerning soil profiles are obtained from Cone Penetration Tests (CPT) and the characteristics of the combi-wall are implemented. From D-Foundation the point and shaft resistances are obtained at eight different locations in section B-B'. These resistances are

implemented in a vertical bearing capacity calculation sheet in Excel, used in the existing design, in order to determine the unity check per CPT. In D-Foundation the resistances are obtained for a not excavated and excavated situation. In the Excel sheet the averages of the two values of the different situations are determined and the sum of the average point- and shaft resistance is the total bearing capacity per CPT,  $R_{c;d}$ . The unity check (UC) per CPT can be calculated as follows:

$$UC = \frac{R_{c;d}}{P_d}$$

So, for these unity checks also the maximum normal force,  $P_d$ , is required. This maximum normal force consists of the maximum resulting vertical force from D-Sheet Piling of 2842 kN, the missing vertical component of the design bolder force and the design surface load on top of the capping beam. These last two forces are calculated as follows:

$$F_{d,bolder} = \gamma_Q \cdot \frac{SWL}{c.t.c.bollard} \cdot \sin(\alpha_{mooring}) \cdot c.t.c.pile = 1.35 \cdot \frac{1500}{15} \cdot \sin(45) \cdot 3.21 = 306 \text{ kN/pile}$$

$$F_{d,surface} = \gamma_Q \cdot F_{surface} \cdot w_{capping\ beam} \cdot c.t.c.piles = 1.35 \cdot 40 \cdot 2.05 \cdot 3.21 = 355 \text{ kN/pile}$$

In which SWL is the Safe Water Load of one bollard and  $\alpha_{mooring}$  the mooring angle. With these values the maximum normal force can be determined:

$$P_d = F_{d,normal} + F_{d,bolder} + F_{d,surface} = 2842 + 306 + 355 = 3503 \text{ kN/pile}$$

Furthermore in this verification  $\xi_3$  is 1.25, because the total amount of CPTs is more than ten. Negative skin friction is not taken into account, because this force is taken into account in the maximum resulting vertical force from D-Sheet Piling. The verification report with the input variables and design calculations of this verification is attached in Appendix P. The results of this verification are given in Table H.6. It follows that the vertical bearing capacity of the combi-wall satisfies at all locations with a toe level of the tubular piles at NAP-27.0 m.

Table H.6 – Vertical bearing capacity check of tubular piles in RC1

CPT	Toe level piles [m NAP]	$P_d$ [kN/pile]	$R_{c;d}$ [kN/pile]	UC
DKM10A	-27.0	3503	3856	0.91
DKM23	-27.0	3503	3550	0.99
DKM22	-27.0	3503	3615	0.97
DKM21	-27.0	3503	3735	0.94
DKM20	-27.0	3503	3970	0.88
DKM19	-27.0	3503	3928	0.89
DKM18	-27.0	3503	3937	0.89
DKM17A	-27.0	3503	3888	0.90

## Appendix I Optimised design of benchmark 1 in SLS with increased $\phi'$

For benchmark 1 also the optimised design in SLS performed, with 10% increased  $\phi'$ , because it is suggested that the  $\phi'$  values of the standards CUR 211 and NEN 9997-1 are significantly lower than in reality. With this design a first insight into the influence of the  $\phi'$  on the design and the construction costs is obtained.

The optimised design in SLS with increased  $\phi'$  is determined following the same design calculations of the optimised design in RC1, presented in Appendix H. The results of the structural dimensions of the optimised design in SLS with increased  $\phi'$  are shown in Table I.1.

Table I.1 – Structural dimensions of optimised design in SLS with increased  $\phi'$

Structural characteristics	Structural dimensions
D <sub>o</sub> piles [mm]	1290
t piles [mm]	14.54
D <sub>o</sub> / t [-]	88.75
Section width combi-wall [m]	3.14
W <sub>eff,y</sub> piles [mm <sup>3</sup> / m]	5,848,624
Toe level piles [m NAP]	-26.4
Length grout body [m]	7.22

In Table I.2 an overview of the construction costs estimation of benchmark 1, excluding Value Added Tax (VAT), is given.

Table I.2 – Construction costs overview of optimised designs

Reliability class	Construction costs (€/m)	Relative increase compared to RC1
RC1	€ 17,380.-	0.00%
RC2	€ 17,570.-	1.08%
RC3	€ 17,980.-	3.42%
SLS with increased $\phi'$	€ 16,980.-	-2.31%

The construction costs of the design in SLS with increased  $\phi'$  are considerably lower than the construction costs of the design in RC1. This is due to the considerable differences in structural dimensions of the different designs. So, it is possible that  $\phi'$  of the soil layers is one of the most important factor influencing the design of benchmark 1.

## Appendix J Influence of the modulus of subgrade reaction on the reliability index of benchmark 1

The influence of the modulus of subgrade reaction on the reliability index of benchmark 1 is investigated by a small sensitivity analysis. In this analysis the modulus of subgrade reaction is varied 20% and these reliability results are presented in Table J.1.

Table J.1 – Reliability results of sensitivity analysis of modulus of subgrade reaction of benchmark 1

Situation	$\beta$ passive resistance inadequate	$\beta$ sheet pile profile fails	$\beta$ tension member anchorage fails
$k_h$ -20%	9.25	7.77	8.15
$k_h$ RC2	9.25	7.81	8.20
$k_h$ +20%	9.25	7.84	8.26

From this analysis follows that the modulus of subgrade reaction is not influencing the  $\beta$  of benchmark 1 a lot. So, modelling the modulus of subgrade reaction as deterministic seems a reasonable estimation.

## Appendix K Reliability results of benchmark 1

For benchmark 1 reliability calculations are performed, for the designs in RC1, RC2 and RC3, but also for the influence of the structural components on  $\beta$ 's. These latter results are used to estimate the influence of the failure mechanisms on the construction costs.

### Appendix K-1 Reliability results of benchmark 1 in RC1, RC2 and RC3

For the different failure mechanisms a first estimation of the relationship between the  $\beta$  and the construction costs is estimated by comparing the costs- and reliability results. These results are plotted in Figure K.1 and a linear trendline between these points is drawn. The trendline is a first estimation of the relationship between the construction costs and  $\beta$  of 'passive resistance inadequate' corresponding to the designs in RC1, RC2 and RC3. It is notable that the trendline is increasing in compliance with the increase of the length of the tubular piles of the designs in different RC's.

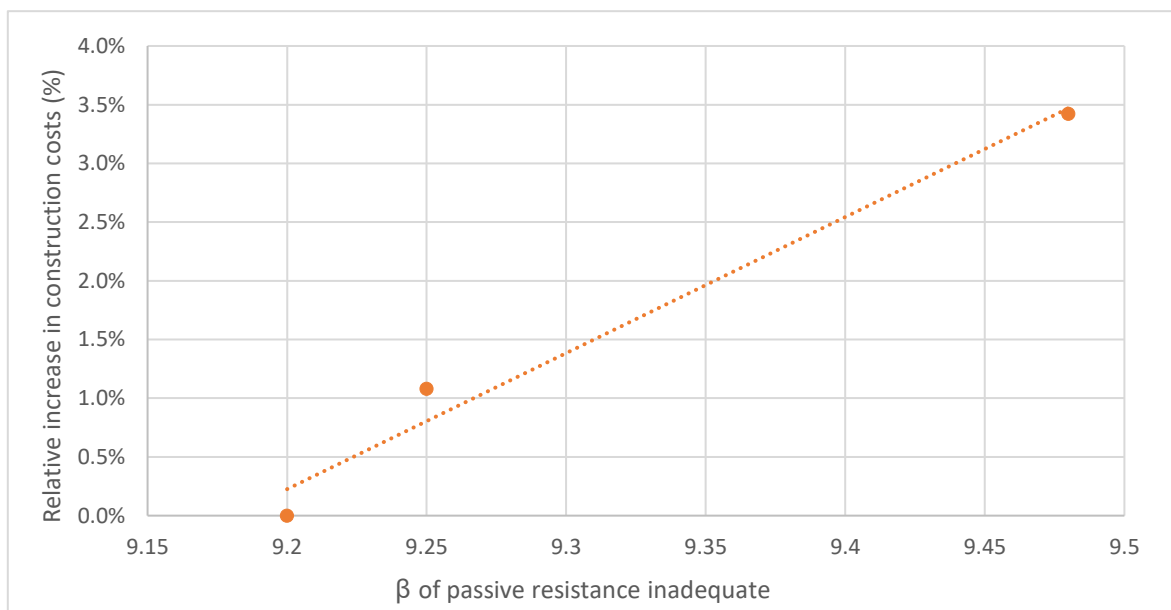


Figure K.1 – Relationship between the construction costs and  $\beta$  of 'passive resistance inadequate' corresponding to the designs in RC1, RC2 and RC3

The reliability results of the failure mechanism 'sheet pile profile fails' are also plotted against the relative increase in the construction costs, together with a linear trendline in between, in Figure K.2. In this way a first estimation of the relationship between the construction costs and  $\beta$  of the failure mechanism 'sheet pile profile fails' corresponding to the designs in RC1, RC2 and RC3 is depicted. This relationship increases also in compliance with the increase of the section modulus of the piles of the designs in different RC's.

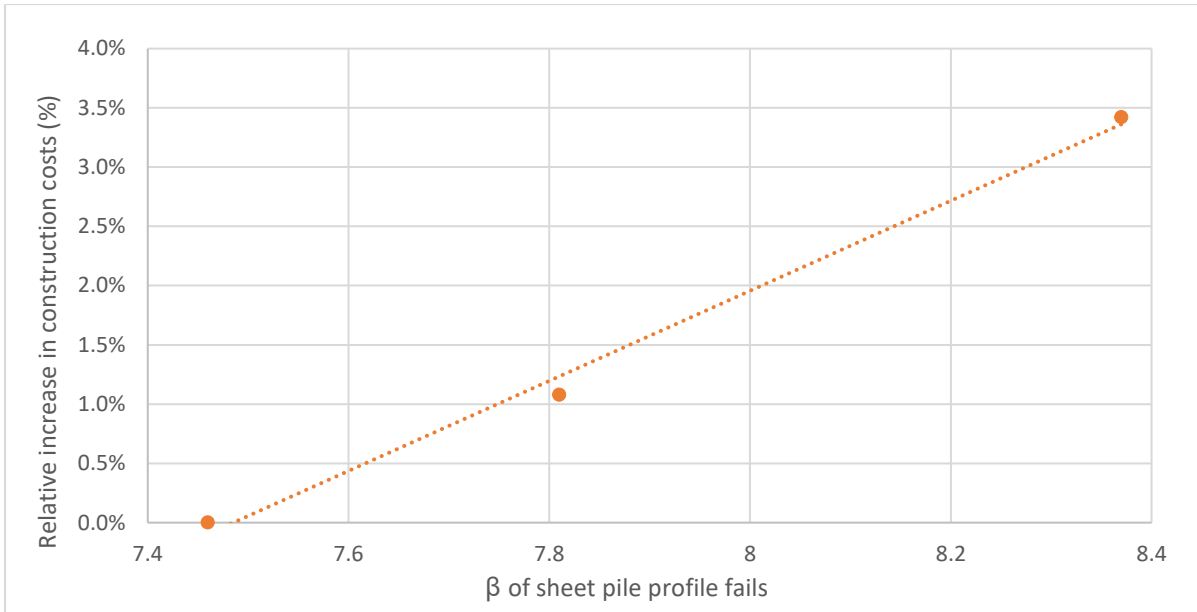


Figure K.2 – Relationship between the construction costs and  $\beta$  of ‘sheet pile profile fails’ corresponding to the designs in RC1, RC2 and RC3

In Figure K.3 the results of the reliability calculations of the failure mechanism ‘tension member anchorage fails’ with respect to the construction costs of benchmark 1 of the designs in different RC’s are shown. Notable is that the calculated  $\beta$ ’s are very similar to each, but a linear trendline is still added in between these results. The trendline is a first estimation of the relationship between the construction costs and  $\beta$  of ‘sheet pile profile fails’ corresponding to the designs in RC1, RC2 and RC3 and is even decreasing. This is mainly explained by the fact that the anchor rod is unchanged in the designs in RC1, RC2 and RC3, but the section width is increased, leading to a larger anchor force and a lower  $\beta$ .

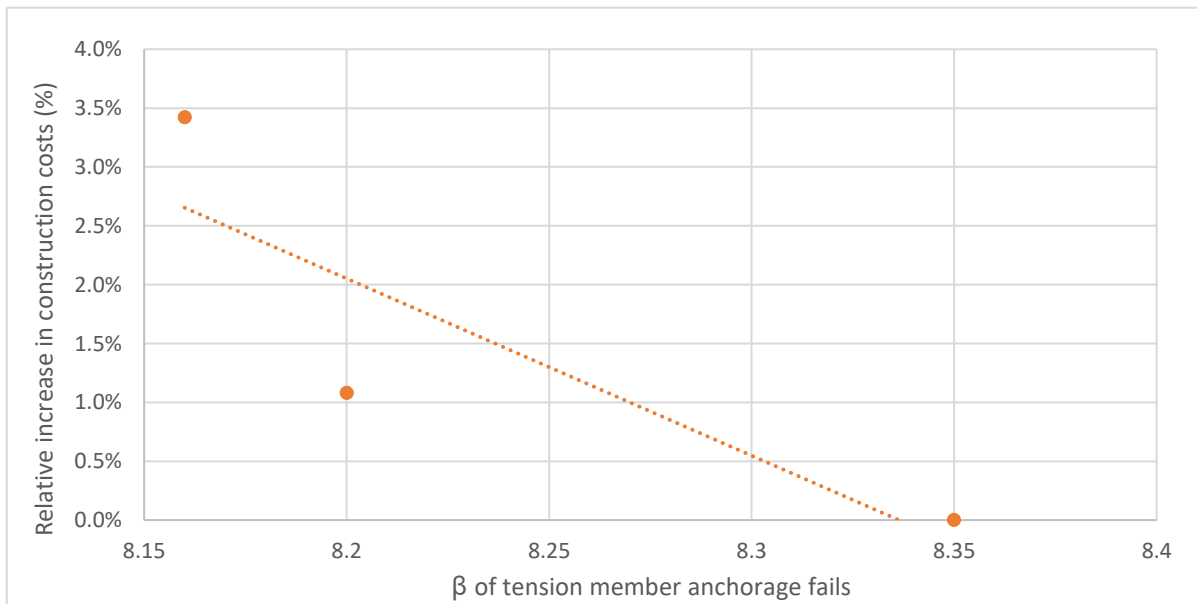


Figure K.3 – Relationship between the construction costs and  $\beta$  of ‘tension member anchorage fails’ corresponding to the designs in RC1, RC2 and RC3

#### Appendix K-2 Influence of structural components on $\beta$

The influence of the length of the tubular piles, the section modulus of the tubular piles and the steel area of the anchor rod on the  $\beta$  of three failure mechanisms is estimated with the help of reliability calculations, based on the starting points of chapter 3.1.6. The results of the reliability calculations of the sensitivity analysis varying structural components are shown in table 4.11. A possible explanation of the high  $\beta$ -values, is that the investigated failure mechanisms are not normative in the design.

Besides that, the partial factors of the Eurocodes are defined such that about 90% of the designs are more reliable than defined. So, extra reliability the design is expected. It is emphasised that the reliability results are first indications and just rough estimations, because model uncertainties and stochastic correlations are not considered and limited different stochastic variables are used.

The reliability results of the sensitivity analysis varying the length of the tubular piles are depicted in Figure K.4. In the figure the relative change of the length of the tubular piles is plotted against the relative change of the  $\beta$  for the three different failure mechanisms. In between these result points, polynomial trendlines are added to the graph, which are a first estimate of the influence of the length of the tubular piles on  $\beta$ . It is notable that the trendline of the failure mechanism 'passive resistance inadequate' is the steepest, which indicates that the length of the tubular piles has a relatively large influence on this failure mechanism. This is, because the length of the tubular piles is directly related to this failure mechanism. Moreover, the influence of the length of the tubular piles on the  $\beta$  of 'passive resistance inadequate' is reasonable and on the  $\beta$  of 'tension member anchorage fails' is relatively low. So, increasing the length of the tubular piles leads to an increase of the  $\beta$  of all three failure mechanisms.

Furthermore, the influence of the length of tubular piles on  $\beta$  is estimated by plotting the reliability results of the sensitivity analysis varying the section modulus of the tubular piles. These results are depicted in Figure K.5. The trendlines are a first estimation of the influence of the section modulus of the tubular piles on  $\beta$ . In this case the trendline of the failure mechanism 'sheet pile profile fails' is the steepest, so the influence of the section modulus of the piles on this  $\beta$  is relatively significant. In this case the section modulus of the tubular piles is directly related to the failure mechanism 'sheet pile profile fails'. From the figure follows also that the influence of the length of the piles on the failure mechanism 'passive resistance inadequate' is relatively low and on the failure mechanism 'tension member anchorage fails' is reasonable. However, the  $\beta$  of 'tension member anchorage fails' decreases, when increasing the section member of the tubular piles. This is, because the anchor rod of the different designs is constant. By increasing the section modulus of the tubular piles, the diameter of the tubular piles increases, the centre to centre distance between the anchors increases and the anchor force increases. So, the same anchor rod must resist an increased anchor force and the  $\beta$  decreases.

Besides that, the reliability results of the sensitivity analysis varying the steel area of the anchor rod are depicted in Figure K.6. Again, the relative change of the steel area is plotted against the relative change of the  $\beta$  for the three different failure mechanisms and polynomial trendlines are added. The trendlines are a first estimation of the influence of the steel area of the anchor rod on  $\beta$ . The steel area of the anchor rod is directly related to the failure mechanism 'tension member anchorage fails', which can be seen in the figure. The trendline of 'tension member anchorage fails' is the steepest, which means that the influence of the steel area of the anchor rod on the failure mechanism 'tension member anchorage fails' is relatively large. From the figure follows also that the influences of the steel area of the anchor rod on the failure mechanisms 'passive resistance inadequate' and 'sheet pile profile fails' are negligible.

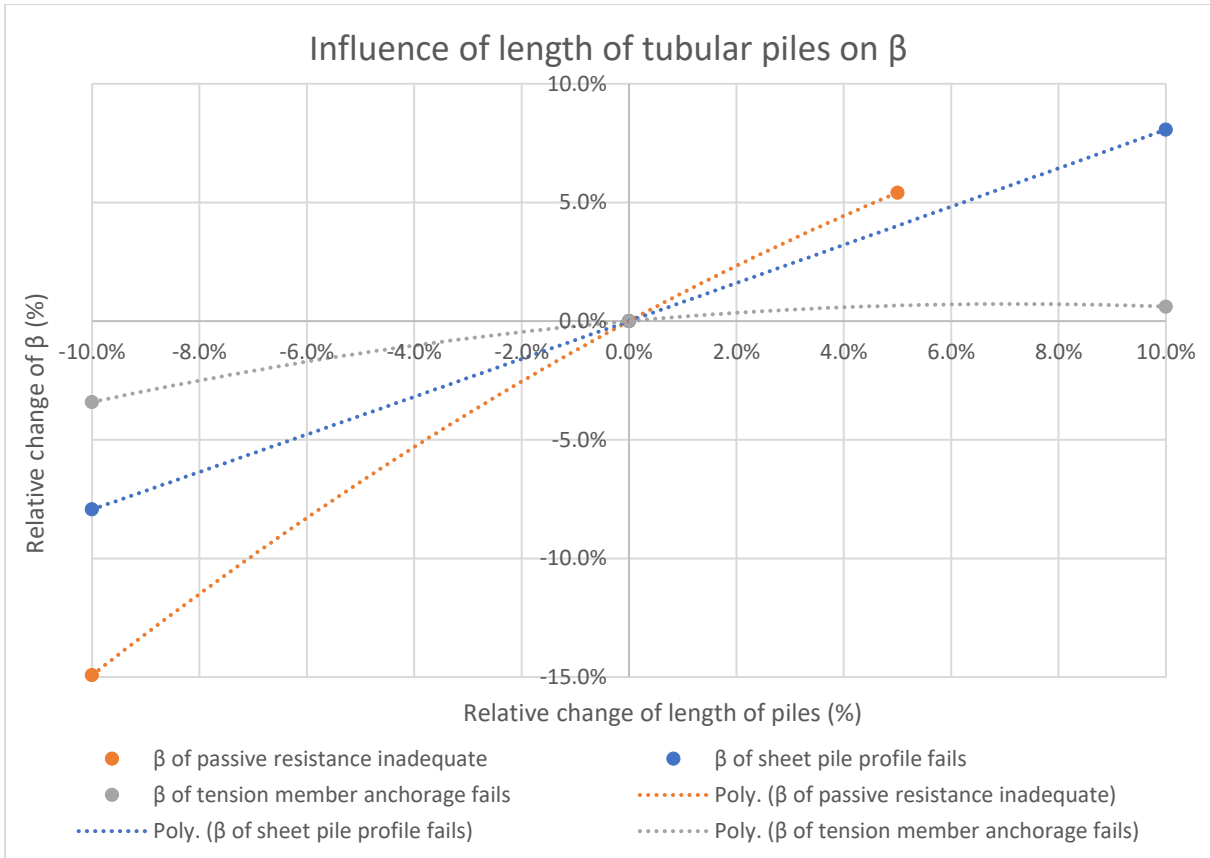


Figure K.4 – Influence of length of tubular piles on  $\beta$

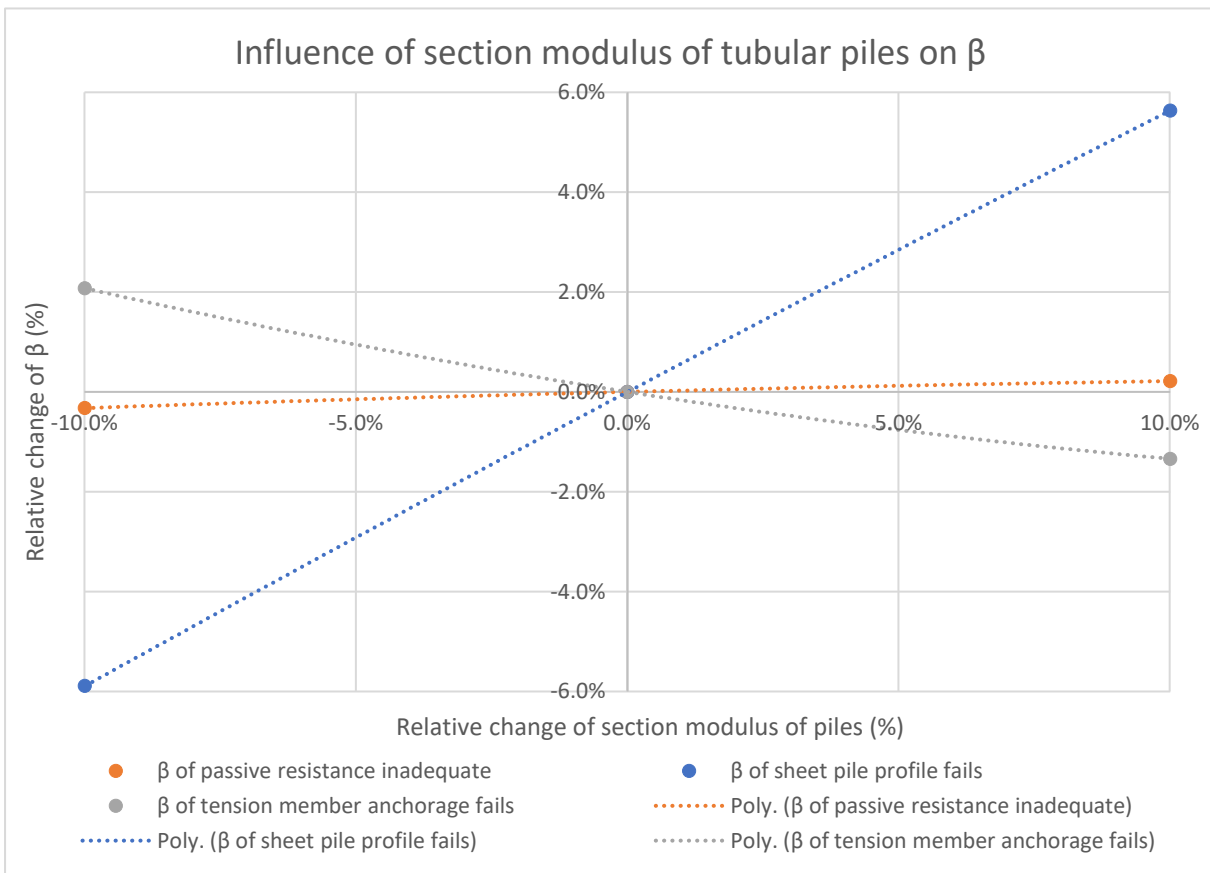


Figure K.5 – Influence of section modulus of tubular piles on  $\beta$

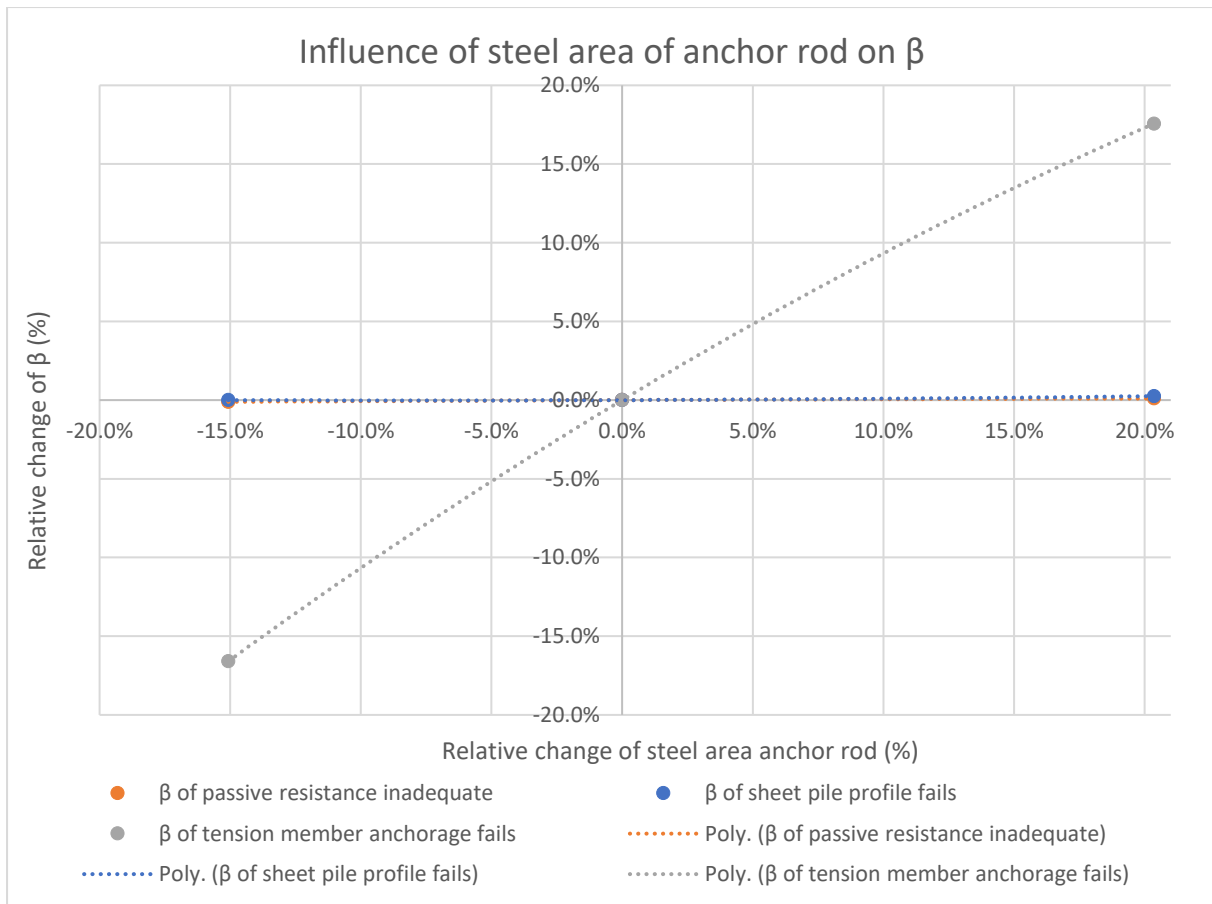


Figure K.6 – Influence of steel area anchor rod on  $\beta$

Appendix L Anchors of Jetmix

Onderdeel		ANKERTABEL JETMIX GROUINJECTIEANKERS													
		ANKERTYPE													
Type	Eenheid	1	2	3	4	5	6	7	8	9	10	11	12	13	14
		Ø 42,4 x 8,0 mm	Ø 42,4 x 11,0 mm	Ø 51,0 x 10,0 mm	Ø 51,0 x 12,5 mm	Ø 60,3 x 12,5 mm	Ø 60,3 x 16,0 mm	Ø 76,1 x 14,2 mm	Ø 76,1 x 17,5 mm	Ø 82,5 x 17,5 mm	Ø 82,5 x 20,0 mm	Ø 101,6 x 17,5 mm	Ø 101,6 x 22,2 mm	Ø 101,6 x 25,0 mm	Ø 101,6 x 28,0 mm
Jetmix															
Buisdiameter	mm	42,4	42,4	51,0	51,0	60,3	60,3	76,1	76,1	82,5	82,5	101,6	101,6	101,6	101,6
Wanddikte	mm	8,0	11,0	10,0	12,5	12,5	16,0	14,2	17,5	17,5	20,0	17,5	22,2	25,0	28,0
Doornende ankermateriasal Anm1g	mm <sup>2</sup>	808	1.038	1.221	1.447	1.849	2.194	2.707	3.190	3.593	3.888	4.578	5.510	5.986	6.442
Gewicht	kgm <sup>1</sup>	6,79	8,52	10,11	11,87	14,74	17,48	21,68	25,29	28,05	30,83	36,30	43,47	47,23	50,82
Minimale vloeispanning fy	Nmm <sup>2</sup>	500	500	500	500	500	500	500	500	500	500	500	500	500	500
Minimale vloeikracht	kN	404	519	610	723	925	1.097	1.354	1.595	1.752	1.944	2.289	2.755	2.993	3.221
Minimale breukspanning fu	Nmm <sup>2</sup>	700	700	700	700	700	700	700	700	700	700	700	700	700	700
Minimale bruukkracht	kN	586	727	855	1.013	1.285	1.536	1.895	2.233	2.462	2.722	3.205	3.857	4.190	4.509
Staalwaaliteit		E470	E470	E470	E470	E470	E470	E470	E470	E470	E470	E470	E470	E470	E470
Diameter Boorlop	mm	180	180	220	220	260	260	300	300	350	350	380	380	380	380

Geen rekening gehouden met vermoeding  
 Geen rekening gehouden met de invloed van nationale bijlagen  
 Geen rekening gehouden met corrosie

Figure L.1 – Anchors of Jetmix Funderingstechniek (Jetmix, 2016)

## Appendix M Designs based on standard dimensions of benchmark 2

The designs based on standard available dimensions of tubular pipes of benchmark 2 are designed using the standard available dimensions of spirally welded steel piles of ArcelorMittal, which are attached in Appendix F. Besides that, the toe level of the tubular piles and vibro piles and the length of the grout body are varied with 10 cm. So, in the design based on standard dimensions, the ratio  $D_o/t$  changes per pile. The designs based on standard dimensions of benchmark 2 are designed based on the optimised designs of benchmark 2, using the pre-2017 bearing capacity verification, containing  $\alpha_p = 1.0$ . An overview of the structural dimension of the designs based on standard dimensions of benchmark 2 in RC1, RC2 and RC3 is given in Table M.1.

Table M.1 – Structural dimension of designs based on standard dimensions of benchmark 2 in RC1, RC2 and RC3

Structural characteristics	RC1	RC2	RC3
<b>D<sub>o</sub> piles [mm]</b>	1220	1320	1520
<b>t piles [mm]</b>	19	20	22
<b>D<sub>o</sub> / t [-]</b>	64.21	66.0	69
<b>Section width combi-wall [m]</b>	3.53	3.63	3.81
<b>W<sub>eff,y</sub> piles [mm<sup>3</sup> / m]</b>	6,004,082	7,203,974	9,979,282
<b>Toe level tubular piles [m NAP]</b>	-34.5	-33.8	-37.0
<b>Toe level piles [m NAP]</b>	-27.8	-27.8	-27.9
<b>Length grout body [m]</b>	7.2	8.0	9.0

The final design based on standard dimensions of benchmark 2 was already performed by designers, but in this study this design is optimised. The buckling and vertical bearing verifications of the tubular piles of the combi-wall are just right in the design of this study. The design calculations are performed in the same way as the optimised design of benchmark 2 in RC1, presented in Appendix N. In order to avoid the repetition of these steps, only a summary of the design steps and results is given.

### Appendix M-1 Construction costs estimation of designs based on standard dimensions

The construction costs of the designs based on standard available dimensions of tubular pipes of benchmark 2 in RC1, RC2 and RC3 are also estimated and the results are collected in Table M.2. It follows that the construction costs estimations are comparable with the construction costs estimations of the optimised designs. The differences are somewhat smaller in the designs based on standard dimensions, but the relationship between these costs and RC is less reliable than for the optimised designs. The reason for this, is that the construction costs are based on standard available tubular pile dimensions and can differ abruptly.

Table M.2 – Construction costs overview of designs based on standard dimensions

Reliability class	Construction costs (€/m)	Relative increase compared to RC1
<b>RC1</b>	€ 34,565.-	0.00%
<b>RC2</b>	€ 34,881.-	0.92%
<b>RC3</b>	€ 36,307.-	5.04%

The relative construction costs increase between the designs in RC1 and RC2 is about 0.9% and between the designs in RC1 and RC3 about 5, due to the used bearing capacity verification, containing  $\alpha_p = 1.0$ . This is further explained in the optimised design results of benchmark 2 in chapter 5.2. An overview of the relative construction costs comparison of the different cost components of the designs based on standard dimensions of benchmark 2 is given in Figure M.1. It is emphasised that the results are cost estimations and give a reasonable first insight into the construction costs considering the functionality of benchmark 2.

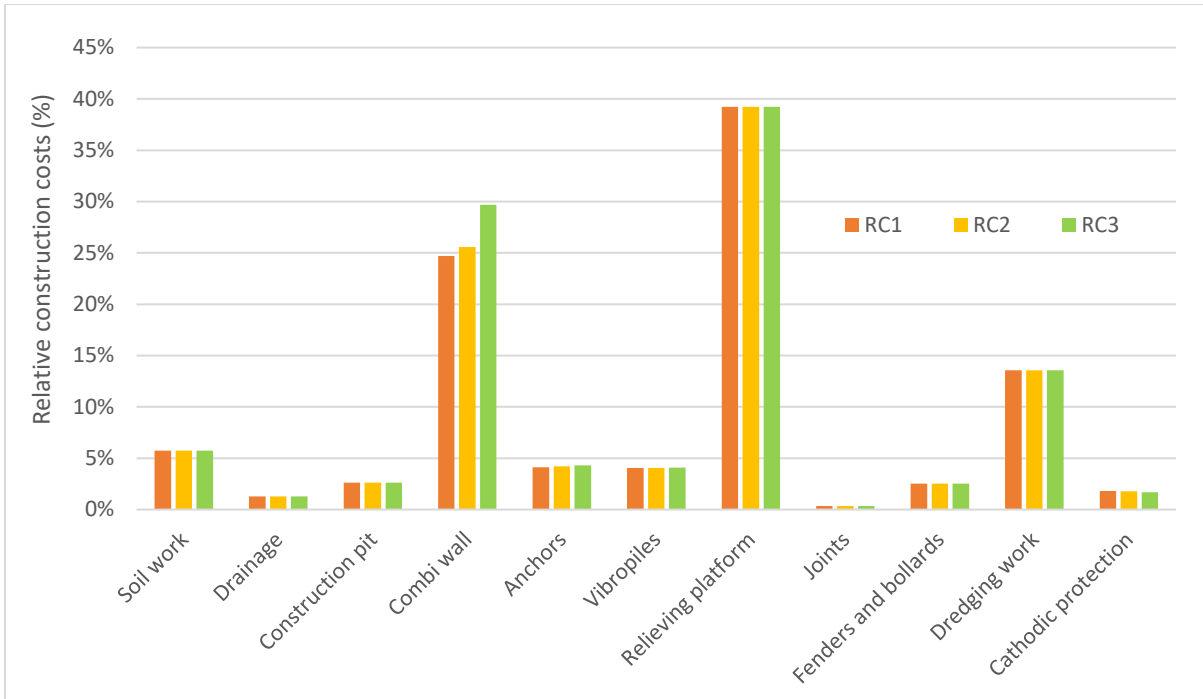


Figure M.1 – Relative construction costs comparison of designs based on standard dimensions of benchmark 2

For the design based on standard dimensions of benchmark 2, the construction costs of the combi-wall, anchors, relieving platform and cathodic differ between the RC's. Therefore, the relative cost increase compared to the design in RC1 of these cost components are shown in Figure M.2. Due to the abrupt design differences between the RC's, the differences between the construction costs of the combi-wall in RC1, RC2 and RC3 and the anchors in RC2 and RC3 are lower for the designs based on standard dimensions. Therefore, the differences between the construction costs of the designs of benchmark 2 in RC1, RC2, RC3 are lower in general for the designs based on standard dimensions.

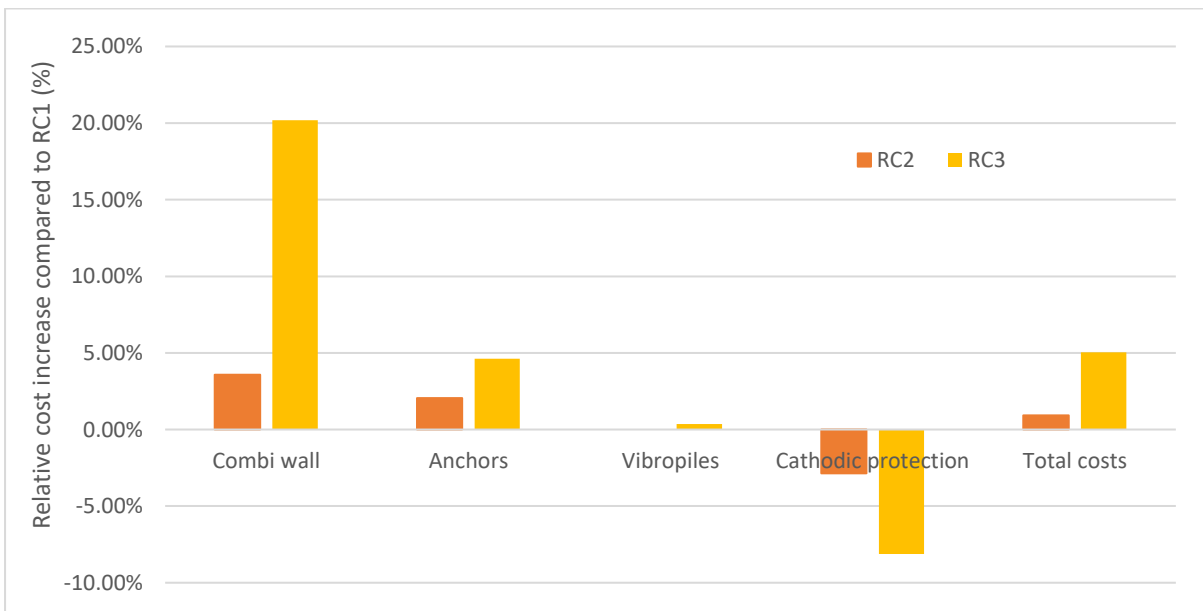


Figure M.2 – Relative cost increase compared to the design in RC1

Appendix N Design calculations of optimised design of benchmark 2 in RC1  
 First, for benchmark 2 an optimised design in RC1 is performed. After several iterations all the design verifications of the optimised design in RC1 are just right and the design meets the requirements. The results of the structural dimensions of the optimised design in RC1 are collected in Table N.1.

Table N.1 – Structural dimensions of optimised design in RC1

Structural characteristics	Structural dimensions
D <sub>o</sub> piles [mm]	1225
t piles [mm]	18.09
D <sub>o</sub> / t [-]	67.72
Section width combi-wall [m]	3.53
W <sub>eff,y</sub> piles [mm <sup>3</sup> / m]	5,769,546
Toe level tubular piles [m NAP]	-34.5
Toe level vibro piles [m NAP]	-27.9
Length grout body [m]	7.3

In the optimised design iterations, the section modulus and toe level of the piles is decreased, until the design meets the local buckling and vertical bearing verification. The required section modules of the piles is about 5,769,546 mm<sup>3</sup>/m and this value is reached with tubular piles with D<sub>o</sub> of 1225 mm and thickness of about 18.09 mm.

With this geometry of the structure, the required toe level of the piles and the length of the grout body is determined using the calculation sheet, used in the existing design. The required toe level of the piles is about NAP-34.5. The vibro piles and anchors are designed based on the obtained geometry. The required toe level of the vibro piles is about NAP-27.8 and the required length of the grout bodies of the anchors is about 7.3 m.

#### Appendix N-1 Internal- and anchor forces

With the help of this geometry the internal- and anchor forces of the quay wall can be determined using the Plaxis 2D model. From the Plaxis calculation in RC1 already follows that the quay wall is stable and 'soil mechanical failure' will not occur. An overview of the internal and anchor forces is given in Table N.2

Table N.2 – Internal and anchor forces of optimised design in RC1

Force	Unity	LC I (SLS / ULS)	LC II (SLS / ULS)	LC IV (SLS / ULS)	LC VIII (SLS / ULS)	LC Kranz I (SLS / ULS)
S <sub>ED combi</sub>	[kN/m]	435 / 556	376 / 480	<b>437 / 567</b>	404 / 493	388 / 492
M <sub>ED combi</sub>	[kNm/m]	1461 / 1995	1262 / 1789	<b>1420 / 2082</b>	1340 / 1732	1185 / 1641
N <sub>ED combi</sub>	[kN/m]	2049 / 2412	<b>2077 / 2502</b>	1587 / 1760	2030 / 2367	1210 / 1242
U <sub>combi max</sub>	[m] (SLS)	0.149	0.120	<b>0.153</b>	0.125	0.127
N <sub>ED vibro</sub>	[kN/m]	1386 / 1383	1447 / 1353	1328 / 1306	<b>1425 / 1384</b>	1204 / 1177
F <sub>anchor</sub>	[kN]	614 / 1145	530 / 1085	<b>718 / 1301</b>	502 / 716	724 / 1190
MSF	[-]	1.29	1.38	<b>1.20</b>	1.30	1.24

It is notable that the MSFs of the 'soil mechanical failure' verification are all above 1.0, which means that geotechnical stability is satisfied. From these results follow that LC I, LC II and LC III can be normative for the capacity of the combi-wall, LC VIII for the bearing capacity of the vibro piles and LC IV for the anchor forces.

#### Appendix N-2 Capacity combi-wall

The capacity of the combi-wall is checked by means of a local buckling verification at the location of the maximum bending moment. This verification is performed following the CUR 211, using a calculation sheet used in the existing design. The required input variables for the local buckling verification consist of, among others, the maximum normal force and the maximum bending moment in the combi-wall. In stead of the maximum normal force, the normal force at the location of the maximum bending moment should have been used, but this difference is negligible. The maximum normal force is directly obtained from the Plaxis results, shown in Table N.2. The maximum bending moment in the combi-wall consists of the first order moment (M<sub>1</sub>), shown in Table N.2, and a second order bending moment (M<sub>2</sub>) as a

result of deflection of the wall. The deflection is the difference between the total displacement of the tubular piles in the middle of the combi-wall and the displacement of the pile due to the displacement of the top of the piles. Based on the design calculation of the design based on standard dimensions of benchmark 2 in RC2, the deflection of the tubular piles is estimated at about  $0.72 \cdot u_{\text{combi max}}$ , which is a conservative value. The second order bending moment is calculated using a calculation sheet, used in the existing design. The calculation sheet with LC I is attached in Appendix Q.

It is assumed that the piles are filled with sand with a relative density of 70% and a  $q_c$  above 10 MPa. Furthermore it is assumed that corrosion has not affected the combi-wall, because the combi-wall is performed including cathodic protectors. From the Plaxis results and the second order bending moment results follows the maximum normal force and the maximum bending moment in the combi-wall, also collected in Table N.3. Using these values the UC of local buckling of LC I can be calculation as follows:

$$UC = \frac{M_{ed}}{M_{Rd}} + \left( \frac{N_{ed}}{N_{Rd}} \right)^{1.7} = \frac{8169}{9545} + \left( \frac{8514}{27841} \right)^{1.7} = 0.989$$

$0.989 \leq 1.0$ , so the structure satisfies

For the other LCs the UC is determined in the same way.

Table N.3 – Input parameters and results of local buckling verification

LC	$\Delta u$ [m]	$M_2$ [kNm]	$M+M_2$ [kNm]	$N_{ED}$ [kN]	$UC_{\text{buckling}}$ [-]
LC I	0.107	1127	8169	8514	0.99
LC II	0.087	925	7240	8832	0.90
LC IV	0.110	794	8143	6213	0.95

From these results follows that the structure just satisfies the local buckling verification. The verification report with the input variables and design calculations of this verification is attached in Appendix Q.

### Appendix N-3 Anchoring

The anchoring is designed following the CUR 166, using a calculation sheet used in the existing design. The verification report with the input variables and design calculations of this verification is attached in Appendix Q. In this verification, the anchor forces are increased with extra load factors described in CUR 166; the load factor for the grout body is 1.1, the load factor for the anchor rod is 1.25. These load factors are independent of the RC.

In the design it is assumed that the shaft friction,  $\alpha_t$ , is 0.015 and 100% of the installed anchors is tested. The anchors are applied from the relieving platform and the c.t.c. distance between the anchors is equal to 2.735 m. In the design based on standard dimensions in RC2 by the designers, the anchors are designed for eleven different CPTs. These CPTs are different than the CPTs used for the design of the combi-wall and vibro piles. For six CPTs the anchor design is equal, for which the anchorage angle is  $12^\circ$  and the grout body is located in between NAP-3.3 m and NAP-5.5 m. In this study all the anchors of the quay wall are designed following these CPTs, in order to obtain a constant anchor design for the whole quay wall. The normative anchor forces are following from the Plaxis calculation LC Kranz I and are showed in Table N.4.

Table N.4 – Normative anchor forces in RC1

LC	$F_{a,\text{rep}}$ [kN]	$F_{a,\text{max}}$ [kN]	$F_{a,\text{max};\text{gr};\text{d}}$ [kN]	$F_{s;\text{A};\text{rod};\text{d}}$ [kN]
Kranz I	718	1301	1431	898

In this verification, corrosion of the anchor rod is considered, because cathodic protectors cannot be applied to anchors. Conform CUR 166 a corrosion layer of 1.5 mm (contaminated soil, stirred soil), corresponding to a design life of 50 years, is taken into account. In the design calculation also the situation is checked that both two anchors of a tubular pile are dropped out. In this situation the adjacent anchors have to accommodate extra anchor forces. So, in the calculation the c.t.c. distance between anchors becomes 4.1 m in stead of 2.735 m. In this ALS the representative anchor loads are used and the extra load factors from the CUR 166 are not applied. The results of the verification of the anchor rod are listed in Table N.5.

Table N.5 – Anchor rod check in RC1

Tube	Type	Length [m]	Angle [°]	$F_{r;A;rod;d}$ [kN]	$UC_{rod}$	$UC_{dropout}$
Grout anchor rod	Jetmix 101.6 x 17.5	27.81	12	2191	0.74	0.49

Furthermore the grout body of the anchor is checked and the results of this verification are showed in Table N.6. From this verification followed that the steel anchor rod is sufficient and the grout body with a diameter of 280 mm must be minimally 7.3 m. It is clear that for benchmark 2 the design check of the grout body is normative for the design of the anchors.

Table N.6 – Grout body check in RC1

Tube	Diameter [m]	Length [m]	$F_{r;A;gr;rep}$ [kN]	$F_{r;A;gr;d}$ [kN]	$UC_{grout}$	$UC_{dropout}$
Grout anchor rod	280	7.3	1734	1445	0.99	0.62

#### Appendix N-4 Vertical bearing capacity tubular piles

The vertical bearing capacity is verified conform NEN 9997-1, using D-Foundation. For the optimised design of benchmark 2, the vertical bearing capacity verification of pre-2017 is used, which means that that  $\alpha_p = 1.0$ . In D-Foundation the concerning soil profiles are obtained from CPTs and the characteristics of the combi-wall are implemented. From D-Foundation the point and shaft resistances are obtained at eleven different locations of the different CPTs. These resistances are implemented in a vertical bearing capacity calculation sheet in Excel, used in the existing design, in order to determine the unity check per CPT. In D-Foundation the resistances are obtained for the unexcavated side (excavation level of NAP-1.0 m) and the excavated side (excavation level of NAP-18.65 m). In the Excel sheet the averages of the two values of the different situations are determined and the sum of the average point- and shaft resistance, reduced by the negative skin fraction, is the total bearing capacity per CPT,  $R_{c;d}$ . For the unexcavated side, the negative skin friction is taken into account till the depth NAP-9.0 m and positive skin friction from the depth NAP-26 m, because from this depth the active zone is not present anymore. For the excavated side, positive skin friction is taken into account from the excavation level. The UC per CPT can be calculated as follows:

$$UC = \frac{R_{c;d}}{P_d}$$

So, for these unity checks also the maximum normal force,  $P_d$ , is required. This maximum normal force follows from the Plaxis results, namely 8832 kN/pile. In this verification  $\xi_3$  is 1.25, because the total amount of CPTs is more than ten. The tubular pile is considered to have a closed tip, because the tubular pile will plug. This is verified following a plug verification of the CUR 2001-8.

The bearing capacity verification report with the input variables and design calculations of this verification is attached in Appendix Q. The results of this verification are given in Table N.7. It follows that the vertical bearing capacity of the combi-wall satisfies at all locations with a toe level of the tubular piles at NAP-34.5 m.

Table N.7 – Vertical bearing capacity check of tubular piles in RC1

CPT	Toe level piles [m NAP]	$P_d$ [kN/pile]	$R_{c;d}$ [kN/pile]	UC
DKP011	-34.5	8832	10181	0.87
EN380	-34.5	8832	13506	0.65
EN381	-34.5	8832	13070	0.68
EN382	-34.5	8832	10485	0.84
EN383	-34.5	8832	12530	0.70
EN384	-34.5	8832	10042	0.88
EN385	-34.5	8832	9476	0.93
EN387	-34.5	8832	9181	0.96
EN388	-34.5	8832	8848	1.00
EN317	-34.5	8832	10477	0.84
EN311	-34.5	8832	10333	0.85

#### Appendix N-5 Vertical bearing capacity vibro piles

The vertical bearing capacity of the vibro piles is also verified conform NEN 9997-1, using D-Foundation and the same CPTs as for the vertical bearing capacity of the tubular piles of the combi-wall. The vibro piles have a diameter of 560 mm and a base plate with a diameter of 685 mm. Because of the large base plate, the point resistance of the vibro piles is significantly larger. From D-Foundation the point and shaft resistances are obtained at eleven different locations of the different CPTs. These resistances are implemented in a vertical bearing capacity calculation sheet in Excel, used in the existing design, in order to determine the unity check per CPT. The point resistance is determined for piles with a diameter of 685 mm, but the positive and negative skin friction is determined for piles with a diameter of 560 mm. In the Excel sheet the point resistance is summed up to the shaft resistance and reduced by the negative skin friction, resulting in the total bearing capacity per CPT,  $R_{c;d}$ . In this verification  $\xi_3$  is 1.25, because the total amount of CPTs is more than ten. The UC per CPT can be calculated as follows:

$$UC = \frac{R_{c;d}}{P_d}$$

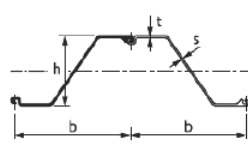
So, for these unity checks also the maximum normal force,  $P_d$ , is required. This maximum normal force follows from the Plaxis results, namely 3655 kN/pile. This value is present in the SLS LC IV. This is because in the ULS the quay structure rotates somewhat, which leads to a reduction of the normal force of the vibro piles.

The bearing capacity verification report with the input variables and design calculations of this verification is attached in Appendix Q. The results of this verification are given in Table N.8. It follows that the vertical bearing capacity of the combi-wall satisfies at all locations with a toe level of the tubular piles at NAP-34.5 m.

Table N.8 – Vertical bearing capacity check of vibro piles in RC1

CPT	Toe level piles [m NAP]	$P_d$ [kN/pile]	$R_{c;d}$ [kN/pile]	UC
DKP011	-27.8	3655	4841	0.76
EN380	-27.8	3655	5828	0.63
EN381	-27.8	3655	4281	0.85
EN382	-27.8	3655	4800	0.76
EN383	-27.8	3655	4200	0.87
EN384	-27.8	3655	3687	0.99
EN385	-27.8	3655	4925	0.74
EN387	-27.8	3655	5118	0.71
EN388	-27.8	3655	5251	0.70
EN317	-27.8	3655	5037	0.73
EN311	-27.8	3655	5103	0.72

## Appendix O Z-type sheet pile profiles of ArcelorMittal



	Width	Height	Thickness		Mass		Moment of inertia	Elastic section modulus
	b mm	h mm	t mm	s mm	single pile kg/m	wall kg/m <sup>2</sup>		
<b>AZ<sup>®</sup>-700 &amp; AZ<sup>®</sup>-770</b>								
AZ 12-770	770	344	8.5	8.5	72.6	<b>94.3</b>	21 430	<b>1 245</b>
AZ 13-770	770	344	9.0	9.0	76.1	<b>98.8</b>	22 360	<b>1 300</b>
AZ 14-770	770	345	9.5	9.5	79.5	<b>103.2</b>	23 300	<b>1 355</b>
AZ 14-770-10/10	770	345	10.0	10.0	82.9	<b>107.7</b>	24 240	<b>1 405</b>
AZ 12-700	700	314	8.5	8.5	67.7	<b>96.7</b>	18 880	<b>1 205</b>
AZ 13-700	700	315	9.5	9.5	74.0	<b>105.7</b>	20 540	<b>1 305</b>
AZ 13-700-10/10	700	316	10.0	10.0	77.2	<b>110.2</b>	21 370	<b>1 355</b>
AZ 14-700	700	316	10.5	10.5	80.3	<b>114.7</b>	22 190	<b>1 405</b>
AZ 17-700	700	420	8.5	8.5	73.1	<b>104.4</b>	36 230	<b>1 730</b>
AZ 18-700	700	420	9.0	9.0	76.5	<b>109.3</b>	37 800	<b>1 800</b>
AZ 19-700	700	421	9.5	9.5	80.0	<b>114.3</b>	39 380	<b>1 870</b>
AZ 20-700	700	421	10.0	10.0	83.5	<b>119.3</b>	40 960	<b>1 945</b>
AZ 24-700	700	459	11.2	11.2	95.7	<b>136.7</b>	55 820	<b>2 430</b>
AZ 26-700	700	460	12.2	12.2	102.9	<b>146.9</b>	59 720	<b>2 600</b>
AZ 28-700	700	461	13.2	13.2	110.0	<b>157.2</b>	63 620	<b>2 760</b>
AZ 24-700N	700	459	12.5	9.0	89.7	<b>128.2</b>	55 890	<b>2 435</b>
AZ 26-700N	700	460	13.5	10.0	96.9	<b>138.5</b>	59 790	<b>2 600</b>
AZ 28-700N	700	461	14.5	11.0	104.1	<b>148.7</b>	63 700	<b>2 765</b>
AZ 36-700N	700	499	15.0	11.2	118.6	<b>169.5</b>	89 610	<b>3 590</b>
AZ 38-700N	700	500	16.0	12.2	126.4	<b>180.6</b>	94 840	<b>3 795</b>
AZ 40-700N	700	501	17.0	13.2	134.2	<b>191.7</b>	100 080	<b>3 995</b>
AZ 42-700N	700	499	18.0	14.0	142.1	<b>203.1</b>	104 930	<b>4 205</b>
AZ 44-700N	700	500	19.0	15.0	149.9	<b>214.2</b>	110 150	<b>4 405</b>
AZ 46-700N	700	501	20.0	16.0	157.7	<b>225.3</b>	115 370	<b>4 605</b>
<b>AZ<sup>®</sup></b>								
AZ 18	630	380	9.5	9.5	74.4	<b>118.1</b>	34 200	<b>1 800</b>
AZ 18-10/10	630	381	10.0	10.0	77.8	<b>123.4</b>	35 540	<b>1 870</b>
AZ 26	630	427	13.0	12.2	97.8	<b>155.2</b>	55 510	<b>2 600</b>
AZ 46	580	481	18.0	14.0	132.6	<b>228.6</b>	110 450	<b>4 595</b>
AZ 48	580	482	19.0	15.0	139.6	<b>240.6</b>	115 670	<b>4 800</b>
AZ 50	580	483	20.0	16.0	146.7	<b>252.9</b>	121 060	<b>5 015</b>

Figure O.1 – Z-type sheet pile profiles ArcelorMittal (Vrijling et al., 2015)

## Appendix P Verification reports of optimised design of benchmark 1 in RC1

### Appendix P-1 D-Sheet Piling report

## Report for D-Sheet Piling 18.2

Design of Diaphragm and Sheet Pile Walls  
Developed by Deltares



# ARCADIS

Design & Consult  
for natural and  
built assets

Company: ARCADIS  
Infrastructure

Date of report: 04/03/2019  
Time of report: 12:58:11  
Report with version: 18.2.900.21437

Date of calculation: 3/4/2019  
Time of calculation: 12:46:51 PM  
Calculated with version: 18.2.900.21437

File name: C:\.\Hoofdwand doorsnede B-B - RC1 - D = 1360 t = 15.32 mm

Project identification: Benchmark 1  
Definitief ontwerp  
Doorsnede B-B'

Verification according to National Annex of Eurocode 7 in the Netherlands (NEN 9997-1:2016)

## 1 Table of Contents

1 Table of Contents	2
2 Summary	3
2.1 Overview per Stage and Test	3
2.2 Anchors and Struts	3
2.3 Overall Stability per Stage	4
2.4 Warnings	4
2.5 CUR Verification Steps	5
3 Input Data for all Stages	6
3.1 General Input Data	6
3.2 Sheet Piling Properties	6
3.2.1 General properties	6
3.2.2 Stiffness EI (elastic behaviour)	6
3.2.3 Maximum allowable moments	6
3.2.4 Properties for vertical balance	6
3.3 Calculation Options	6
4 Outline Stage 1: Huidig	12
5 Overall Stability Stage 1: Huidig	13
5.1 Overall Stability	13
6 Outline Stage 2: Aanleg+ voorspannen ankers	14
7 Overall Stability Stage 2: Aanleg+ voorspannen ankers	15
7.1 Overall Stability	15
8 Outline Stage 3: Constructiediepte	16
9 Overall Stability Stage 3: Constructiediepte	17
9.1 Overall Stability	17
10 Outline Stage 4: BC I	18
11 Overall Stability Stage 4: BC I	19
11.1 Overall Stability	19
12 Outline Stage 5: BC II	20
13 Overall Stability Stage 5: BC II	21
13.1 Overall Stability	21
14 Outline Stage 6: BC III	22
15 Overall Stability Stage 6: BC III	23
15.1 Overall Stability	23
16 Outline Stage 7: BC IV (extreem laag water)	24
17 Overall Stability Stage 7: BC IV (extreem laag water)	25
17.1 Overall Stability	25
18 Outline Stage 8: BC V (falen drainage)	26
19 Overall Stability Stage 8: BC V (falen drainage)	27
19.1 Overall Stability	27
20 Outline Stage 9: BC VI (aanleg bodembescherming)	28
21 Overall Stability Stage 9: BC VI (aanleg bodembescherming)	29
21.1 Overall Stability	29

## 2 Summary

### 2.1 Overview per Stage and Test

Stage nr.	Verification	Displacement [mm]	Moment [kNm]	Shear force [kN]	Mob. perc. moment [%]	Mob. perc. resistance [%]	Vertical balance
1	EC7(NL)-Step 6.1		539.72	-311.19	<b>0.0</b>	17.3	Upwards
1	EC7(NL)-Step 6.2		314.92	-239.77	<b>0.0</b>	17.4	Upwards
1	EC7(NL)-Step 6.3		539.72	-311.19	<b>0.0</b>	17.3	Upwards
1	EC7(NL)-Step 6.4		314.92	-239.77	<b>0.0</b>	17.4	Upwards
1	EC7(NL)-Step 6.5	4.2	455.42	-269.16	<b>0.0</b>	14.1	Upwards
1	EC7(NL)-Step 6.5 * 1.20		546.50	-322.99			
2	EC7(NL)-Step 6.1		726.73	726.31	<b>0.0</b>	16.9	Not sufficient
2	EC7(NL)-Step 6.2		-486.45	693.29	<b>0.0</b>	17.0	Not sufficient
2	EC7(NL)-Step 6.3		726.73	726.31	<b>0.0</b>	16.9	Not sufficient
2	EC7(NL)-Step 6.4		-486.45	693.29	<b>0.0</b>	17.0	Not sufficient
2	EC7(NL)-Step 6.5	-9.0	548.08	666.16	<b>0.0</b>	13.7	Not sufficient
2	EC7(NL)-Step 6.5 * 1.20		657.70	799.40			
3	EC7(NL)-Step 6.3		4901.37	-1062.26	<b>0.0</b>	25.4	Not sufficient
3	EC7(NL)-Step 6.4		4483.85	-998.34	<b>0.0</b>	26.0	Not sufficient
3	EC7(NL)-Step 6.5	45.8	3907.26	-837.98	<b>0.0</b>	20.2	Not sufficient
3	EC7(NL)-Step 6.5 * 1.20		4688.72	-1005.58			
4	EC7(NL)-Step 6.3		7902.28	-1594.46	<b>0.0</b>	36.6	Not sufficient
4	EC7(NL)-Step 6.4		7434.00	-1570.87	<b>0.0</b>	<b>38.4</b>	Not sufficient
4	EC7(NL)-Step 6.5	88.5	6512.94	-1360.28	<b>0.0</b>	29.4	Not sufficient
4	EC7(NL)-Step 6.5 * 1.20		7815.53	-1632.34			
5	EC7(NL)-Step 6.3		6789.38	-1453.13	<b>0.0</b>	34.3	Not sufficient
5	EC7(NL)-Step 6.4		6695.04	-1449.03	<b>0.0</b>	34.7	Not sufficient
5	EC7(NL)-Step 6.5	87.3	6372.64	-1322.11	<b>0.0</b>	29.3	Not sufficient
5	EC7(NL)-Step 6.5 * 1.20		7647.16	-1586.54			
6	EC7(NL)-Step 6.3		7607.76	-1578.98	<b>0.0</b>	36.7	Not sufficient
6	EC7(NL)-Step 6.4		7393.91	-1570.71	<b>0.0</b>	37.6	Not sufficient
6	EC7(NL)-Step 6.5	88.4	6431.72	-1353.99	<b>0.0</b>	29.4	Not sufficient
6	EC7(NL)-Step 6.5 * 1.20		7718.07	-1624.78			
7	EC7(NL)-Step 6.3		6544.50	-1367.29	<b>0.0</b>	29.9	Not sufficient
7	EC7(NL)-Step 6.4		6490.31	-1361.34	<b>0.0</b>	29.8	Not sufficient
7	EC7(NL)-Step 6.5	89.8	6544.50	-1367.29	<b>0.0</b>	29.9	Not sufficient
7	EC7(NL)-Step 6.5 * 1.20		7853.40	-1640.75			
8	EC7(NL)-Step 6.3		6660.57	-1377.59	<b>0.0</b>	30.3	Not sufficient
8	EC7(NL)-Step 6.4		6640.36	-1375.63	<b>0.0</b>	30.3	Not sufficient
8	EC7(NL)-Step 6.5	<b>91.8</b>	6660.57	-1377.59	<b>0.0</b>	30.3	Not sufficient
8	EC7(NL)-Step 6.5 * 1.20		<b>7992.68</b>	<b>-1653.11</b>			
9	EC7(NL)-Step 6.3		6912.94	-1449.19	<b>0.0</b>	35.0	Not sufficient
9	EC7(NL)-Step 6.4		6769.25	-1450.45	<b>0.0</b>	35.6	Not sufficient
9	EC7(NL)-Step 6.5	90.8	6559.68	1364.76	<b>0.0</b>	30.1	Not sufficient
9	EC7(NL)-Step 6.5 * 1.20		7871.61	1637.71			
Max		<b>91.8</b>	<b>7992.68</b>	<b>-1653.11</b>	<b>0.0</b>	<b>38.4</b>	Not sufficient

### 2.2 Anchors and Struts

Stage nr.	Verification type	Anchor/strut Groutanker 1		Anchor/strut Groutanker 2	
		Force [kN]	State	Force [kN]	State
2	EC7(NL)-Step 6.1	802.50	Elastic	802.50	Elastic
2	EC7(NL)-Step 6.2	802.50	Elastic	802.50	Elastic
2	EC7(NL)-Step 6.3	802.50	Elastic	802.50	Elastic
2	EC7(NL)-Step 6.4	802.50	Elastic	802.50	Elastic
2	EC7(NL)-Step 6.5 * 1.20	963.00	Elastic	963.00	Elastic

Stage nr.	Verification type	Anchor/strut Groutanker 1		Anchor/strut Groutanker 2	
		Force [kN]	State	Force [kN]	State
3	EC7(NL)-Step 6.1	-		-	
3	EC7(NL)-Step 6.2	-		-	
3	EC7(NL)-Step 6.3	979.42	Elastic	977.25	Elastic
3	EC7(NL)-Step 6.4	931.00	Elastic	929.42	Elastic
3	EC7(NL)-Step 6.5 * 1.20	1085....	Elastic	1084....	Elastic
4	EC7(NL)-Step 6.1	-		-	
4	EC7(NL)-Step 6.2	-		-	
4	EC7(NL)-Step 6.3	1305....	Elastic	1299....	Elastic
4	EC7(NL)-Step 6.4	1225....	Elastic	1219....	Elastic
4	EC7(NL)-Step 6.5 * 1.20	1393....	Elastic	1387....	Elastic
5	EC7(NL)-Step 6.1	-		-	
5	EC7(NL)-Step 6.2	-		-	
5	EC7(NL)-Step 6.3	1270....	Elastic	1264....	Elastic
5	EC7(NL)-Step 6.4	1257....	Elastic	1251....	Elastic
5	EC7(NL)-Step 6.5 * 1.20	1448....	Elastic	1443....	Elastic
6	EC7(NL)-Step 6.1	-		-	
6	EC7(NL)-Step 6.2	-		-	
6	EC7(NL)-Step 6.3	1331....	Elastic	1324....	Elastic
6	EC7(NL)-Step 6.4	1310....	Elastic	1304....	Elastic
6	EC7(NL)-Step 6.5 * 1.20	<b>1455....</b>	Elastic	<b>1449....</b>	Elastic
7	EC7(NL)-Step 6.1	-		-	
7	EC7(NL)-Step 6.2	-		-	
7	EC7(NL)-Step 6.3	1185....	Elastic	1181....	Elastic
7	EC7(NL)-Step 6.4	1200....	Elastic	1195....	Elastic
7	EC7(NL)-Step 6.5 * 1.20	1422....	Elastic	1417....	Elastic
8	EC7(NL)-Step 6.1	-		-	
8	EC7(NL)-Step 6.2	-		-	
8	EC7(NL)-Step 6.3	1194....	Elastic	1189....	Elastic
8	EC7(NL)-Step 6.4	1191....	Elastic	1186....	Elastic
8	EC7(NL)-Step 6.5 * 1.20	1433....	Elastic	1427....	Elastic
9	EC7(NL)-Step 6.1	-		-	
9	EC7(NL)-Step 6.2	-		-	
9	EC7(NL)-Step 6.3	1182....	Elastic	1178....	Elastic
9	EC7(NL)-Step 6.4	1186....	Elastic	1181....	Elastic
9	EC7(NL)-Step 6.5 * 1.20	1416....	Elastic	1410....	Elastic
Max		<b>1455....</b>		<b>1449....</b>	

Due to multiplication of the representative value a force bigger than yield or buckling force may be present.

### 2.3 Overall Stability per Stage

Stage name	Stability factor [-]
Huidig	4.52
Aanleg+ voorspannen ankers	4.52
Constructiediepte	2.26
BC I	1.90
BC II	1.96
BC III	1.89
BC IV (extreem laag water)	2.30
BC V (falen drainage)	2.29
BC VI (aanleg bodembescherming)	1.97

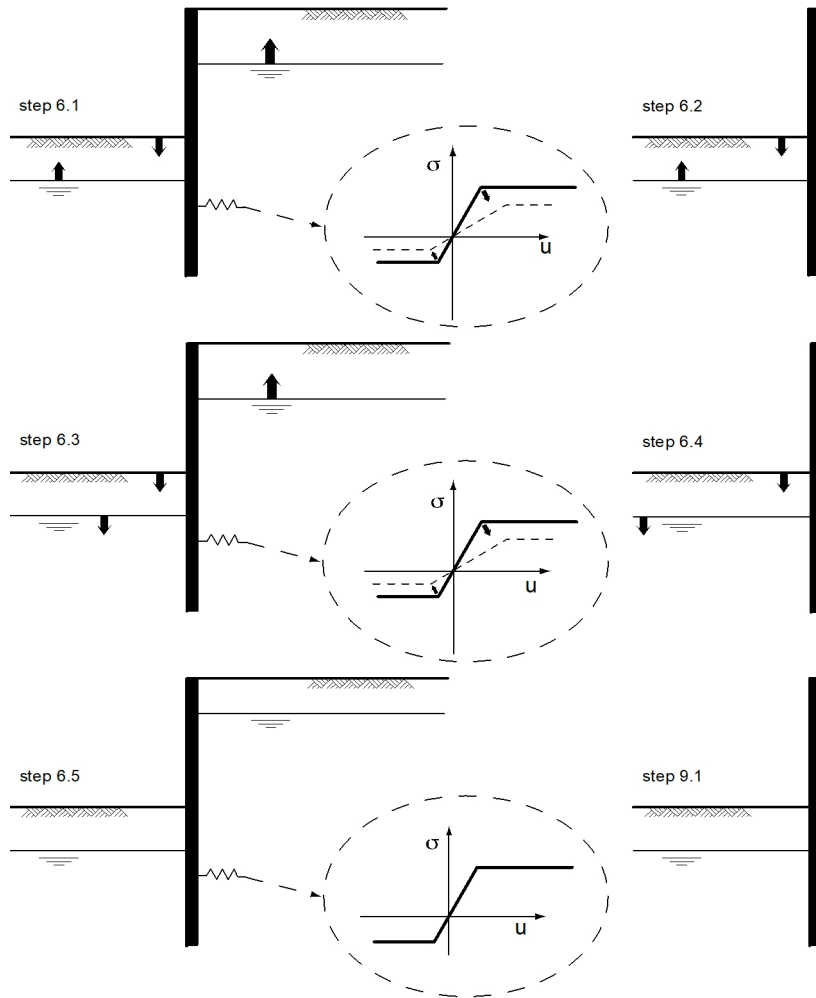
### 2.4 Warnings

**\* Vertical stability**

The vertical balance cannot be calculated correctly under combined walls. It is not possible to indicate CPT resistances for both toe levels. The calculation only takes into account the lower toe resistance, the upper toe resistance is neglected.

**\* Vertical balance:** The resultant vertical friction force is directed upward in stage 1, 1, 1, 1 & 1 because the friction force on the passive side exceeds that on the active side. This might be prevented by reducing the friction angle Delta on the passive side.

2.5 CUR Verification Steps



### 3 Input Data for all Stages

#### 3.1 General Input Data

Verification according to National Annex of Eurocode 7 in the Netherlands (NEN 9997-1:2016)

Model	Sheet piling
Check vertical balance	Yes
Number of construction stages	9
Unit weight of water	9.81 kN/m <sup>3</sup>
Number of curves for spring characteristics	3
Unloading curve on spring characteristic	No
Elastic calculation	Yes

#### 3.2 Sheet Piling Properties

Length	30.60 m
Level top side	3.60 m
Number of sections	2
q <sub>b</sub> ;max	10.00 MPa
Xi factor	1.25

##### 3.2.1 General properties

Section name	From [m]	To [m]	Material type	Acting width [m]
d1360 t15.32 X...	-17.50	3.60	Steel	3.21
d1360 t15.32 X70	-27.00	-17.50	Steel	1.36

##### 3.2.2 Stiffness EI (elastic behaviour)

Section name	Elastic stiffness EI [kNm <sup>2</sup> /m']	Red. factor on EI [-]	Corrected elas. stiffness EI [kNm <sup>2</sup> ]	Note to reduction factor
d1360 t15.32 X...	1.0316E+06	1.00	3.3115E+06	
d1360 t15.32 X70	2.2596E+06	1.00	3.0730E+06	

##### 3.2.3 Maximum allowable moments

Section name	Mr;char;el [kNm/m']	Modification factor [-]	Material factor [-]	Red. factor allow. moment [-]	Mr;d;el [kNm]
d1360 t15.32 X...	3747.72	1.00	1.00	1.00	12030.18
d1360 t15.32 X70	7674.26	1.00	1.00	1.00	10436.99

##### 3.2.4 Properties for vertical balance

Section name	From [m]	To [m]	Height [mm]	Coating area [m <sup>2</sup> /m <sup>2</sup> wall]	Section area [cm <sup>2</sup> /m']
d1360 t15.32 X...	-17.50	3.60	400.00	1.35	545.70
d1360 t15.32 X70	-27.00	-17.50	400.00	1.35	231.20

#### 3.3 Calculation Options

First stage represents initial situation	No
Calculation refinement	Coarse
Reduce delta(s) according to CUR	Yes
Verification	EC7 NA NL - method B: Partial factors (design values) in verification according to Eurocode 7 using the factors as described in the National Annex of the Netherlands. It is basically design approach III.

Verification of stage	1: Huidig
Multiplication factor for anchor stiffness	1.000
Used partial factor set	RC 1
Factors on loads	
- Permanent load, unfavourable	1.00
- Permanent load, favourable	1.00
- Variable load, unfavourable	1.00
- Variable load, favourable	0.00
Factors on representative values	
- Partial factor on M, D and Pmax	1.20
Material factors	
- Cohesion	1.15
- Tangent phi	1.15
- Delta (wall friction angle)	1.15
- Modulus of low representative subgrade reaction	1.30
Geometry modification	
- Increase retaining height	0.00 % User defined
- Maximum increase retaining height	0.00 m User defined
- Reduction in phreatic line on passive side	0.00 m User defined
- Raise in phreatic line on active side	0.00 m User defined
Overall stability factors	
- Cohesion	1.30
- Tangent phi	1.20
- Factor on unit weight soil	1.00
Vertical balance factors	
- Partial factor base resistance (gamma_b)	1.20
Verification of stage	2: Aanleg+ voorspannen ankers
Multiplication factor for anchor stiffness	1.000
Used partial factor set	RC 1
Factors on loads	
- Permanent load, unfavourable	1.00
- Permanent load, favourable	1.00
- Variable load, unfavourable	1.00
- Variable load, favourable	0.00
Factors on representative values	
- Partial factor on M, D and Pmax	1.20
Material factors	
- Cohesion	1.15
- Tangent phi	1.15
- Delta (wall friction angle)	1.15
- Modulus of low representative subgrade reaction	1.30
Geometry modification	
- Increase retaining height	0.00 % User defined
- Maximum increase retaining height	0.00 m User defined
- Reduction in phreatic line on passive side	0.00 m User defined
- Raise in phreatic line on active side	0.00 m User defined
Overall stability factors	
- Cohesion	1.30
- Tangent phi	1.20
- Factor on unit weight soil	1.00

Vertical balance factors	
- Partial factor base resistance (gamma_b)	1.20
Verification of stage	3: Constructiediepte
Multiplication factor for anchor stiffness	1.000
Used partial factor set	RC 1
Factors on loads	
- Permanent load, unfavourable	1.00
- Permanent load, favourable	1.00
- Variable load, unfavourable	1.00
- Variable load, favourable	0.00
Factors on representative values	
- Partial factor on M, D and Pmax	1.20
Material factors	
- Cohesion	1.15
- Tangent phi	1.15
- Delta (wall friction angle)	1.15
- Modulus of low representative subgrade reaction	1.30
Geometry modification	
- Increase retaining height	0.00 % User defined
- Maximum increase retaining height	0.00 m User defined
- Reduction in phreatic line on passive side	0.00 m User defined
- Raise in phreatic line on active side	0.00 m User defined
Overall stability factors	
- Cohesion	1.30
- Tangent phi	1.20
- Factor on unit weight soil	1.00
Vertical balance factors	
- Partial factor base resistance (gamma_b)	1.20
Verification of stage	4: BC I
Multiplication factor for anchor stiffness	1.000
Used partial factor set	RC 1
Factors on loads	
- Permanent load, unfavourable	1.00
- Permanent load, favourable	1.00
- Variable load, unfavourable	1.00
- Variable load, favourable	0.00
Factors on representative values	
- Partial factor on M, D and Pmax	1.20
Material factors	
- Cohesion	1.15
- Tangent phi	1.15
- Delta (wall friction angle)	1.15
- Modulus of low representative subgrade reaction	1.30
Geometry modification	
- Increase retaining height	0.00 % User defined
- Maximum increase retaining height	0.00 m User defined
- Reduction in phreatic line on passive side	0.00 m User defined
- Raise in phreatic line on active side	0.00 m User defined
Overall stability factors	
- Cohesion	1.30

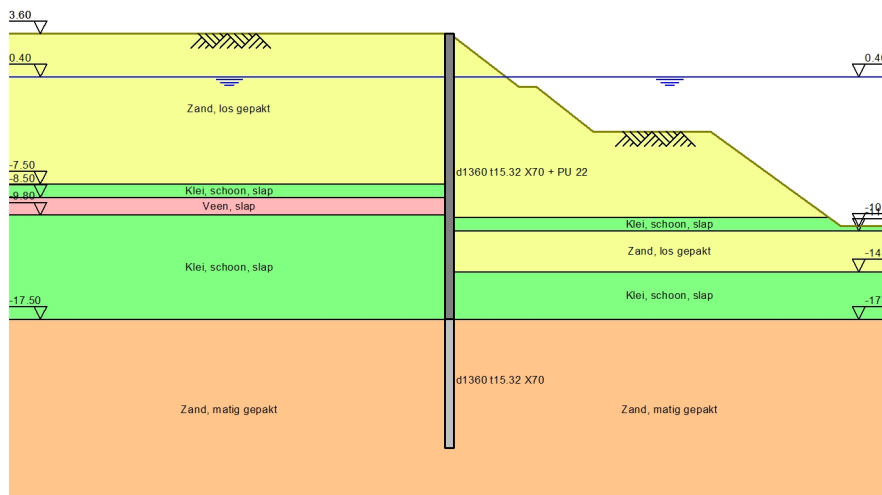
- Tangent phi	1.20
- Factor on unit weight soil	1.00
Vertical balance factors	
- Partial factor base resistance (gamma_b)	1.20
Verification of stage	
	5: BC II
Multiplication factor for anchor stiffness	
	1.000
Used partial factor set	
	RC 1
Factors on loads	
- Permanent load, unfavourable	1.00
- Permanent load, favourable	1.00
- Variable load, unfavourable	1.00
- Variable load, favourable	0.00
Factors on representative values	
- Partial factor on M, D and Pmax	1.20
Material factors	
- Cohesion	1.15
- Tangent phi	1.15
- Delta (wall friction angle)	1.15
- Modulus of low representative subgrade reaction	1.30
Geometry modification	
- Increase retaining height	0.00 % User defined
- Maximum increase retaining height	0.00 m User defined
- Reduction in phreatic line on passive side	0.00 m User defined
- Raise in phreatic line on active side	0.00 m User defined
Overall stability factors	
- Cohesion	1.30
- Tangent phi	1.20
- Factor on unit weight soil	1.00
Vertical balance factors	
- Partial factor base resistance (gamma_b)	1.20
Verification of stage	
	6: BC III
Multiplication factor for anchor stiffness	
	1.000
Used partial factor set	
	RC 1
Factors on loads	
- Permanent load, unfavourable	1.00
- Permanent load, favourable	1.00
- Variable load, unfavourable	1.00
- Variable load, favourable	0.00
Factors on representative values	
- Partial factor on M, D and Pmax	1.20
Material factors	
- Cohesion	1.15
- Tangent phi	1.15
- Delta (wall friction angle)	1.15
- Modulus of low representative subgrade reaction	1.30
Geometry modification	
- Increase retaining height	0.00 % User defined
- Maximum increase retaining height	0.00 m User defined
- Reduction in phreatic line on passive side	0.00 m User defined
- Raise in phreatic line on active side	0.00 m User defined

Overall stability factors	
- Cohesion	1.30
- Tangent phi	1.20
- Factor on unit weight soil	1.00
Vertical balance factors	
- Partial factor base resistance (gamma_b)	1.20
Verification of stage	7: BC IV (extrem laag water)
Multiplication factor for anchor stiffness	1.000
Used partial factor set	RC 0 RC0 is added for simple constructions. To be compared with CUR class I
Factors on loads	
- Permanent load, unfavourable	1.00
- Permanent load, favourable	1.00
- Variable load, unfavourable	1.00
- Variable load, favourable	0.00
Factors on representative values	
- Partial factor on M, D and Pmax	1.20
Material factors	
- Cohesion	1.00
- Tangent phi	1.00 User defined
- Delta (wall friction angle)	1.00 User defined
- Modulus of low representative subgrade reaction	1.00 User defined
Geometry modification	
- Increase retaining height	0.00 % User defined
- Maximum increase retaining height	0.00 m User defined
- Reduction in phreatic line on passive side	0.00 m User defined
- Raise in phreatic line on active side	0.00 m User defined
Overall stability factors	
- Cohesion	1.00 User defined
- Tangent phi	1.00 User defined
- Factor on unit weight soil	1.00
Vertical balance factors	
- Partial factor base resistance (gamma_b)	1.00 User defined
Verification of stage	8: BC V (falen drainage)
Multiplication factor for anchor stiffness	1.000
Used partial factor set	RC 0 RC0 is added for simple constructions. To be compared with CUR class I
Factors on loads	
- Permanent load, unfavourable	1.00
- Permanent load, favourable	1.00
- Variable load, unfavourable	1.00
- Variable load, favourable	0.00
Factors on representative values	
- Partial factor on M, D and Pmax	1.20
Material factors	
- Cohesion	1.00
- Tangent phi	1.00 User defined
- Delta (wall friction angle)	1.00 User defined

- Modulus of low representative subgrade reaction	1.00 User defined
Geometry modification	
- Increase retaining height	0.00 % User defined
- Maximum increase retaining height	0.00 m User defined
- Reduction in phreatic line on passive side	0.00 m User defined
- Raise in phreatic line on active side	0.00 m User defined
Overall stability factors	
- Cohesion	1.00 User defined
- Tangent phi	1.00 User defined
- Factor on unit weight soil	1.00
Vertical balance factors	
- Partial factor base resistance (gamma_b)	1.00 User defined
Verification of stage	9: BC VI (aanleg bodembescherming)
Multiplication factor for anchor stiffness	1.000
Used partial factor set	RC 1
Factors on loads	
- Permanent load, unfavourable	1.00
- Permanent load, favourable	1.00
- Variable load, unfavourable	1.00
- Variable load, favourable	0.00
Factors on representative values	
- Partial factor on M, D and Pmax	1.20
Material factors	
- Cohesion	1.15
- Tangent phi	1.15
- Delta (wall friction angle)	1.15
- Modulus of low representative subgrade reaction	1.30
Geometry modification	
- Increase retaining height	0.00 % User defined
- Maximum increase retaining height	0.00 m User defined
- Reduction in phreatic line on passive side	0.00 m User defined
- Raise in phreatic line on active side	0.00 m User defined
Overall stability factors	
- Cohesion	1.30
- Tangent phi	1.20
- Factor on unit weight soil	1.00
Vertical balance factors	
- Partial factor base resistance (gamma_b)	1.20

**4 Outline Stage 1: Huidig**

Outline - Stage 1: Huidig

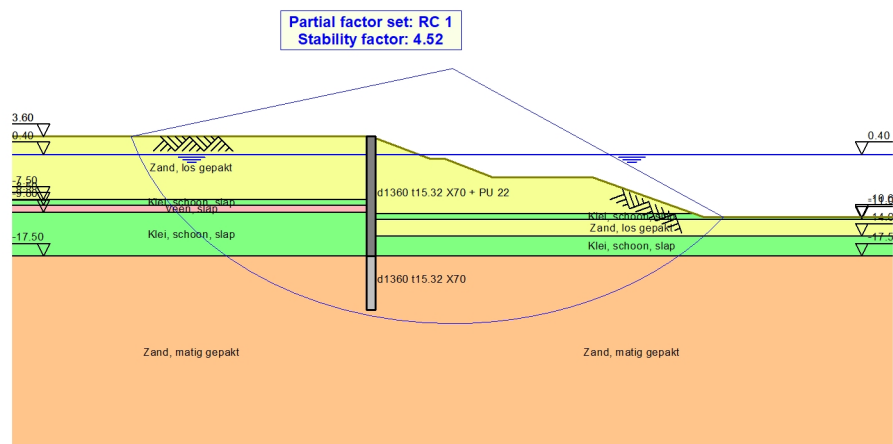


## 5 Overall Stability Stage 1: Huidig

Stability factor : 4.52

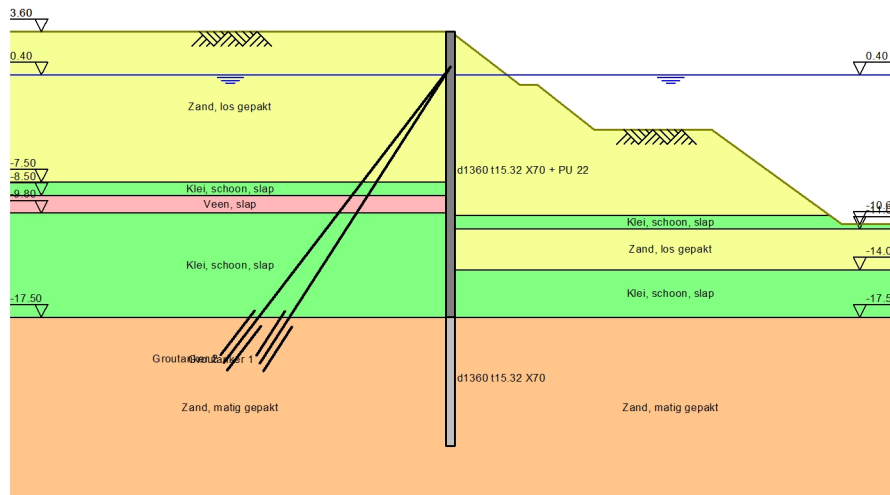
### 5.1 Overall Stability

Overall Stability - Stage 1: Huidig



## 6 Outline Stage 2: Aanleg+ voorspannen ankers

Outline - Stage 2: Aanleg+ voorspannen ankers

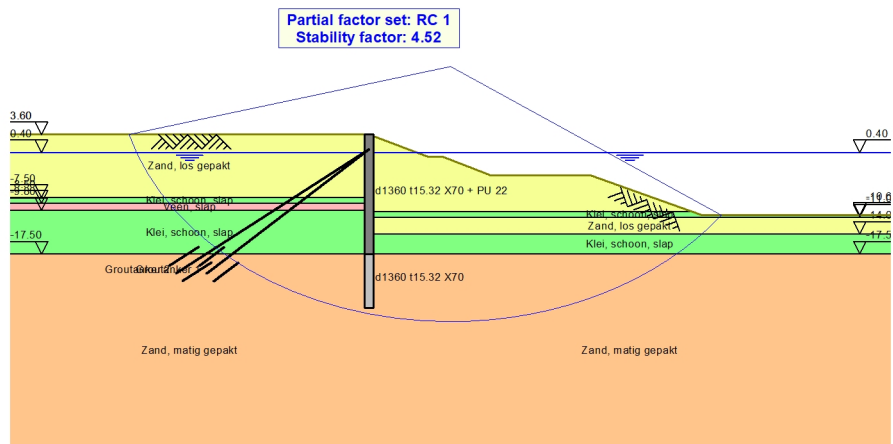


## 7 Overall Stability Stage 2: Aanleg+ voorspannen ankers

Stability factor : 4.52

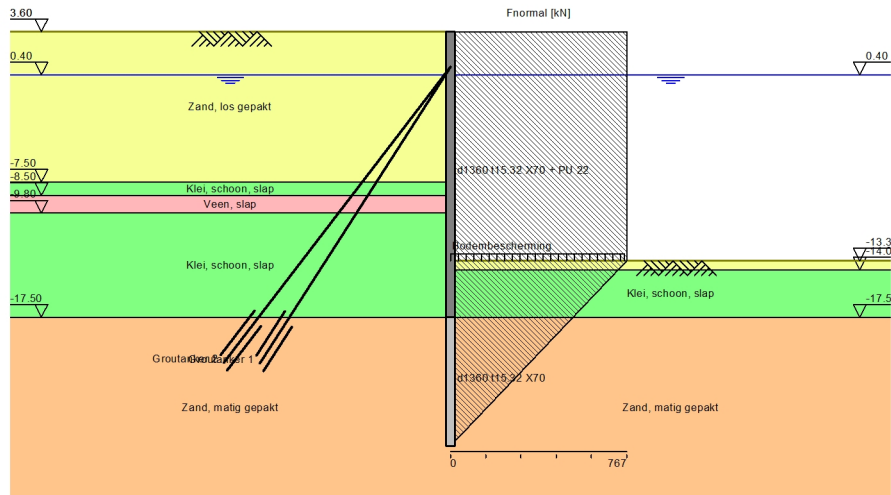
### 7.1 Overall Stability

Overall Stability - Stage 2: Aanleg+ voorspannen ankers



**8 Outline Stage 3: Constructiediepte**

Outline - Stage 3: Constructiediepte

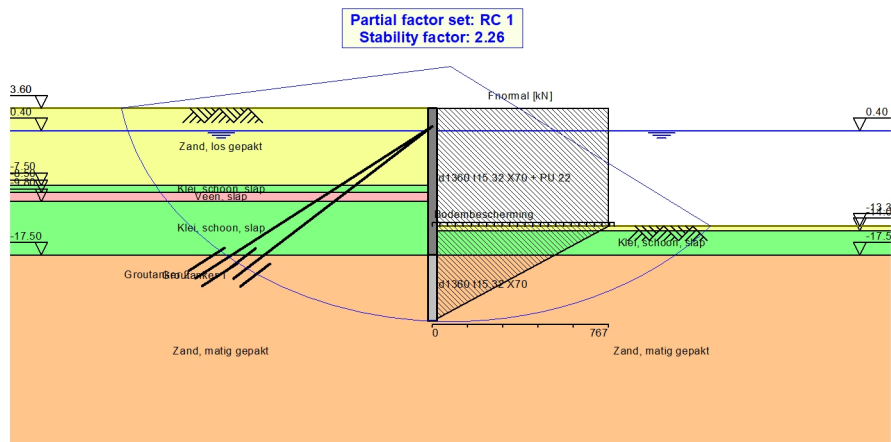


## 9 Overall Stability Stage 3: Constructiediepte

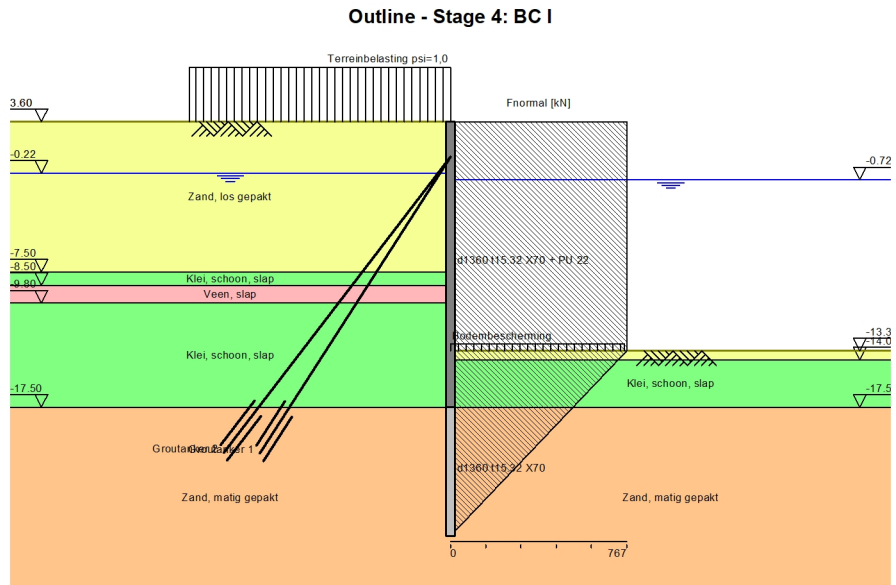
Stability factor : 2.26

### 9.1 Overall Stability

Overall Stability - Stage 3: Constructiediepte



10 Outline Stage 4: BC I

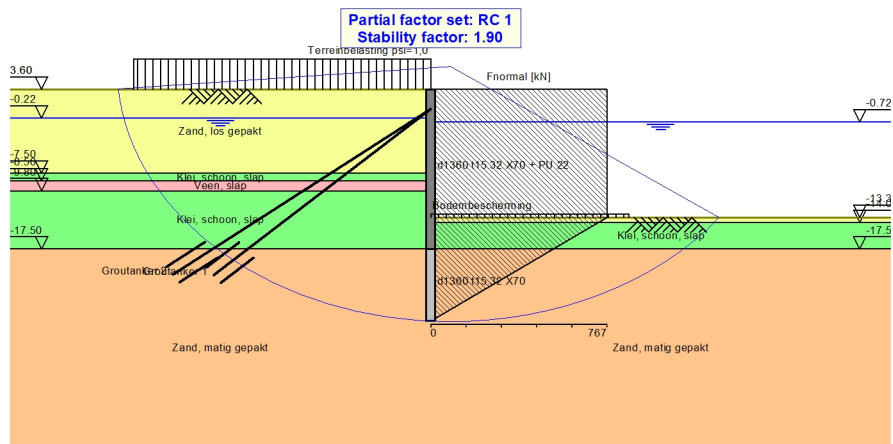


## 11 Overall Stability Stage 4: BC I

Stability factor : 1.90

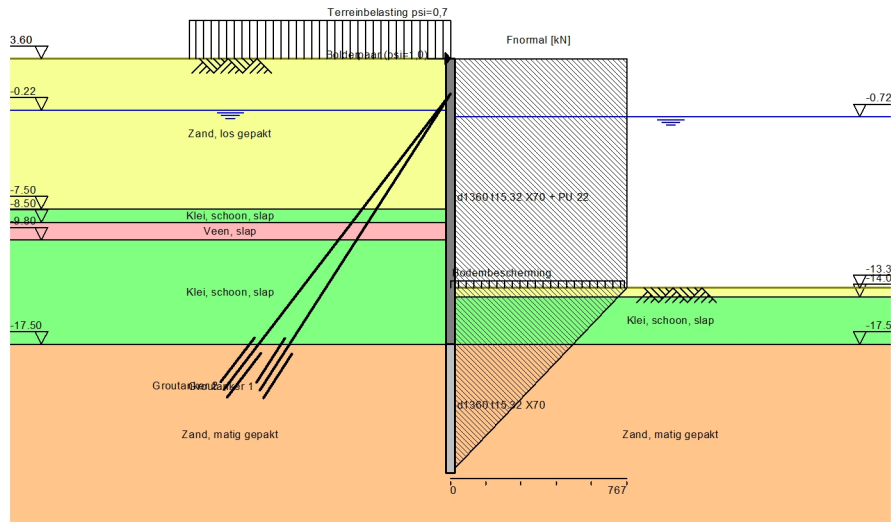
### 11.1 Overall Stability

Overall Stability - Stage 4: BC I



12 Outline Stage 5: BC II

Outline - Stage 5: BC II

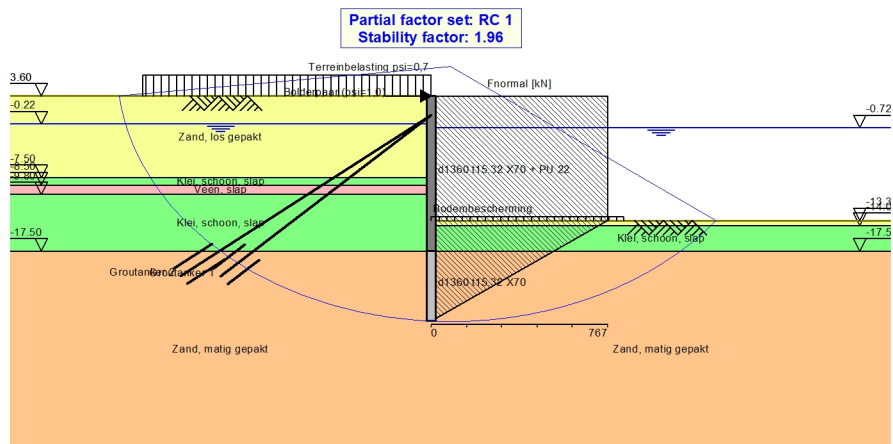


### 13 Overall Stability Stage 5: BC II

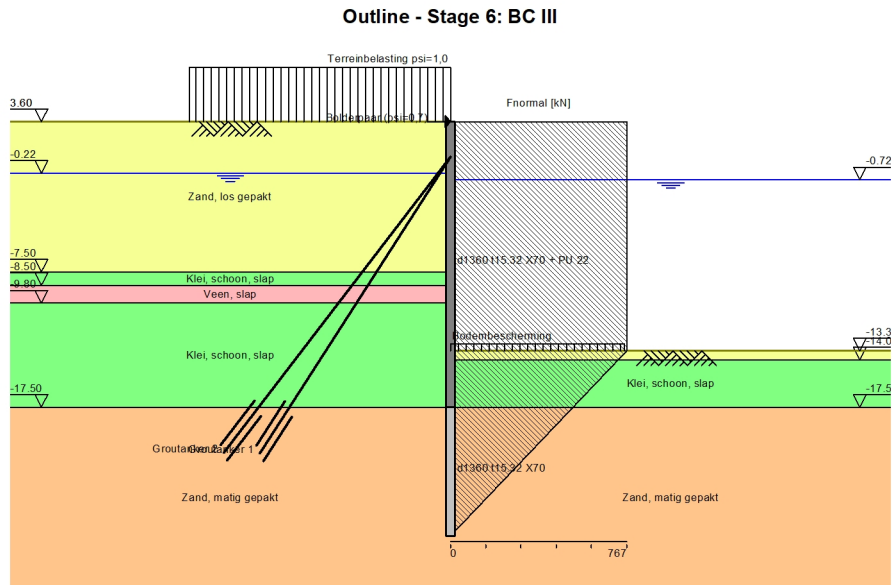
Stability factor : 1.96

#### 13.1 Overall Stability

Overall Stability - Stage 5: BC II



**14 Outline Stage 6: BC III**

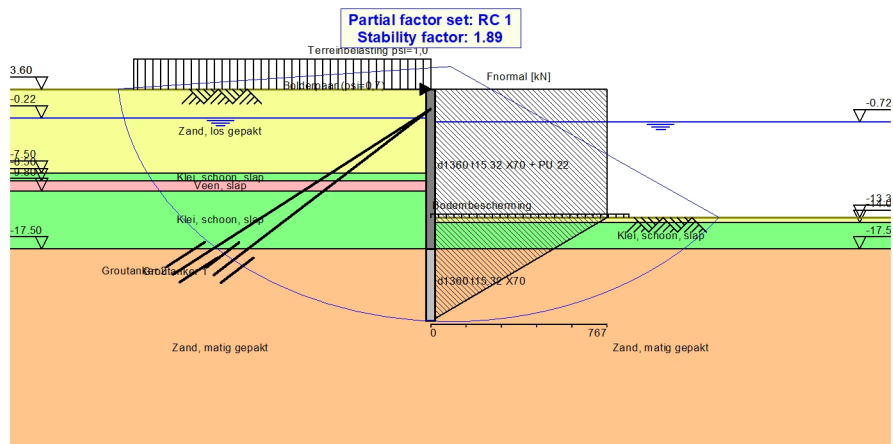


### 15 Overall Stability Stage 6: BC III

Stability factor : 1.89

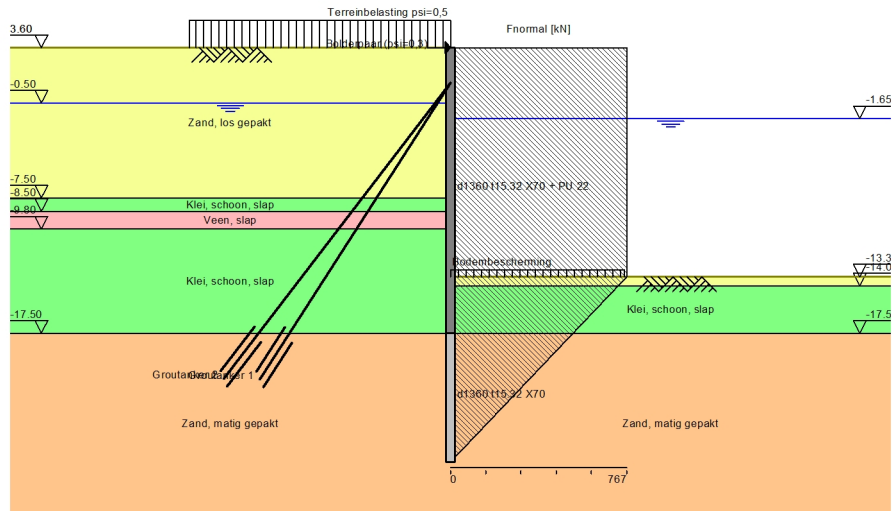
#### 15.1 Overall Stability

Overall Stability - Stage 6: BC III



16 Outline Stage 7: BC IV (extrem laag water)

Outline - Stage 7: BC IV (extrem laag water)

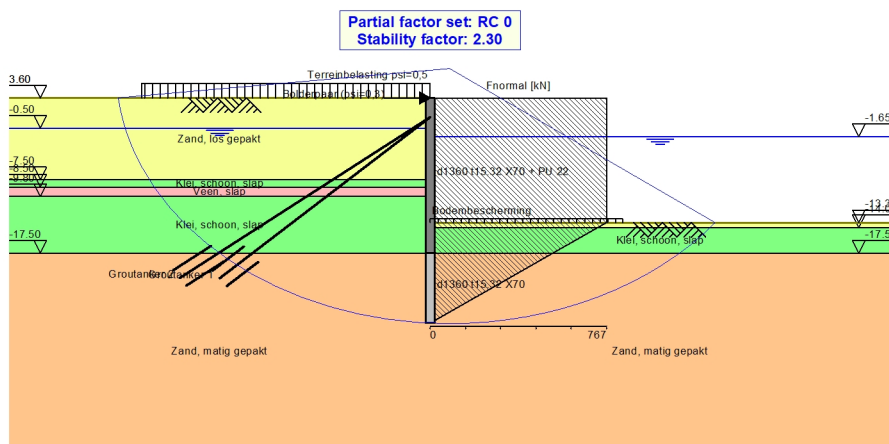


### 17 Overall Stability Stage 7: BC IV (extreem laag water)

Stability factor : 2.30

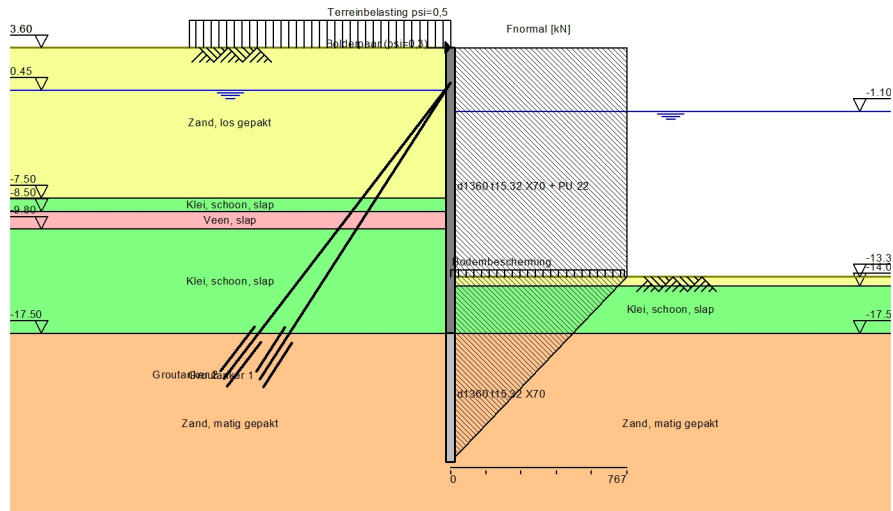
#### 17.1 Overall Stability

Overall Stability - Stage 7: BC IV (extreem laag water)



18 Outline Stage 8: BC V (falen drainage)

Outline - Stage 8: BC V (falen drainage)

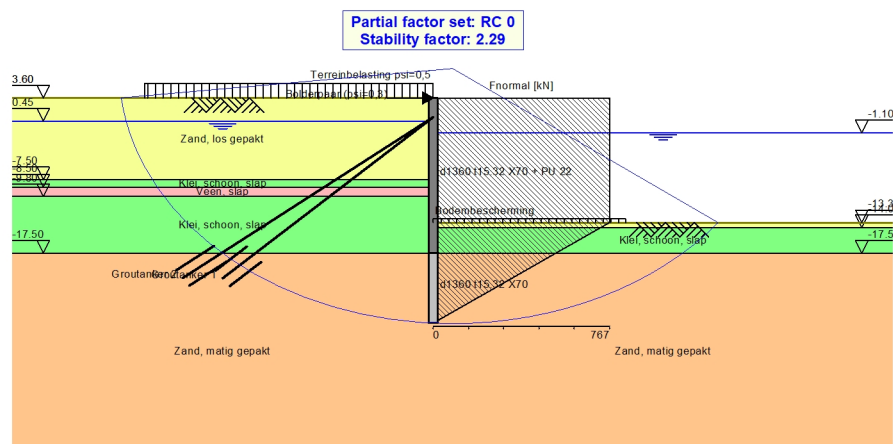


### 19 Overall Stability Stage 8: BC V (falen drainage)

Stability factor : 2.29

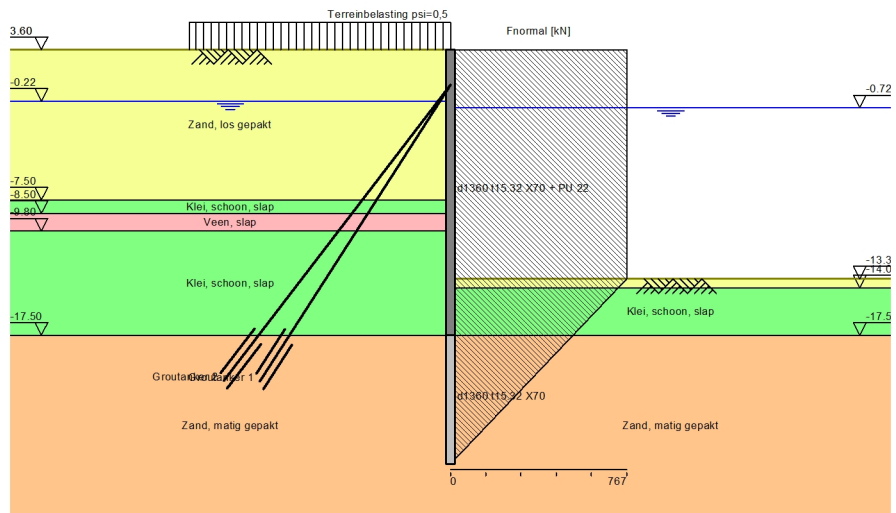
#### 19.1 Overall Stability

Overall Stability - Stage 8: BC V (falen drainage)



**20 Outline Stage 9: BC VI (aanleg bodembescherming)**

**Outline - Stage 9: BC VI (aanleg bodembescherming)**

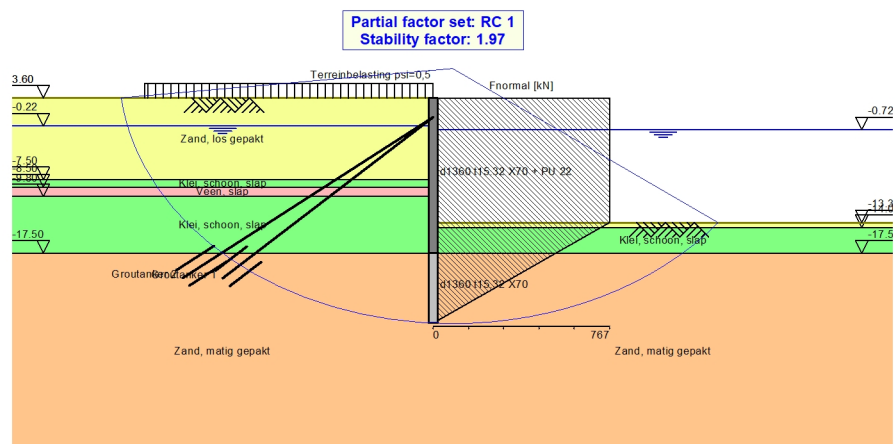


## 21 Overall Stability Stage 9: BC VI (aanleg bodembescherming)

Stability factor : 1.97

### 21.1 Overall Stability

Overall Stability - Stage 9: BC VI (aanleg bodembescherming)



End of Report

## Appendix P-2 Local buckling



## Local buckling according to Quay Wall Handbook

### Limitations: Piles

- Method to be used for steel quality up to X70 ( $f_y = 483 \text{ MPa}$ )
- The formulas are valid for water head differences less than 4 m.
- Critical strain formula for pile fill with sand is only valid for  $70 < \frac{D}{t} \leq 120$
- Alternatively EN 1993-1-6 may be used for piles filled with sand. In that case the resistance may be increased with a factor 1.13. This is only allowed for  $D/t < 100$  and for  $D/t\epsilon^2 < 170$ .

### Fill

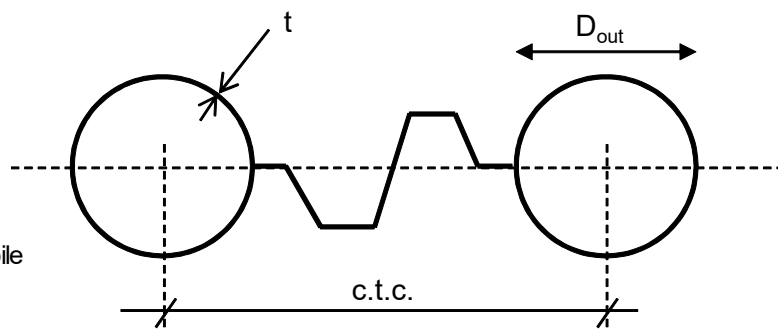
- Sand shall be present in the area of the section subject to evaluation of the resistance. Sand may be loose or medium dense, if naturally available.
- In actively filled piles the sand fill shall be compacted, obtaining 70% relative density or  $q_c > 10 \text{ MPa}$ .
- Clay filled piles shall be considered as empty piles. Sand filled piles with thin ( $< 0.5 D$ ) intermediate clay layers may be considered as sand filled piles.
- The results of this work should not be used for dolphin piles or for other applications where plastic deformation capacity is required. The effect of use of the recommendations for these type of structures may result in choosing larger  $D/t\epsilon^2$  values, which is not recommendable.

### Geometry:

$z_t$ :  m -> Top level of pile  
 $z_b$ :  m -> Tip level of pile  
 $c_{tc}$ :  m -> c.t.c of piles  
 (0 means only pile)

### Pile:

$D_o$ :  mm -> Outside section of pile  
 $t$ :  mm -> Wall thickness



$D_i := D_o - 2t = 1329 \cdot \text{mm}$  -> Internal section of pile  
 middle surface

$$r := \frac{(D_o - t)}{2} = 672.34 \cdot \text{mm} \quad \text{-> Radius of}$$

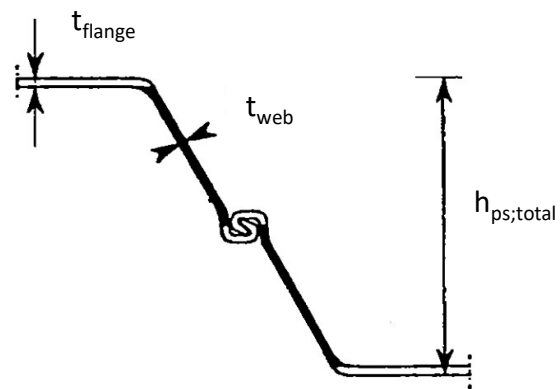
$A_{\text{pile}} := 2\pi \cdot r \cdot t = 64.7 \times 10^3 \cdot \text{mm}^2$  -> Area

$$W_{\text{pile}} := \pi r^3 \cdot \frac{2}{D_o} = 21.5 \times 10^6 \cdot \text{mm}^3 \quad \text{-> Section modulus}$$

$I_{\text{pile}} := \pi r^3 t = 1.463 \times 10^{10} \cdot \text{mm}^4$  -> Moment of inertia

### Sheet Pile:

$t_{fl}$ :  mm -> flange thickness  
 $t_{web}$ :  mm -> web thickness  
 $h_{sp}$ :  mm -> height sheet pile



**PROJECT:**  
**SUBJECT:**  
**CROSS-SECTION:**

Kadeconstructie Recobel  
 Plooi en sterkte buispaal  
 B-B'

**Material properties:**

E : N/mm<sup>2</sup> -> Modulus of Elasticity

Pile : N/mm<sup>2</sup> -> Steel quality pile

$$f_{yp} = 482 \cdot \frac{N}{mm^2} \quad \text{-> Yield strength pile}$$

SP : N/mm<sup>2</sup> -> Steel quality sheet pile

$$f_{ySp} = 355 \cdot \frac{N}{mm^2} \quad \text{-> Yield strength sheet pile}$$

Y<sub>M0</sub> : -> Safety factor because tubular piles tend to be not perfectly round, and this reduces the critical strain. Handbook Design of quay walls second edition, page 274.

**Classification of pile according to NEN-EN-1993-1-1, 5.5.2 / Table 5.2:**

D [mm]	t [mm]	f <sub>y</sub> [N/mm <sup>2</sup> ]	ε [-]	d/tε <sup>2</sup> [-]	
1360	15,32	482	0,698	182	class 1: d/tε <sup>2</sup> <=50 / class 2: 50<d/tε <sup>2</sup> <=70 class 3: 70<d/tε <sup>2</sup> <=90 / class 4: 90<d/tε <sup>2</sup>

Class 4: cross-sections are those in which local buckling will occur before the attainment of yield stress in one or more parts of the cross-section.

**Local buckling of pile according to NEN-EN-1993-1-6, D.1.2.2 (5):**

Cylinders need not be checked against meridional shell buckling if they satisfy:

$$\frac{r}{t} \leq 0.03 \cdot \frac{E}{f_{yp}} \quad \frac{r}{t} = 43.886 \quad 0.03 \cdot \frac{E}{f_{yp}} = 13.1$$

x\_ctrl = "Check buckling"

**Load cases:**

**From sheet pile:**

$$M_{sd.sheet} := \frac{1}{4} \cdot t_{web} \cdot f_{ySp} = 8 \cdot \frac{kNm}{m} \quad \text{-> Maximum moment from sheet pile}$$

$$w_{y.Ed} := \text{if} \left[ t_{fl} = 0,0, \frac{2 \cdot M_{sd.sheet}}{(h_{sp} - t_{fl})} \right] = 36.6 \cdot \frac{kN}{m} \quad \text{-> Maximal support reaction}$$

**From soil and pile:**

Soil loads are passive and/or active soil pressures, inside pile neutral soil pressure.

Amount of cases [min 1 / max 5, Left side is water/excavation side]:

Cases : -> i := 1 .. cases

Case	Level [m +NAP]	Soil					Pile loads	
		Left		Right		Intern	N <sub>ed</sub> [kN]	M <sub>ed</sub> [kNm]
		σ <sub>h</sub> [kN/m <sup>2</sup> ]	σ <sub>water</sub> [kN/m <sup>2</sup> ]	σ <sub>h</sub> [kN/m <sup>2</sup> ]	σ <sub>water</sub> [kN/m <sup>2</sup> ]	σ <sub>h</sub> [kN/m <sup>2</sup> ]		
1	-8,5	0,0	77,0	82,0	94,0	30,0	3105	7905

**Type of pile:**

Pile : -> Choose type of pile (empty or fill)



**Soil pressure:**

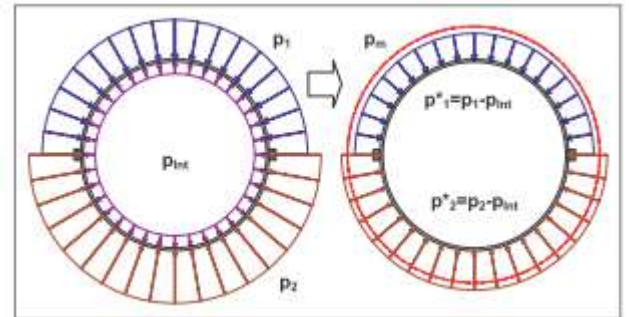
External soil pressure should be calculated with a factor c.t.c/Do (pressure acting on the pile is equal to de c.t.c between piles per m width of pile)

$$q_{L_i} := \text{if} \left( \text{ctc} = 0, 1, \frac{\text{ctc}}{D_o} \right) \cdot \sigma'_{hL_i} + \sigma_{wL_i} \quad q_{R_i} := \text{if} \left( \text{ctc} = 0, 1, \frac{\text{ctc}}{D_o} \right) \cdot \sigma'_{hR_i} + \sigma_{wR_i} \quad q_{Int_i} := \sigma'_{hI_i}$$

The pressures outside the tube had been averaged for the determination of the mean pressure on the tube

$$q_i := \max \left[ \left[ \frac{(q_{L_i} + q_{R_i})}{2} - q_{Int_i} \right] \text{ if } q_{L_i} \neq 0 \frac{\text{kN}}{\text{m}^2}, 0 \frac{\text{kN}}{\text{m}^2} \right. \\ \left. \left[ (q_{R_i}) - q_{Int_i} \right] \text{ otherwise} \right]$$

Case	q <sub>L</sub>	q <sub>R</sub>	q <sub>int</sub>	q
	[kN/m <sup>2</sup> ]	[kN/m <sup>2</sup> ]	[kN/m <sup>2</sup> ]	[kN/m <sup>2</sup> ]
1	77,0	287,5	30,0	152,3



**Out of roundness:**

No re-rounding effect caused by soil support to the sides of the tube has been taken in account

**a- Due to fabrication [NEN-EN 1993-1-6, tabel 8.1]:**

Cl:  $U_{r,max}(Cl, D_o) = 0.015$  → class [A:Excellent/B:High/C:Normal]

$$e_a := \frac{1}{4} \cdot U_{r,max}(Cl, D_o) \cdot D_o = 5.10 \cdot \text{mm}$$

**b- Due to tensile forces from secondary members [NEN-EN 1993-5, D.2.1]:**

$$EI := \frac{E \cdot t^3}{12} \quad e_b := \min \left[ 0.1 \cdot r, \frac{1}{2} \cdot \left( \frac{2}{\pi} - \frac{1}{2} \right) \cdot w_y \cdot Ed \cdot \frac{r^3}{EI} \right] = 12.07 \cdot \text{mm}$$

**c- Due to soil pressure:**

$$e_{c_i} := \begin{cases} \frac{1}{24} \cdot \frac{q_i \cdot r^4}{EI} & \text{if } q_L = 0 \frac{\text{kN}}{\text{m}^2} \\ \left( \frac{1}{12} \cdot \frac{q_i \cdot r^4}{EI} \right) & \text{otherwise} \end{cases} \quad e_c^T = (41.21) \cdot \text{mm}$$

**d- Ovalization as a second order effect:**

$$\kappa_i := \frac{M_{ed_i}}{E \cdot I_{pile}} \quad e_{d_i} := \frac{(\kappa_i)^2 \cdot r^5}{t^2} \quad e_d^T = (3.88) \cdot \text{mm}$$

**Radius of top and bottom side of the tube due to ovalisation [ $r'$ ]:**

$$k_{\text{steel}} := \frac{12 \cdot EI}{r} = 3.695 \cdot \frac{\text{MN}}{\text{m}^3}$$

$$k_{\text{sand}} := \frac{10 \text{MPa}}{r} = 14.873 \cdot \frac{\text{MN}}{\text{m}^3} \quad (E_{\text{sand}} := 10 \cdot \text{MPa, see article 6.6.6.4, bending moment evaluation for sand-filled tube})$$

$$k := \frac{k_{\text{steel}}}{k_{\text{steel}} + k_{\text{sand}}} = 0.199$$

$$e_{\text{tot}_i} := e_a + e_b + e_{c_i} + e_{d_i} \quad e_{t_i} := \begin{cases} (e_{\text{tot}_i} \cdot k) & \text{if Pile} = 2 \\ e_{\text{tot}_i} & \text{otherwise} \end{cases} \quad r'_i := \frac{r}{1 - 3 \cdot \frac{e_{t_i}}{r}}$$

$$e_t^T = (12.4) \cdot \text{mm}$$

$$r'^T = (711.7) \cdot \text{mm}$$

**Bending moment evaluation:**

**Critical strain:**  $\frac{D_o}{t} = 88.773 \quad \epsilon_y := \frac{f_{yp}}{E}$

$$\epsilon_{\text{cr}_i} = \begin{cases} \text{if Pile} = 1 & \epsilon_{\text{cr}} = (3.244 \times 10^{-3}) \\ \left( \begin{cases} \left( 0.25 \cdot \frac{t}{r'_i} - 0.0025 \right) & \text{if } \frac{D_o}{t} < 120 \\ \left( 0.1 \cdot \frac{t}{r'_i} \right) & \text{otherwise} \end{cases} \right) & \\ \text{if Pile} = 2 & \\ \left( \begin{cases} 7 \cdot \left( \frac{t}{r'_i} \right)^2 & \text{if } 67 < \frac{D_o}{t} \leq 120 \\ \text{"Out of range, to be calculated as empty pile"} & \text{otherwise} \end{cases} \right) & \end{cases}$$

**Parameter  $\mu$ :**  $\mu_i := \frac{\epsilon_{\text{cr}_i}}{\epsilon_y} \quad \mu^T = (1.41)$

**Plasticity rate:**  $\varphi_i := \begin{cases} \frac{\pi}{2} & \text{if } \mu_i \leq 1 \\ \text{asin}\left(\frac{1}{\mu_i}\right) & \text{otherwise} \end{cases} \quad \varphi^T = (45)^\circ$

**Bending moment as function of the plasticity rate:**

$$M_{el.d} := \frac{W_{pile} \cdot f_{yp}}{\gamma_{M0}} = 9426 \cdot \text{kNm}$$

$$M_{pl.d} := \frac{(2 \cdot r)^2 \cdot t \cdot f_{yp}}{\gamma_{M0}} = 12138 \cdot \text{kNm}$$

$$M_{R_i} := \begin{cases} \frac{1}{2} \cdot \left( \frac{\varphi_i}{\sin(\varphi_i)} + \cos(\varphi_i) \right) \cdot M_{pl.d} & \text{if } \mu_i > 1 \\ \mu_i \cdot M_{el.d} & \text{otherwise} \end{cases}$$

$$M_R = \boxed{11031} \cdot \text{kNm}$$

**Reduced bending moment and normal force:**

$m_{eff.Sd}$  due to tensile forces from secondary members is:

$$m_{eff.Sd.1} := \frac{\left( \frac{1}{\pi} \cdot w_y \cdot E_d \cdot r \right) + \left( \frac{1}{2} - \frac{1}{\pi} \right) \cdot w_y \cdot E_d \cdot r}{2}$$

$$m_{eff.Sd.1} = 6.1 \cdot \frac{\text{kNm}}{\text{m}}$$

$m_{eff.Sd}$  due to soil:

$$m_{eff.Sd.2_i} := \begin{cases} \frac{\left[ \left( \frac{1}{8} \cdot q_i \cdot r^2 \right) + \left( \frac{3}{8} - \frac{2}{3\pi} \right) \cdot q_i \cdot r^2 \right]}{2} & \text{if } q_L = 0 \frac{\text{kN}}{\text{m}^2} \\ \frac{\left( \frac{1}{4} \cdot q_i \cdot r^2 + \frac{1}{4} \cdot q_i \cdot r^2 \right)}{2} & \text{otherwise} \end{cases}$$

$$m_{eff.Sd.2} = \boxed{17.2} \cdot \frac{\text{kNm}}{\text{m}}$$

$$m_{pl.Rd} := \frac{t^2}{4} \cdot \frac{f_{yp}}{\gamma_{M0}}$$

$$m_{pl.Rd} = 25.711 \cdot \frac{\text{kNm}}{\text{m}}$$

$$c1_i := \sqrt{4 - 2 \cdot \sqrt{3} \cdot \frac{(m_{eff.Sd.1} + m_{eff.Sd.2_i})}{m_{pl.Rd}}}$$

$$c1^T = (0.92)$$

$$g0_i := \frac{c1_i}{6} + \frac{2}{3}$$

$$g0^T = (0.82)$$

$$\beta_{g_i} := 1 - \frac{2 \cdot e_{t_i}}{3 \cdot r}$$

$$\beta_g^T = (0.99)$$

$$\beta_{s_i} := \beta_{s1}(\text{Pile}, \mu_i)$$

$$\beta_s^T = (0.92)$$

$$M_{Rd_i} := g0_i \cdot \beta_{g_i} \cdot \beta_{s_i} \cdot M_{R_i}$$

$$M_{Rd} = \boxed{8231} \cdot \text{kNm}$$

$$N_{pl} := A_{pile} \cdot \frac{f_{yp}}{\gamma_{M0}} \text{ and } N_{Rd_i} := g0_i \cdot N_{pl}$$

$$N_{Rd} = \boxed{23271} \cdot \text{kN}$$

**PROJECT:**  
**SUBJECT:**  
**CROSS-SECTION:**

Kadeconstructie Recobel  
Plooi en sterkte buispaal  
B-B'

**Combined bending and normal force evaluation:**

$$N_{ed,1} = \boxed{3105} \cdot \text{kN} \quad M_{ed,1} = \boxed{7905} \cdot \text{kNm}$$

**UC:** 
$$\frac{M_{ed,1}}{M_{Rd,1}} + \left( \frac{N_{ed,1}}{N_{Rd,1}} \right)^{1.7} =$$
  
$$\boxed{0.993}$$

**Ctrl:** 
$$x_{ctrl} = \boxed{\text{"OK"}}$$

## Appendix P-3 Anchoring

### 3. Uitvoer van de berekening

**Naam** : Toetsing groutinjectieankers  
**Project** : Benchmark 1  
**Onderdeel** : Verankering  
**Bran** : CUR 166, 6e druk  
**Opsteller** : R. Wesstein  
**Versie** : 1.0  
**Datum** : 10-09-2018  
**Gecontroleerd door** : -

Doorsnede		-	-	B-B' (DKM25 t/m 33)	B-B' (DKM25 t/m 33)	
Ankerrij		-	-	1	2	
<b>Belasting:</b>						
F <sub>a,max</sub>	=	-	-	452.65	450.78	[kN/m]
F <sub>a,max/anker</sub>	=	-	-	1453.00	1447.00	[kN]
F <sub>a,rep</sub>	=	-	-	376.95	375.39	[kN/m]
F <sub>a,rep/anker</sub>	=	-	-	1210.00	1205.00	[kN]
F <sub>a,rep/anker bij anker uitval</sub>	=	-	-	1815.00	1807.50	[kN]
<b>Verankering:</b>						
hoek met de horizontaal	=	-	-	45	40	[°]
hart op hart afstand ankers	=	-	-	3.21	3.21	[m]
lengte groutprop	=	-	-	7.66	7.66	[m]
vrije ankerlengte	=	-	-	27.58	30.34	[m]
lengte bevestiging (indicatief)	=	-	-	0.50	0.50	[m]
totale ankerlengte	=	-	-	35.74	38.50	[m]
ankerniveau tpv hart wand	=	-	-	1.00	1.00	[m tov NAP]
ankerniveau tpv bk grout	=	-	-	-18.50	-18.50	[m tov NAP]
ankerniveau tpv ok grout	=	-	-	-23.92	-23.42	[m tov NAP]
soort	=	-	-	Jetmix Ø 101,6 mm x 17,5 mm	Jetmix Ø 101,6 mm x 17,5 mm	
buitendiameter stang/streng	=	-	-	101.60	101.60	[mm]
binnendiameter	=	-	-	17.50	17.50	[mm]
staalkwaliteit	=	-	-	E-470	E-470	
<b>Sondering:</b>						
gem. consusweerstand tpv groutprop	=	-	-	DKM 26	DKM 26	
				14	14	[MPa]
<b>Toetsing groutlichaamlengte (CUR166, Hfst 7 deel I en 4.9.4 deel II):</b>						
F <sub>g,max,grout</sub> = 1,1 x F <sub>a,max</sub>	=	-	-	1598	1592	[kN/anker]
F <sub>g,grout</sub>	=	-	-	1600	1600	[kN/anker]
unity check (eis: ≥ 1)	=	-	-	1.00	0.99	[-]
Toetsing groutprop:				voldoet	voldoet	
<b>Toetsing groutlichaam bij ankeruitval (stap 9.4, CUR166)</b>						
per m wand:						
F <sub>rep</sub>	=	-	-	376.95	375.39	[kN/m]
γ <sub>F,A</sub>	=	-	-	1.0	1.0	[-]
F <sub>s,A,gr,rep</sub>	=	-	-	376.95	375.39	[kN/m]
per staaf:						
F <sub>t,A,gr,rep</sub>	=	-	-	1920.36	1920.36	[kN/anker]
F <sub>s,A,gr,rep</sub>	=	-	-	1815.00	1807.50	[kN/anker]
u.c. =	=	-	-	0.95	0.94	[-]
Toetsing:				Voldoet	Voldoet	
<b>Toetsing ankerstaaf (stap 9, CUR166):</b>						
per m wand:						
F <sub>t,A,sl,d</sub>	=	-	-	656.69	656.69	[kN/m]
F <sub>A,max</sub>	=	-	-	452.65	450.78	[kN/m]
γ <sub>F,A</sub>	=	-	-	1.25	1.25	[-]
F <sub>s,A,sl,d</sub>	=	-	-	565.8099688	563.4735202	[kN/m]
u.c. = (eis: >1)	=	-	-	0.86	0.86	[-]
				Voldoet	Voldoet	
per staaf:						
F <sub>t,A,sl,d</sub>	=	-	-	2107.98	2107.98	[kN]
F <sub>s,A,sl,d</sub>	=	-	-	1816.25	1808.75	[kN]
u.c. = (eis: >1)	=	-	-	0.86	0.86	[-]
Toetsing:				Voldoet	Voldoet	
<b>Toetsing ankeruitval (stap 9.4, CUR166):</b>						
per m wand:						
F <sub>rep</sub>	=	-	-	376.95	375.39	[kN/m]
γ <sub>F,A</sub>	=	-	-	1.0	1.0	[-]
F <sub>s,A,sl,rep</sub>	=	-	-	376.95	375.39	[kN/m]
per staaf:						
F <sub>t,A,rep</sub>	=	-	-	2107.98	2107.98	[kN]
F <sub>s,A,sl,rep</sub> (=F <sub>a,rep</sub> * 1,5)	=	-	-	1815.00	1807.50	[kN]
u.c. = (eis: >1)	=	-	-	0.86	0.86	[-]
Toetsing:				Voldoet	Voldoet	

## Appendix P-4 Vertical bearing capacity

BUISPAAL GEGEVENS		Rekenwaarde LAAG			Rekenwaarde HOOG			Rekenwaarde GEMIDDELD			DRAAGKRACHTBEREKENING		
Sondering	P.P.N. [m NAP]	Schacht [kN]	Punt [kN]	Kleef [kN]	Schacht [kN]	Punt [kN]	Kleef [kN]	Schacht [kN]	Punt [kN]	Kleef [kN]	Rekenwaarde [kN]	Normaalkracht UGT [kN]	UC [-]
DKM10A	-27,0	3.349	90	0	2.234	2.040	0	2791	1065	0	3856	3503	0,91
DKM23	-27,0	2.812	143	0	3.929	216	0	3371	179	0	3550	3503	0,99
DKM22	-27,0	2.773	220	0	3.906	331	0	3340	276	0	3615	3503	0,97
DKM21	-27,0	2.951	207	0	4.002	311	0	3476	259	0	3735	3503	0,94
DKM20	-27,0	3.087	235	0	4.264	355	0	3675	295	0	3970	3503	0,88
DKM19	-27,0	3.101	191	0	4.276	287	0	3688	239	0	3928	3503	0,89
DKM18	-27,0	2.934	303	0	4.183	455	0	3558	379	0	3937	3503	0,89
DKM17A	-27,0	2.969	180	0	4.355	271	0	3662	226	0	3888	3503	0,90

Appendix Q Verification reports of optimised design of benchmark 2 in RC1  
Appendix Q-1 Second order bending moment of the combi-wall

$$D := 1225\text{mm (buiten)}$$

$$t := 18.1\text{mm}$$

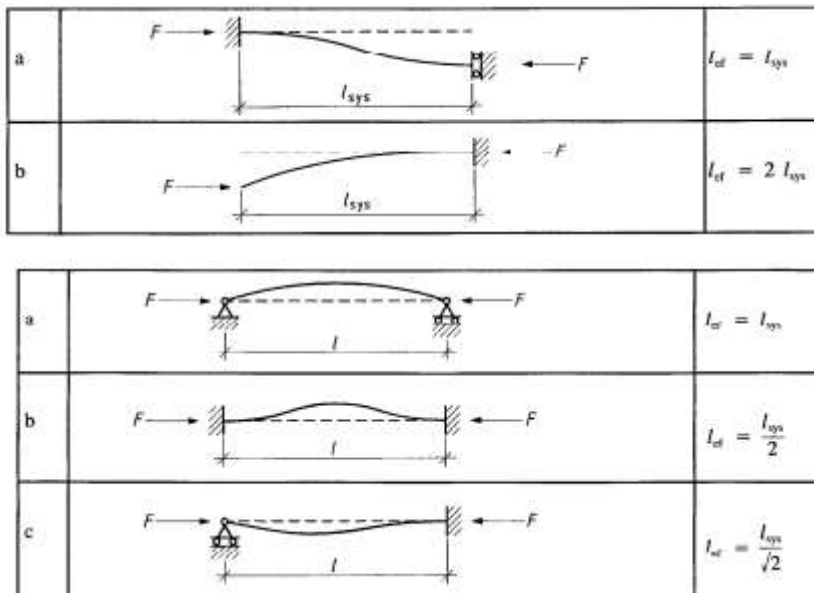
$$D_i := D - 2t$$

$$A := \frac{\pi(D^2 - D_i^2)}{4} = 68628 \cdot \text{mm}^2$$

$$I := \frac{\pi(D^4 - D_i^4)}{64} = 12498272517 \cdot \text{mm}^4$$

$$W := I \cdot \frac{2}{D} = 20405343 \cdot \text{mm}^3$$

$$E := 210000 \frac{\text{N}}{\text{mm}^2} = 210000000 \cdot \text{kPa}$$



$$\sigma_{x70} := 485 \frac{\text{N}}{\text{mm}^2} \quad M_{el} := \sigma_{x70} \cdot W = 9897 \cdot \text{kN} \cdot \text{m} \quad N_{el} := \sigma_{x70} \cdot A = 33284 \cdot \text{kN}$$

$$M_d := 7042 \text{kN} \cdot \text{m} \quad N_d := 8514 \text{kN}$$

$$\delta_{BGT} := 0.107 \text{m}$$

$$l_{y.buc} := 0.7 \cdot 34.2 \text{m} \quad N_{ye} := \frac{\pi^2 \cdot E \cdot I}{l_{y.buc}^2} = 45198 \cdot \text{kN}$$

$$n := \frac{N_{ye}}{N_d} = 5 \quad \frac{n}{n-1} = 1.23$$

$$M_{2e} := \frac{n}{(n-1)} \cdot N_d \cdot \delta_{BGT} = 1122 \cdot \text{kN} \cdot \text{m}$$

$$M_d + M_{2e} = 8164 \cdot \text{kN} \cdot \text{m}$$

## Appendix Q-2 Local buckling



## Local buckling according to Quay Wall Handbook

### Limitations: Piles

- Method to be used for steel quality up to X70 ( $f_y = 483 \text{ MPa}$ )
- The formulas are valid for water head differences less than 4 m.
- Critical strain formula for pile fill with sand is only valid for  $70 < \frac{D}{t} \leq 120$
- Alternatively EN 1993-1-6 may be used for piles filled with sand. In that case the resistance may be increased with a factor 1.13. This is only allowed for  $D/t < 100$  and for  $D/t\epsilon^2 < 170$ .

### Fill

- Sand shall be present in the area of the section subject to evaluation of the resistance. Sand may be loose or medium dense, if naturally available.
- In actively filled piles the sand fill shall be compacted, obtaining 70% relative density or  $q_c > 10 \text{ MPa}$ .
- Clay filled piles shall be considered as empty piles. Sand filled piles with thin ( $< 0.5 D$ ) intermediate clay layers may be considered as sand filled piles.
- The results of this work should not be used for dolphin piles or for other applications where plastic deformation capacity is required. The effect of use of the recommendations for these type of structures may result in choosing larger  $D/t\epsilon^2$  values, which is not recommendable.

### Geometry:

$z_t$ :  m -> Top level of pile

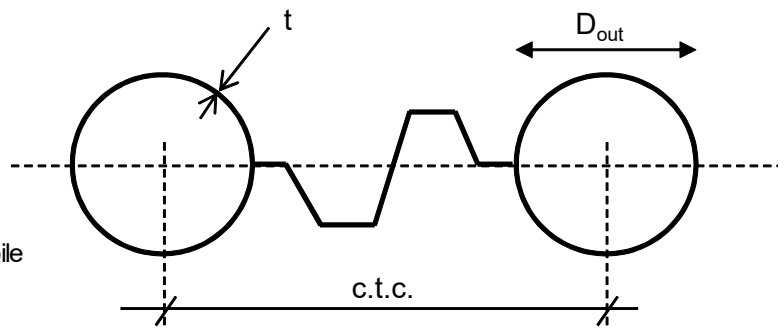
$z_b$ :  m -> Tip level of pile

ctc:  m -> c.t.c of piles  
(0 means only pile)

### Pile:

$D_o$ :  mm -> Outside section of pile

$t$ :  mm -> Wall thickness



$D_i := D_o - 2t = 1189 \cdot \text{mm}$  -> Internal section of pile  
middle surface

$$r := \frac{(D_o - t)}{2} = 603.455 \cdot \text{mm} \quad \text{-> Radius of}$$

$A_{\text{pile}} := 2\pi \cdot r \cdot t = 68.6 \times 10^3 \cdot \text{mm}^2$  -> Area

$$W_{\text{pile}} := \pi r^3 t \cdot \frac{2}{D_o} = 20.4 \times 10^6 \cdot \text{mm}^3 \quad \text{-> Section modulus}$$

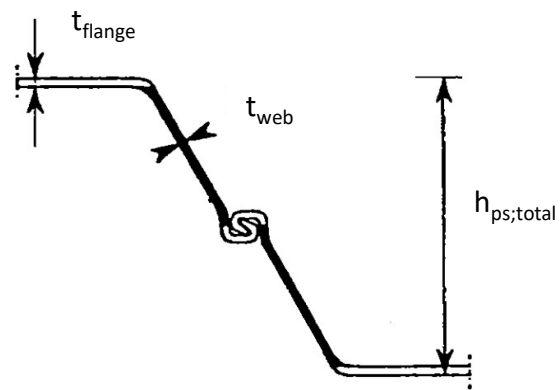
$I_{\text{pile}} := \pi r^3 t = 1.249 \times 10^{10} \cdot \text{mm}^4$  -> Moment of inertia

### Sheet Pile:

$t_{fl}$ :  mm -> flange thickness

$t_{web}$ :  mm -> web thickness

$h_{sp}$ :  mm -> height sheet pile



PROJECT:  
SECTION:  
ANNEX:

Engie biomassakade  
Plooi en sterkte buispaal  
H

X of document XXX

**Material properties:**

E :  N/mm<sup>2</sup> -> Modulus of Elasticity

Pile :  N/mm<sup>2</sup> -> Steel quality pile

$f_{yp} = 482 \cdot \frac{N}{mm^2}$  -> Yield strength pile

SP :  N/mm<sup>2</sup> -> Steel quality sheet pile

$f_{ySp} = 355 \cdot \frac{N}{mm^2}$  -> Yield strength sheet pile

$Y_{M0}$  :  -> Safety factor because tubular piles tend to be not perfectly round, and this reduces the critical strain. Handbook Design of quay walls second edition, page 274.

**Classification of pile according to NEN-EN-1993-1-1, 5.5.2 / Table 5.2:**

D [mm]	t [mm]	$f_y$ [N/mm <sup>2</sup> ]	$\epsilon$ [-]	$d/t\epsilon^2$ [-]	
1225	18.09	482	0.698	139	class 1: $d/t\epsilon^2 \leq 50$ / class 2: $50 < d/t\epsilon^2 \leq 70$ class 3: $70 < d/t\epsilon^2 \leq 90$ / class 4: $90 < d/t\epsilon^2$

Class 4: cross-sections are those in which local buckling will occur before the attainment of yield stress in one or more parts of the cross-section.

**Local buckling of pile according to NEN-EN-1993-1-6, D.1.2.2 (5):**

Cylinders need not be checked against meridional shell buckling if they satisfy:

$\frac{r}{t} \leq 0.03 \cdot \frac{E}{f_{yp}}$        $\frac{r}{t} = 33.358$        $0.03 \cdot \frac{E}{f_{yp}} = 13.1$

x\_ctrl = "Check buckling"

**Load cases:**

**From sheet pile:**

$M_{sd, sheet} := \frac{1}{4} \cdot t_{web} \cdot f_{ySp} = 8 \cdot \frac{kNm}{m}$  -> Maximum moment from sheet pile

$w_{y, Ed} := \text{if} \left[ t_{fl} = 0, 0, \frac{2 \cdot M_{sd, sheet}}{(h_{sp} - t_{fl})} \right] = 36.9 \cdot \frac{kN}{m}$  -> Maximal support reaction

**From soil and pile:**

Soil loads are passive and/or active soil pressures, inside pile neutral soil pressure.

Amount of cases [min 1 / max 5, Left side is water/excavation side]:

Cases :  -> i := 1..cases

Case	Level [m +NAP]	Soil					Pile loads	
		Left		Right		Intern	$N_{ed}$ [kN]	$M_{ed}$ [kNm]
		$\sigma_h$ [kN/m <sup>2</sup> ]	$\sigma_{water}$ [kN/m <sup>2</sup> ]	$\sigma_h$ [kN/m <sup>2</sup> ]	$\sigma_{water}$ [kN/m <sup>2</sup> ]	$\sigma_h$ [kN/m <sup>2</sup> ]		
1	-12	0.0	120.0	33.0	120.0	50.0	8514	8169
2	-12	0.0	120.0	33.0	120.0	50.0	8832	7240
3	-14	0.0	140.0	39.6	140.0	60.0	6213	8143

**Type of pile:**

Pile :  -> Choose type of pile (empty or fill)



**Soil pressure:**

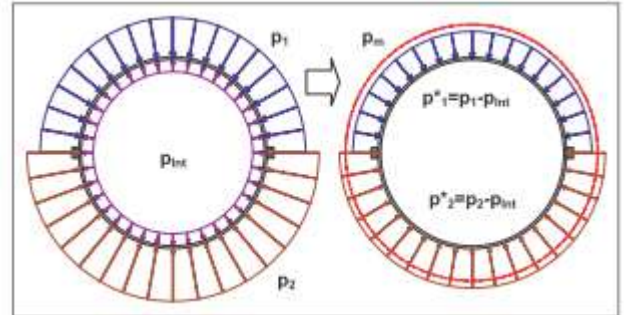
External soil pressure should be calculated with a factor c.t.c/Do (pressure acting on the pile is equal to de c.t.c between piles per m width of pile)

$$q_{L_i} := \text{if} \left( \text{ctc} = 0, 1, \frac{\text{ctc}}{D_o} \right) \cdot \sigma'_{hL_i} + \sigma_{wL_i} \quad q_{R_i} := \text{if} \left( \text{ctc} = 0, 1, \frac{\text{ctc}}{D_o} \right) \cdot \sigma'_{hR_i} + \sigma_{wR_i} \quad q_{Int_i} := \sigma'_{hI_i}$$

The pressures outside the tube had been averaged for the determination of the mean pressure on the tube

$$q_i := \max \left[ \left[ \frac{(q_{L_i} + q_{R_i})}{2} - q_{Int_i} \right] \text{ if } q_{L_i} \neq 0 \frac{\text{kN}}{\text{m}^2}, 0 \frac{\text{kN}}{\text{m}^2} \right. \\ \left. \left[ (q_{R_i}) - q_{Int_i} \right] \text{ otherwise} \right]$$

Case	q <sub>L</sub>	q <sub>R</sub>	q <sub>int</sub>	q
	[kN/m <sup>2</sup> ]	[kN/m <sup>2</sup> ]	[kN/m <sup>2</sup> ]	[kN/m <sup>2</sup> ]
1	120.0	215.2	50.0	117.6
2	120.0	215.2	50.0	117.6
3	140.0	254.3	60.0	137.1



**Out of roundness:**

No re-rounding effect caused by soil support to the sides of the tube has been taken in account

**a- Due to fabrication [NEN-EN 1993-1-6, tabel 8.1]:**

Cl:   $U_{r,max}(Cl, D_o) = 0.016$  -> class [A:Excellent/B:High/C:Normal]

$$e_a := \frac{1}{4} \cdot U_{r,max}(Cl, D_o) \cdot D_o = 4.75 \cdot \text{mm}$$

**b- Due to tensile forces from secondary members [NEN-EN 1993-5, D.2.1]:**

$$EI := \frac{E \cdot t^3}{12} \quad e_b := \min \left[ 0.1 \cdot r, \frac{1}{2} \cdot \left( \frac{2}{\pi} - \frac{1}{2} \right) \cdot w_y \cdot Ed \cdot \frac{r^3}{EI} \right] = 5.35 \cdot \text{mm}$$

**c- Due to soil pressure:**

$$e_{c_i} := \begin{cases} \frac{1}{24} \cdot \frac{q_i \cdot r^4}{EI} & \text{if } q_L = 0 \frac{\text{kN}}{\text{m}^2} \\ \left( \frac{1}{12} \cdot \frac{q_i \cdot r^4}{EI} \right) & \text{otherwise} \end{cases} \quad e_c^T = (12.55 \quad 12.55 \quad 14.63) \cdot \text{mm}$$

**d- Ovalization as a second order effect:**

$$\kappa_i := \frac{M_{ed_i}}{E \cdot I_{pile}} \quad e_{d_i} := \frac{(\kappa_i)^2 \cdot r^5}{t^2} \quad e_d^T = (2.37 \quad 1.86 \quad 2.36) \cdot \text{mm}$$

**Radius of top and bottom side of the tube due to ovalisation [r']:**

$$k_{\text{steel}} := \frac{12 \cdot EI}{r^4} = 9.375 \cdot \frac{\text{MN}}{\text{m}^3}$$

$$k_{\text{sand}} := \frac{10 \text{kPa}}{r} = 0.017 \cdot \frac{\text{MN}}{\text{m}^3} \quad (E_{\text{sand}} := 10 \cdot \text{kPa, see article 6.6.6.4, bending moment evaluation for sand-filled tube})$$

$$k := \frac{k_{\text{steel}}}{k_{\text{steel}} + k_{\text{sand}}} = 0.998$$

$$e_{\text{tot}_i} := e_a + e_b + e_{c_i} + e_{d_i} \quad e_{t_i} := \begin{cases} (e_{\text{tot}_i} \cdot k) & \text{if Pile} = 2 \\ e_{\text{tot}_i} & \text{otherwise} \end{cases} \quad r'_i := \frac{r}{1 - 3 \cdot \frac{e_{t_i}}{r}}$$

$$e_t^T = (25 \quad 24.5 \quad 27) \cdot \text{mm}$$

$$r'^T = (689 \quad 687 \quad 697.1) \cdot \text{mm}$$

**Bending moment evaluation:**

**Critical strain:**  $\frac{D_o}{t} = 67.717 \quad \epsilon_y := \frac{f_{yp}}{E}$

$$\epsilon_{\text{cr}_i} = \begin{cases} \text{if Pile} = 1 \\ \left| \begin{cases} \left( 0.25 \cdot \frac{t}{r'_i} - 0.0025 \right) & \text{if } \frac{D_o}{t} < 120 \\ \left( 0.1 \cdot \frac{t}{r'_i} \right) & \text{otherwise} \end{cases} \right. \\ \text{if Pile} = 2 \\ \left| \begin{cases} 7 \cdot \left( \frac{t}{r'_i} \right)^2 & \text{if } 67 < \frac{D_o}{t} \leq 120 \\ \text{"Out of range, to be calculated as empty pile"} & \text{otherwise} \end{cases} \right. \end{cases} \quad \epsilon_{\text{cr}} = \begin{pmatrix} 4.826 \times 10^{-3} \\ 4.854 \times 10^{-3} \\ 4.713 \times 10^{-3} \end{pmatrix}$$

**Parameter  $\mu$ :**  $\mu_i := \frac{\epsilon_{\text{cr}_i}}{\epsilon_y} \quad \mu^T = (2.1 \quad 2.11 \quad 2.05)$

**Plasticity rate:**  $\varphi_i := \begin{cases} \frac{\pi}{2} & \text{if } \mu_i \leq 1 \\ \text{asin} \left( \frac{1}{\mu_i} \right) & \text{otherwise} \end{cases} \quad \varphi^T = (28.4 \quad 28.2 \quad 29.1) \cdot ^\circ$

**Bending moment as function of the plasticity rate:**

$$M_{el.d} := \frac{W_{pile} \cdot f_{yp}}{\gamma_{M0}} = 8935 \cdot \text{kNm}$$

$$M_{R_i} := \begin{cases} \frac{1}{2} \cdot \left( \frac{\varphi_i}{\sin(\varphi_i)} + \cos(\varphi_i) \right) \cdot M_{pl.d} & \text{if } \mu_i > 1 \\ \mu_i \cdot M_{el.d} & \text{otherwise} \end{cases}$$

$$M_{pl.d} := \frac{(2 \cdot r)^2 \cdot t \cdot f_{yp}}{\gamma_{M0}} = 11546 \cdot \text{kNm}$$

$$M_R = \begin{matrix} 11095 \\ 11100 \\ 11072 \end{matrix} \cdot \text{kNm}$$

**Reduced bending moment and normal force:**

$m_{eff.Sd}$  due to tensile forces from secondary members is:

$$m_{eff.Sd.1} := \frac{\left( \frac{1}{\pi} \cdot w_y \cdot Ed \cdot r \right) + \left( \frac{1}{2} - \frac{1}{\pi} \right) \cdot w_y \cdot Ed \cdot r}{2}$$

$$m_{eff.Sd.1} = 5.6 \cdot \frac{\text{kNm}}{\text{m}}$$

$m_{eff.Sd}$  due to soil:

$$m_{eff.Sd.2_i} := \begin{cases} \frac{\left[ \left( \frac{1}{8} \cdot q_i \cdot r^2 \right) + \left( \frac{3}{8} - \frac{2}{3\pi} \right) \cdot q_i \cdot r^2 \right]}{2} & \text{if } q_L = 0 \frac{\text{kN}}{\text{m}^2} \\ \frac{\left( \frac{1}{4} \cdot q_i \cdot r^2 + \frac{1}{4} \cdot q_i \cdot r^2 \right)}{2} & \text{otherwise} \end{cases}$$

$$m_{eff.Sd.2} = \begin{matrix} 10.7 \\ 10.7 \\ 12.5 \end{matrix} \cdot \frac{\text{kNm}}{\text{m}}$$

$$m_{pl.Rd} := \frac{t^2}{4} \cdot \frac{f_{yp}}{\gamma_{M0}}$$

$$m_{pl.Rd} = 35.849 \cdot \frac{\text{kNm}}{\text{m}}$$

$$c1_i := \sqrt{4 - 2 \cdot \sqrt{3} \cdot \frac{(m_{eff.Sd.1} + m_{eff.Sd.2_i})}{m_{pl.Rd}}}$$

$$c1^T = (1.56 \quad 1.56 \quad 1.50)$$

$$g0_i := \frac{c1_i}{6} + \frac{2}{3}$$

$$g0^T = (0.93 \quad 0.93 \quad 0.92)$$

$$\beta_{g_i} := 1 - \frac{2 \cdot e_{t_i}}{3 \cdot r}$$

$$\beta_g^T = (0.97 \quad 0.97 \quad 0.97)$$

$$\beta_{s_i} := \beta_{s1}(\text{Pile}, \mu_i)$$

$$\beta_s^T = (0.96 \quad 0.96 \quad 0.95)$$

$$M_{Rd_i} := g0_i \cdot \beta_{g_i} \cdot \beta_{s_i} \cdot M_{R_i}$$

$$M_{Rd} = \begin{matrix} 9545 \\ 9562 \\ 9384 \end{matrix} \cdot \text{kNm}$$

$$N_{pl} := A_{pile} \cdot \frac{f_{yp}}{\gamma_{M0}} \quad \text{and} \quad N_{Rd_i} := g0_i \cdot N_{pl}$$

$$N_{Rd} = \begin{matrix} 27841 \\ 27841 \\ 27560 \end{matrix} \cdot \text{kN}$$

**PROJECT:**  
**SECTION:**  
**ANNEX:**

Engie biomassakade  
Plooi en sterkte buispaal  
H

X of document XXX

**Combined bending and normal force evaluation:**

$$N_{ed,i} = \begin{array}{|c|} \hline 8514 \\ \hline 8832 \\ \hline 6213 \\ \hline \end{array} \cdot \text{kN}$$

$$M_{ed,i} = \begin{array}{|c|} \hline 8169 \\ \hline 7240 \\ \hline 8143 \\ \hline \end{array} \cdot \text{kNm}$$

**UC:**  $\frac{M_{ed,i}}{M_{Rd,i}} + \left( \frac{N_{ed,i}}{N_{Rd,i}} \right)^{1.7} = \begin{array}{|c|} \hline 0.989 \\ \hline 0.899 \\ \hline 0.947 \\ \hline \end{array}$

**Ctrl:**  $x_{ctrl} = \begin{array}{|c|} \hline "OK" \\ \hline "OK" \\ \hline "OK" \\ \hline \end{array}$

## Appendix Q-3 Anchoring

### 3. Uitvoer van de berekening

**Naam** : Berekening groutanker en schroefinjectieankers  
**Project** : Benchmark 2  
**Onderdeel** : Kadeconstructie  
**Bron** : CUR 166, 6e druk  
**Opsteller** : R. Wesstein  
**Versie** : 0.1  
**Datum** : 18-12-2018  
**Gecontroleerd door** : -



		EN408 - DKP004 - EN409 - DKP005 -				
		DKP007 - EN412	-	-	-	-
		1	-	-	-	-
<b>Doorsnede</b>						
Ankerrij						
<b>Belasting:</b>						
Fa,max	=	475.69	-	-	-	[kN/m]
Fa,max/anker	=	1301.00	-	-	-	[kN]
Fa,rep	=	262.52	-	-	-	[kN/m]
Fa,rep/anker	=	718.00	-	-	-	[kN]
Fa,rep/anker bij anker uitval	=	1077.00	-	-	-	[kN]
<b>Verankering:</b>						
hoek met de horizontaal	=	12	-	-	-	[°]
hart op hart afstand ankers	=	2.74	-	-	-	[m]
lengte groutprop	=	7.30	-	-	-	[m]
vrije ankerlengte	=	20.01	-	-	-	[m]
lengte bevestiging (indicatief)	=	0.50	-	-	-	[m]
totale ankerlengte	=	27.81	-	-	-	[m]
ankerniveau tpv hart wand	=	0.90	-	-	-	[m tov NAP]
ankerniveau tpv bk grout	=	0.00	-	-	-	[m tov NAP]
ankerniveau tpv ok grout	=	-4.78	-	-	-	[m tov NAP]
soort	=	Jetmix Ø 101,6 mm x 17,5 mm	-	-	-	
buitendiameter stang/streng	=	101.60	-	-	-	[mm]
binnendiameter	=	17.50	-	-	-	[mm]
staalkwaliteit	=	E-470	-	-	-	
<b>Sondering:</b>						
gem. consusweerstand tpv groutprop	=	EN408/409/410 DKP004/005	-	-	-	
	=	18	-	-	-	[MPa]
<b>Toetsing groutlichaamlengte (CUR166, Hfst 7 deel I en 4.9.4 deel II):</b>						
F <sub>u,max,gr,d</sub> = 1,1 x F <sub>u,max</sub>	=	1431	-	-	-	[kN/anker]
F <sub>u,gr,d</sub>	=	1445	-	-	-	[kN/anker]
unity check (eis: <1)	=	0.99	-	-	-	[-]
Toetsing groutprop:	=	voldoet	-	-	-	
<b>Toetsing groutlichaam bij ankeruitval (stap 9.4, CUR166)</b>						
per m wand: F <sub>rep</sub>	=	262.52	-	-	-	[kN/m]
γ <sub>F,A</sub>	=	1.0	-	-	-	[-]
F <sub>s,A,gr,rep</sub>	=	262.52	-	-	-	[kN/m]
per staaf: F <sub>r,A,gr,rep</sub>	=	1733.78	-	-	-	[kN/anker]
F <sub>s,A,gr,rep</sub>	=	1077.00	-	-	-	[kN/anker]
u.c. =	=	0.62	-	-	-	[-]
Toetsing:	=	Voldoet	-	-	-	
<b>Toetsing ankerstaaf (stap 9, CUR166):</b>						
per m wand: F <sub>r,A,sl,d</sub>	=	801.02	-	-	-	[kN/m]
F <sub>A,max</sub>	=	475.69	-	-	-	[kN/m]
γ <sub>F,A</sub>	=	1.25	-	-	-	[-]
F <sub>s,A,sl,d</sub>	=	594.606947	-	-	-	[kN/m]
u.c. = (eis: <1)	=	0.74	-	-	-	[-]
	=	Voldoet	-	-	-	
per staaf: F <sub>r,A,sl,d</sub>	=	2190.78	-	-	-	[kN]
F <sub>s,A,sl,d</sub>	=	1626.25	-	-	-	[kN]
u.c. = (eis: <1)	=	0.74	-	-	-	[-]
Toetsing:	=	Voldoet	-	-	-	
<b>Toetsing ankeruitval (stap 9.4, CUR166):</b>						
per m wand: F <sub>rep</sub>	=	262.52	-	-	-	[kN/m]
γ <sub>F,A</sub>	=	1.0	-	-	-	[-]
F <sub>s,A,sl,rep</sub>	=	262.52	-	-	-	[kN/m]
per staaf: F <sub>r,A,rep</sub>	=	2190.78	-	-	-	[kN]
F <sub>s,A,sl,rep</sub> (=F <sub>A,rep</sub> * 1,5)	=	1077.00	-	-	-	[kN]
u.c. = (eis: <1)	=	0.49	-	-	-	[-]
Toetsing:	=	Voldoet	-	-	-	

## Appendix Q-4 Vertical bearing capacity tubular piles

BUISPAAL GEGEVENS		HOOG			LAAG			TOTAAL			DRAAGKRACHTBEREKENING			
Sondering	P.P.N. [m NAP]	Punt [kN]	Schacht [kN]	Kleef [kN]	Punt [kN]	Schacht [kN]	Kleef [kN]	Punt [kN]	Schacht [kN]	Kleef [kN]	Representatief [kN]	Rekenwaarde [kN]	Normaalkracht UGT [kN]	UC [-]
DKP011	-34.5	15061	2912	328	7106	3105	0	11084	3009	164	13928	10181	8832	0.87
EN380	-34.5	17535	2932	325	12908	3903	0	15222	3418	163	18477	13506	8832	0.65
EN381	-34.5	17535	2837	337	12736	2989	0	15136	2913	169	17880	13070	8832	0.68
EN382	-34.5	13867	2884	373	8835	3473	0	11351	3179	187	14343	10485	8832	0.84
EN383	-34.5	17535	2729	298	12266	2051	0	14901	2390	149	17142	12530	8832	0.70
EN384	-34.5	15061	2767	334	7873	2107	0	11467	2437	167	13737	10042	8832	0.88
EN385	-34.5	11954	2867	331	7709	3726	0	9832	3297	166	12963	9476	8832	0.93
EN387	-34.5	13666	2751	331	6250	2782	0	9958	2767	166	12559	9181	8832	0.96
EN388	-34.5	13733	2612	329	6098	2094	0	9916	2353	165	12104	8848	8832	1.00
EN317	-34.5	15456	2905	325	7959	2671	0	11708	2788	163	14333	10477	8832	0.84
EN311	-34.5	15229	2921	307	7719	2708	0	11474	2815	154	14135	10333	8832	0.85

## Appendix Q-5 Vertical bearing capacity vibro piles

Sondering	Puntniveau [m NAP]	Punt Ø685 [kN]	Schacht Ø560 [kN]	Negatieve kleef Ø560 [kN]	Represenatief [kN]	Rekenwaarde [kN]	Normaalkracht UGT [kN]	UC [-]
DKP011	-27.8	4981	1809	168	6622	4841	3655	0.76
EN380	-27.8	5528	2617	172	7973	5828	3655	0.63
EN381	-27.8	4343	1694	181	5856	4281	3655	0.85
EN382	-27.8	4429	2328	191	6566	4800	3655	0.76
EN383	-27.8	4379	1526	159	5746	4200	3655	0.87
EN384	-27.8	3877	1342	175	5044	3687	3655	0.99
EN385	-27.8	4928	1981	172	6737	4925	3655	0.74
EN386	-27.8	5165	1997	161	7001	5118	3655	0.71
EN387	-27.8	5528	1825	169	7184	5251	3655	0.70
EN388	-27.8	5217	1846	172	6891	5037	3655	0.73
EN317	-27.8	5079	2072	170	6981	5103	3655	0.72